The spatiotemporal control of CDK activity

Emma Roberts

The Francis Crick Institute

and

Imperial College London

Department of Clinical Sciences

PhD Supervisor: Sir Paul Nurse

A thesis submitted for the degree of

Doctor of Philosophy

Imperial College London

February 2022

Declaration

I, Emma Roberts, confirm that the work presented in this thesis is my own. Where information has been derived from other sources, I confirm that this has been indicated in the thesis.

The work presented in this thesis was done in parallel with related work which is published in (Basu, Roberts, Jones, Swaffer, Snijders and Nurse; 2020). Aspects of the published work informs the discussion in this thesis, and the rationale behind some experiments presented here. Where the work of other authors is presented, it is made clear in the text and figure legend, and the publication is referenced.

The copyright of this thesis rests with the author. Unless otherwise indicated, its contents are licensed under a Creative Commons Attribution-Non Commercial 4.0 International Licence (CC BY-NC). Under this licence, you may copy and redistribute the material in any medium or format. You may also create and distribute modified versions of the work. This is on the condition that: you credit the author and do not use it, or any derivative works, for a commercial purpose. When reusing or sharing this work, ensure you make the licence terms clear to others by naming the licence and linking to the licence text. Where a work has been adapted, you should indicate that the work has been changed and describe those changes.

Please seek permission from the copyright holder for uses of this work that are not included in this licence or permitted under UK Copyright Law

Abstract

The oscillating activity of cyclin-dependent kinases (CDKs) in complex with cyclins drives progression through the eukaryotic cell cycle. It has long been appreciated that the temporal control of cyclin-CDK activity is critical to cell cycle progression, but there is increasing evidence that the spatial control of cyclin-CDK activity is also important in cell cycle regulation. The centrosome (metazoa) and spindle pole body (SPB, yeast) act as key signalling hubs in cell cycle transitions including mitotic entry. Understanding CDK localisation and regulation at the centrosome and SPB will inform our understanding of the importance of CDK spatial regulation and how it impacts cell cycle progression.

I have studied the localisation of the mitotic cyclin Cdc13 in the fission yeast *S. pombe*, identifying that the hydrophobic patch region of Cdc13 is responsible for Cdc13 localisation to the SPB in early G2. A hydrophobic patch mutant (HPM) of Cdc13 does not localise to the SPB, and does not enter mitosis. Restoring the SPB localisation of $Cdc13^{HPM}$-Cdc2 promotes a wave of mitotic entry, leading to the hypothesis that cyclin-CDK activity at the SPB is essential for entry into mitosis. Unlike human Cyclin B1, Cyclin $B1^{HPM}$ is not detected at the centrosome, suggesting that the involvement of the Cyclin B hydrophobic patch in SPB and centrosomal localisation is similar between fission yeast and human cells.

I also show that there is a hydrophobic patch-independent mechanism of Cdc13 localisation to the SPB after Polo kinase localisation to the SPB in late G2/mitosis, which operates when there is a wild-type copy of Cdc13 present in cells. Finally, I present initial work developing a system to compare CDK substrate phosphorylation across different subcellular locations. Overall, this work supports the body of work indicating that the SPB and centrosome play an important role in mitotic entry.

Acknowledgement

Firstly, thank you to Paul for mentoring me through my PhD and encouraging me to develop a project around my interests and take ownership of it. I joined the lab wanting a challenge and now at the end I can look back and see how much I've learnt and progressed in my time here. It has been a real privilege to have done my PhD under your guidance, and I am very grateful for your support.

Thank you also to the members of the Nurse lab past and present, who have been friends as well as colleagues. In particular, thank you to Saz for all the time you spent teaching me throughout, the many scientific (and many non-scientific) discussions, and for the collaboration. To Jess and Helena, it has been so valuable to me to have you as friends and role models, and if I end up half the scientist you two are I would be so proud. And thank you to Clovis, for making me laugh and never failing to be up for a drink, I count myself lucky to have gone through the PhD with you. Thank you as well to Scott, Joe and Theresa for the constant good humour and support throughout, and to Jacky for sharing your infinite knowledge and insight. Special thanks to Paul, Jess, Saz, Theresa and Joe for critical reading of this thesis. Thank you as well to Sofi and Ryoko for keeping the lab running so smoothly; it makes such a difference and I am very thankful for it. I am also very grateful to the Lord Leonard and Lady Estelle Wolfson Foundation, Cancer Research UK, and the Wellcome Trust for funding, and my thesis committee, Silvia Santos, Luis Aragon-Alcaide and Sila Ultanir for their advice and guidance.

Thank you as well to my friends, especially Priya, Holly, Caroline and Chandni, for always being supportive and understanding through the good and bad times of the PhD, even if it has always been just 'something to do with yeast'. Thank you to my family for the constant patience and support. Mum, I hope you know how much our daily calls have helped me over the years. And finally, the biggest thank you of course to Jack. This PhD has definitely been a team effort, and I can't imagine what it would have been like without you by my side. From listening to every complaint after every failed experiment, to helping me celebrate the small wins, to having a cup of tea to come home to after the longest days, your support has been constant and I'm so grateful for it.

Table of Contents

Abstract **3**
Acknowledgement **4**
Table of Contents **5**
Table of figures **7**
List of tables **9**
Abbreviations **10**
Chapter 1. Introduction **12**
1.1 Cyclin-CDK control of cell cycle progression **12**
1.1.1 CDKs control cell cycle progression 13
1.1.2 *S. pombe* as a model to study CDK control of the cell cycle 14
1.2 Molecular regulation of CDK activity **17**
1.2.1 Cyclin binding is necessary for CDK activity 17
1.2.2 T-loop phosphorylation 19
1.2.3 T14 and Y15 phosphorylation inhibit CDK activity 21
1.2.4 CDK activity is regulated by Suc1/Cks1 and CDK inhibitors 25
1.2.5 Phosphatases oppose CDK substrate phosphorylation 27
1.2.6 Cyclin docking sites 30
1.2.7 The regulation of CDK activity is critical for controlling cell cycle progression 33
1.3 The temporal control of CDK activity is critical to ordering the cell cycle **34**
1.3.1 Quantitative vs qualitative model 34
1.3.2 Ordering CDK substrate phosphorylation 37
1.3.3 The spatial regulation of CDK activity is also important for cell cycle progression 38
1.4 Localisation of CDK and its regulators **39**
1.4.1 Localisation of cyclin-CDK complexes 39
1.4.2 Localisation of other cell cycle regulators 40
1.5 Role and importance of localisation in cell cycle progression **42**
1.5.1 Regulation of substrate specificity and access 42
1.5.2 Concentration of enzymes to aid switch-like transitions 43
1.5.3 Signalling hubs and scaffold-assisted signalling cascades 44
1.6 Role of the centrosome and SPB in cell cycle regulation **45**
1.6.1 Structure and dynamics of the SPB and centrosome 45
1.6.2 SPB as a signalling hub at mitotic entry 46
1.6.3 SPB and centrosome in other cell cycle transitions 51
1.6.4 Importance of the centrosome is contested 52
1.7 Cyclin localisation to the SPB and centrosome **54**
Chapter 2. Materials & Methods **55**
2.1 Fission yeast growth and synchronisation **55**
2.2 Human cell line culture **56**
2.3 Fluorescence microscopy **57**
2.4 Flow cytometry and cell cycle progression analysis **59**
2.5 Protein extraction, immunoprecipitation and Western blotting **59**
2.6 Antibody generation and immunofluorescence **61**
2.7 Phosphoproteomics **62**
Chapter 3. Localisation of Cdc13 to the SPB **70**

3.1 Localisation of cyclin-CDK through the cell cycle 71
3.2 Cdc13 localisation to the SPB involves the hydrophobic patch 78
3.3 Cdc13^{HPM} is enriched at the SPB in mitosis 81
3.3.1 Cdc13^{HPM} is not enriched at the SPB in a G2 arrest 81
3.3.2 Cdc13^{HPM} accumulates at the SPB after Polo kinase 86
3.4 Discussion 88
Chapter 4. Localisation of Cyclin B1 to the centrosome 93
4.1 Expressing Cyclin B1^{HPM} in human cells 95
4.2 Localisation of Cyclin B1^{HPM}-mCherry 99
4.3 Discussion 104
Chapter 5. Raising Cdc13^{HPM} activity at the SPB 106
5.1 Localisation of Cdc13^{HPM} in the absence of wild-type Cdc13 107
5.2 Developing a system to relocalise Cdc13^{HPM}/Cdc2 to the SPB 111
5.3 Can the mitotic defect of Cdc13^{HPM} be rescued by fusing Cdc13 and Cdc2 or raising Cdc2 activity? 119
5.4 Relocalising Cdc13^{HPM}-Cdc2 to the SPB 128
5.5 Discussion 136
Chapter 6. Measuring CDK substrate phosphorylation in different cellular compartments 140
6.1 Novel phosphospecific antibodies against CDK substrates 142
6.2 Measuring CDK substrate phosphorylation on Western blots 148
6.3 Testing Spo15 antibodies for use in immunofluorescence 155
6.4 Discussion 164
Chapter 7. Discussion 166
7.1 A localisation model to explain the effect of Cdc13^{HPM} 168
7.2 The role of the cyclin hydrophobic patch in substrate docking and localisation 169
7.2.1 Are there different roles for the hydrophobic patch in G1/S vs mitotic cyclins? 170
7.2.2 Are there different roles for the hydrophobic patch between different organisms? 171
7.2.3 The involvement of the cyclin hydrophobic patch in SPB and centrosomal localisation 172
7.3 Importance of the hydrophobic patch and SPB localisation 174
7.3.1 Is Cdc13 SPB localisation essential for cell cycle progression? 174
7.3.2 What might be the essential roles of Cdc13-Cdc2 at the SPB? 176
7.3.3 Importance of substrate specific docking via the hydrophobic patch 177
7.4 Hydrophobic patch-independent localisation of Cdc13 179
7.4.1 How might Polo kinase activity at the SPB influence Cdc13 SPB recruitment? 180
7.4.2 What is the role of the hydrophobic patch independent mechanism of Cdc13 SPB accumulation in late G2/mitosis? 181
7.5 The role of localisation in substrate sensitivity to CDK activity 184
7.6 Concluding remarks 187
Chapter 8. Appendix 188
Reference List 191

Table of figures

Figure 1.1 | Cell cycle of *S. pombe* 15
Figure 1.2 | Cyclin-CDK regulation of the cell cycle 18
Figure 1.3 | Structure of Cyclin A-Cdk2 bound to ATP 21
Figure 1.4 | Core network regulating CDK Y15 dephosphorylation 24
Figure 1.5 | Structure of Cyclin A-Cdk2 bound to p27 31
Figure 1.6 | Schematic of the fission yeast SPB 46
Figure 1.7 | Regulation of mitotic entry at the SPB 49
Figure 3.1 | Localisation of core cell cycle regulators through the cell cycle 74
Figure 3.2 | Segmentation to create SPB and 'surround' mask 75
Figure 3.3 | Intensity measurements of cell cycle regulators at the SPB 76
Figure 3.4 | Cdc13^{HPM}-sfGFP is only enriched at the SPB in longer cells 80
Figure 3.5 | Cdc13-sfGFP localisation and accumulation in a *cdc25-22* G2 arrest 82
Figure 3.6 | Cdc13-sfGFP concentration in *cdc2(as)* G2-arrested cells 84
Figure 3.7 | Cdc13^{HPM}-sfGFP does not localise to the SPB in a G2 arrest 85
Figure 3.8 | Cdc13^{HPM}-sfGFP localises to the SPB after Plo1-mCherry 87
Figure 4.1 | Cdc13 and Cyclin B1 hydrophobic patch sequence conservation 95
Figure 4.2 | Western blot of transfected Cyclin B1-mCherry constructs 97
Figure 4.3 | Transfected Cyclin B1-mCherry constructs can interact with Cdk1 98
Figure 4.4 | Cyclin B1^{HPM}-mCherry is not enriched at the centrosome 100
Figure 4.5 | Cyclin B1^{WT}-mCherry localisation in mitosis 102
Figure 4.6 | Cyclin B1^{HPM}-mCherry localisation in mitosis 103
Figure 5.1 | Release from G1 arrest of cells expressing Cdc13$^{WT/HPM}$-sfGFP 108
Figure 5.2 | Localisation of Cdc13^{HPM}-sfGFP when wild-type Cdc13 is not present 109
Figure 5.3 | Cdc2-GBP-mCherry colocalises with Cut12-NEGFP 113
Figure 5.4 | Strains with Cdc2 tethered at the SPB are diploids 114
Figure 5.5 | The Cdc13-Cdc2 fusion protein tethered to the SPB is not tolerated well even in the presence of inhibitor 115
Figure 5.6 | Inducing Cdc13^{HPM}-L-Cdc2(as)-GBP-mCherry can drive mitosis in the absence of GFP 117

Figure 5.7 | Induction of Cdc13^{HPM}-L-Cdc2(as)-GBP-mCherry 120
Figure 5.8 | Phenotype of cells driven by Cdc13^{HPM}-L-Cdc2 in a Cdc2-M26 background..... 122
Figure 5.9 | Phenotype of cells driven by Cdc13^{HPM}-L-Cdc2 in an *nmt41:cdc13 ΔCC* background..... 125
Figure 5.10 | Quantitation of septation events in cells driven by Cdc13^{HPM}-L-Cdc2 in an *nmt41:cdc13 ΔCC* background 126
Figure 5.11 | Phenotype of cells driven by Cdc13^{HPM}-L-Cdc2(as)^{AF}..... 127
Figure 5.12 | Experimental design for Cdc13^{HPM}-Cdc2 SPB tethering experiment 130
Figure 5.13 | G2 accumulation after release from N-arrest..... 131
Figure 5.14 | Cdc2(as)-M17-GBP-mCherry induction 133
Figure 5.15 | Restoring SPB localisation of Cdc13^{HPM}-Cdc2 promotes a wave of mitotic entry..... 135
Figure 6.1 | Phosphorylation of selected CDK substrates after release from a G2 block..... 143
Figure 6.2 | Validating antibodies against selected CDK substrates..... 146
Figure 6.3 | Cdc13-L-Cdc2$^{WT/AF}$ protein level through the time course 149
Figure 6.4 | Bqt4 phosphorylation by Cdc13-L-Cdc2$^{WT/AF}$ 152
Figure 6.5 | Spo15 phosphorylation by Cdc13-L-Cdc2$^{WT/AF}$ 153
Figure 6.6 | Immunofluorescence with Spo15 phosphospecific pS121 antibody . 156
Figure 6.7 | Immunofluorescence with the Spo15-ctrl antibody 157
Figure 6.8 | Testing what Spo15-ctrl staining is dependent on CDK activity..... 158
Figure 6.9 | Intensity measurements of Spo15-ctrl staining in Cdc2-inhibited cells 160
Figure 6.10 | Testing what Spo15-ctrl signal is specific to Spo15..... 162
Figure 8.1 | Identification of phosphosites dependent on the Cdc13 hydrophobic patch..... 188
Figure 8.2 | Cdc13^{HPM}-sfGFP SPB localisation is downstream of Plo1 SPB localisation..... 190

List of tables

Table 2.1 | *S. pombe* strains used in this study 66
Table 2.2 | Plasmids used in this study 67
Table 2.3 | Fusion protein details 69
Table 6.1 | Selected CDK substrates 142

Abbreviations

APC/C	Anaphase-promoting complex/cyclosome
AU	Arbitrary units
CAK	CDK activating kinase
CAKAK	CAK activating kinase
CDK	Cyclin-dependent kinase
CKI	CDK inhibitor
CLS	Centrosomal localisation sequence
CRS	Cytoplasmic retention sequence
eGFP	Enhanced GFP
GBP	GFP-binding protein
GFP	Green fluorescent protein
IC50	Half maximal inhibitory concentration
MEN	Mitotic exit network
mNG	mNeonGreen fluorescent protein
MPF	Maturation-promoting factor
mRFP	Red fluorescent protein
MTOC	Microtubule-organising centre
NE	Nuclear envelope
NEBD	Nuclear envelope break-down
PCM	Peri-centriolar matrix
PP1	Protein phosphatase 1
PP2A	Protein phosphatase 2A
SIN	Septation initiation network
sfGFP	Super folding-GFP
SPB	Spindle pole body
cdc	Cell division cycle mutant phenotype
$Cdc2^{AF}$	Cdc2-T14AY15F allele
Cdc2(as)	Cdc2 analogue-sensitive allele
HP	Hydrophobic patch
HPM	Hydrophobic patch mutant

U2OS	Human osteosarcoma cell line
WT	Wild-type
ΔCC	*cig1Δcig2Δ*
DAPI	4',6-diamidino-2-phenylindole
DMSO	Dimethyl sulfoxide
EMM4S	Edinburgh minimal media with adenine, leucine, uridine and histidine
YE4S	Yeast extract (media) with adenine, leucine, uridine and histidine

Chapter 1. Introduction

The cell cycle governs some of the most fundamental processes for eukaryotic cells: the duplication of the genome, and its subsequent segregation into two daughter cells. It is critical that these processes are error-free and occur in the correct order. DNA replication must occur once and only once per mitotic cell cycle, and chromosome segregation must result in an equal distribution of genetic material to each daughter cell. Over- or under-replication of the genome and chromosome mis-segregation can result in genome instability, cell death, or disease. As such, misregulation of the cell cycle is a hallmark of cancer.

Given its importance, both as a highly conserved fundamental eukaryotic process and in disease, expanding our understanding of cell cycle regulation is crucial. Extensive research in the field has identified many key players in cell cycle control, including cyclin-dependent kinases (CDKs) in complex with their partner cyclins, and their regulators. The activity of cyclin-CDK complexes drives progression through the cell cycle, and therefore understanding how cyclin-CDK activity is regulated is a major aspect of understanding cell cycle regulation.

1.1 Cyclin-CDK control of cell cycle progression

Identification of many of the key genes involved in eukaryotic cell cycle control came from studies in the budding yeast *Saccharomyces cerevisiae* and the fission yeast *Schizosaccharomyces pombe*. Genetic screens to search for mutants defective in the cell division cycle (termed *cdc* mutants) proved invaluable not only in identifying many of the proteins involved but also in providing a genetic toolkit with which to study the function of these proteins. Hundreds of temperature-sensitive *cdc* mutants were isolated in *S. cerevisiae* and *S. pombe*, in which the protein in question is functional when grown at permissive temperature, but at a restrictive temperature becomes non-functional, often through protein destabilisation and/or degradation (Hartwell et al., 1970, Hartwell et al., 1973, Nurse, 1975, Nurse et al., 1976). This approach allows for the study of essential genes which is valuable as many of the proteins important for cell cycle control are

indispensable for cell viability. These *cdc* mutants defined multiple different genes involved in the cell cycle, and understanding how the proteins produced by these genes work together to coordinate the cell cycle became a key focus of research.

One of the proteins identified to be important in cell cycle control was Cdc2 in *S. pombe*, homologous to Cdc28 in *S. cerevisiae* (Nurse et al., 1976, Hartwell et al., 1973, Nurse and Bissett, 1981). In parallel, studies in *Rana pipiens* (frog) oocytes had identified a cytoplasmic maturation-promoting factor, or MPF, which promoted entry into the first meiotic division (maturation) when injected into immature oocytes, and therefore represented a major regulator of cell cycle progression (Masui and Markert, 1971). In addition, a class of proteins was identified in sea urchin eggs that increased in protein level through the cell cycle before their destruction at cell division; the periodic nature of their synthesis and degradation resulted in the allocation of the name ‘cyclin’ to these proteins (Evans et al., 1983). The demonstration that MPF consisted of a homologue of Cdc2, in complex with a cyclin, unified these advances that had been made in different model systems (Dunphy et al., 1988, Gautier et al., 1988, Labbe et al., 1989a, Labbe et al., 1989b). *cdc2* and its homologues encode cyclin-dependent kinases (CDKs), protein kinases whose activities are dependent on binding to a partner cyclin protein. The activity of cyclin-CDK complexes is essential for cell cycle progression, and they are at the centre of the regulatory network controlling the cell cycle. Many of the other genes identified as cell cycle genes in the yeast screens regulate CDK activity. As such, the function and regulation of cyclin-CDK complexes have been, and continue to be, extensively studied.

1.1.1 CDKs control cell cycle progression

Cyclin-CDK is a major regulator of the cell cycle. Progression through the cell cycle is driven by increasing cyclin-CDK activity, until cyclin-CDK is inactivated to promote mitotic exit and a new cell cycle. Cyclin-CDK is essential for both major cell cycle events, which are DNA replication (in S phase) and mitosis (Nurse and Bissett, 1981, D'Urso et al., 1990).

CDKs are serine/threonine protein kinases, and they phosphorylate hundreds of substrates involved in the processes of the cell cycle, including substrates essential for S-phase such as Drc1 (Sld2) and Sld3, and mitosis, such as the condensin subunit Cut3 (SMC4) (Noguchi et al., 2002, Fukuura et al., 2011, Sutani et al., 1999). CDKs have a strong requirement for a proline at position +1, recognising a minimal consensus sequence of S/T-P, with an extended optimal consensus sequence of S/T-P-X-K/R (Songyang et al., 1994).

Given the importance of the faithful ordering and execution of the processes in the cell cycle, cyclin-CDK activity is tightly regulated through the cell cycle. In order to gain an understanding of how the cell cycle is controlled, it is necessary to understand how CDK drives progression through the cell cycle, how it maintains the order of the different processes it drives, and how it is regulated. Just as the fission yeast *S. pombe* provided a powerful system in the initial studies that identified key cell cycle genes, it is also an excellent system in which to study how cyclin-CDK regulates cell cycle progression.

1.1.2 *S. pombe* as a model to study CDK control of the cell cycle

Studies in the fission yeast *S. pombe* have contributed a lot to our understanding of eukaryotic cell cycle control. *S. pombe* cells grow by tip extension throughout G2, with cell length increasing whilst cell width is maintained, until cells reach mitosis when they cease growing, at around 14 μm in length in wild-type cells (Mitchison, 1970) (Figure 1.1). Mitotic cells then undergo nuclear division, resulting in a binucleate cell that is in G1. G1 phase is short in wild-type *S. pombe* cells in the growth media used in this thesis. In wild-type cells in these media, a septum forms in the centre of the binucleate cell at approximately the time that S-phase finishes, and the cell divides at the septum to form two daughter cells that are in early G2. This means that progression through the cell cycle can be monitored by cell length in *S. pombe*. Spindle pole body (SPB, the yeast centrosome equivalent) separation at early mitosis, binucleation and septation are also useful markers of cell cycle stage. It also means that gene products that influence the rate of cell cycle entry can be identified due to a difference in cell length at septation in a strain deleted for

or with altered expression of the gene in question. Cells that enter mitosis more quickly septate at shorter lengths, and cells that are delayed in mitotic entry septate at longer lengths. This technique has been valuable in identifying the key players in the cell cycle regulatory network (Nurse, 1975, Navarro and Nurse, 2012, Hayles et al., 2013, Moris et al., 2016).

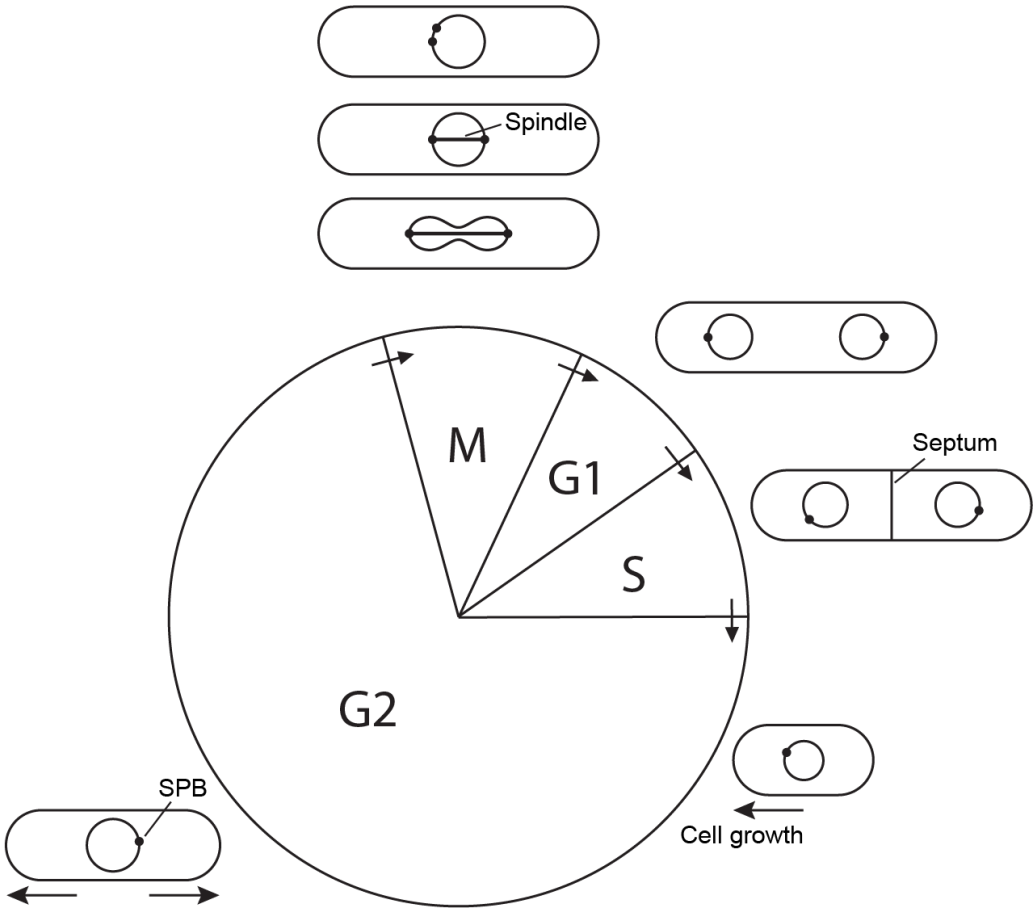


Figure 1.1 | Cell cycle of *S. pombe*

A schematic showing the cell cycle of *S. pombe*. A newly born cell grows by tip extension through G2 phase, until it reaches mitosis. SPB separation, spindle formation and nuclear division occur and the cell becomes a binucleate. A septum is formed in the centre of the cell in G1/S phase, where cytokinesis will occur coincidentally with the end of S-phase to form two daughter cells that are in G2 phase.

The ease of genetic manipulation in *S. pombe* has made it a very powerful system with which to dissect the genetic control of the cell cycle. Moreover, whilst human cells contain multiple CDKs that drive progression through the cell cycle, *S. pombe* only has one cell cycle CDK, Cdc2. This simplicity makes *S. pombe* an ideal system in which to study CDK control of the cell cycle. The cell cycle network can be simplified even further; although *S. pombe* has four cyclins that bind Cdc2 in the mitotic cell cycle (the mitotic cyclin *cdc13,* the G1/S cyclins *cig1* and *cig2,* and the G1 cyclin *puc1*), only *cdc13* is essential, and it can drive the whole mitotic cell cycle (Booher and Beach, 1988, Fisher and Nurse, 1996).

Despite its relative simplicity, what is learned in *S. pombe* is often relevant to more complex eukaryotes such as humans. The importance of the cell cycle means that many of the core principles underlying its control, as well as many of the proteins involved, are highly conserved throughout eukaryotes. This is highlighted by the striking observation that the human Cdk1 protein can function in place of its homologue Cdc2 in *S. pombe* cells, demonstrating remarkable conservation (Lee and Nurse, 1987). Thus, studies of CDK regulation of the cell cycle in *S. pombe* can be informative of wider eukaryotic cell cycle control.

Given the key importance of CDKs, their activity is tightly regulated, and extensive work on this in *S. pombe* and other systems has identified several mechanisms that regulate CDK activity. The aim of the work in this thesis is to further our understanding of cyclin-CDK regulation, particularly at mitotic entry, specifically focussing on cyclin-CDK spatial regulation and how it affects cell cycle progression and substrate phosphorylation. In this Introduction, I will discuss the multiple ways in which cyclin-CDK activity is regulated, and the importance of considering both the temporal and spatial dynamics of CDK activity, before outlining the open questions driving this work.

1.2 Molecular regulation of CDK activity

CDK activity is regulated by multiple factors, including cyclin binding, phosphorylation of CDK itself, the binding of accessory factors or inhibitors to CDK, and phosphatases that counteract CDK substrate phosphorylation. In this section I will cover these major mechanisms of CDK activity regulation.

1.2.1 Cyclin binding is necessary for CDK activity

Cyclin binding is necessary for CDK activity, so cyclins provide a major point of regulation for CDK. Cyclin binding alters the tertiary structure of CDK, making the substrate binding cleft more accessible. In *S. pombe* there are four cyclins (Puc1, Cig1, Cig2 and Cdc13) and one CDK (Cdc2) that act in the mitotic cell cycle (summarised in Figure 1.2). Puc1-Cdc2 acts in G1, while Cig1-Cdc2 and predominantly Cig2-Cdc2 drive the G1/S transition and S-phase (Martin-Castellanos et al., 2000, Fisher and Nurse, 1996). Cdc13-Cdc2 is the only complex that can drive mitosis in an unperturbed cell cycle, and it can also drive the entire cell cycle in the absence of the other cyclins (Fisher and Nurse, 1996). Like *S. pombe*, *S. cerevisiae* has just one cell cycle CDK (Cdc28), but it has multiple cyclins that act in the mitotic cell cycle. The Cln-type cyclins Cln1-3 act in G1, driving progression through Start, which is the point at which cells are committed to the mitotic cell cycle (Richardson et al., 1989, Enserink and Kolodner, 2010). The B-type Clb cyclins function in the other major events of the cell cycle. Clb5 and Clb6 drive S-phase, Clb3 and Clb4 act in G2, and Clb1 and Clb2 drive progression through mitosis (Enserink and Kolodner, 2010). In vertebrates, cell cycle control is more complex, with multiple CDKs as well as multiple cyclins (Satyanarayana and Kaldis, 2009). Cdk4 and Cdk6 in partnership with D-type cyclins drive G1, and E-type and A-type cyclins in complex with Cdk2 drive S-phase. A-type and B-type cyclins in complex with Cdk1 initiate and drive progression through mitosis, with Cyclin A-Cdk1 important to initiate mitosis and activate Cyclin B-Cdk1, and Cyclin B-Cdk1 important for progression through mitosis (Hegarat et al., 2020). There are multiple cyclins within each cyclin class, with some cyclin isoforms being primarily

expressed in specific cell types. The major mitotic cyclin isoforms are Cyclin A2, and Cyclin B1 (Satyanarayana and Kaldis, 2009).

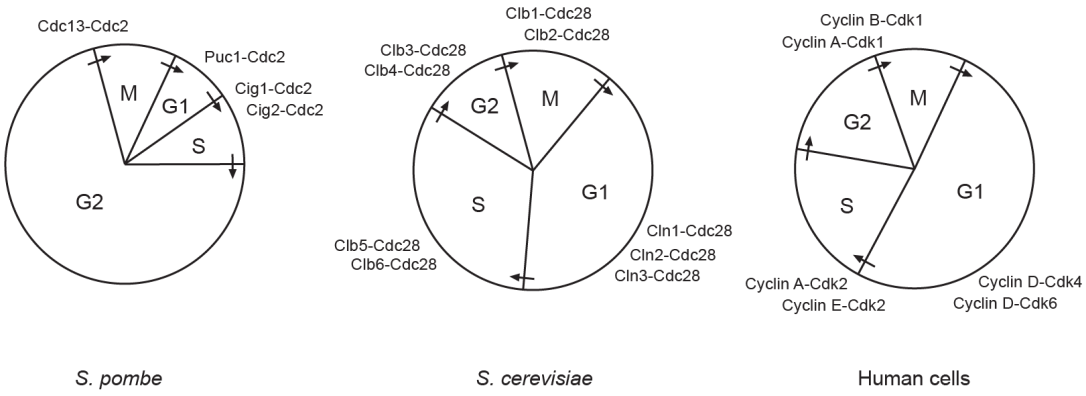


Figure 1.2 | Cyclin-CDK regulation of the cell cycle

Schematics to show when different cyclin-CDK complexes act in the cell cycle in different eukaryotes.

The mechanism by which cyclin binding activates CDK was demonstrated by comparing the structure of Cyclin A-bound Cdk2 with free monomeric Cdk2 (complex shown in Figure 1.3) (Jeffrey et al., 1995). When Cyclin A binds Cdk2, there are a number of conformational changes. As well as forming interactions with the N-terminal sheet and C-terminal lobe of Cdk2, Cyclin A interacts with two key regions of Cdk2: the T-loop; and the PSTAIRE helix. In free Cdk2, the T-loop blocks the entrance to the catalytic cleft, and the orientation of the PSTAIRE region results in key residues of the active site that are involved in ATP phosphate orientation being misaligned. Upon cyclin binding, the T-loop significantly changes conformation and position, resulting in its orientation away from blocking the catalytic cleft. This also exposes the conserved threonine 160 residue to phosphorylation (discussed in the next section). Furthermore, cyclin binding induces conformational changes in the PSTAIRE region, resulting in its movement and rotation towards the catalytic cleft and the alignment in the active site of the residues important for ATP phosphate orientation.

Thus the kinase activity of CDK is dependent on association with cyclin, and the availability of cyclins can be a limiting factor affecting CDK activity. Although the

protein level of Cdc2 is constant throughout the cell cycle in a synchronised population in *S. pombe* (Simanis and Nurse, 1986) the periodic synthesis and degradation of cyclins acts as a mechanism which broadly regulates CDK activity throughout the cycle. In general, mitotic cyclin synthesis as the cell cycle progresses drives an increase in CDK activity, and cyclin degradation mediated by the anaphase-promoting complex/cyclosome (APC/C) at mitotic exit leads to CDK deactivation, in effect 'resetting' the cell cycle (Sudakin et al., 1995, King et al., 1995, Moreno et al., 1989). In *S. pombe, S. cerevisiae*, and more complex eukaryotes, there are multiple cyclins, which have different patterns of synthesis and degradation, and therefore different cyclins are expressed at different times.

Cyclin binding can activate CDK to a basal level, but subsequent direct phosphorylation of CDK on several conserved residues can also influence CDK activity.

1.2.2 T-loop phosphorylation

Upon cyclin binding to CDK, the conformational changes in CDK expose a conserved threonine residue in the T-loop that was previously inaccessible (Thr160 in human Cdk2, or Thr167 in *S. pombe* Cdc2) (shown in Figure 1.3) (Jeffrey et al., 1995). This threonine is phosphorylated by the CDK-activating kinase complex (CAK), and is necessary (though not sufficient) for full CDK activity (Gould et al., 1991, Kaldis, 1999).

In metazoans CAK is a cyclin-CDK complex, composed of Cyclin H and Cdk7 in complex with an assembly factor, Mat1 (Poon et al., 1993, Tassan et al., 1994, Fisher and Morgan, 1994, Kaldis, 1999, Devault et al., 1995, Tassan et al., 1995, Fisher et al., 1995). In synchronised populations of HeLa cells neither CAK activity nor complex formation are cell cycle regulated, with both remaining constant through the cell cycle (Tassan et al., 1994). Metazoan CAK is also part of the TFIIH complex involved in transcriptional regulation. In *S. cerevisiae*, the Cdk7 homologue (encoded by *KIN28*) does not have CAK activity but is involved in transcriptional regulation via TFIIH (Cismowski et al., 1995). Instead, CAK activity

is provided by Cak1p, which is a monomeric kinase that is relatively divergent from cyclin-dependent kinases (Kaldis et al., 1996). In *S. pombe* there are two CAKs, one which is homologous to the Cyclin H-Cdk7 complex (Mcs2-Mcs6), and one that is related to the *S. cerevisiae* Cak1p (Csk1) (Buck et al., 1995, Hermand et al., 1998). Csk1 acts upstream of Mcs6, as a CAK activating kinase (CAKAK) (Hermand et al., 1998), and does not phosphorylate Cdc2 *in vivo* (Hermand et al., 2001).

Although cyclin binding can activate CDK to a basal level *in vitro*, subsequent phosphorylation on the T-loop further increases CDK activity (Poon et al., 1993). T-loop phosphorylation causes a further shift in the position of the T-loop away from the catalytic cleft, which increases access to the substrate binding site (Russo et al., 1996b). It also promotes more contacts between Cyclin A and Cdk2 to stabilise the structure.

T-loop phosphorylation is critical to regulating CDK activity, but in HeLa cells CAK activity is constant throughout the cell cycle (Tassan et al., 1994). However, some CDK inhibitors (discussed later in section 1.2.4) prevent CAK phosphorylation of CDK, possibly by making CDK inaccessible to CAK, providing one mechanism by which CDK T-loop phosphorylation may be regulated (Aprelikova et al., 1995). Furthermore, it has been shown that the T-loop of CDK is dephosphorylated at anaphase after cyclin degradation in *Xenopus* extracts, and this is thought to be important for CDK inactivation (Lorca et al., 1992). T-loop dephosphorylation is also important for mitotic exit in *S. pombe*, as a Cdc2 T167E mutant is delayed in progression through mitosis and has defects in cell division, resulting in polyploid cells (Gould et al., 1991).

Whilst cyclin binding and then T-loop phosphorylation are both necessary for full CDK activation, they are not the only ways in which CDK activity is regulated. Throughout interphase, CDK is phosphorylated on a highly conserved tyrosine residue, which has an inhibitory effect on CDK. The removal of this inhibitory phosphorylation is needed for the full activation of CDK that drives the cell from G2 into mitosis.

1.2.3 T14 and Y15 phosphorylation inhibit CDK activity

Inhibitory phosphorylation on conserved threonine and tyrosine residues on CDK (threonine 14 and tyrosine 15 in *S. pombe* Cdc2) provide a critical mechanism of regulation of CDK activity, with tyrosine phosphorylation being particularly important (residue shown in Figure 1.3). Cdc2 Y15 phosphorylation is thought to inhibit CDK activity primarily through blocking substrate binding (Welburn et al., 2007). Additionally, whilst Y15-phosphorylated Cdc2 can bind ATP, the phosphorylated Y15 residue promotes the stabilisation of a conformation of the terminal group of ATP that does not support phosphotransfer.

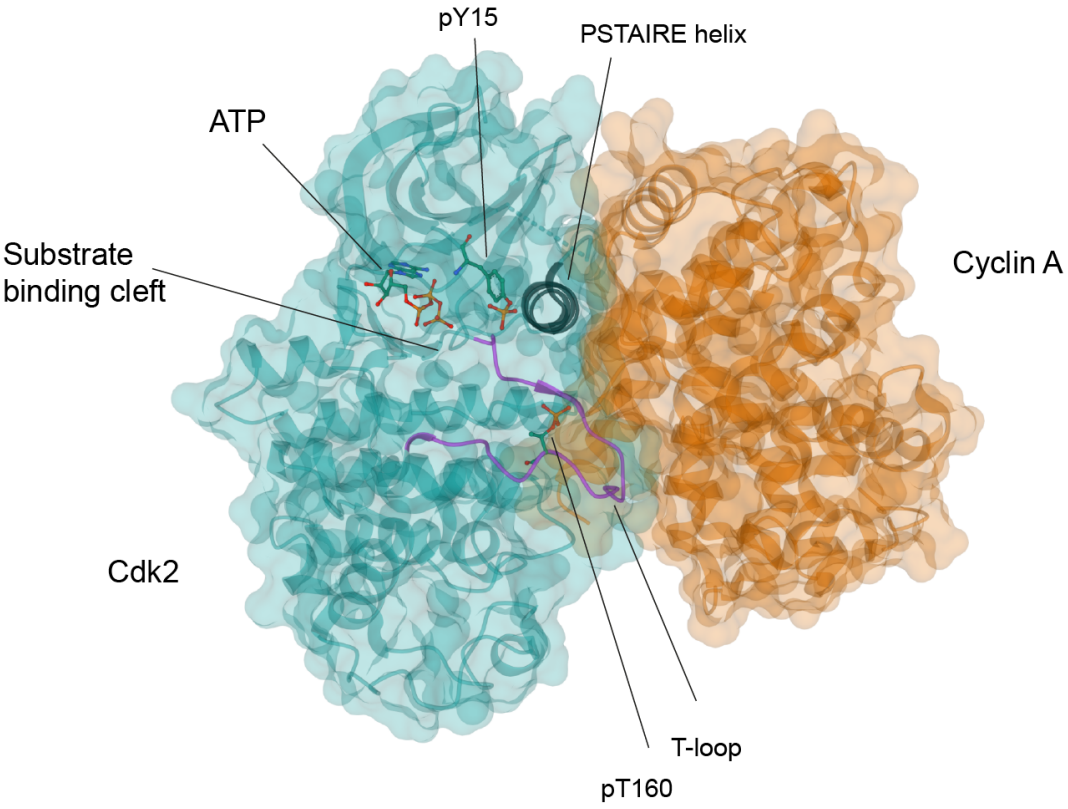


Figure 1.3 | Structure of Cyclin A-Cdk2 bound to ATP

Structure of Cyclin A (orange) bound to Cdk2 (green). ATP is shown in ball-and-stick format, as are the phosphorylated Y15 and phosphorylated T160 residues on Cdk2. The T-loop of Cdk2 is in magenta, and the PSTAIRE helix is shown in dark grey. Structure from (Welburn et al., 2007), PDB ID 2CJM, and created using Mol* (Sehnal et al., 2021) and RSCB PDB.

Y15 phosphorylation is carried out by the kinase Wee1, and to a lesser extent the kinase Mik1 (Myt1 in human cells) (Lundgren et al., 1991, Featherstone and Russell, 1991, McGowan and Russell, 1993, Mueller et al., 1995b). Dephosphorylation, resulting in CDK activation, is carried out predominantly by the phosphatase Cdc25 (Cdc25A-C in human cells), as well as the phosphatase Pyp3 in fission yeast (Russell and Nurse, 1986, Gautier et al., 1991, Millar et al., 1992, Millar et al., 1991). T14 is also phosphorylated by Wee1 in *S. pombe* and Myt1 in more complex eukaryotes (Den Haese et al., 1995, Mueller et al., 1995b), and dephosphorylated by Cdc25 (Gautier et al., 1991).

Y15 remains phosphorylated throughout G1, S and G2, and its dephosphorylation results in a substantial increase in CDK activity that pushes the cell from G2 into mitosis (Gould and Nurse, 1989, Krek and Nigg, 1991b, Krek and Nigg, 1991a). Thus, Cdc2 Y15 phosphorylation is the major point of mitotic entry regulation, and therefore the balance of Wee1 and Cdc25 signalling determines the timing of mitotic commitment. Whilst phosphorylation on T14 and Y15 both inhibit CDK activity, Y15 phosphorylation is a particularly important point of regulation and a stronger effect on the timing of mitotic entry is seen when mutating Y15 alone than T14 alone (Gould and Nurse, 1989, Den Haese et al., 1995, Krek and Nigg, 1991b). In *S. pombe*, Cdc2 T14 phosphorylation can be detected in an S-phase arrest, but is not detected in a G2 arrest, supporting the finding that Y15 dephosphorylation is the major point of regulation for mitotic entry with regulation of T14 phosphorylation having a more minor effect (Den Haese et al., 1995).

A double negative feedback loop exists between CDK and Wee1, as CDK inhibits Wee1, while Wee1 inhibits CDK (Figure 1.4) (Tang et al., 1993, Mueller et al., 1995a, McGowan and Russell, 1995). There is also a positive feedback loop between CDK and Cdc25, with CDK activating Cdc25, as well as Cdc25 activating CDK (Hoffmann et al., 1993, Lu et al., 2012).

Polo kinase (known as Plo1, Cdc5, Plx1 and Plk1 in *S. pombe*, *S. cerevisiae, Xenopus* and human cells respectively) is a serine/threonine kinase that has also been implicated in the feedback loops that act on CDK tyrosine phosphorylation. Plo1 activity measured *in vitro* peaks in mitosis in *S. pombe*, and this mitotic

activation requires Cdc2 activation, suggesting that Plo1 is involved in amplifying CDK activation rather than initiating it (Tanaka et al., 2001). Plk1 activation in human cells also involves CDK activity. Cyclin B1-Cdk1 phosphorylates Bora, a protein essential for efficient activation of Plk1 by the kinase Aurora A, and this phosphorylation of Bora by Cdk1 is required for Plk1 activation *in vitro* and *in vivo* (Thomas et al., 2016). Active Polo kinase can then promote CDK activation. In *Xenopus* extracts*,* Plx1 phosphorylates Cdc25 to promote Cdc25 activation of Cdc2, and immunodepletion of Plx1 prevents the abrupt activation of Cdc2 that results from the amplification of the positive feedback loop between Cdc2 and Cdc25 (Kumagai and Dunphy, 1996, Abrieu et al., 1998, Karaiskou et al., 1999). In budding yeast, Cdc5 interacts with and phosphorylates Swe1 (the Wee1 homologue), and in human cells Plk1 phosphorylates Wee1 to target it for degradation (Bartholomew et al., 2001, Watanabe et al., 2004). In *S. pombe*, early recruitment and activation of Plo1 at the SPB is able to suppress a temperature sensitive mutant of *cdc25* at otherwise lethal temperatures, thought to be via inhibition of Wee1 (Hudson et al., 1990, Mulvihill et al., 1999, MacIver et al., 2003, Hagan and Grallert, 2013).

Wee1 and Cdc25 phosphorylation by CDK exhibit ultrasensitivity, in which low levels of CDK activity do not result in full phosphorylation of Wee1 and Cdc25, but high levels of CDK activity are required for the full phosphorylation and therefore inhibition/activation of Wee1 and Cdc25 respectively, and this transition happens over a small change in CDK activity (Kim and Ferrell, 2007, Trunnell et al., 2011). The feedback loops and ultrasensitivity result in a bistable system, in which global CDK is either stably in the ‘low activity’ state (Y15 phosphorylated) that cannot drive mitosis, or in the ‘high activity’ state with Y15 dephosphorylated that is competent to promote mitosis (Pomerening et al., 2003). CDK activation also exhibits hysteresis, a property of bistable systems, which results in the interphase to mitosis transition occurring at a higher CDK activity threshold than the mitosis to interphase transition. This bistability ensures that the G2/M transition is a robust, switch-like, all-or-nothing transition (Pomerening et al., 2003). Accordingly, interfering with these feedback mechanisms reduces the bistability of the system. Mutating Y15 and T14 on Cdc2/Cdk1 to non-phosphorylatable residues (T14AY15F mutant, here referred to as $Cdc2^{AF}$ or $Cdk1^{AF}$), not only accelerates entry into

mitosis due to the lack of inhibition by Wee1, but also results in CDK activation as measured by a mitotic CDK activity sensor being less switch-like (Gould and Nurse, 1989, Krek and Nigg, 1991b, Coudreuse and Nurse, 2010, Patterson et al., 2021).

There is also evidence for CDK regulation of Myt1 activity in *Xenopus* and human cells. *Xenopus* and human Myt1 both become hyperphosphorylated in a mitotic arrest, and Myt1 kinase activity is also severely reduced in this arrest (Mueller et al., 1995b, Booher et al., 1997). Human Cyclin B1-Cdk1 can phosphorylate Myt1 *in vitro*, and although Cdk1 phosphorylation of Myt1 does not appear to directly affect Myt1 activity *in vitro*, it has been shown in *Xenopus* that Cdc2 phosphorylation of Myt1 creates a docking site for Plx1, and this binding of Plx1 inhibits Myt1 (Booher et al., 1997, Inoue and Sagata, 2005). It is not clear whether this regulation by Cdc2 applies to Mik1 in *S. pombe*.

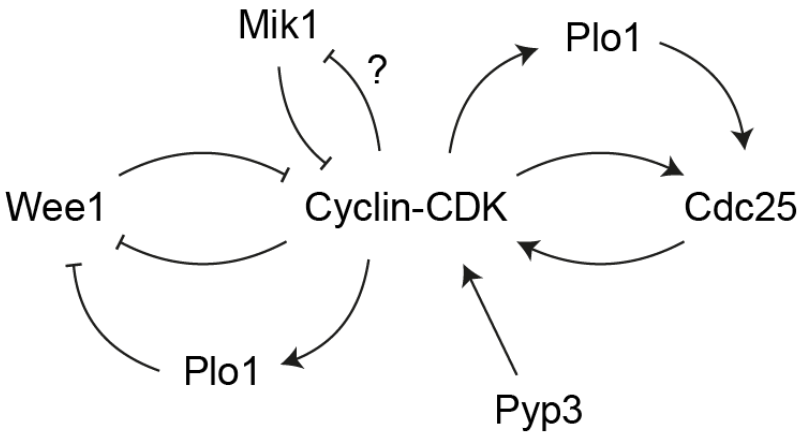


Figure 1.4 | Core network regulating CDK Y15 dephosphorylation

The core regulators of Y15 dephosphorylation, and therefore activation, of Cdc2 in *S. pombe*. There is evidence for CDK regulation of Myt1 (Mik1) in human cells and *Xenopus*, but it is not clear if Mik1 is similarly regulated in *S. pombe*.

While increased cyclin expression and cyclin binding result in a gradual increase of CDK activity from G1 through to G2, Cdc2 Y15 dephosphorylation results in a large jump in CDK activity at the G2/M transition. Several signalling pathways act on Y15 phosphorylation in order to affect cell cycle progression. These include the cell geometry network, in which Wee1 is increasingly inhibited at increasing cell size,

providing one mechanism by which cell size information is coupled to mitotic entry in *S. pombe* (Moseley et al., 2009). In addition, the DNA damage sensing pathway inhibits Cdc25 to prevent premature entry into mitosis (discussed further in Section 1.5.1) (Takizawa and Morgan, 2000), as well as activating Wee1 (O'Connell et al., 1997). Nutrient availability and the stress response pathway are also coupled to mitotic entry through Plo1, which is part of the feedback loops acting on Y15 dephosphorylation (Petersen and Hagan, 2005, Petersen and Nurse, 2007, MacIver et al., 2003).

1.2.4 CDK activity is regulated by Suc1/Cks1 and CDK inhibitors

Cyclin-CDK can form a complex with a highly conserved protein known as Suc1 in *S. pombe*, and Cks1/Cks2 in many other organisms including humans. Suc1 was initially identified in *S. pombe* as a high copy suppressor of certain *cdc2* mutations (Hayles et al., 1986b). It is an essential gene whose product physically interacts with Cdc2 (Hayles et al., 1986a, Brizuela et al., 1987). Whilst Suc1 clearly plays an important role in cell cycle control (Hayles et al., 1986a), elucidating its function *in vivo* has proved difficult. A diploid yeast strain haploinsufficient for *suc1*, which only has one copy of *suc1*, divides at a shorter length than wild-type indicating an acceleration of entry into mitosis (Moris et al., 2016). This is consistent with the finding that overproducing Suc1 results in a mitotic delay (Hayles et al., 1986a), and indicates that Suc1 acts as an inhibitor of mitotic entry.

Suc1/Cks1 has also been shown to contain a phospho-binding pocket, and can direct multisite phosphorylation of CDK substrates by binding specific phosphosites (Arvai et al., 1995, McGrath et al., 2013, Koivomagi et al., 2013). Solving the structure of human Cks1 bound to Cdk2 demonstrated that the Cks1 binding site is on the C-terminal lobe of Cdk2, relatively far away from the cyclin binding site and regulatory phosphorylation sites on Cdk2 (Bourne et al., 1996). Cks1 in *S. cerevisiae* has also been implicated in binding to Swe1 (the Wee1 homologue), providing a possible mechanism by which it may aid CDK inhibition (McGrath et al., 2013). Whilst it is not yet known if these mechanisms of Suc1/Cks1 activity explain

the *in vivo* phenotypes seen upon *suc1* deletion or overproduction, it is clear that Suc1/Cks1 plays an important role in regulating CDK activity.

CDK activity is also regulated by CDK inhibitors (CKIs). In mammalian cells, there are two broad families of CKIs. Inhibitors belonging to the INK4 family (p16, p15, p18 and p19) associate with CDK4/6 and prevent them from binding with Cyclin D, and therefore influence the early events in the cell cycle. Proteins belonging to the CIP/KIP family (p21, p27 and p57) affect the activity of cyclin-CDK complexes including D, E, A or B-type cyclins (Besson et al., 2008). The structure of Cdk2-Cyclin A bound to p27 demonstrates that it interacts with Cyclin A through the cyclin hydrophobic patch substrate docking region (discussed in section 1.2.6) and inserts into the catalytic site of Cdk2, preventing ATP binding to inhibit CDK activity (Russo et al., 1996a). In addition to their well-established inhibitory role, CIP/KIP family proteins have also been suggested to have a role in promoting the association and therefore activity of Cyclin D-Cdk4 complexes (LaBaer et al., 1997). The role of CDK inhibitors in regulating the G1/S transition is well described, with CIP/KIP protein sequestration into Cyclin D-CDK4 complexes both activating Cyclin D-Cdk4 and relieving inhibition on Cyclin E-Cdk2 complexes, and active Cyclin E-Cdk2 promoting p27 proteolysis (Sherr and Roberts, 1999). The double-negative feedback loop between Cyclin E-Cdk2 and p27 contributes to abrupt Cdk2 activation and the G1/S transition being switch-like (Barr et al., 2016). CIP/KIP family protein inhibition of cyclin-CDK can itself be regulated, for example by interactions with other proteins and phosphorylation (Besson et al., 2008).

In budding yeast, the p27 homologue Sic1 has been well-studied (Barberis et al., 2005). Sic1 is important both in negatively regulating the G1/S transition (Mendenhall, 1993) and promoting mitotic exit (Visintin et al., 1998). Sic1 degradation (mediated by phosphorylation of Sic1 by CDK) at the G1/S transition is necessary for S phase entry, with mutants of Sic1 that cannot be phosphorylated on sites critical for its degradation inhibiting DNA replication (Verma et al., 1997). Another CDK inhibitor, Far1, also acts early in the cell cycle, and is necessary for the cell cycle arrest induced in response to mating pheromone (Chang and Herskowitz, 1990). An analogue of p21 has also been identified in *S. cerevisiae*,

known as Cip1, which inhibits CDK in complex with G1 cyclins and results in a G1 arrest upon overexpression (Chang et al., 2017).

In *S. pombe*, the only CDK inhibitor (other than Suc1, Wee1 and Mik1) identified to date is encoded by the *rum1* gene. Rum1 was first identified as a regulator of G1, with overexpression resulting in repeated rounds of S phase with no intervening mitosis, and deletion resulting in a failure of cells to arrest in G1 upon nitrogen starvation (Moreno and Nurse, 1994). Rum1 is expressed in G1, and acts as a specific inhibitor of Cdc13-Cdc2 by targeting Cdc13 for degradation (Correa-Bordes and Nurse, 1995, Correa-Bordes et al., 1997). This inhibits the mitotic kinase activity of Cdc13-Cdc2 in G1, explaining the repeated rounds of S-phase without mitosis occurring when Rum1 is overexpressed in G2 (Correa-Bordes and Nurse, 1995). Cig1-Cdc2 is insensitive to Rum1 inhibition, with Cig2-Cdc2 displaying an intermediate effect, being inhibited by Rum1, but to a lesser extent than Cdc13-Cdc2 (Correa-Bordes and Nurse, 1995). Transient inhibition of Cig2-Cdc2 is thought to prevent S-phase entry occurring prematurely in G1, until Cig2 levels are high enough to overcome inhibition (Martin-Castellanos et al., 1996). Cig1-Cdc2 can phosphorylate Rum1, and deletion of *cig1* results in delayed Rum1 degradation upon release from a G1 arrest, suggesting that Cig1-Cdc2 contributes to Rum1 degradation at the G1/S transition which in turn allows for the accumulation of Cdc13 (Correa-Bordes et al., 1997). The G1/S cyclins are not essential for Rum1 degradation, as a *cig1Δ cig2Δ puc1Δ* strain can still degrade Rum1, however Rum1 degradation is delayed in this mutant, as is the G1/S transition (Martin-Castellanos et al., 2000). Deletion of *rum1* abolishes the increased G1 population of a *cig1Δ cig2Δ puc1Δ* strain, indicating that it is Rum1 activity that opposes Cdc13-Cdc2 activity to delay S-phase in the absence of the G1/S cyclins (Martin-Castellanos et al., 2000). Whilst Rum1 regulation is important in G1, it does not play a role in mitotic exit in *S. pombe*.

1.2.5 Phosphatases oppose CDK substrate phosphorylation

Substrate phosphorylation, the functional output of CDK activity, is always an interplay of the activities of CDK and antagonising phosphatases *in vivo*. In

S. pombe, CDK substrates have a fast turnover time, with a half-life of roughly 2 minutes at 25 °C, highlighting the constant action of CDK-antagonising phosphatases (Swaffer et al., 2016). Phosphatases play a critical role in 'resetting' the cell cycle back to G1 at mitotic exit, by reversing the phosphorylation events catalysed by CDK and other mitotic kinases. However, the role of phosphatases is not restricted to mitotic exit; a number of phosphatases have been implicated in earlier stages of cell cycle control including the G2/M transition. As well as antagonising CDK substrate phosphorylation, phosphatases can directly affect CDK activity via the feedback loops that act on CDK Y15 dephosphorylation. The main phosphatases known to oppose CDK substrate phosphorylation and affect CDK activity are the PP2A (protein phosphatase 2A) and PP1 (protein phosphatase 1) holoenzymes and the Cdc14-like phosphatases (Mochida and Hunt, 2012).

The PP2A holoenzyme consists of a catalytic subunit, a scaffold subunit, and a regulatory subunit; the different regulatory subunits (referred to as B subunits) confer different substrate specificity to the holoenzyme. PP2A-B55δ plays a particularly important role in cell cycle progression. The activity of PP2A-B55δ displays the reverse pattern of Cdc2/Cdk1 activity, with PP2A-B55δ being inhibited at mitosis and active in interphase. Mitotic inhibition of PP2A-B55δ is achieved by CDK activation of the Greatwall kinase, which then phosphorylates its substrates ENSA and ARPP-19, which specifically inhibit PP2A-B55δ by outcompeting other substrates (Castilho et al., 2009, Gharbi-Ayachi et al., 2010, Mochida et al., 2010). Without inhibition of PP2A-B55δ, CDK substrates in *Xenopus* extracts do not become fully phosphorylated, even if CDK is fully activated, and the extracts do not enter M phase (Mochida et al., 2010). PP2A has also been implicated in opposing the hyperphosphorylation of Cdc25 that results in its activation (Karaiskou et al., 1999). Genetic deletion *ppa2* (one of the catalytic subunits of PP2A) in fission yeast results in accelerated entry into mitosis, highlighting the role of PP2A in counteracting CDK activity at mitotic entry in yeast (Kinoshita et al., 1993).

PP1 also antagonises CDK activity, playing an important role in mitotic exit (Wu et al., 2009). In fission yeast, PP1 is also involved in counteracting the Plo1/Cdc25/Cdc2 feedback loops that result in tyrosine dephosphorylation, thus

regulating mitotic entry (discussed further in section 1.6.2) (Grallert et al., 2013a). PP1 phosphorylation by CDK both acts as a mild phosphodegron and inhibits PP1 activity, keeping PP1 activity relatively low while CDK activity is high (Grallert et al., 2015, Dohadwala et al., 1994). CDK inactivation in anaphase then allows PP1 to autoreactivate, and subsequently reactivate PP2A-B55 and PP2A-B56, to coordinate mitotic exit (Grallert et al., 2015)

The phosphatase Cdc14 (Clp1/Flp1 in *S. pombe*) is essential in budding yeast for mitotic exit, dephosphorylating CDK substrates (Visintin et al., 1998, Mocciaro and Schiebel, 2010). Cdc14 dephosphorylation of Sic1 functions to stabilise Sic1, dephosphorylation of the transcription factor Swi5 results in increased Sic1 expression, and dephosphorylation of the APC/C subunit Cdh1 activates the APC/C, all leading to CDK inactivation mediated by Sic1 binding and cyclin degradation (Visintin et al., 1998, Bardin and Amon, 2001). Cdc14 homologues are found in more complex eukaryotes, but the specific functions of Cdc14 in these organisms are not clear (Mocciaro and Schiebel, 2010). In fission yeast Clp1 is not required for mitotic exit but plays an important role in the septation initiation network, coupling cytokinesis to nuclear division (Trautmann et al., 2001). Clp1 also plays a role in regulating the G2/M transition, as highlighted by the accelerated entry into mitosis in a *clp1Δ* strain (Trautmann et al., 2001). A possible mechanism for the negative effect of Clp1 on mitotic entry is by negative regulation of Cdc2 activation (Trautmann et al., 2001).

Therefore the phosphatases that counteract and regulate CDK influence cell cycle control. These phosphatases can themselves be regulated by phosphorylation, localisation, inhibition, and regulatory subunit binding. It is also worth noting that where substrate phosphorylation is discussed or used to reflect CDK activity, it more specifically reflects the balance of CDK and phosphatase activities, or the net CDK activity.

1.2.6 Cyclin docking sites

As well as influencing the catalytic activity of CDK, cyclins contain docking sites that can directly interact with other proteins or CDK substrates. The most well-characterised cyclin docking site is the hydrophobic patch binding groove, which is found in A, E, and B-type cyclins in yeasts and more complex eukaryotes, and generally has a high level of sequence conservation among these eukaryotes.

The hydrophobic patch was identified as a substrate binding site on human Cyclin A, when the structure of Cyclin A-Cdk2 in complex with the inhibitory N-terminus of the CKI p27 was solved, with the hydrophobic patch acting as a docking site for p27 at the conserved RXLFG region on p27 (Figure 1.5) (Russo et al., 1996a). The α1, α3 and α4 helices of the cyclin box region form the binding groove, with highly conserved residues from the α1 helix (in the region comprised of MRAILVDW) suggested to be particularly important for peptide interaction (Russo et al., 1996a). Mutation of three of these key residues in human Cyclin A (M210A, L214A, W217A) generated a hydrophobic patch mutant (HPM) of Cyclin A that does not affect its affinity for Cdk2 or its histone H1 kinase activity, but severely reduces its affinity for substrates with RXL motifs, also known as Cy motifs, resulting in reduced phosphorylation of these substrates by Cdk2 (Schulman et al., 1998). The authors also found that, unlike Cyclin A^{WT}, an overexpression of Cyclin A^{HPM} did not result in a reduction of G1 cells in a population indicating that the hydrophobic patch plays an important role in cyclin function *in vivo* (Schulman et al., 1998). The role of the hydrophobic patch as a substrate docking site is conserved in the Clb5 cyclin in *S. cerevisiae* (Cross and Jacobson, 2000), and it is responsible for Clb5 specificity towards S-phase CDK substrates, allowing CDK activity to be targeted to substrates that need to be phosphorylated early in the cell cycle via interaction with R/KXL motifs (Loog and Morgan, 2005). Thus the role and importance of the hydrophobic patch as a substrate docking site in G1/S cyclins has been extensively demonstrated.

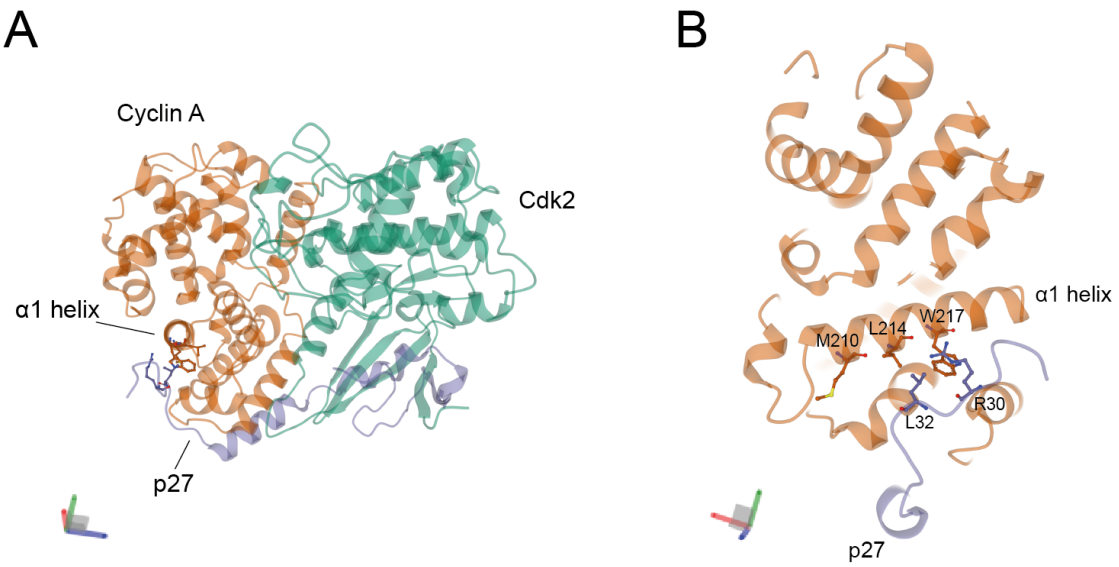


Figure 1.5 | Structure of Cyclin A-Cdk2 bound to p27

A: Structure of Cyclin A (orange) bound to Cdk2 (green) and p27 (purple). p27 interacts with the hydrophobic patch binding groove on Cyclin A and the substrate binding site of Cdk2. The α1 helix of Cyclin A (labelled) contributes to the hydrophobic patch binding groove. Three of the key resides contributing to the hydrophobic patch binding groove of Cyclin A (M210, L215, W217) and the key residues in the RXL motif of p27 (R30 and L32) are shown in ball-and-stick form (see B for a more detailed view). Structure from (Russo et al., 1996a), PDB ID 1JSU, and created using Mol* (Sehnal et al., 2021) and RSCB PDB.
B: Closer, lengthways view of the hydrophobic patch binding groove interacting with p27. Labels and colour scheme as in (A).

In contrast, mutating the hydrophobic patch of the mitotic *S. cerevisiae* cyclin Clb2 did not have a large effect on substrate phosphorylation via RXL motifs *in vitro* (Loog and Morgan, 2005). However, it does affect Clb2 activity *in vivo* as Clb2^{HPM} is unable to rescue a *clb2* temperature-sensitive mutant in the absence of *clb1, clb3* and *clb4* (Cross and Jacobson, 2000). Later studies demonstrated that the Clb2 hydrophobic patch does in fact mediate specificity for some substrates *in vitro* and *in vivo*, but via an LXF motif on substrates, that does not affect Clb5-Cdc28 phosphorylation of these substrates (Ord et al., 2019). It was also found that the 'HPM' mutations affected the localisation of Clb2, resulting in a strong nuclear accumulation, and a failure to localise to the mother bud neck even when cytoplasmic localisation is restored (Bailly et al., 2003). Consistent with a role for the hydrophobic patch in cyclin localisation, experiments in BS-C-1 monkey kidney cells using truncations of human Cyclin B1 fused to eGFP demonstrated that the C

terminus of Cyclin B1 is needed for localization to centrosomes, leading the authors to hypothesise that the hydrophobic patch may be important for centrosomal localization, though this was not tested using the previously described 'HPM' point mutations in the full-length cyclin (Bentley et al., 2007). Mutating I213 (the I in MRAIL) as well as E220, E224, and K226 to arginine in human Cyclin A prevents it binding to centrosomes, and residues 201-255 (which include the MRAIL hydrophobic patch) were found to be sufficient for centrosomal binding, demonstrating that the hydrophobic patch of Cyclin A is involved in targeting it to the centrosome (Pascreau et al., 2010). However, the rat Cyclin E centrosomal localization sequence has been shown to be in a different region of the cyclin, suggesting that not all cyclins that possess a hydrophobic patch depend on it for centrosomal localisation (Matsumoto and Maller, 2004). Supporting this, the investigation into $Clb2^{HPM}$ localisation in *S. cerevisiae* did not report any defects in localisation to the SPB (the yeast centrosome equivalent) (Bailly et al., 2003). However, the hydrophobic patch of the *S. cerevisiae* G2 cyclin Clb3, which specifically recognises PXF motifs, influences its localisation to the SPB and nuclear envelope (Ord et al., 2020).

It should be noted that one report found that Cyclin A^{HPM} had defects in nuclear localization and kinase activity in HeLa cells due to impaired binding of Cyclin A^{HPM} to Cdk2 (Jackman et al., 2002). However, other investigations into hydrophobic patch mutants of cyclins in both mammalian cells and budding yeast have found that the hydrophobic patch mutant is able to bind its partner CDK and does not affect its intrinsic activity against substrates without RXL motifs (Schulman et al., 1998, Cross and Jacobson, 2000, Loog and Morgan, 2005).

The hydrophobic patch-RXL interaction is not the only docking interaction that has been identified in cyclins. In *S. cerevisiae*, LXF motifs are recognised specifically by the Clb2 hydrophobic patch, PXF motifs are recognised specifically by the hydrophobic patch of the G2 cyclin Clb3 (Ord et al., 2020, Ord et al., 2019), and NLXXXL motifs are specifically recognised by the S phase cyclins Clb5 and Clb6 (Faustova et al., 2021). The *S. cerevisiae* Cln-type cyclins display substrate specificity that is dependent on LP regions (rich in leucine and proline resides) in substrates which bind to a region on cyclin distinct from the hydrophobic patch

(Koivomagi et al., 2011, Bhaduri et al., 2015). However, *in vitro* studies suggest that LXF and PXF motifs do not significantly affect substrate phosphorylation directed by the mammalian Cyclins E, A and B (Ord et al., 2020). Therefore, the interaction of the hydrophobic patch with LXF/PXF motifs may not be as widely conserved across eukaryotes as the hydrophobic patch-R/KXL interaction.

Additionally, a phosphate binding pocket in human Cyclin B1 has recently been identified that interacts with separase, providing another mechanism by which cyclins can bind to substrates (Yu et al., 2021). This is conserved amongst the B-type cyclins in yeast, and is required for hyperphosphorylation of the CDK substrate Ndd1 *in vitro* after priming phosphorylations in *S. cerevisiae* (Asfaha et al., 2022).

1.2.7 The regulation of CDK activity is critical for controlling cell cycle progression

CDK activity can thus be regulated in multiple ways: cyclin binding and T-loop phosphorylation activate CDK to a basal level; removal of the inhibitory phosphorylations on T14 and in particular Y15 substantially increase CDK activity at mitosis; Suc1/Cks1 binding can further modulate CDK activity; CKIs can interfere with cyclin or substrate binding to CDK; phosphatases counteract CDK substrate phosphorylation and can affect CDK activity via the feedback loops that act on Y15 dephosphorylation; and docking sites on cyclin can target CDK activity to specific substrates. It has been clear for a long time that CDK activity regulation is key to orderly progression through the cell cycle. There has historically been some debate as to how this is achieved, with two key models proposed known as the qualitative and the quantitative model.

1.3 The temporal control of CDK activity is critical to ordering the cell cycle

1.3.1 Quantitative vs qualitative model

A key question in cell cycle control is how a single CDK is able to drive ordered cell cycle progression in the yeasts *S. cerevisiae* and *S. pombe*. Given that CDK phosphorylates substrates involved in both S-phase and mitosis, to confer order on the cell cycle, CDK substrate phosphorylation itself must be ordered.

The qualitative model proposes that the main factor resulting in ordered CDK activity is the sequential binding of different cyclins to CDK, that have different substrate specificities. In this model, cyclins expressed early in the cell cycle target CDK activity towards G1 and S-phase substrates, while cyclins expressed later in the cell cycle result in the phosphorylation of mitotic substrates. Such cyclin specificity has been demonstrated most extensively in *S. cerevisiae*. As described in the previous section 1.2.6, the S-phase cyclin Clb5 is specific for a subset of substrates, which it recognises via the hydrophobic patch on Clb5 and R/KXL motifs on the substrates (Loog and Morgan, 2005). Further studies demonstrated that different docking sites are recognised by different cyclins in *S. cerevisiae*, with the G1 Cln-type cyclins, S-phase Clb5, G2/M Clb3 and mitotic Clb2 all recognising different motifs in substrates, via the hydrophobic patch or a different docking site (Loog and Morgan, 2005, Bhaduri et al., 2015, Faustova et al., 2021, Ord et al., 2020, Ord et al., 2019, Koivomagi et al., 2011). Furthermore, this work found that the activity of Cdc28 (*S. cerevisiae* Cdk1) to the full CDK consensus sequence increased as it sequentially bound the cyclins in the order G1-S-G2-M, and that different cyclin-Cdc28 complexes had slight differences in preference for residues around the minimum CDK consensus site (Koivomagi et al., 2011). Thus these data are consistent with a model in which cyclins expressed early in the cycle target CDK activity to S-phase substrates, and the later cyclins result in a higher CDK activity towards the full consensus sequence that results in more general substrate phosphorylation, meaning that non-S-phase substrates are phosphorylated, possibly aided to some extent by cyclin-specific substrate docking (Koivomagi and Loog, 2011, Koivomagi et al., 2011, Loog and Morgan, 2005).

However, whilst cyclin specificity clearly exists, and it provides one mechanism by which the cycle could be ordered, it has been demonstrated that there is significant redundancy between cyclins in multiple systems. This is most plainly illustrated in *S. pombe*, where the entire mitotic cell cycle can be driven by one cyclin-CDK complex, Cdc13-Cdc2 (Fisher and Nurse, 1996, Coudreuse and Nurse, 2010). Thus differing substrate specificity of different cyclins cannot explain how CDK substrate phosphorylation, and therefore the cell cycle, can be ordered by one cyclin-CDK complex. An alternative model, known as the quantitative model, was first proposed by Stern and Nurse and suggests that the cell cycle is ordered by a progressive increase in net CDK activity through the cycle, with S-phase occurring at a low activity threshold, and mitosis having a higher activity threshold (Stern and Nurse, 1996). A major endorsement of the quantitative model came from the demonstration that the cell cycle can be ordered by modulating the activity of a chimeric fusion protein of Cdc13 and Cdc2 separated by a linker (Cdc13-L-Cdc2) with a chemical inhibitor (Coudreuse and Nurse, 2010). A further prediction of the quantitative model is that, as well as a mitotic cyclin being able to drive S-phase, an S-phase cyclin should be able to drive mitotic phosphorylation if its activity is raised sufficiently. Accordingly, the substrates phosphorylated *in vivo* by Cdc2 when fused to the S-phase cyclin Cig2 substantially overlap with those phosphorylated by Cdc13-L-Cdc2, and Cig2-L-Cdc2 is able to drive mitosis if the CDK antagonising phosphatase Dis2 (PP1) is removed from the SPB, raising the net *in vivo* CDK activity (Basu et al., 2021). Thus it has been clearly demonstrated that, though there are minor differences in substrate phosphorylation directed between S-phase and M-phase cyclins in *S. pombe*, the cell cycle can be ordered by the increasing activity of a single cyclin-CDK complex.

Subsequently it has been shown that a single cyclin-CDK complex, Clb2-Cdc28, is able to drive ordered substrate phosphorylation and ordered progression of the processes of S-phase, chromosome segregation, and nuclear division, in the absence of other cyclins in *S. cerevisiae*, though there is a requirement for Cln cyclins for cell viability as they are essential for the morphological process of budding (Pirincci Ercan et al., 2021). There is evidence of significant cyclin and CDK redundancy in more complex eukaryotes as well. Despite mammalian cells

having multiple cell-cycle CDKs, with Cdk1 driving mitosis and Cdk2, Cdk3, Cdk4 and Cdk6 having roles in interphase, Cdk1 (the homologue of *S. pombe* Cdc2) is the only essential CDK for the cell cycle in mouse embryos (Santamaria et al., 2007). Mouse models also suggest that many cyclins are also redundant, with Cyclin A2 and B1 being the cyclins with least redundancy (Satyanarayana and Kaldis, 2009). Cyclin A2 is required in mammalian cells for mitotic entry, and Cyclin B1 is subsequently required for nuclear envelope breakdown (NEBD) and completion of mitosis (Hegarat et al., 2020). However, approximately 90% of mitotic Cdk1 phosphosites are phosphorylated efficiently by Cyclin A2 in the absence of Cyclin B1, suggesting a large overlap in substrate preference between the two cyclins (Hegarat et al., 2020). Furthermore, Cyclin B1-Cdk1, which normally drives mitosis but not DNA replication, is able to promote S-phase in *Xenopus* egg extracts when localised to the nucleus (Moore et al., 2003), indicating that, with modified localisation, this single cyclin can drive both S-phase and mitosis. Supporting the theory that increasing CDK activity levels are needed to drive cell cycle progression, a FRET sensor developed to measure Cyclin B1-Cdk1 activity was used to demonstrate that different events in mitosis are triggered at different levels of Cyclin B1-Cdk1 activity in HeLa cells, with cell rounding occurring at lower activity levels than NEBD (Gavet and Pines, 2010b). Therefore, there is evidence that a quantitative increase in CDK activity is also important for cell cycle progression in mammalian cells, though there may be an increased requirement for cyclin and CDK specificity in these more complex systems.

It is clear from the extensive *in vitro* studies in *S. cerevisiae*, as well as studies in mammalian cells, that different cyclins can have different substrate specificities. However, the observation that the *S. pombe* cell cycle can be driven by a single cyclin-CDK complex, with S-phase and mitosis occurring at different activity thresholds, is a clear endorsement of the quantitative model and incompatible with the suggestion that different cyclin specificities are necessary to provide order to the cell cycle (Fisher and Nurse, 1996, Coudreuse and Nurse, 2010). The observation that a single cyclin-CDK can drive ordered S phase and nuclear division in *S. cerevisiae* suggests that the quantitative model is also the best description of *S. cerevisiae* cell cycle control (Pirincci Ercan et al., 2021). Reconciling these observations leads to a model for yeast cell cycle control where

the quantitative increase in CDK activity provides the primary, broad mechanism by which to order the events of S-phase and mitosis, with differing cyclin specificity providing fine-tuning to cell cycle control (Stern and Nurse, 1996, Coudreuse and Nurse, 2010, Swaffer et al., 2016, Pirincci Ercan et al., 2021). The significant redundancy between cyclins and CDKs in mammalian cells suggests that the quantitative model is also relevant for cell cycle control in more complex eukaryotes.

1.3.2 Ordering CDK substrate phosphorylation

Further investigation into how a single cyclin-CDK complex can order the cell cycle in *S. pombe* utilised phosphoproteomics to study *in vivo* global phosphorylation dynamics through the cell cycle. This showed that CDK substrate phosphorylation is also ordered, with different substrates being phosphorylated at different CDK activity levels (Swaffer et al., 2016). Substrates phosphorylated early in the cell cycle, at relatively low CDK activity levels, are enriched for proteins involved in DNA replication, whereas substrates phosphorylated late in the cell cycle at high activity levels are enriched for those involved in mitotic processes (Swaffer et al., 2016). Furthermore, this study provided an *in vivo* measure of global substrate phosphorylation, the functional output of net CDK activity, throughout the cycle. This demonstrated that CDK activity rises throughout the cycle, with a substantial increase in CDK activity at mitosis. This narrows the question of how a single cyclin-CDK orders S-phase and mitosis, into how different substrate sensitivities to CDK activity are generated to ensure ordered substrate phosphorylation.

There are a number of factors that could influence substrate sensitivity to CDK activity. One such factor is the presence of docking sites on the substrates that bind to cyclins, such as the R/KXL motifs that dock to the cyclin hydrophobic patch. Another important factor is the action of phosphatases. The measurement of substrate phosphorylation level reflects the local balance of CDK and phosphatase activity, so if different substrates have different sensitivities to antagonising phosphatases, this would impact on the substrate's net phosphorylation level at a given CDK activity level. The *in vivo* role of Suc1 is still not well known, but its

involvement in binding phosphorylated residues provides another mechanism by which CDK activity may be preferentially recruited to certain substrates. The sequence surrounding the phosphosite itself could influence sensitivity, however in *S. pombe* there does not seem to be any relationship between substrate sensitivity and the minimal/full CDK consensus site (Swaffer et al., 2016).

Another important factor to consider, both for its potential impact on CDK substrate sensitivity, and more widely in CDK regulation of cell cycle control, is the localisation of cyclin-CDK. Whilst it has long been appreciated that the temporal control of CDK activity is critical for cell cycle control, and the studies outlined above emphasise this further, in the past few decades the spatial regulation of CDK activity has also been much more widely studied.

1.3.3 The spatial regulation of CDK activity is also important for cell cycle progression

Cyclin-CDK localisation changes throughout the cell cycle, as does the localisation of several key CDK regulators; it cannot be assumed that CDK activity is homogenous throughout the cell. Although using phosphoproteomics to measure global substrate phosphorylation provides a powerful measure of the temporal dynamics of CDK activity, it does not provide information of the spatial dynamics of CDK activity, nor do many of the widely used measures of CDK activity such as histone H1 phosphorylation in whole cell extracts.

There is substantial evidence to suggest that the spatial regulation of cyclin-CDK and its regulators is important for their function and therefore cell cycle progression. In order to discuss the role and importance of localisation in CDK control of the cell cycle, I will first outline the current understanding of the localisation of cyclin-CDK and some of its key regulators.

1.4 Localisation of CDK and its regulators

1.4.1 Localisation of cyclin-CDK complexes

Cyclin-CDK complexes exhibit dynamic localisation through the mitotic cell cycle. In *S. pombe*, Cdc13 has been shown to colocalise with Cdc2 in the nucleus and at the spindle-pole body (SPB, the centrosome equivalent) in G2 and at the spindle in mitosis in both immunofluorescence studies (Alfa et al., 1989, Booher et al., 1989, Alfa et al., 1990) and in live cells expressing fluorescently-tagged proteins (Decottignies et al., 2001). Cig2 also localises at the SPB and in the nucleus (Decottignies et al., 2001). These studies did not investigate the localisation of the other G1 and G1/S cyclins that act in the mitotic cell cycle (Puc1 and Cig1). The observation that Cdc2 localisation becomes diffuse upon cyclin degradation suggests that it is primarily cyclins that mediate the localisation of the complex (Alfa et al., 1989, Booher et al., 1989, Decottignies et al., 2001).

Immunofluorescence of Cdk1 in HeLa cells shows that human Cdk1 localisation is similar to that of Cdc2 in *S. pombe*, demonstrating nuclear and cytoplasmic localisation, as well as centrosomal localisation in late G2/M (Bailly et al., 1989). Studies in *Xenopus* and mammalian cells show Cyclin B1, the major mitotic cyclin, is continuously shuttling between the cytoplasm and nucleus, with nuclear export being more efficient than nuclear import in interphase resulting in a predominantly cytoplasmic localisation (Pines and Hunter, 1991, Pines and Hunter, 1994, Jackman et al., 1995, Hagting et al., 1998, Toyoshima et al., 1998). At the entry to mitosis, Cyclin B1 is phosphorylated at multiple sites within its cytoplasmic retention sequence (CRS) by several kinases including Cdk1 and Plk1, which has been suggested to result in an abrogation of its nuclear export as well as rapid nuclear import, resulting in a rapid nuclear accumulation (Pines and Hunter, 1994, Li et al., 1995, Li et al., 1997, Yang et al., 1998, Hagting et al., 1999, Yang et al., 2001, Santos et al., 2012). However, it has also been suggested that the phosphorylation of the Cyclin B1 CRS is not the cause of the rapid nuclear accumulation of Cyclin B1, and that it may instead be due to general changes to the nuclear import machinery, possibly as a result of CDK activation (Gavet and Pines, 2010a). Despite the contention surrounding the mechanism, it is clear that

the rapid nuclear import of Cyclin B1 is critical for mitotic entry, and mutants of Cyclin B1 that do not accumulate in the nucleus do not drive mitosis (Li et al., 1997). The nuclear translocation of Cyclin B1 has been shown to exhibit spatial positive feedback, with nuclear Cyclin B1-Cdk1 promoting the net nuclear translocation of Cyclin B1-Cdk1 (Santos et al., 2012). Cyclin B1 has also been described to localise to microtubules in interphase, as well as the spindle, centrosome, chromatin and unattached kinetochores (Jackman et al., 1995, Bentley et al., 2007). In contrast, immunofluorescence in HeLa cells indicates that Cyclin B2 colocalises with the Golgi apparatus, and does not translocate into the nucleus (Jackman et al., 1995). Immunofluorescence of Cyclin A in human cells shows that, unlike the B-type cyclins, it remains mainly nuclear from S-phase through to its degradation in mitosis (Pines and Hunter, 1991). Cyclin E is also predominantly nuclear (Ohtsubo et al., 1995), while Cyclin D1 was found to accumulate in the nucleus in G1 before being exported to the cytoplasm in S phase (Baldin et al., 1993). Cyclin A and E are also enriched at the centrosome (Pascreau et al., 2010, Matsumoto and Maller, 2004).

1.4.2 Localisation of other cell cycle regulators

The localisation of major CDK regulators also changes throughout the cycle. In *S. pombe*, Wee1 accumulates in the nucleus through G2 and at the SPB in late G2, as well as localising to cortical nodes surrounding the nucleus (Masuda et al., 2011, Allard et al., 2018). Cdc25 accumulates in the nucleus in G2 and decreases in anaphase (Lopez-Girona et al., 1999). Polo kinase (Plo1) accumulates at the SPB in late G2 and remains associated with the SPBs and spindle during mitosis (Mulvihill et al., 1999, Grallert et al., 2013b).

Immunofluorescence in HeLa cells shows that Wee1 is located in the nucleus, but appears to be excluded from the nucleolus (McGowan and Russell, 1995), and is exported from the nucleus in prophase (Baldin and Ducommun, 1995). Cdc25 is found in 3 isoforms in human cells, with the different isoforms all implicated in mitosis but having some specific functions (Takizawa and Morgan, 2000, Lindqvist et al., 2005). Cdc25A is mainly nuclear (Hoffmann et al., 1994), though it has been

reported that a fraction of cells also have Cdc25A in the cytoplasm (Kallstrom et al., 2005). Cdc25B is predominantly nuclear, but also localises to the cytoplasm in G2, and there is also a population at the centrosome, where Cdc25B is implicated in the activation of Cyclin B1-Cdk1 (Gabrielli et al., 1997, Dutertre et al., 2004, Lindqvist et al., 2004, Lindqvist et al., 2005, Kramer et al., 2004). Cdc25C localisation is similar to that of Cyclin B1; it is located in the cytoplasm during interphase, and translocates to the nucleus coincidentally with Cyclin B1 translocation at the entry to mitosis (Heald et al., 1993, Dalal et al., 1999, Kumagai and Dunphy, 1999, Takizawa and Morgan, 2000). Human Plk1 localises to the centrosomes in late G2 and early mitosis, as well as the kinetochore, midzone microtubules in late mitosis and the midbody during cytokinesis (Golsteyn et al., 1995, Schmucker and Sumara, 2014).

The specific and often dynamic localisation of cyclin-CDK and its regulators, seen in yeasts and more complex eukaryotes including human cells, suggests that localisation plays an important role in cell cycle progression.

1.5 Role and importance of localisation in cell cycle progression

Localisation can affect cellular signalling in multiple ways. It can be used to concentrate enzymes, regulators and substrates, and this can be regulated temporally. It can also affect specificity of signalling pathways, for example by affecting which substrates an enzyme is able to access. A number of studies have demonstrated that the localisation of cell cycle regulators is important to their function, and therefore cell cycle progression. In this section, examples of how the localisation of regulators can influence signalling and cell cycle progression are discussed.

1.5.1 Regulation of substrate specificity and access

Restricting the localisation of a protein restricts the substrates and interactors that it comes into contact with. Localisation is thought to be a major determinant of the substrate specificity of human Cyclin B1 and Cyclin B2. Whilst both Cyclin B1-Cdk1 and Cyclin B2-Cdk1 can promote Golgi disassembly, normally only Cyclin B1-Cdk1 promotes chromosome condensation, nuclear envelope disassembly and microtubule reorganisation. However, relocalising Cyclin B1 to the Golgi using the N-terminal region of Cyclin B2 restricted its assayed activities to solely promoting Golgi disassembly, but not chromosome condensation, nuclear envelope disassembly or microtubule reorganisation (Draviam et al., 2001). Furthermore, promoting Cyclin B2 diffuse cytoplasmic localisation by replacing its N terminus with that of Cyclin B1 resulted in Cyclin B2 being able to promote both Golgi disassembly and microtubule reorganisation. Cytoplasmic Cyclin B2 did not promote nuclear envelope disassembly or chromosome condensation, consistent with its lack of nuclear translocation. These experiments strongly suggest that the localisation of Cyclins B1 and B2 have a major role in determining their substrate specificity and function.

Further emphasising the importance of localisation in determining the output of CDK activity, Cyclin B1, normally restricted to a role in mitosis, is able to promote

S-phase if prematurely targeted to the nucleus in *Xenopus* egg extracts (Moore et al., 2003). Cyclin B1 can only promote mitosis upon its nuclear translocation (Li et al., 1997), supporting the theory that Cyclin B1 is retained in the cytoplasm in interphase to prevent mitosis occurring prematurely. Further demonstrating the importance of the localisation of Cdk1 activity for mitosis, high levels of cytoplasmic Cdk1 activity are not sufficient to drive mitosis, if the nucleus is protected from high Cdk1 activity levels by Wee1 (Heald et al., 1993).

The localisation of cell cycle regulators can also be altered during the cell cycle in order to halt cell cycle progression in certain scenarios. Cdc25C cytoplasmic localisation in interphase is mediated in part through phosphorylation of Cdc25C creating a binding site for the 14-3-3 phosphoserine binding proteins, leading to Cdc25C retention in the cytoplasm (Peng et al., 1997, Kumagai et al., 1998, Kumagai and Dunphy, 1999). In response to unreplicated DNA, or DNA damage, phosphorylation of this site by the checkpoint kinases Cds1/Chk2 and Chk1 is stabilised, leading to Cdc25C retention in the cytoplasm, contributing to inhibition of Cdk1 activation to prevent mitosis (Peng et al., 1997, Matsuoka et al., 1998, Takizawa and Morgan, 2000). Cdc25B is also exported to the cytoplasm in response to DNA damage, mediated by phosphorylation of a 14-3-3 binding site on Cdc25B (Lindqvist et al., 2004). Similarly, in *S. pombe*, the 14-3-3 protein Rad24 binds to Cdc25 when Cdc25 is phosphorylated by Chk1 or Cds1 in response to DNA damage, leading to the nuclear export of Cdc25 (Furnari et al., 1999, Lopez-Girona et al., 1999).

1.5.2 Concentration of enzymes to aid switch-like transitions

As well as affecting the substrate specificity of enzymes, localisation can affect the dynamics of signalling pathways, including changing a graded response to a switch-like response. The rapid nuclear import of both Cyclin B1 and Cdc25C at mitotic entry was proposed to contribute to making CDK activation, and therefore mitotic entry, a more switch-like event (Ferrell, 1998). The concurrent translocation of both Cyclin B1-Cdk1 and its activator to the nucleus generates a potential source of ultrasensitivity, as it results in increased nuclear Cyclin B1-Cdk1, as well as

increased dephosphorylation of Cyclin B1-Cdk1 in the nucleus, which together result in higher concentration of active nuclear Cyclin B1-Cdk1 (Ferrell, 1998).

It was subsequently shown that the forced nuclear translocation of one population of Cyclin B1 promotes the nuclear translocation of a different population of Cyclin B1, suggesting that Cyclin B1 nuclear import, a result of Cdk1 activation, is part of a spatial positive feedback loop that promotes further Cyclin B1 nuclear translocation (Santos et al., 2012). Compromising the abruptness of Cyclin B1 nuclear import resulted in longer, more variable mitosis, indicating that rapid nuclear import of Cyclin B1 is physiologically important. The spatial positive feedback acting on Cyclin B1 nuclear translocation has therefore been proposed to contribute to making Cdk1 activation at mitosis a robust, all-or-nothing event (Santos et al., 2012).

1.5.3 Signalling hubs and scaffold-assisted signalling cascades

The concentration of enzymes by regulated localisation can also increase the rate of enzymes encountering substrates or regulators, and therefore the rate of signalling. Creating a signalling hub can also facilitate the convergence of different signalling pathways, for example by concentrating multiple upstream regulators of an enzyme. A signalling hub can focus around a scaffold, with which different proteins in a signalling pathway can physically associate.

A key scaffold/signalling hub in cell cycle control is the centrosome or SPB (Doxsey et al., 2005). The SPB of both budding yeast and fission yeast has been shown to be an important hub of major cell cycle signalling networks acting at mitotic exit: the mitotic exit network (MEN) in budding yeast; and the septation initiation network (SIN) in fission yeast (Arquint et al., 2014). In fission yeast, the SPB has also been implicated as a signalling hub important for mitotic entry, consistent with evidence to suggest that the centrosome of more complex eukaryotes is important at mitotic entry. In the following section, I discuss the SPB and centrosome, and their role and importance in CDK regulation of cell cycle progression with a particular focus on mitotic entry.

1.6 Role of the centrosome and SPB in cell cycle regulation

1.6.1 Structure and dynamics of the SPB and centrosome

The centrosome (found in metazoans) and SPB (in yeast) are functional equivalents, both acting as the major microtubule-organizing centre (MTOC) in the cell. Their structures are different, though many SPB and centrosome components are conserved, and both use γ-tubulin to nucleate microtubules. The SPB is a laminar structure, with an extension to one side known as the half-bridge (Figure 1.6) (Bestul et al., 2017). The centrosome consists of a pair of centrioles surrounded by a peri-centriolar matrix (PCM), which contains a number of proteins including the γ-tubulin ring complex that nucleates microtubules (Fu et al., 2015).

Like DNA, the SPB and centrosome are duplicated once, and only once, per cell cycle. The half bridge of the mother SPB is extended in late mitosis, to form a full bridge structure, onto which the daughter SPB assembles in G1 (Uzawa et al., 2004, Ruthnick and Schiebel, 2018). In metazoans, the two centrioles disengage from each other in G1, and a new centriole begins to form to the side of each mother centriole in G1/S, and is extended in G2 phase to reach the same length as the mother centriole (Fu et al., 2015). Both the SPB and centrosome undergo a stage of maturation in late G2/mitosis, which involves increased incorporation of components for the SPB, and for the centrosome, involves a substantial expansion of the PCM and an increase in microtubule nucleation (Walde and King, 2014, Fu et al., 2015). However, there is also evidence that both fission yeast SPBs and mammalian centrioles can take more than one cell cycle to fully mature, suggesting that full maturation may be incremental over multiple cycles (Grallert et al., 2004, Vorobjev and Chentsov Yu, 1982).

The centrosome is a cytoplasmic structure, and NEBD during mitosis in mammalian cells allows the centrosome to nucleate a mitotic spindle that can access chromosomes, a mechanism known as open mitosis. In contrast, *S. pombe* performs a closed mitosis, with the nuclear envelope remaining largely intact for mitosis (McCully and Robinow, 1971). The SPB is also cytoplasmic in interphase, so in order to construct a mitotic spindle to segregate chromosomes, the SPB must

insert into the nuclear envelope during mitosis. Thus, the SPB enters and leaves the nuclear envelope during the cell cycle (Ding et al., 1997). During interphase, it is cytoplasmic, with the 'nuclear face' of the SPB adjacent to the nuclear envelope (NE), and the 'cytoplasmic face' facing the cytoplasm. During mitosis, there is localised nuclear envelope fenestration underneath the SPB to allow SPB insertion, at which point the SPB is in contact with both the nucleus and cytoplasm (Ruthnick and Schiebel, 2018). Although the SPB is cytoplasmic in interphase, the SUN-domain containing protein Sad1 localises in the nucleus adjacent to the NE under the SPB throughout the cell cycle (Figure 1.6) (Hagan and Yanagida, 1995, Bestul et al., 2017).

The SPB and centrosome have a clear role in the cell division cycle through their role as the MTOCs that organise the mitotic spindle. However, there is also evidence that they may play a key role as signalling hubs in cell cycle progression, including in mitotic entry.

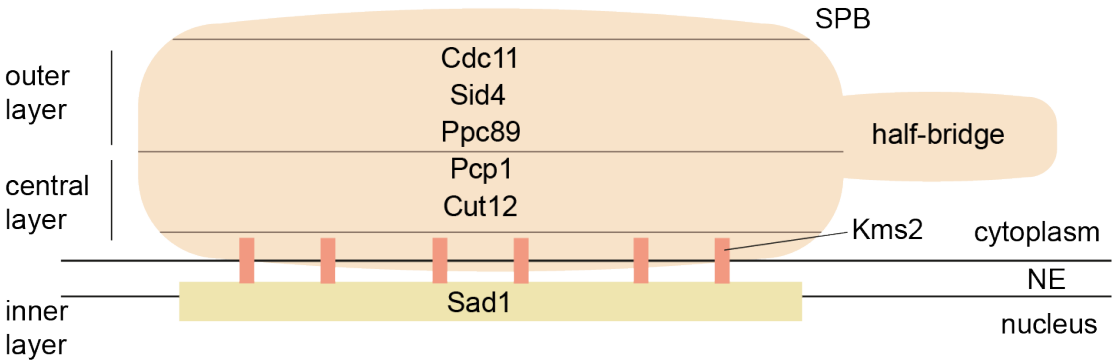


Figure 1.6 | Schematic of the fission yeast SPB

Simplified schematic showing the *S. pombe* spindle-pole body with key SPB components labelled. SPB component positional information is from (Bestul et al., 2017).

1.6.2 SPB as a signalling hub at mitotic entry

Extensive work in *S. pombe* has uncovered a role for signalling at the SPB in mitotic commitment. In *S. pombe*, cyclin-CDK can be detected at the SPB

throughout G2 and mitosis (Alfa et al., 1990, Decottignies et al., 2001). As discussed in Section 1.2.3, mitotic entry requires the full activation of CDK that occurs with its dephosphorylation on Y15. This requires activation of the positive and double-negative feedback loops involving Cdc25 and Wee1, and Polo kinase plays a key role in these feedback loops. The signalling network regulating mitotic entry involves the SPB component Cut12, which is essential for bipolar spindle formation, and was implicated in mitotic entry from its discovery.

Cut12 was initially identified in a screen for mutants that suppressed the lethal phenotype of the temperature-sensitive *cdc25.22* mutant, where it was designated the name *stf1* (for suppressor of twenty-five) (Hudson et al., 1990). The mutant *stf1.1* (known as both *stf1.1* or *cut12.s11* and from here on referred to as *cut12.s11*) was able to rescue the otherwise lethal *cdc25-22* at temperatures up to 35 °C (Hudson et al., 1990). Later work on a mutant *cut12.1*, that results in a failure to establish a bipolar spindle, identified that *cut12* encoded an SPB component and was allelic to *stf1*, providing the first link between the SPB and CDK regulation of mitotic entry, and raising the question of how a mutant in an SPB component was able to rescue *cdc25-22* (Bridge et al., 1998). Further insight into the mechanism involved was provided by a series of studies investigating the genetic and physical interactions of Cut12 with Plo1, the fission yeast Polo kinase. It was observed that Plo1 localises to the SPB around late G2/mitotic entry, and that this localisation is accelerated in *cut12.s11* cells (Mulvihill et al., 1999, Grallert et al., 2013b). Given that Polo kinase is involved in amplification of the positive and double-negative feedback loops involving Cdc25, Wee1 and Cdc2 that result in active Y15-dephosphorylated Cdc2, the early recruitment of Plo1 to the SPB was suggested to be the basis by which *cut12.s11* cells bypass the requirement for fully functional *cdc25* (Mulvihill et al., 1999). Supporting this, investigation into the activity of Plo1 at SPBs showed that the *cut12.s11* rescue of *cdc25-22* depends on Polo activity, and that the Plo1 recruited to the SPB early in *cut12.s11* is active, as *cut12.s11* cells have an increased number of SPBs staining with the antibody MPM2, which detects a phosphorylated epitope at the SPB dependent on Plo1 activity (MacIver et al., 2003, Grallert et al., 2013b). It was also shown that Plo1 interacts with Cut12 (MacIver et al., 2003), and interfering with Plo1 recruitment to the SPB in *cut12.s11*

cdc25-22 cells reduced the observed levels of mitotic rescue (Petersen and Hagan, 2005).

Study of the mechanism by which Plo1 is recruited to the SPB early in *cut12.s11* demonstrated that Cut12 contains a bipartite PP1 docking motif, and that the mutation in *cut12.s11* (G71V) maps to this docking motif (Grallert et al., 2013a). The gain of function mutant *cut12.s11* disrupted Dis2 (one of two catalytic PP1 subunits in fission yeast) docking to Cut12, while the loss of function mutant *cut12.1* had enhanced binding to Dis2, suggesting that Dis2 docking to the SPB may be involved in the *cut12.s11* rescue of *cdc25-22*. It was shown that eviction of Dis2 from Cut12 normally occurs in G2 phase, and is mediated by phosphorylation on two residues within the PP1 docking motif in Cut12 (T75 and T78) by Cdc2 and the NIMA kinase Fin1 (Figure 1.7) (Grallert et al., 2013a). Mutations that perturb Dis2 docking to Cut12 result in early recruitment of Plo1 to the SPB, while mutations enhancing Dis2 and Cut12 interaction delay Plo1 SPB recruitment, suggesting that Dis2 activity at the SPB influences Plo1 recruitment. Furthermore, it was shown that Dis2 eviction from Cut12 was required for *cut12.s11* suppression of *cdc25-22*. Thus, the *cut12.s11* mutant is able to suppress *cdc25-22* due to an early eviction of Dis2 from Cut12, which is correlated with an early recruitment of Plo1 to the SPB. Consistently, simultaneous mutation of both parts of the PP1 docking motif in Cut12 removes the requirement for Cdc25 for cell viability. This work demonstrates that Dis2 signalling at the SPB specifically can influence the recruitment of Plo1 and the requirement for Cdc25 activity, suggesting that signalling at the SPB plays a critical role in mitotic entry (Grallert et al., 2013a).

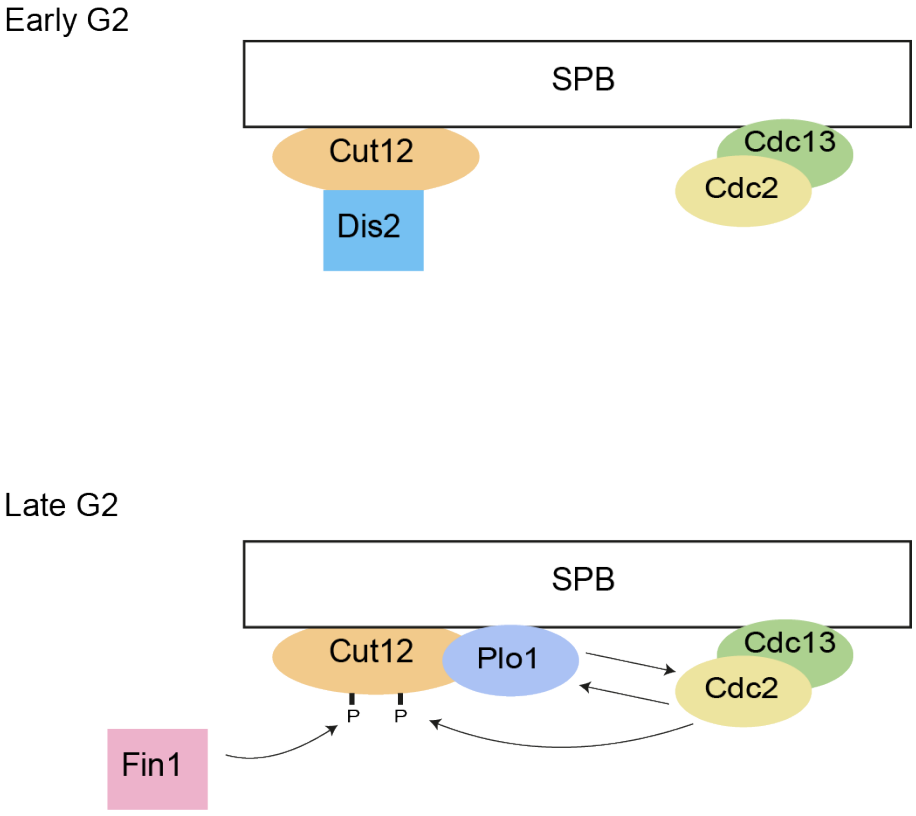


Figure 1.7 | Regulation of mitotic entry at the SPB

Simplified schematic of the model to describe the regulation and SPB recruitment of key regulators of the G2/M transition, detailed in (Grallert et al., 2013a). In early G2, Dis2 (PP1) docks to Cut12 (an SPB component) via a bipartite PP1 docking site in Cut12. Dis2 opposes Plo1 recruitment to the SPB. Cdc13-Cdc2 localises to, or near to, the SPB via an unknown interaction. In late G2, Cdc2 and Fin1 phosphorylate Cut12 on two residues (T75 and T78) in the PP1 docking motif, resulting in the eviction of Dis2. This allows the recruitment of Plo1, possibly to Cut12, and the local activation of the feedback loops involving Cdc2. Propagation of the feedback loop to the rest of the cell is thought to initially be restrained by the activities of Wee1 and phosphatases, until these activities are overcome and the cell enters mitosis (Grallert et al., 2013b).

The suggestion that Plo1 signalling at the SPB can influence mitotic commitment was cemented by experiments showing that tethering a constitutively active Plo1-GBP (GFP-binding protein) to Cut12-NEGFP promotes a wave of mitosis in G2 cells, but tethering it to other regions in the cell does not have the same effect (Grallert et al., 2013b). This study also identified that Plo1 localisation to the SPB relies on continuous Cdc2 activity. A similar promotion of mitotic commitment is

seen upon tethering of Cdc2Y15F-GBP (which is insensitive to inhibition from Wee1 and Mik1) to Cut12-NEGFP, and this relies on Plo1 activity.

These studies have demonstrated that active Cdc2 or Plo1 at SPBs specifically can promote mitotic commitment, and related studies demonstrated that Plo1 signalling at SPBs influences mitotic commitment in response to stress or environmental cues (Petersen and Hagan, 2005, Petersen and Nurse, 2007). Upon temperature shift to induce heat stress, Plo1 became phosphorylated at Ser402, with this phosphorylation being dependent on the stress response pathway MAP kinase Sty1 and its activating kinase Wis1 (Petersen and Hagan, 2005). This phosphorylation of Plo1 promotes early recruitment of Plo1 to the SPB, and a Plo1S402A mutant takes longer to cycle again after return from heat shock. Similarly, nutrient availability affects TOR signalling, which in turn influences the activity of Sty1 and the recruitment of Polo to the SPB (Petersen and Nurse, 2007). Inhibition of TOR advances mitotic onset in a manner dependent on Polo recruitment to the SPB. Thus Plo1 signalling at the SPB is important for the integration of signals from environmental cues to influence the timing of mitotic commitment.

This work has demonstrated that signalling at the SPB, involving the key cell cycle regulators Dis2, Plo1, Cdc2 and Fin1, can influence mitotic commitment. Although much of this work has focussed on the role of Plo1 at the SPB, it showed that Plo1 association with the SPB requires Cdc2 activity, and that Cdc2Y15F can promote mitotic entry when tethered to the SPB, but not when tethered to other subcellular locations (Grallert et al., 2013b). Moreover, this work proposes that a key role of Plo1 signalling at the SPB in driving mitotic commitment is through promoting Cdc2 activation, and that the SPB is the location at which the decision to enter mitosis might be made, triggering global activation of Cdc2 (Grallert et al., 2013b, Hagan and Grallert, 2013). Understanding Cdc2 signalling dynamics at the SPB is therefore crucial to understanding mitotic commitment.

There are indications to suggest that the centrosome may play a key role in cell cycle signalling in other organisms too. Notably, immunofluorescence to detect an autophosphorylation site on Cyclin B1 shows that the first active population of

Cyclin B1-Cdk1 in human cells is at the centrosome (Jackman et al., 2003). Subsequently it was shown that Chk1 is enriched at the centrosome in interphase but not mitosis in human cells, and that removal of Chk1 from the centrosome results in activation of centrosomal Cyclin B1-Cdk1 (Kramer et al., 2004). Inhibiting Chk1 resulted in increased Cyclin B1-Cdk1 activation, as measured by Cdk1 Y15 dephosphorylation, and promoted centrosome separation and mitosis. By targeting Chk1 specifically to the centrosome, the authors showed that wild-type Chk1 at the centrosome inhibited Cdk1 activation at centrosomes and in the cytoplasm, and also inhibited normal mitotic progression resulting in polyploid cells, whereas targeting kinase-dead Chk1 to the centrosome promoted early Cdk1 activation and early centrosome separation. Underpinning the suggested importance of Cyclin B1-CDK activity regulation at the centrosome, mutations in genes implicated in microcephaly result in a loss of Chk1 from the centrosome and corresponding premature activation of Cyclin B1-Cdk1 (Tibelius et al., 2009). Activation of Cyclin B1-Cdk1 at the centrosome is mediated by the relief of Chk1 inhibition of Cdc25B, as well as Aurora A activation of Cdc25B (Kramer et al., 2004, Lindqvist et al., 2005, Dutertre et al., 2004). There is also an involvement of the fission yeast Aurora kinase (Ark1) in promoting mitotic entry on recovery from a mitotic delay induced by nutrient enrichment, with Ark1 phosphorylating Plo1 on S402 to recruit it to the SPB as described above (Halova and Petersen, 2011).

1.6.3 SPB and centrosome in other cell cycle transitions

The SPB and centrosome have also been implicated in other cell cycle transitions. Work in cultured mammalian cells suggests that the centrosome is needed for the G1/S transition. Microsurgery of cultured vertebrate cells to separate the centrosome from the nucleus in interphase, resulting in karyoplasts (acentrosomal cells), does not prevent these karyoplasts forming a mitotic spindle and undergoing mitosis, but does result in arrest at the G1/S transition (Hinchcliffe et al., 2001). Supporting the requirement for intact centrosomes for full cell cycle progression in cultured vertebrate cells, when one centrosome is laser-ablated in vertebrate cells during metaphase, the acentrosomal daughter cells arrest at the following G1/S transition (Khodjakov and Rieder, 2001). Expression of a peptide encompassing

the Cyclin E centrosomal localisation sequence (CLS) in mammalian cells displaces both Cyclin E and Cyclin A from centrosomes, and inhibits the initiation of DNA synthesis, in a manner that is rescued upon retargeting of Cyclin E back to the centrosome (Matsumoto and Maller, 2004, Ferguson and Maller, 2010). This suggests that a requirement for Cyclin E/Cyclin A centrosomal localisation for S-phase could be a potential mechanism contributing to the observed G1 arrest upon centrosomal removal.

The SPB acts as a signalling hub at the mitotic exit network (MEN) in budding yeast and the septation initiation network (SIN) in fission yeast (Bardin and Amon, 2001, Krapp et al., 2004). These require mitotic cyclin-CDK inactivation, and the CDK-counteracting phosphatases Cdc14/Clp1 play a major role in promoting the MEN/SIN pathways (Visintin et al., 1998, Bardin and Amon, 2001). Interestingly, the SIN scaffold protein Sid4 can also impact the mitotic entry signalling network at the SPB, indicating that the same scaffold proteins can function in multiple signalling pathways (Chan et al., 2017). Attachment to the SPB is essential for SIN function in fission yeast, and laser ablation of both SPBs in metaphase results in a failure of cytokinesis, supporting an important role for the yeast SPB in cell cycle progression (Magidson et al., 2006, Chan et al., 2017). Similarly, laser ablation of the centrosome during mitosis leads to increased defects in cytokinesis in vertebrate cells (Khodjakov and Rieder, 2001).

1.6.4 Importance of the centrosome is contested

Despite the evidence outlined above to suggest that the centrosome and SPB are key sites of cell cycle regulation, their importance is questioned by the observation that *Drosophila* cells without centrioles due to a mutation in *DSas-4*, a protein essential for centriole replication, are able to perform the entire cell cycle (Basto et al., 2006). These cells did not contain PCM markers including γ-tubulin, Aurora A and Centrosomin, indicating that centrosomes were not intact in these cells. However, the effect of localisation of key cell cycle regulators in this system, such as Cyclin B1-Cdk1, is unknown. It is also not clear if the centrosome normally plays a role in cell cycle progression, but there is a mechanism by which *Drosophila* cells

are able to compensate. Furthermore, although the microsurgery experiment in cultured mammalian cells discussed above did not suggest a requirement for centrosomes for G2/M, it did not rule out that the MTOC that forms is able to fulfil the potential role of the centrosome in G2/M signalling (Hinchcliffe et al., 2001). In these experiments, centrioles are not detected at the MTOCs in the karyoplasts, but γ-tubulin and pericentrin are detected at the MTOC, indicating that whilst the karyoplasts do not contain full centrosomes, they do still contain MTOCs with some proteins normally associated with the centrosome (Hinchcliffe et al., 2001). Thus, whilst a fully intact centrosome does not appear to be necessary for the G2/M transition in all systems, it is not clear how Cyclin B1-Cdk1 localisation and signalling is affected in these cells. It is also possible that the centrosome plays an important role in the G2/M transition when it is present in cells, but that when removed there are compensatory mechanisms for some important centrosomal functions.

Furthermore, there is contention surrounding the suggested role of Cyclin B1-Cdk1 signalling at the centrosome and SPB. Although it is suggested that centrosomes are the site for Cyclin B1-Cdk1 activation in human cells, it is suggested that the nucleus, not the centrosome, is the site for Cdk1 activation in *Xenopus* (Jackman et al., 2003, Afanzar et al., 2020, Nolet et al., 2020).

1.7 Cyclin localisation to the SPB and centrosome

The work discussed in the previous sections has demonstrated that cyclin localisation is important for cell cycle control, influencing CDK substrate specificity, cell cycle progression, and potentially the switch-like nature of cell cycle transitions. The key role of the SPB in mitotic entry indicates that cyclin-CDK localisation to the SPB, and possibly the centrosome, is important, but it is not known if it is essential for mitotic entry. *S. pombe* provides an ideal model to study the importance of cyclin-CDK localisation to the SPB. As mitosis is driven by just one cyclin-CDK complex, Cdc13-Cdc2, we can study the role of SPB localisation in this relatively simple system. To study the importance of Cdc13-Cdc2 SPB localisation and the impact of preventing this localisation, the determinant of cyclin-CDK localisation to the SPB first needs to be identified.

Furthermore, although it is clear that the temporal control of CDK activity is important in cell cycle regulation, it is less clear how this fits with what is known of cyclin-CDK localisation in *S. pombe*. For example, it is not known if CDK activity is homogenous throughout the cell, or if activity can be detected in one location before it is detected in the rest of the cell. It is also unknown whether the localisation of CDK and its substrates affect the timing of their phosphorylation.

These questions drive the work in this thesis. The determinant for Cdc13 and Cyclin B1 localisation to the SPB and centrosome is studied in the first two Results chapters. In the third chapter I present work addressing the importance of Cdc13 localisation to the SPB, and in the final Results chapter I present initial work developing a system that has potential to provide spatial information of CDK substrate phosphorylation.

Chapter 2. Materials & Methods

2.1 Fission yeast growth and synchronisation

Fission yeast media and cell culture are as described previously (Moreno et al., 1991). Cells were grown in YE4S medium (yeast extract with the supplements adenine, leucine, histidine and uridine at 0.25 g/L) at 25 °C unless stated otherwise, apart from experiments involving the thiamine repressible *nmt41* promoter, in which cells were grown in EMM4S (Edinburgh minimal media with the supplements adenine, leucine, histidine and uridine at 0.15 g/L) on agar plates or EMM + adenine or EMM + adenine + leucine (in liquid culture, for the G1 arrest experiments) at 32 °C unless stated otherwise. All experiments were carried out in exponential growth. Strain construction was performed by mating followed by random spore analysis, or transformation (Moreno et al., 1991), and confirmed by colony PCR. Strains and plasmids used in this study are listed in Table 2.1 and Table 2.2 respectively. Where strains or plasmids were gifted from others, it is noted in the origin column of Table 2.1, Table 2.2 and Table 2.3. The following plasmids were both gifts from Michael Nick Boddy and bought from Addgene: pFA6a-KanMX-tetO-pCyc1 (TetP) (Addgene plasmid # 41023; http://n2t.net/addgene:41023; RRID:Addgene_41023); and pDM291-tetR-tup11Δ70 (Addgene plasmid # 41027; http://n2t.net/addgene:41027; RRID:Addgene_41027). pFA6a-GBP-mCherry-kanMX6 was a gift from Quanwen Jin (Addgene plasmid # 89068; http://n2t.net/addgene:89068; RRID:Addgene_89068).

G2 arrest of *cdc25-22* cells was performed by shifting cells to 36 °C until no septated cells were seen under the microscope (2 hours 40 minutes). G2 arrest of *cdc2(as)-M17* cells was performed by addition of 1 μM 1-NmPP1 (Toronto Research Chemicals) dissolved in dimethyl sulfoxide (DMSO) for one generation. G1 arrest of cells was performed by taking an exponentially growing culture at a density of 2 x 10^6 cells/mL and washing three times in media containing no ammonium chloride and no amino acid supplements. Cells were held in the nitrogen starvation for between 16-18 hours at 25 °C, before release by washing 3-4 times into EMM media (containing nitrogen) + supplements (adenine for the experiment in section 5.1, and adenine + leucine in the experiment in section 5.4).

To repress the thiamine repressible *nmt41* promoter, thiamine hydrochloride (Sigma) dissolved in water was added to a final concentration of 30 μM, 1 hour before release from the nitrogen arrest, and to the media used to release the cells.

To induce protein expression under the tetracycline-inducible enoTetP promoter described in (Patterson et al., 2019), anhydrous tetracycline dissolved in DMSO was added to a final concentration of 0.3125 μg/mL. To induce protein expression from the TetP promoter described in (Zilio et al., 2012), a final concentration of 1.25 μg/mL was used. For the experiments in section 5.4, strains were maintained in 10 μM 1-NmPP1 throughout growth before the experiment, and after release from the nitrogen starvation, until 1-NmPP1 wash-out.

2.2 Human cell line culture

The U2OS human osteosarcoma cell line stably expressing γ-tubulin-eGFP was a gift from Jonathan Higgins (Dai et al., 2009). P-cyclinB1-mcherry (1958) was a gift from Jonathon Pines (Addgene plasmid #26063; http://n2t.net/addgene:26063; RRID:Addene_26063) (Gavet and Pines, 2010b). Cyclin B1-YFP plasmid was a gift from Silvia Santos, and described in (Gong et al., 2007). pIRES-Centrin1-mCherry was a gift from Matthieu Piel (Addgene plasmid # 64338; http://n2t.net/addgene:64338; RRID:Addgene_64338). To create Cyclin $B1^{HPM}$-YFP and Cyclin $B1^{HPM}$-mCherry, the plasmids above were modified to introduce the M201A, L205A, and W208A substitutions using the following primers: 5' – gcaattgacgcgctagtacaggttcaaatgaaattc – 3' and 5' – gatggctctagcgtttccagtgacttcccg – 3'. The primers were used to introduce the desired mutations using KAPA HiFi HotStart Readymix (KAPA Biosystems) according to the manufacturers protocol, using an annealing temperature of 56 °C. The product was incubated with KLD mix (New England BioLabs) to digest the template DNA and phosphorylate and ligate the product. The ligated plasmid was introduced into NEB 5-alpha competent cells (New England BioLabs) by transformation, and the plasmid subsequently purified using a QIAGEN Plasmid kit.

HeLa Kyoto and U2OS cells were cultured in Dulbecco's modified Eagle's medium (DMEM, Gibco) containing 10 % FBS, 50 U/mL penicillin and 50 µg/mL streptomycin at 37 °C and 5 % CO_2. Transfection was carried out using Lipofectamine 3000 (Thermo-Fisher) according to manufacturer's protocol in Opti-MEM media (Gibco). Cell lines were tested for mycoplasma by the Cell Services Science Technology Platform at the Francis Crick Institute.

2.3 Fluorescence microscopy

Fluorescence microscopy was performed as described before (Basu et al., 2020), also outlined below for clarity. A Nikon Ti2 inverted microscope was used, equipped with a Perfect Focus System and Okolab environmental chamber, and a Prime sCMOS or BSI camera (Photometrics). Micro-Manager v2.0 software (Open-imaging) was used to control the microscope (Edelstein et al., 2014). Fluorescence excitation was carried out using a SpectraX LED light engine (Lumencor) fitted with the following standard filters: 395/25 for imaging DAPI/calcofluor, 470/24 for imaging sfGFP/eGFP; and 575/25 for imaging mCherry/mRFP; with either a dual-edge ET-eGFP/mCherry dichroic beamsplitter (Chroma 59022bs), or a 409/493/573/652 nm BrightLine® quad-edge dichroic beamsplitter (Semrock). The following emission filters were used: Semrock, 438/24 nm BrightLine® single-band bandpass filter for imaging DAPI/calcofluor; Chroma, ET - EGFP single-band bandpass filter ET525_50m for imaging sfGFP/eGFP; and Semrock, 641/75 nm BrightLine® single-band bandpass filter FF02_641_75 for imaging mCherry/mRFP. ImageJ software (NIH) was used to measure pixel intensity, adjust brightness and contrast, apply a pixel range to images, and render maximum projection images (Schindelin et al., 2012).

For *S. pombe* experiments, a 100X Plan Apochromat oil-immersion objective (NA 1.45) was used and microscopy performed at 25 °C. Cells (from live-cell imaging and fixed cell imaging) were segmented using Ilastik, with segmentation training files supplied by Scott Curran or developed using brightfield images from the experiment (Berg et al., 2019). SPBs were also segmented using Ilastik, based on Sid4-mRFP signal. The resulting masks were dilated by 3 pixels using ImageJ

software to ensure that they covered SPB signal, and the mean of the top 10 pixels within the mask were measured as a readout of SPB intensity. Fluorescence intensity measurements were performed on maximum intensity projection images. For intensity measurements performed in Chapter 3, the mean value of background autofluorescence was removed, measured using a strain in the same experimental conditions but not expressing the fluorophore being measured. The presence of Cdc13-sfGFP, Plo1-mCherry or Spo15 foci at the SPB was judged by eye. In strains with Sid4-mRFP, any cells without Sid4-mRFP signal (presumed to be out of focus) were excluded from analysis.

For experiments with U2OS cells, cells were seeded 24 hours before transfection in 35 mm glass-bottom dishes (MatTek Corporation). Fluorescence imaging was performed 24 hours after transfection, with the environmental chamber heated to 37 °C with 5 % CO_2 supply. A 40X Plan Apochromat Fluor objective (NA 0.95) was used. For time-lapse experiments, z-stacks were acquired every 10 minutes. For experiments identifying Cyclin B1-mCherry accumulation at the centrosome, cells with Cyclin B1-mCherry expression above 9000 AU were excluded from analysis as high levels of Cyclin B1 overexpression could result in its mislocalisation. Cells with signal intensity below ~1000 AU were excluded as the signal was too close to background for Cyclin B1 localisation to be determined. Cells in which the centrosome was not in focus (judged by γ-tubulin-eGFP signal) were also excluded from analysis. Cyclin B1-mCherry centrosomal localisation was determined by eye and by checking for an overlapping peak of γ-tubulin-eGFP and Cyclin B1-mCherry signal using line scans drawn with the FIJI plot profile function. Graphs of vertically-averaged pixel intensity across a line scan shown in Chapter 4 were produced using the FIJI plot profile function, using a line 3 pixels in height that was drawn through the centrosome.

Brightfield microscopy of *S. pombe* cells on plates (in Sections 5.2 and 5.3) was performed using an Axioskop 40 plate microscope (Zeiss), with a 50X CF Plan objective (NA 0.55) and a Sony NEX-5N camera.

2.4 Flow cytometry and cell cycle progression analysis

DNA content analysis on *S. pombe* cells was performed by flow cytometry. Cells were fixed in 70 % ice-cold ethanol, before being washed and resuspended in 50 mM sodium citrate. Samples were incubated with 0.1 mg/mL RNase A at 37 °C for at least 3 hours. DNA was stained with Sytox Green (1 µM, Invitrogen). 100,000 events were acquired on either an LSRII or BD LSRFortessa, using FACS Diva software. DNA content is displayed on a linear scale after gating for single cells in FlowJo v10.3 (Treestar Inc).

Binucleation and septation analyses were performed by heat-fixing cells on a microscope slide at 70 °C before staining with 4',6-diamidino-2-phenylindole (DAPI) (SlowFade Diamond Antifade Mountant with DAPI, Invitrogen) and Calcofluor (Sigma).

2.5 Protein extraction, immunoprecipitation and Western blotting

For U2OS cell denatured protein extract, transfected U2OS cells were resuspended in lysis buffer (Laemmli sample buffer (BioRad), 10 % β-mercaptoethanol) and incubated at 99 °C for 8 minutes. Protein detection by Western blotting was carried out using 1:2000 Cyclin B1 (V152) mouse monoclonal antibody from Cell Signalling (Cat# 4135, RRID:AB_2233956).

For immunoprecipitation experiments, U2OS cell extract preparation and immunoprecipitation was carried out using RFP-trap (Chromotek) according to the manufacturer's instructions. 1.9 x 10^6 cells were seeded in 10 cm dishes, and roughly 24 hours later cells were transfected with the relevant plasmid. Roughly 24 hours after transfection, cells were washed in ice-cold phosphate-buffered saline (PBS), and cells were collected into a pre-cooled tube. Cells were washed with ice-cold PBS two more times. Cells were then lysed by resuspension in 200 µL ice-cold lysis buffer (10 mM Tris/Cl pH 7.5, 150 mM NaCl, 0.5 mM ethylenediamine tetraacetic acid (EDTA), 0.5 % Nonidet P40 substitute, 1 mM phenylmethylsufonyl

fluoride (PMSF), 1X protease inhibitor cocktail set III (EDTA free, CalBiochem) and 1X PhosSTOP phosphatase inhibitor cocktail (Roche)) followed by incubation on ice for 30 min, during which time the suspension was mixed by pipetting every 10 min. Cell lysate was spun down and the supernatant transferred to an ice-cold tube, followed by addition of 300 µL dilution buffer (10 mM Tris/Cl pH 7.5, 150 mM NaCl, 0.5 mM EDTA, 1 mM PMSF, 1X protease inhibitor cocktail set III (EDTA free, CalBiochem) and 1X PhosSTOP phosphatase inhibitor cocktail (Roche)). The RFP-trap magnetic agarose beads were equilibrated in dilution buffer, and the diluted lysate was added to the equilibrated beads and incubated at 4 °C for 1 hour whilst rotating. The beads were washed 3 times in wash buffer (10 mM Tris/Cl pH 7.5, 150 mM NaCl, 0.5 mM EDTA, 0.05 % Nonidet P40 subsitute), transferring the beads to a new tube on the last wash step. The washed beads were then resuspended in SDS-sample buffer and boiled at 95 °C for 5 min to elute immunocomplexes. Protein detection was carried out using anti-Cyclin B1 antibody as described above or 1:500 anti-CDK1 [A17] mouse monoclonal from Abcam (Cat# ab18, RRID:AB_2074906).

S. pombe protein extracts for Western blotting were prepared by addition of ice-cold 100 % w/v trichloroacetic acid (TCA) to a final volume of 10 % to a cell culture. Cells were kept on ice for at least 30 minutes before being washed in ice-cold acetone. Dry pellets were stored at -80 °C, before being washed and resuspended in lysis buffer (8 M urea, 50 mM ammonium bicarbonate, 5 mM ethylenediamine tetraacetic acid (EDTA), 1 mM phenylmethylsufonyl fluoride (PMSF), 1X protease inhibitor cocktail set III (EDTA free, CalBiochem), and 1X PhosSTOP phosphatase inhibitor cocktail (Roche)). Cells were lysed by beating with glass beads (using a FastPrep120), and the supernatant collected after cell debris was pelleted. Mitotic cell extracts were made by first adding 1 µM 1-NmPP1 to *cdc2(as)-M17* cells for at least 1 generation to arrest cells in G2. Cells were released by 1-NmPP1 removal, and TCA was added to the culture between 8-10 minutes after release to collect a mitotic cell extract. Kinase-dead extract was made by adding 10 µM 1-NmPP1 to *cdc2(as)-M17* cells for 30 min, before TCA addition. Ponceau staining was performed using Ponceau S solution (Sigma). Antibodies used in *S. pombe* studies were: Cdc2 Y63.2 mouse monoclonal antibody (1:40,000 dilution, lab stock); and novel antibodies generated in the course of this study (dilution indicated in figure

legend), that are covered later in the methods. Western blot quantitation was performed using Image Studio Lite software (Li-Cor). For Ponceau staining quantitation, a blank lane (PBS + loading buffer) was used to determine the background using the Assign Shape function. For antibody quantitation, background was calculated for each lane by taking the median signal from the top/bottom of the measured rectangle.

For all protein detection via Western blotting, the secondary antibodies used were: 1:5000 anti-mouse IgG HRP-linked whole antibody from sheep (GE Healthcare Cat# NA931, RRID:AB_772210); 1:5000 anti-rabbit IgG HRP-linked whole antibody from donkey (GE healthcare, Cat# NA934, RRID:AB_772206). Signal was detected with SuperSignal West Femto Maximum Sensitivity Substrate (Cat # 34095, Life Technologies), and images taken on an Amersham Imager 600.

2.6 Antibody generation and immunofluorescence

Novel antibodies used in this study (against Bqt4-T272, Bit61-S132, Crf1-T316, Dnt1-T225 and Spo15-S121) were generated and purified by an external company (Covalab) against a peptide encompassing the phosphosite of interest. Antisera was incubated with a non-phosphorylated peptide to isolate the Bqt4-ctrl, Bit61-ctrl, Crf1-ctrl, Dnt1-ctrl and Spo15-ctrl antibodies, and the remaining antisera was incubated with a phosphorylated peptide to isolate the Bqt4-pT272, Bit61-pS132, Crf1-pT316, Dnt1-pT225 and Spo15-pS121 antibodies.

For immunofluorescence, 15 mL cells were fixed by adding 5 mL of 16 % paraformaldehyde solution (methanol-free, Agar Scientific, Cat# AGR1026) to a final concentration of 4 %. Samples were processed as described previously with a few minor changes (Hagan, 2016). Samples were incubated at room temperature (19 – 23 °C) whilst rocking for 35 - 50 minutes, before washing cells 3 times in PEM (100 mM PIPES pH 6.9, 1 mM ethylene glycol bis(2-aminoethyl)tetraacetic acid (EGTA) pH 8.0, 1 mM $MgSO_4$). Cells were resuspended in PEMS (PEM, 1 M sorbitol) with 0.5 mg Lysing enzyme from *Trichoderma harzanum* (novozyme) (Sigma) and 0.25 mg Zymolyase-20T (stock 20000 U/gm, ICN Biomedicals) and

incubated at 37 °C for 8-10 minutes. Cells were washed in PEMS and resuspended in PEMS with 1% Triton for 2 min. Cells were washed 3 times in PEM, before resuspension in PEMBAL (PEM, 100 mM lysine hydrochloride, 1 % BSA, 0.1 % NaN_3) and rotation at room temperature for at least 30 min. Cells were pelleted and resuspended in 100 µL primary antibody (1:50 dilution in PEMBAL) and incubated overnight on a rotating wheel at room temperature. Cells were then washed 3 times in PEMBAL before resuspension in PEMBAL and rotation at room temperature for at least 30 minutes. Cells were then incubated with 1:1000 donkey anti-rabbit Alexa-488 conjugated secondary antibody (lab stock) in PEMBAL overnight at room temperature, before being washed and stored for at least 48 hours in PEMBAL at 4 °C. Samples were mixed with DAPI on a microscope slide and imaged immediately.

2.7 Phosphoproteomics

The experiment inducing Cdc13-L-Cdc2 fusion proteins under the tet inducible promoter was designed and performed by Souradeep Basu. Protein extraction was performed by Souradeep Basu, and sample preparation for phosphoproteomics and mass spectrometry analysis were performed by Andrew Jones. Subsequent data analysis was performed by Souradeep Basu. Details of phosphoproteomic sample preparation and analysis were provided by Andrew Jones, and described in (Basu et al., 2021).

Protein extraction was performed as described above for Western blotting, with the exception that the lysis buffer consisted of 8 M urea, 50 mM ammonium bicarbonate, 1X cOmplete mini EDTA-free protease inhibitor and 1X phosSTOP phosphatase inhibitor cocktail.

Each protein sample (400 µg) was reduced with 5 mM dithiothreitol (DTT) for 25 min at 56 °C, alkylated with 10 mM iodoacetamide for 30 min at room temperature in the dark and then quenched with 7.5 M DTT. Samples were digested using SP3 on-bead methodology (Hughes *et al*, 2019) with the variation that 50 mM HEPES (pH 8.5) was used in place of ammonium bicarbonate. Briefly,

proteins were bound to the SP3 beads (10:1 beads:protein (w/w)) in 50 % ethanol (v/v) and then washed three times in 80 % ethanol, prior to resuspension in 50 mM HEPES (pH 8.5) with 1:40 (trypsin:protein (w/w)) overnight at 37 °C. The digested samples were arranged in sets of 16 and labelled using the TMTpro 16plex Isobaric Label Reagent Set (Thermo Fisher), as per the manufacturer's instructions. Following labelling and mixing, multiplexed samples were desalted using a C18 SepPak column. Phosphopeptide enrichment was performed by Sequential Enrichment from Metal Oxide Affinity Chromatography (SMOAC, Thermo Fisher) with initial enrichment using the HighSelect TiO2 Phosphopeptide Enrichment Kit followed by the HighSelect Fe-NTA Phosphopeptide Enrichment Kit (both Thermo Scientific) for the non-bound flow through fractions. Phosphopeptides and non-bound flow through fractions were desalted and fractionated using the High pH Reversed-Phase Peptide Fractionation Kit (Pierce) and analysed on an Orbitrap Fusion Lumos mass spectrometer (Thermo Fisher) coupled to an UltiMate 3000 HPLC system for online liquid chromatographic separation. Each run consisted of a 3 hour gradient elution from a 75 µm × 50 cm C18 column. MaxQuant (version 1.6.14.0) was used for all data processing. The data were searched against a PomBase (Lock et al., 2019) extracted *S. pombe* proteome FASTA file. Default MaxQuant parameters were used with Phospho(STY) being added as a variable modification, MaxQuant output files were imported into Perseus (version 1.6.14.0).

Name	Genotype		Origin
PN5605	*sid4-mRFP:kanMX6_ura4-D18_leu1-32_ade6-*	h+	(Kume et al., 2019)
ER109	*cdc2-mNeonGreen:kanMX6_sid4-mRFP:kanMX6_ura4-D18_ade6-_leu1-32*	h-	This study
ER106	*suc1-mNG:kanMX6_sid4-mRFP:kanMX6_ura4-D18_ade6-*	h+	This study
ER107	*cdc13-sfGFP_sid4-mRFP:kanMX6*	h?	This study
ST946	*cdc13-sfGFP*	h90	(Kamenz et al., 2015)
ER94	*cdc25-mNeonGreen:kanMX6_sid4-mRFP:kanMX6_ura4-D18*	h?	This study
ER61	*leu1-32Δ::cdc13P-cdc13(wt)-sfGFP-cdc13T:hphMX6_sid4-mRFP:kanMX6_ura4-D18_ade6-*	h+	This study
ER62	*leu1-32Δ::cdc13P-cdc13(M235A, L239A, W242A)sfGFP-*	h+	This study

	cdc13T:hphMX6_sid4-mRFP:kanMX6_ura4-D18_ade6-		
ER74	*cdc25-22 leu1Δ::cdc13P-cdc13(wt)sfGFP-cdc13T:hphMX6 sid4-mRFP:kanMX6_ura4-D18_ade6-*	h-	This study
ER75	*cdc25-22 leu1Δ::cdc13P-cdc13(M235A, L239A, W242A)sfGFP-cdc13T:hphR_sid4-mRFP:kanMX6_ura4-D18_ade6-*	h-	This study
ER60	*cdc25-22_sid4-mRFP:kanMX6_ura4-D18_ade6-*	h-	This study
PN5478	*cdc2(as)-M17:bsdMX6*	h+	(Aoi et al., 2014)
ER123	*cdc2(as)-M17:bsdMX6_leu1Δ::cdc13P-cdc13(M235A, L239A, W242A)sfGFP-cdc13T:hphMX6*	h+	This study
ER125	*cdc2(as)-M17:bsdMX6_leu1Δ:cdc13P-cdc13(wt)sfGFP-cdc13T:hphMX6*	h+	This study
PN 5745	*plo1-mCherry:natMX6_ade6-M210_leu1-*	h-	(Heinrich et al., 2012)
ER76	*leu1-32Δ::cdc13P-cdc13(wt)sfGFP-cdc13T:hphMX6_ade6-M210_plo1-mCherry:natMX6*	h-	This study
ER77	*leu1-32Δ::cdc13P-cdc13(M235A, L239A, W242A)sfGFP-cdc13T:hphMX6_ade6-M210_plo1-mCherry:natMX6*	h-	This study
ER298	*cdc13Δ::ura4+_pREP41::cdc13int LEU2+_leu1Δ::cdc13P-cdc13(M235A, L239A, W242A)sfGFP-cdc13T:hphMX6_Δcig1::ura4+_Δcig2::ura4+_sid4-mRFP:kanMX6_ade-_ura4-D18*	h+	This study
ER299	*cdc13Δ::ura4+_pREP41::cdc13int LEU2+_leu1Δ::cdc13P-cdc13(wt)sfGFP-cdc13T:hphMX6_Δcig1:ura4+_Δcig2:ura4+_sid4-mRFP:kanMX6_ade-_ura4-D18*	h+	This study
IH1356	*cut12-NEGFP:ura4_leu1-32_ura4-D18*	h-	(Bridge et al., 1998)
ER286	*cdc13Δ::ura4+_pREP41::cdc13int LEU2+_leu1Δ::cdc13P-cdc13(M235A, L239A, W242A)-cdc13T:hphMX6_cdc2-GBP-mCherry:hphMX6_cig1Δ::ura4+_cig2Δ::ura4+_ura4-D18*	h+	This study
ER342	*cdc13Δ::ura4+_pREP41::cdc13int LEU2+_leu1Δ::cdc13P-cdc13(M235A, L239A, W242A)-cdc13T:hphMX6_cdc2-GBP-mCherry:hphMX6_cig1Δ::ura4+_cig2Δ::ura4+_lys+::adh1P-GFP-adh1T:natMX6_ura4-D18*	h+	This study
ER339	*cdc13Δ::ura4+_ura4-D18 pREP41::cdc13int LEU2+_cig1Δ::ura4+_cig2Δ::ura4+_cut12-NEGFP:ura4+_ade6-_leu1-32Δ::cdc13P-cdc13(M235A, L239A, W242A)-L-cdc2(F84G)-GBP-mCherry-cdc13T:hphMX6*	h-	This study
ER296	*cdc13Δ::ura4+_ura4-D18 pREP41::cdc13int LEU2+_cig1Δ::ura4+_cig2Δ::ura4+_cut12-NEGFP:ura4+_ade6-_leu1-32*	h-	This study
ER320	*cdc2-M26_ura4-D18:tetR-tup11Δ70::ura4+_leu1Δ::enoTetP-*	h-	This study

	cdc13(M235A, L239A, W242A)-L-cdc2(F84G)-GBP-mCherry-adh1T:hphMX6		
ER321	*cdc2-M26_ura4-D18:tetR-tup11Δ70::ura4+_cut12-NEGFP:ura4+_leu1-32Δ::enoTetP-cdc13(M235A, L239A, W242A)-L-cdc2(F84G)-GBP-mCherry-adh1T:hphMX6*	h-	This study
ER323	*cdc2-m26_leuΔ::cdc13P-cdc13-L-cdc2(F84G)-cdc13T:hphMX6*	h-	This study
ER325	*cdc2-M26_leuΔ::cdc13P-cdc13(M235A, L239A, W242A)-L-cdc2(F84G)-GBP-mCherry-cdc13T:hphMX6*	h-	This study
ER334	*cdc2-m26_leuΔ::cdc13P-cdc13(M235A, L239A, W242A)-L-cdc2(F84G)-cdc13T:hphMX6*	h-	This study
ER335	*cdc2-M26_cdc13Δ::ura4+_ura4-D18_pREP41::cdc13int:LEU2+_leu1-32Δ:cdc13P-cdc13(M235A, L239A, W242A)-L-cdc2(F84G)-GBP-mCherry-cdc13T:hphMX6_ade6-_cig1Δ::ura4+_cig2Δ::ura4+*	h?	This study
PN1813	*cdc13Δ::ura4+_ura4-D18_pREP41::cdc13int:LEU2+_leu1-32_ade6-_cig1Δ::ura4+_cig2Δ::ura4+*	h+	Lab stock
ER324	*cdc13Δ::ura4+_ura4-D18_pREP41::cdc13int LEU2+_ade6-_cig1Δ::ura4+_cig2Δ::ura4+_leuΔ::cdc13P-cdc13-L-cdc2(F84G)-Cdc13T:hphMX6*	h+	This study
ER328	*cdc13Δ::ura4+_ura4-D18_pREP41::cdc13int:LEU2+_leu1-32Δ::cdc13P-cdc13(M235A, L239A, W242A)-L-cdc2(F84G)-GBP-mCherry-Cdc13T:hphMX6_ade6-_cig1Δ::ura4+_cig2Δ::ura4+*	h+	This study
ER329	*cdc13Δ::ura4+_ura4-D18_pREP41::cdc13int:LEU2+_leu1-32Δ::cdc13P-cdc13-L-cdc2(F84G)-GBP-mCherry-cdc13T:hphMX6_ade6-_cig1Δ::ura4+_cig2Δ::ura4+*	h+	This study
ER330	*cdc13Δ::ura4+_ura4-D18_pREP41::cdc13int:LEU2+_leu1-32Δ::cdc13P-cdc13(M235A, L239A, W242A)-L-cdc2(F84G)-cdc13T:hphMX6_ade6-_cig1Δ::ura4+_cig2Δ::ura4+*	h+	This study
ER343	*cdc13Δ::ura4+_ura4-D18_pREP41::cdc13int:LEU2+_ade6-_cig1Δ::ura4+_cig2Δ::ura4+ leu1-32Δ:cdc13P-cdc13(wt)sfGFP-L-cdc2(T14A,Y15F,F84G)-cdc13T-hphMX6*	h+	This study
ER198	*cdc13Δ::ura4+_ura4-D18_pREP41::cdc13int:LEU2+_ade6-_cig1Δ::ura4+_cig2Δ::ura4+_leu1-32Δ::cdc13P-cdc13(M235A, L239A, W242A)-L-cdc2(T14A,Y15F,F84G)-cdc13T:hphMX6*	h+	This study
ER191	*cdc13Δ::ura4+_ura4-D18_pREP41::cdc13int:LEU2+_ade6-_cig1Δ::ura4+_cig2Δ::ura4+_leu1-32Δ::cdc13P-cdc13(M235A, L239A, W242A)sfGFP-L-cdc2(T14A,Y15F,F84G)-cdc13T:hphMX6*	h+	This study
ER338	*cdc13Δ::ura4+_ura4-D18_pREP41::cdc13int:LEU2+_leu1-32Δ::cdc13P-cdc13(M235A, L239A, W242A)-sfGFP-L-cdc2(F84G):hphMX6_ade6-_cig1Δ::ura4+_cig2Δ::ura4+*	h+	This study
PN1	*wild-type*	h-	Lab stock
ER262	*dnt1Δ::kanMX6*	h-	This study

ER132	*bit61Δ::kanMX6_ade6-_leu1-32_ura4-D18*	h+	(Kim et al., 2010)
ER133	*crf1Δ::kanMX6_ade6-_leu1-32_ura4-D18*	h+	(Kim et al., 2010)
ER143	*spo15Δ::kanMX6_ade6-_leu1-32_ura4-D18*	h+	(Kim et al., 2010)
ER177	*bqt4Δ:kanMX6_cut11:GFP:ura4+ leu- ura4-*	h-	Kazunori Kume
ER235	*cdc2(as)-M17:bsdMX6_sid4-mRFP:kanMX6_ura4-D18_ade6-*	h+	This study
ER352	*cdc13Δ::ura4+_ura4-D18_pREP41::cdc13int LEU2+_cig1Δ::ura4+_cig2Δ::ura4+_tetR-tup11Δ70:ura4+_cut12-NEGFP:ura4+_leu1Δ::cdc13P-cdc13(M235A, L239A, W242A)-cdc13T:hphMX6_lys1^{+}::tetP-Cdc2(as)-M17-GBP-mCherry-adh1T:natMX6_ade6-*	h-	This study
ER353	*cdc13Δ::ura4+_ura4-D18_pREP41::cdc13int LEU2+_cig1Δ::ura4+_cig2Δ::ura4+_tetR-tup11Δ70:ura4+_leu1Δ::cdc13P-cdc13(M235A, L239A, W242A)-cdc13T:hphMX6_ lys1^{+}::tetP-Cdc2(as)-M17-GBP-mCherry-adh1T:natMX6_ade6-*	h+	This study

Table 2.1 | *S. pombe* strains used in this study

The following are worth noting: the thiamine-repressible *nmt41* promoter is referred to by the genotype pREP41; the HPM mutation in *S. pombe* Cdc13 is denoted by the specific residue changes M235A, L239A, W242A; the AF mutation in Cdc2 is denoted by the specific residue changes T14A, Y15F; the original analogue-sensitive (as) mutation in Cdc2 is used in the Cdc13-L-Cdc2 fusion proteins and denoted by the residue change F84G (Bishop et al., 2000); the optimised analogue sensitive Cdc2 allele Cdc2(as)-M17 is used where Cdc2 is monomeric (Aoi et al., 2014); *cdc13P* refers to the *cdc13* promoter region; *cdc13T* refers to the *cdc13* terminator region; *tetP* refers to the tetracycline-inducible promoter described in (Zilio et al., 2012); *enoTetP* refers to the tetracycline-inducible promoter described in (Patterson et al., 2019); *adh1P* refers to the *adh1* promoter region; *adh1T* refers to the *adh1* terminator region; *LEU2+* refers to the *S. cerevisiae LEU2* gene.

Plasmid number	Name	Integration site	Digest with	Origin
ERp3	*pFA6a_leu::cdc13P-cdc13-sfGFP-cdc13T:hphMX6*	leu1	PvuII	This study
ERp4	*pFA6a_leu::cdc13P-cdc13(M235A, L239A, W242A)-sfGFP-cdc13T:hphMX6*	leu1	PvuII	This study
Addgene 26063	*Cyclin B1-mCherry*			(Gavet and Pines, 2010b)
ARC1353	*Cyclin B1(M201A,L205A,W208A)-mCherry*			This study
ARC1349	*Cyclin B1-YFP*			(Gong et al., 2007)
Addgene 64338	*Centrin 1-mCherry*			Matthieu Piel (unpublished)
ARC1350	*Cyclin B1(M201A,L205A,W208A)-YFP*			This study
ERp48	*PCST3-adh1P-GFP-adh1T:natMX6*	lys1	Blp1	This study
ERp43	*leu::enoTetP-cdc13(M235A, L239A, W242A)-L-cdc2(F84G)-GBP-mCherry-adh1T:hphMX6*	leu1	Swa1	This study
MSp290	*pFA6a_leu::cdc13P-cdc13-L-cdc2(F84G)-cdc13T-nmt1T-HphMX6*	leu1	PvuII	Matthew Swaffer
MSp291	*pFA6a_leu::cdc13P-cdc13(M235A, L239A, W242A)-L-cdc2(F84G)-cdc13T-nmt1T-HphMX6*	leu1	PvuII	Matthew Swaffer
Addgene 89068	*pFA6a-GBP-mCherry-kanMX6*			(Chen et al., 2017)
ERp44	*pFA6a_leu::cdc13P-cdc13(M235A, L239A, W242A)-L-cdc2(F84G)-GBP-mcherry-cdc13T:hphMX6*	leu1	PvuII	This study
ERp45	*pFA6a_leu::cdc13P-cdc13-L-cdc2(F84G)-GBP-mcherry-cdc13T:hphMX6*	leu1	PvuII	This study
ARC1284	*pFA6a_leu::cdc13P-cdc13(M235A, L239A, W242A)-L-cdc2(T14A;Y15F;F84G)-cdc13T:hphMX6*	leu1	PvuII	Souradeep Basu
ARC1321	*pFA6a_leu::cdc13P-cdc13(M235A, L239A, W242A)sfGFP-L-cdc2(T14A;Y15F;F84G)-cdc13T:hphMX6*	leu1	PvuII	Souradeep Basu
ERp50	*pFA6a_leu::cdc13P-cdc13sfGFP-L-cdc2(T14A;Y15F;F84G)-cdc13T:hphMX6*	leu1	PvuII	This study
SBp22	*pFA6a_leu::cdc13P-cdc13(M235A, L239A, W242A)sfGFP-L-cdc2(F84G)-cdc13T:hphMX6*	leu1	PvuII	Souradeep Basu
Addgene 41023	*pFA6a_KanMX-tetO-pCyc1* (referred to as TetP)			(Zilio et al., 2012)
Addgene 41027	*pDM291-tetR-tup11Δ70*	3' of ura4	BamH1	(Zilio et al., 2012)
ERp53	*pCST3_tetP-cdc2(as)-M17-GBP-mCherry:natMX6*	lys1	Blp1	This study

Table 2.2 | Plasmids used in this study

Fusion Protein	Origin	Tag location	Linker sequence
Sid4-mRFP	(Kume et al., 2019)	RFP is C-terminal of Sid4	(Kume et al., 2019)
Cdc2-mNeonGreen	Scott Curran (Nurse lab)	mNeonGreen is immediately C-terminal of ORF	(Cdc2)…gattttcat – **gattctgctggatcagctggcgactctgcaggctctgctgga** – atggtttct (mNeonGreen)
Suc1-mNeonGreen	Scott Curran (Nurse lab)	mNeonGreen is immediately C-terminal of ORF	(Suc1)…cggggtggt – **gattctgctggatcagctggcgactctgcaggctctgctgga** – atggtttct (mNeonGreen)
Cdc13-sfGFP (at endogenous Cdc13 locus)	(Kamenz et al., 2015)	Internal – circularly permuted sfGFP inserted between Ser177 and Val178 of Cdc13	An additional Gly residue as a spacer
LeuΔ::Cdc13P-Cdc13-sfGFP-Cdc13T and derivatives (used where Cdc13 is introduced exogenously: ERp3, ERp4)	This study	Circularly permuted sfGFP is internal to Cdc13 between Ser177 and Val178 (as above)	An additional Met residue on N terminus of sfGFP
Cdc25-mNeonGreen	Scott Curran (Nurse lab)	mNeonGreen is immediately C-terminal of ORF	(Cdc25)…agaagattt – **gattctgctggatcagctggcgactctgcaggctctgctgga** – atggtttct (mNeonGreen)
Plo1-mCherry	(Heinrich et al., 2012)	mCherry is C-terminal of Plo1	(Heinrich et al., 2012)
Cut12-NEGFP	(Bridge et al., 1998)	N terminal; GFP is inserted at Met33 of Cut12	None
Cdc2-GBP-mCherry (at endogenous locus, in strains ER286, ER342)	Souradeep Basu (Nurse lab)	GBP-mCherry immediately C-terminal of Cdc2 ORF	*Cdc2-GBP linker*: (Cdc2)…gattttcat – **cggatccccgggttaattaacatggctgat** - gtccaactg…(GBP) *GBP-mCherry linker*: (GBP)…gtctcctct – **agc** – atggtgagc (mCherry)
Cdc13-L-Cdc2 (all constructs using Cdc13-L-Cdc2 contain the same linker)	(Coudreuse and Nurse, 2010)	Cdc2 is C-terminal of Cdc13	(Cdc13)…gaagaatgg – **gcggccgcaggtggtggttctggtggtggttctggtggtggatcc** – atggagaat…(Cdc2)

Cdc13-L-Cdc2(as)-GBP-mCherry and derivatives (ERp43, 44, 45)	This study	GBP-mCherry immediately C-terminal of Cdc2 ORF	*Cdc2-GBP linker:* (Cdc2)…gattttcat – **gggttgataaatatggccgac** – gttcaatta…(GBP) *GBP-mCherry linker*: (GBP)…gtctcctct – **tcc** – atggtgagc (mCherry)
Cdc2(as)-M17-GBP-mCherry (introduced as exogenous copy) (ERp53)	This study	GBP-mCherry immediately C-terminal of Cdc2 ORF	*Cdc2-GBP linker:* (Cdc2)…gattttcat – **gcggccgcaggtggtggttctggtggtggttctggtggt ggatccatggccgac** – gttcaatta (GBP) *GBP-mCherry linker*: (GBP)…gtctcctct – **tcc** – atggtgagc (mCherry)
TetR-tup11Δ70	(Zilio et al., 2012)	Tup11Δ70 is C-terminal of TetR	(tetR)…agtggatct - **gttagtatgcagccgtcacttagaagtgagtatgagtacc ctgttttttctcatgttcaggcagggatgttctcacctaagct tagaacctttaccaaaggtgatgcggagagatgggtaag cggtacc** – tacgaaaaa (tup11Δ70)
Cdc13-sfGFP-L-Cdc2-AF(as) and derivatives (ARC1321 and ERp50)	Souradeep Basu (Nurse lab) and this study	Circularly permuted sfGFP is internal to Cdc13 between Ser177 and Val178 (as above) Cdc2 is C-terminal to Cdc13 (as above)	Additional Met residue on N terminus of sfGFP Cdc13-L-Cdc2 linker as above
Cut11-GFP	Kazunori Kume	GFP is C-terminal of Cut11	

Table 2.3 | Fusion protein details

Details of all of the fusion protein constructs used in this thesis, including the location of the fusion proteins relative to each other. Details of the linker sequences of constructs made in this study are included, as are details of the linker sequences for previously published constructs where this information is available. The nucleotide sequences of the linkers are shown in bold, with the immediately neighbouring nucleotides of the flanking proteins also shown.

Chapter 3. Localisation of Cdc13 to the SPB

As discussed in the Introduction, cyclin-CDK localisation to the SPB and centrosome is thought to be important for cell cycle control. In this Chapter I investigate the localisation of the *S. pombe* major mitotic B-type cyclin Cdc13 to the SPB.

Despite the suggested importance of cyclin localisation to the SPB and centrosome, it is currently unknown how Cdc13 localises to the SPB in *S. pombe*, or what happens to cell cycle progression if this localisation is prevented. Finding the region of Cdc13 (or one of its binding partners) that is responsible for its SPB localisation would provide insight into the mechanism involved as well as generating another tool to study the role of cyclin SPB localisation in cell cycle control. As discussed in the Introduction, the human Cyclin A centrosomal localisation sequence (CLS) includes the MRAIL hydrophobic patch, while the rat Cyclin E and budding yeast Clb2 do not require an intact hydrophobic patch to localise to the centrosome and SPB respectively (Bailly et al., 2003, Matsumoto and Maller, 2004, Pascreau et al., 2010). The hydrophobic patch of Cdc13 is therefore a candidate SPB-localisation sequence.

In this Chapter I first describe Cdc13/Cdc2/Suc1 localisation through the cycle. I then investigate Cdc13 localisation to the SPB, identifying that the hydrophobic patch of Cdc13 is responsible for its enrichment at the SPB in G2 phase, and revealing a previously unreported hydrophobic patch-independent localisation to the SPB in late G2/mitosis.

3.1 Localisation of cyclin-CDK through the cell cycle

To describe cyclin-CDK localisation through the cell cycle, asynchronous populations of strains expressing Cdc13 (Kamenz et al., 2015), Cdc2 or Suc1 fused to fluorophores were imaged. As Cdc13 and Cdc2 have been previously described to localise to the SPB (Alfa et al., 1990, Decottignies et al., 2001), an SPB component, Sid4, was also fused to a different fluorophore in these strains. For Cdc13, an allele that contains an internal circularly-permuted super-folding GFP (Cdc13-sfGFP) was used, as Cdc13 tolerates this internal tag better than a C-terminal fluorescent protein tag (Kamenz et al., 2015). Because *S. pombe* cells grow by tip extension, cell length can be used to estimate cell cycle stage, along with physiological events such as SPB separation, binucleation or septation (see Figure 1.1).

Fluorescence microscopy of Cdc13-sfGFP and Cdc2-mNG showed they accumulate in the nucleus as the cell grows throughout G2, with a subpopulation becoming visibly enriched at the SPB during G2 and the spindle in mitosis (Figure 3.1), which agrees with published immunofluorescence of Cdc13 and Cdc2, and fluorescence microscopy of Cdc13-YFP and Cdc2-YFP (Alfa et al., 1990, Alfa et al., 1989, Booher et al., 1989, Decottignies et al., 2001). Suc1-mNG was also seen in the nucleus and SPB in G2 and on the spindle in mitosis. In mitosis, when Cdc13 is degraded, I observed that Cdc2-mNG and Suc1-mNG lose their nuclear and SPB enrichment and disperse throughout the cell, which is also in agreement with published observations of Cdc2 localisation (Alfa et al., 1989, Alfa et al., 1990, Booher et al., 1989, Decottignies et al., 2001). The protein level of Cdc2 remains constant throughout the cell cycle in a population of synchronised cells, and Cdc2-mNG and Suc1-mNG overall concentration remain constant over increasing cell lengths in an asynchronous population (Simanis and Nurse, 1986)(Scott Curran, personal communication). In addition, Cdc2 nuclear accumulation is dependent on Cdc13, indicating that the disappearance of Cdc2 and Suc1 from the nucleus and SPB is to be likely due to a change in localisation once Cdc13 is degraded (Alfa et al., 1989, Booher et al., 1989, Decottignies et al., 2001). Cdc13-sfGFP, Cdc2-mNG

and Suc1-mNG are all seen to start accumulating in the nucleus of binucleate cells, which are in G1 or S phase of the cell cycle.

Thus Cdc13-sfGFP, Cdc2-mNG and Suc1-mNG all accumulate at the SPB throughout G2, appearing to become brighter at the SPB in comparison to the nucleus as the cells grow and progress towards mitosis. To measure this, the signal intensity of Cdc13-sfGFP, Cdc2-mNG and Suc1-mNG was measured at the SPB and compared to cell length. As Cdc13-sfGFP, Cdc2-mNG and Suc1-mNG do not appear strongly enriched at the SPB in all cell cycle stages, and they also accumulate in other cellular compartments (for example, the nucleus, and possibly the nucleolus), measuring the top pixels in the whole cell will not necessarily always result in a measurement of signal at the SPB. Therefore, to measure signal intensity at the SPB specifically, Sid4-mRFP signal was used to create a mask encompassing the SPB, which was dilated by 3 pixels (forming the 'SPB mask') (Figure 3.2). The initial mask was generated using a pixel classification workflow using Ilastik (Berg et al., 2019). The dilation of the initial mask by 3 pixels (in order to form the 'SPB mask') was performed to increase the chance that all Cdc13-sfGFP/Cdc2-mNG/Suc1-mNG SPB signal was included, even if the signal was slightly offset from the Sid4-mRFP focus. The resulting SPB masks vary in size and likely encompass a larger area than the SPB, so the mean of the top 10 pixels in this mask was taken as a readout of SPB intensity to ensure that signal intensity was being measured over the same area in all SPBs.

However, a protein that accumulates in the nucleus but is not enriched at the SPB would also show increasing intensity in the SPB mask throughout the cell cycle, so a measure of nuclear accumulation is also necessary to compare. To do this, a mask was created that comprises the pixels immediately neighbouring the SPB mask. The mean of the top 10 pixels of this 'surround' mask was taken as a readout of nuclear signal (Figure 3.2). Thus this method provides a way to measure Cdc13-sfGFP/Cdc2-mNG/Suc1-mNG signal specifically at the SPB, and compare it to nuclear intensity.

In many cells the SPB resides on the edge of the nucleus, meaning that the 'surround' mask would intersect both the nucleus and cytoplasm; it is assumed that

the top 10 pixels will be in the nucleus, as Cdc13-sfGFP, Cdc2-mNG and Suc1-mNG are more concentrated in the nucleus than the cytoplasm. For comparison, Cdc25 tagged with mNeonGreen was also included in this analysis as it accumulates in the nucleus but is not specifically enriched at the SPB (Figure 3.1D) (Lopez-Girona et al., 1999).

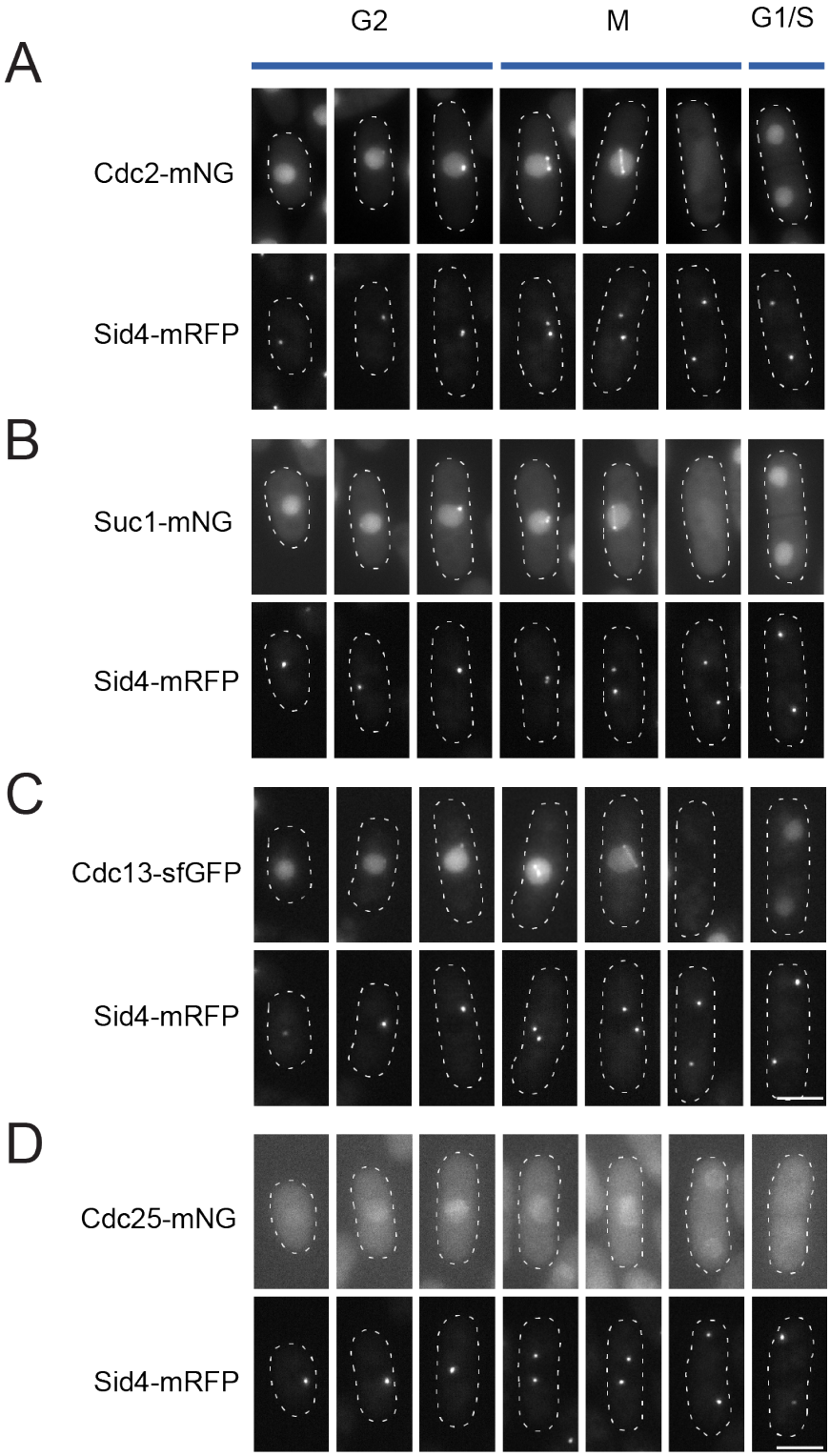


Figure 3.1 | Localisation of core cell cycle regulators through the cell cycle

Maximum projection images of different cells of increasing length from an asynchronous population expressing Sid4-mRFP and (A) Cdc2-mNeonGreen; (B) Suc1-mNeonGreen; (C) Cdc13-sfGFP; (D) Cdc25-mNG. Cell cycle stage is judged by cell length and SPB dynamics. Scale bars, 5 μm. The same pixel range has been applied to all images of the same channel for each strain.

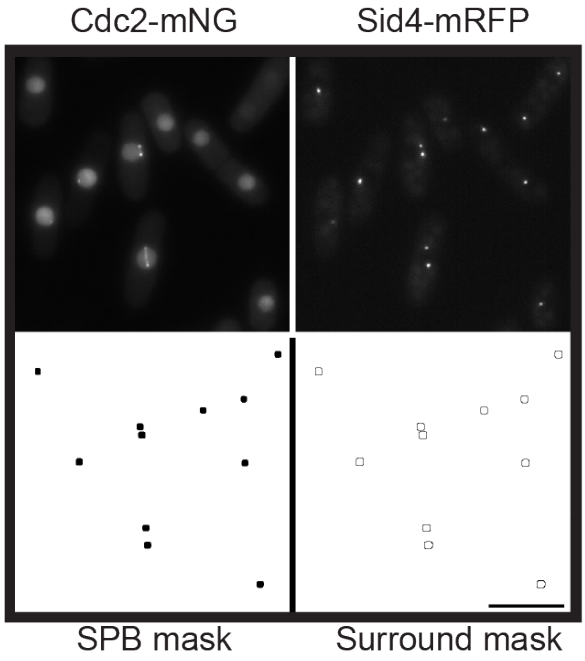


Figure 3.2 | Segmentation to create SPB and 'surround' mask

Example SPB and ‘surround’ masks to demonstrate segmentation. Sid4-mRFP signal was used to create a mask around the SPB. This mask was dilated by one pixel, and the ‘SPB mask’ removed, to create the ‘surround’ mask. The mean of the top 10 pixels was measured within each mask. Within the SPB mask, this is assumed to measure the SPB signal. Within the ‘surround’ mask, this is assumed to measure nuclear signal as all three proteins accumulate in the nucleus, resulting in a higher nuclear than cytoplasmic signal. Scale bar, 10 μm.

In this analysis only cells with one SPB were included to study SPB accumulation dynamics only in G2. In early G2, at shorter cell lengths, the signal intensity of Cdc13-sfGFP, Cdc2-mNG and Suc1-mNG in the SPB and surround mask is very similar, with both increasing as cell length increases for all three proteins (Figure 3.3A-C). At longer cell lengths, later in G2, the signal intensity in the SPB mask diverges from the surround mask, with a higher mean signal in the SPB mask, suggesting that at these cell lengths Cdc13-sfGFP, Cdc2-mNG and Suc1-mNG have a higher population mean signal at the SPB than the nucleus immediately proximal to the SPB. As expected for a protein that accumulates in the nucleus but not the SPB, the signal intensity in the SPB and surround masks for Cdc25-mNG remain the same throughout the cell cycle (Figure 3.3D). The observed divergence in Cdc13-sfGFP, Cdc2-mNG and Suc1-mNG signal in the SPB and surround mask

supports the conclusion that all three proteins are enriched at the SPB for at least part of the cell cycle.

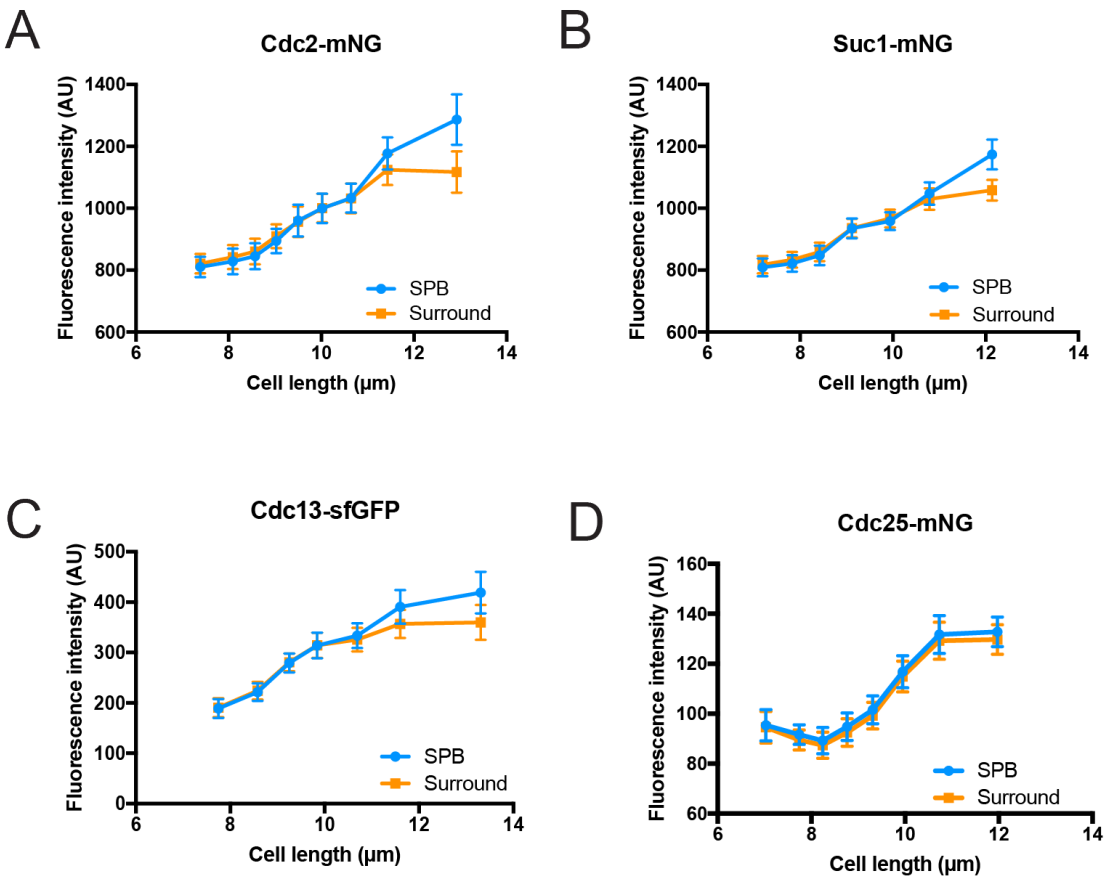


Figure 3.3 | Intensity measurements of cell cycle regulators at the SPB

Intensity measurements of (A) Cdc2-mNeonGreen; (B) Suc1-mNeonGreen; (C) Cdc13-sfGFP; (D) Cdc25-mNG at the SPB (blue) and surrounding area (orange). Cells with 2 SPBs were excluded from the dataset. Mean value of background autofluorescence (measured from a strain expressing Sid4-mRFP) is subtracted from the data. Data was placed into cohorts by cell length, and within each cohort the mean cell length was plotted against the mean and 95% CI of the intensity measurements. N numbers: (A) total n = 892 cells, ≥ 99 per cohort; (B) total n = 755 cells, ≥ 107 per cohort; (C) total n = 553 cells, ≥ 78 per cohort; (D) total n = 837 cells, ≥ 104 per cohort.

These results recapitulate previous observations that Cdc13, Cdc2 and Suc1 have dynamic localisation through the cell cycle, being enriched at the nucleus and SPB in G2 and early mitosis, and the spindle in early mitosis. In addition, signal intensity is quantified at the SPB and nucleus in G2 cells, to demonstrate Cdc13-sfGFP/Cdc2-mNG/Suc1-mNG enrichment at the SPB in late G2. The redistribution of Cdc2-mNG and Suc1-mNG coincident with Cdc13 degradation is consistent with the view that Cdc13 is responsible for the localisation of the complex to the nucleus, SPB and spindle (Alfa et al., 1989, Booher et al., 1989, Decottignies et al., 2001). I therefore next set out to identify the region on Cdc13 responsible for SPB localisation, starting with the possibility that it was the hydrophobic patch.

3.2 Cdc13 localisation to the SPB involves the hydrophobic patch

To study the impact of the hydrophobic patch on Cdc13 localisation to the SPB, a previously described hydrophobic patch mutant (HPM) was used that has three key residues in the hydrophobic patch mutated to alanine to prevent it docking to R/KxL motifs (M235A, L239A, W242A in *S. pombe* Cdc13) (Schulman et al., 1998, Basu et al., 2020). These mutations were made in Cdc13-sfGFP (Kamenz et al., 2015).

It has been previously shown that cells driven by $Cdc13^{HPM}$ perform S phase but not mitosis, with cells elongating as is typical of an interphase cell cycle arrest, suggesting they arrest in G2 (Basu et al., 2020). Therefore, an exogenous copy of $Cdc13^{WT}$-sfGFP or $Cdc13^{HPM}$-sfGFP under the Cdc13 promoter was introduced into the *leu1* locus, whilst the endogenous Cdc13 was present in the cells but not fused to a fluorophore. This allowed the study of the localisation of only the exogenous copy of Cdc13 whilst retaining cell viability.

Exogenous $Cdc13^{WT}$-sfGFP and $Cdc13^{HPM}$-sfGFP were introduced into a strain containing Sid4-mRFP to mark the SPB, and an asynchronous population was imaged. Uninucleate cells from this population were analysed for a focus of Cdc13-sfGFP signal at the SPB, excluding the small proportion of cells with no Cdc13 signal due to Cdc13 degradation in anaphase. Whilst both $Cdc13^{WT}$-sfGFP and $Cdc13^{HPM}$-sfGFP were enriched at the SPB in some cells of the population, a much lower percentage of cells had an SPB focus of $Cdc13^{HPM}$-sfGFP than $Cdc13^{WT}$-sfGFP, indicating that $Cdc13^{HPM}$-sfGFP has severely defective localisation to the SPB (Figure 3.4A-B). Dividing the uninucleate population into cells with either a single SPB (mainly interphase cells) or separated SPBs (mitotic cells) demonstrated that whilst a similar percentage of cells in the uninucleate population had $Cdc13^{WT}$-sfGFP and $Cdc13^{HPM}$-sfGFP enriched at separated SPBs, the percentage of cells with a single focus of $Cdc13^{HPM}$-sfGFP was markedly lower than that of $Cdc13^{WT}$-sfGFP, at 2.3 % compared to 35.9 % (Figure 3.4B).

To study this further, the lengths of cells with a Cdc13-sfGFP focus were compared for both strains. Whilst the lengths of cells with SPB-localised $Cdc13^{WT}$-sfGFP span a wide range of the cell lengths in the entire uninucleate population, $Cdc13^{HPM}$-sfGFP is only localised to the SPB in the longest cells in the population, which are in late G2 or M (Figure 3.4C). This demonstrates that $Cdc13^{HPM}$-sfGFP has defective localisation to the SPB in shorter cells but localises to the SPB in the longest cells of the population. Two possibilities that could result in this delayed localisation to the SPB are the increased protein level of Cdc13 later in the cell cycle, or progression to a late cell cycle stage. In the next section, I describe experiments to address these possibilities.

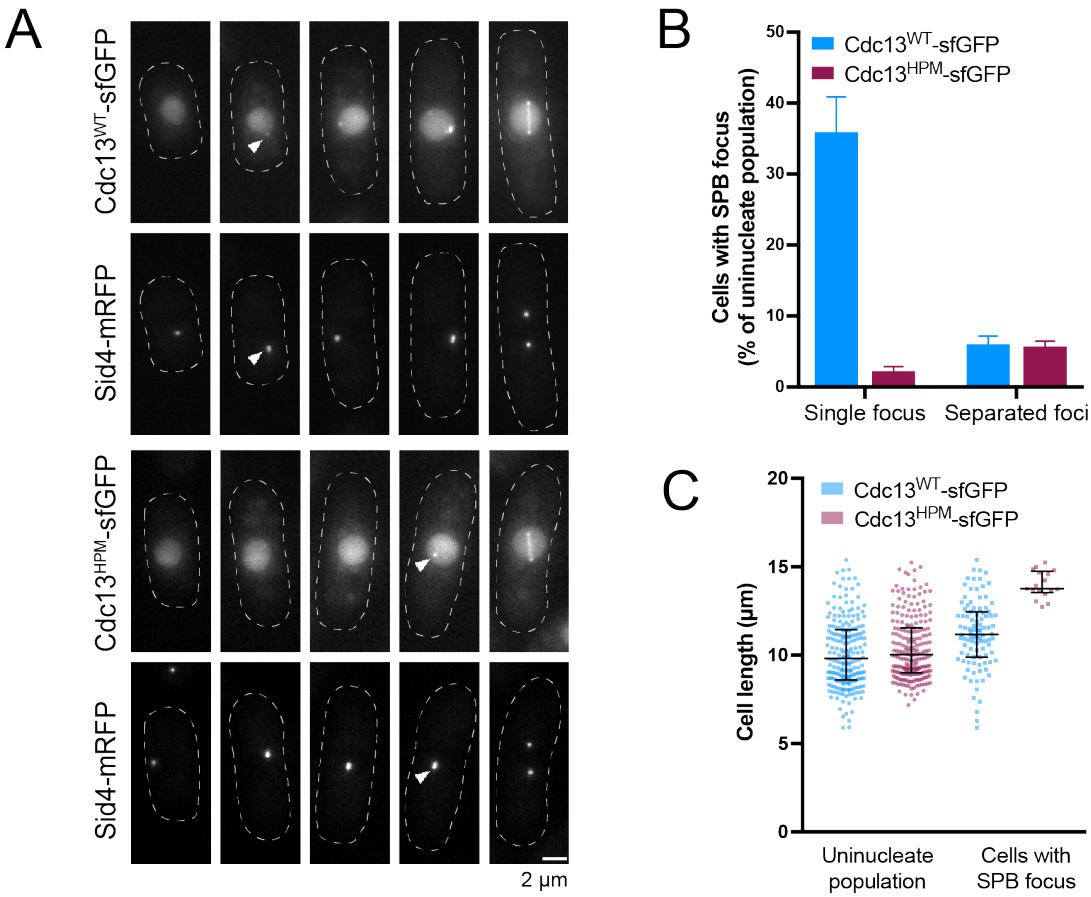


Figure 3.4 | Cdc13^{HPM}-sfGFP is only enriched at the SPB in longer cells

A: Representative maximum projection images of different cells of increasing length from an asynchronous population expressing exogenous Cdc13^{WT}-sfGFP or Cdc13^{HPM}-sfGFP. Endogenous Cdc13 is expressed but is not fused to a fluorophore. Sid4-mRFP marks the SPB. Arrows show first appearance of a Cdc13-sfGFP SPB focus in the montage. The same pixel range has been applied to all images from the same channel.
B: Uninucleate cells were analysed by eye for Cdc13 signal at single (interphase) or separated (mitotic) SPBs. The mean and SD of 3 replicates are shown. Uninucleate population n > 200 cells per replicate, total n = 824 total for Cdc13^{WT} and 954 for Cdc13^{HPM}.
C: Cell lengths of the entire uninucleate population and of cells with a Cdc13-sfGFP SPB focus from one replicate of the experiment described in (B). Bars represent median, with whiskers delimiting the 25th and 75th percentiles. Uninucleate population n = 212 for Cdc13^{WT} and 214 for Cdc13^{HPM}.

3.3 Cdc13^{HPM} is enriched at the SPB in mitosis

3.3.1 Cdc13^{HPM} is not enriched at the SPB in a G2 arrest

To uncouple Cdc13 protein level from cell cycle progression, cells were arrested in G2 phase, preventing cell cycle progression whilst still allowing Cdc13 to accumulate in cells with increasing cell length (Booher et al., 1989). Cdc13^{WT}-sfGFP and Cdc13^{HPM}-sfGFP were introduced to cells containing Sid4-mRFP to mark the SPB and the temperature-sensitive allele *cdc25-22*, which results in a G2 arrest at the restrictive temperature of 36 °C. After shifting to 36 °C, cells were analysed for SPB foci of Cdc13^{WT}-sfGFP or Cdc13^{HPM}-sfGFP. Whilst Cdc13^{WT}-sfGFP was enriched at the SPB in the large majority of arrested cells, Cdc13^{HPM}-sfGFP was not (Figure 3.5A-B). However, Cdc13^{HPM}-sfGFP signal in arrested cells did not appear as bright as Cdc13^{WT}-sfGFP, so the mean cellular intensity of both strains was compared before and after the arrest. Whilst both strains had similar intensities of Cdc13^{WT}-sfGFP and Cdc13^{HPM}-sfGFP in an asynchronous population before the arrest, the spread of intensities was different after the arrest (Figure 3.5C-D). Cdc13^{WT}-sfGFP concentration continues to increase in the G2 arrest as expected, but Cdc13^{HPM}-sfGFP concentration appears to remain relatively flat. It is not clear why Cdc13^{HPM}-sfGFP behaves differently to Cdc13^{WT}-sfGFP in this G2 arrest at 36 °C, but it means that a conclusion cannot be drawn from this experiment about whether increasing Cdc13^{HPM}-sfGFP concentration in G2 results in Cdc13^{HPM}-sfGFP localisation to the SPB. I considered that the temperature shift to 36 °C may have affected these cells, so sought a way of arresting cells in G2 without shifting temperature.

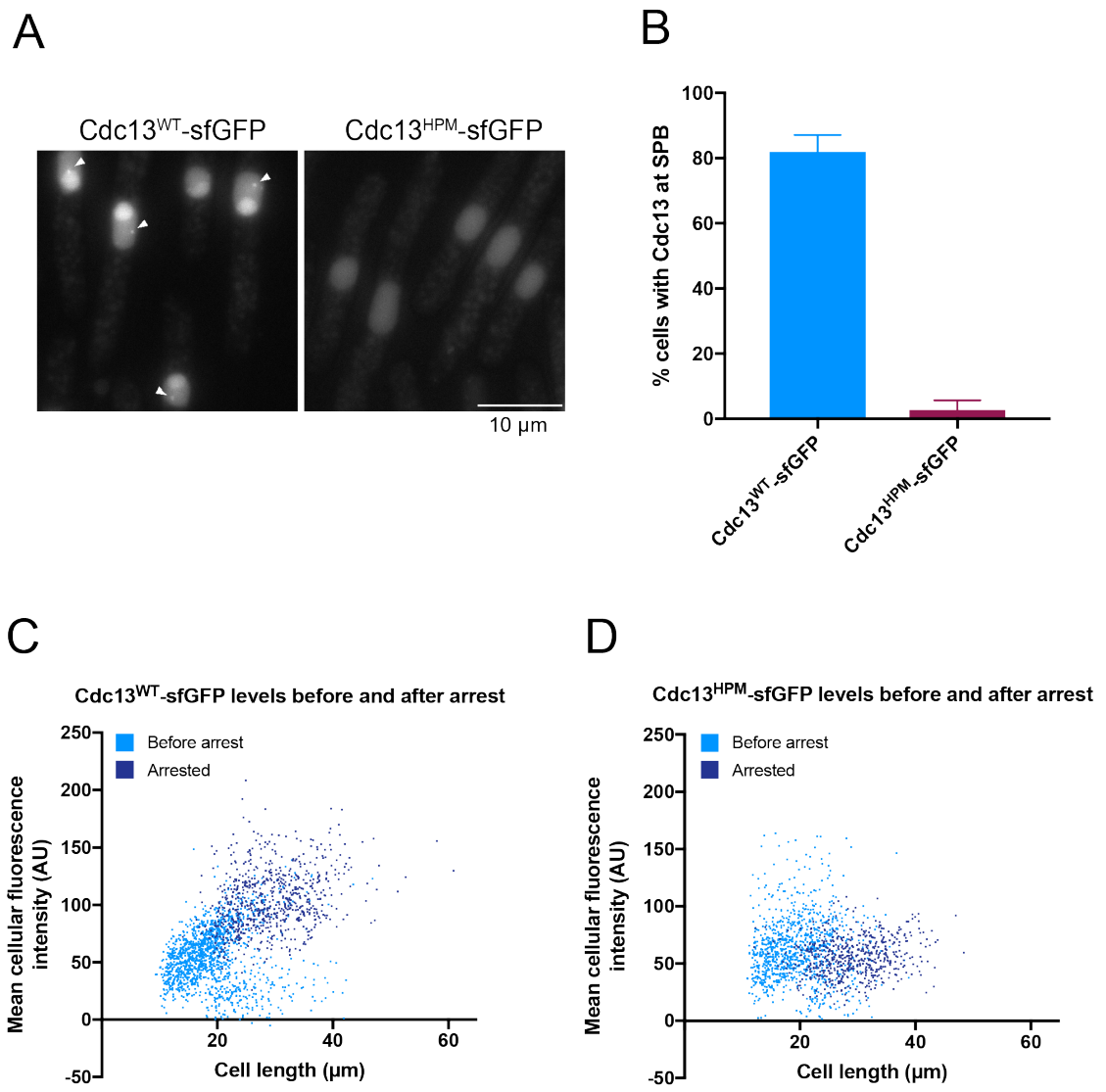


Figure 3.5 | Cdc13-sfGFP localisation and accumulation in a *cdc25-22* G2 arrest

A: Representative maximum projection images of *cdc25-22 sid4-mRFP* cells arrested in G2 by shifting to 36°C for one cell cycle containing an exogenous copy of either Cdc13^{WT}-sfGFP or Cdc13^{HPM}-sfGFP. The endogenous Cdc13 is expressed but not fused to a fluorophore. Arrows indicate Cdc13-sfGFP foci. The same pixel range is applied to both images.
B: The percentage of G2-arrested cells with Cdc13-sfGFP SPB foci, which was judged by eye. n > 210 cells per condition per replicate. The mean and SD of 3 replicates are shown. Total n = 663 cells for Cdc13^{WT} and 693 cells for Cdc13^{HPM}.
C: Cell length plotted against mean whole-cell fluorescence intensity of Cdc13^{WT}-sfGFP in cells from an asynchronous population (before arrest) and after one generation at 36°C (arrested), with the mean value of background autofluorescence subtracted. Data is from one replicate from (B). Before arrest n = 1385, arrested n = 721.
D: Same as C, with Cdc13^{HPM}-sfGFP. Before arrest n = 998, arrested n = 563.

Cdc13^{WT}-sfGFP and Cdc13^{HPM}-sfGFP were introduced to cells containing an analogue-sensitive allele of *cdc2* (*cdc2(as)-M17*) that can be inhibited by a bulky ATP analogue, 1-NmPP1 (Bishop et al., 2000, Aoi et al., 2014). 1 μM 1-NmPP1 was added to cells for one generation time to arrest them in G2, resulting in elongated cells. The mean whole-cell fluorescence intensity of Cdc13^{WT}-sfGFP and Cdc13^{HPM}-sfGFP was compared before and after the G2 arrest. Before the arrest, the asynchronous populations had a similar spread of Cdc13^{WT}-sfGFP and Cdc13^{HPM}-sfGFP mean cellular intensities, suggesting that there are no major differences in expression (Figure 3.6A). Comparing the intensities before and after the arrest shows that both Cdc13^{WT}-sfGFP and Cdc13^{HPM}-sfGFP accumulate with increasing cell length during the G2 arrest, with the majority of the arrested population having a Cdc13-sfGFP level at least as high as the peak of the asynchronous population (Figure 3.6B-C).

Analysing the arrested population for Cdc13-sfGFP foci demonstrated that while most arrested cells had a focus of Cdc13^{WT}-sfGFP, very few had a focus of Cdc13^{HPM}-sfGFP, despite the increase in Cdc13-sfGFP levels (Figure 3.7). This suggests that it is not solely an increase in Cdc13^{HPM}-sfGFP concentration that results in Cdc13^{HPM}-sfGFP accumulation at the SPB in longer cells.

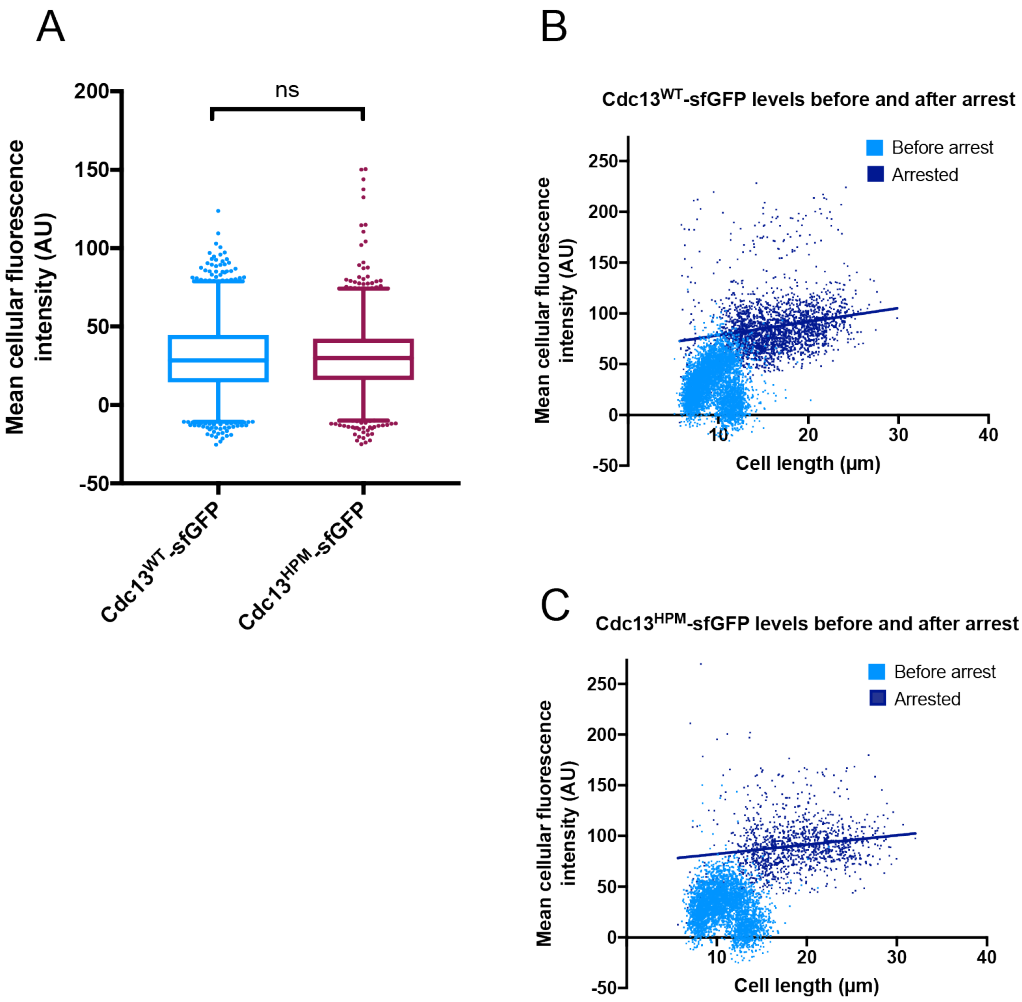


Figure 3.6 | Cdc13-sfGFP concentration in *cdc2(as)* G2-arrested cells

A: Mean whole-cell fluorescence intensity of Cdc13^{WT}-sfGFP and Cdc13^{HPM}-sfGFP in an asynchronous population. Strains also contain the *cdc2(as)-M17* allele but are not in the presence of 1-NmPP1. Box represents median and IQR, with whiskers delimiting the 1st and 99th percentiles. Mann-Whitney p = 0.5178 (ns; not significant).
B: Cell length plotted against mean whole-cell fluorescence intensity of Cdc13^{WT}-sfGFP in cells from an asynchronous population (before arrest) (data from A) and 1 generation after 1 μM 1-NmPP1 addition (arrested), with the mean value of background autofluorescence removed. Regression line calculated using Prism and plotted through arrested population, slope = 1.3. Before arrest n = 4363 cells, arrested n = 2361.
C: Same as B, with Cdc13^{HPM}-sfGFP. Regression line calculated using Prism and plotted through arrested population, slope = 0.9. Before arrest n = 3561, arrested n = 1213.

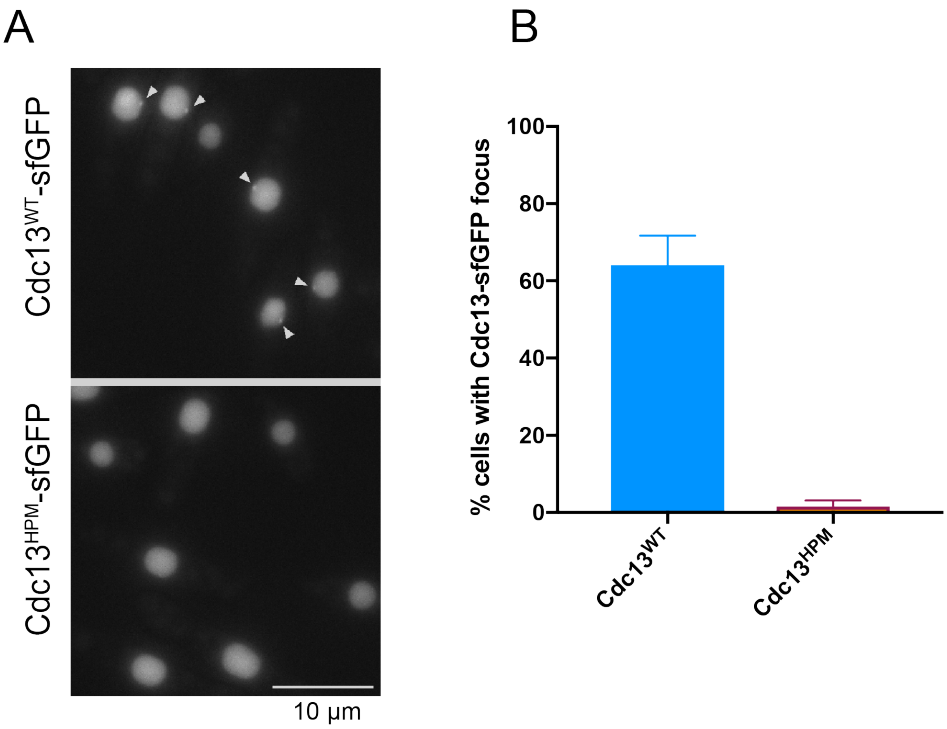


Figure 3.7 | Cdc13^{HPM}-sfGFP does not localise to the SPB in a G2 arrest

A: Representative maximum projection images of *cdc2(as)-M17* cells containing an exogenous copy of either Cdc13^{WT}-sfGFP or Cdc13^{HPM}-sfGFP, arrested in G2 by addition of 1 µM 1-NmPP1 for one cell cycle. The endogenous Cdc13 is expressed but not fused to a fluorophore. Arrows indicate Cdc13-sfGFP foci. The pixel range shown is the same for both Cdc13^{WT} and Cdc13^{HPM}.
B: The percentage of G2-arrested *cdc2(as)-M17* cells with Cdc13-sfGFP foci, judged by eye. N > 250 cells per condition per replicate. The mean and SD of 4 replicates are shown. Total n = 1339 cells for Cdc13^{WT} and 1351 cells for Cdc13^{HPM}.

3.3.2 Cdc13^{HPM} accumulates at the SPB after Polo kinase

To narrow down the timing of Cdc13^{HPM}-sfGFP localisation to the SPB, Cdc13^{WT}-sfGFP or Cdc13^{HPM}-sfGFP were expressed in cells containing Polo kinase (Plo1) fused to mCherry. In fission yeast, Plo1 localisation to the SPB occurs in late G2/early mitosis (Mulvihill et al., 1999, Grallert et al., 2013b), so the timing of Cdc13^{WT}-sfGFP or Cdc13^{HPM}-sfGFP localisation to the SPB was compared with that of Plo1-mCherry. In an asynchronous population, there were fewer Cdc13^{HPM}-sfGFP foci than Cdc13^{WT}-sfGFP foci, as noted previously, but both strains had a similar percentage of cells with Plo1-mCherry foci (Figure 3.8B). Notably, although more than 20% of the population had Cdc13^{WT}-sfGFP foci with no Plo1-mCherry foci, this was very rarely seen with Cdc13^{HPM}-sfGFP. On the other hand, it was more common for cells to have Plo1-mCherry foci with no Cdc13-sfGFP foci in the HPM strain than the WT strain (Figure 3.8A-B). Comparing the percentage of cells with Cdc13-sfGFP or Plo1-mCherry foci against cell length shows that while Cdc13^{WT}-sfGFP foci appear in shorter cells than Plo1-mCherry foci, the opposite is true for Cdc13^{HPM}-sfGFP, which starts to form foci in longer cells than Plo1-mCherry (Figure 3.8C-D). These data suggest that while Cdc13^{WT}-sfGFP becomes visibly enriched at the SPB before Plo1-mCherry, Cdc13^{HPM}-sfGFP only accumulates at the SPB after Plo1-mCherry, in late G2/early mitosis. It is worth noting that the cells with Cdc13^{HPM}-sfGFP only enter and execute mitosis due to the endogenous, untagged copy of wild-type *cdc13*, and without this copy of Cdc13 cells would arrest at G2, possibly before the observed localisation of Cdc13^{HPM}-sfGFP to the SPB (Basu et al., 2020).

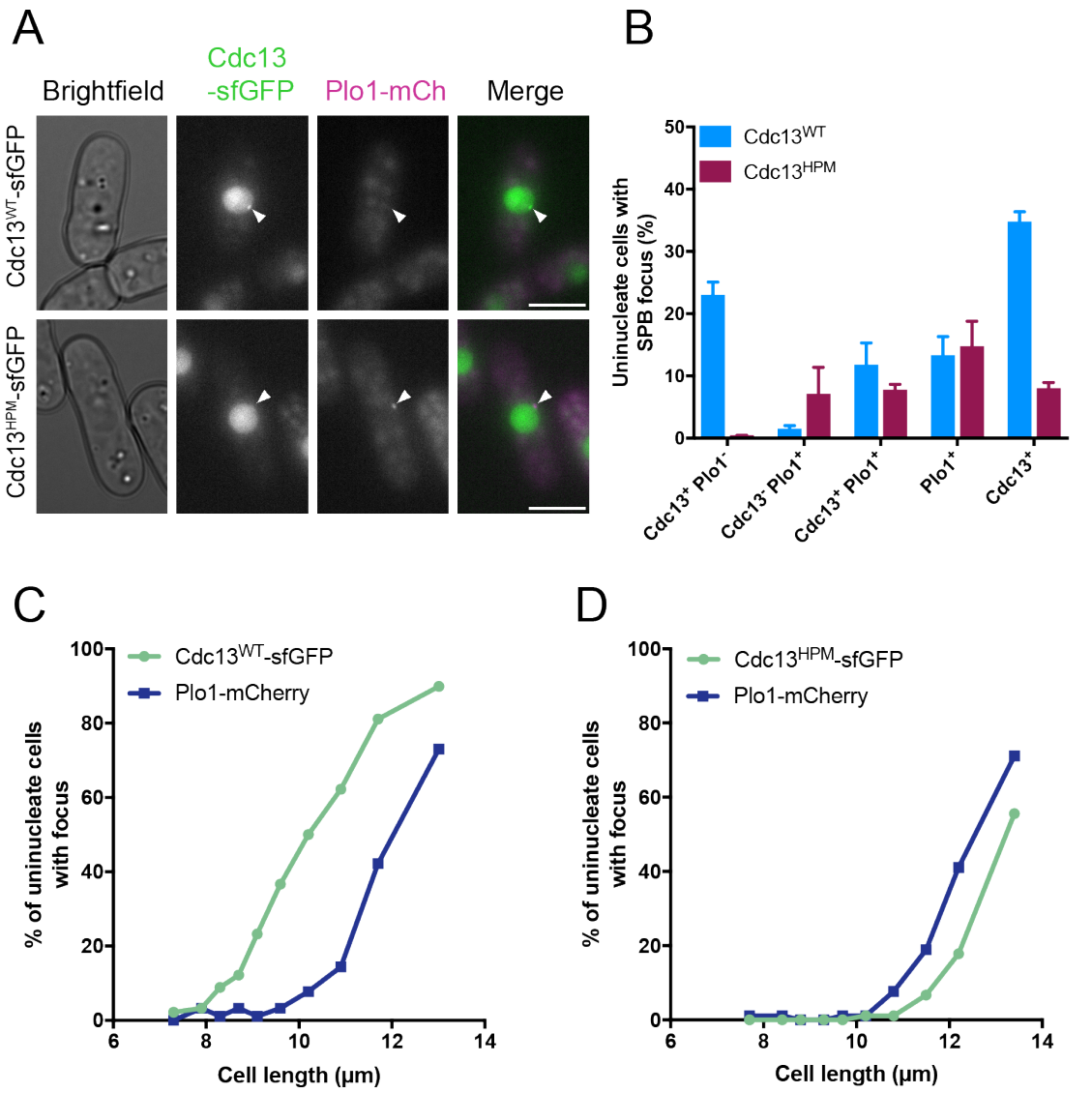


Figure 3.8 | Cdc13^{HPM}-sfGFP localises to the SPB after Plo1-mCherry

A: Representative maximum projection images of example cells from an asynchronous population expressing Plo1-mCherry and an exogenous copy of either Cdc13^{WT}-sfGFP or Cdc13^{HPM}-sfGFP. Endogenous Cdc13 is expressed but not fused to a fluorophore. The same pixel range is applied to all images from the same channel. Scale bars, 5 µm.
B: Uninucleate cells were analysed for the presence ($^{+}$) or absence ($^{-}$) of a focus of Cdc13-sfGFP and Plo1-mCherry signal in the nucleus. Data shows mean and SD of 3 replicates: n ≥ 200 cells per strain per replicate; total n = 899 cells for Cdc13^{WT}-sfGFP and 903 cells for Cdc13^{HPM}-sfGFP.
C: Length of cells compared to presence of Plo1-mCherry and Cdc13^{WT}-sfGFP foci. Data pooled from 3 replicates; mean cell length per cohort is plotted against % of cells within that cohort with Plo1-mCherry or Cdc13-sfGFP foci at the SPB. n ≥ 89 cells per cohort.
D: As (C), with Cdc13^{HPM}-sfGFP.

3.4 Discussion

The initial work detailed in this Chapter describes Cdc13-sfGFP, Cdc2-mNG and Suc1-mNG localisation to the nucleus, SPB and mitotic spindle, confirming previous reports. Signal intensity analysis suggests that the population mean Cdc13-sfGFP, Cdc2-mNG and Suc1-mNG signal at the SPB diverges from nuclear signal in G2, suggesting an enrichment of these proteins at the SPB for part of the cell cycle.

The next conclusion of this chapter is that the hydrophobic patch of Cdc13 is necessary for its accumulation at the SPB in G2 before Plo1-mCherry localisation to the SPB. Whilst budding yeast Clb2 and mammalian Cyclin E do not require an intact hydrophobic patch to localise to the centrosome, human Cyclin A does, demonstrating that the involvement of the hydrophobic patch in localisation to the SPB or centrosome is similar in an *S. pombe* B-type cyclin and a human A-type cyclin (Bailly et al., 2003, Matsumoto and Maller, 2004, Pascreau et al., 2010). A study of the localisation of truncated regions of human Cyclin B1 identified a 45 amino-acid region encompassing the hydrophobic patch as necessary for Cyclin B1 localisation to the centrosome, suggesting that the hydrophobic patch may also be involved in the centrosomal localisation of Cyclin B1, though this has not been tested using point mutations specifically at the hydrophobic patch in the full-length Cyclin B1 (Bentley et al., 2007). As the major mitotic B-type cyclin in *S. pombe*, Cdc13 is functionally most similar to Cyclin B1, so it would be of interest to identify whether the hydrophobic patch is involved in human Cyclin B1 centrosomal localisation. This is investigated in the next Chapter.

It remains to be identified how the hydrophobic patch mediates Cdc13 localisation to the SPB. A likely scenario is that the Cdc13 hydrophobic patch directly interacts with a/multiple SPB-localised protein(s), though it is also possible that the hydrophobic patch is indirectly required for SPB localisation, for example if it were needed for a different interaction that itself is needed for Cdc13 SPB localisation. The hydrophobic patch has been shown to bind R/KXL motifs, as well as LXF motifs in the *S. cerevisiae* mitotic cyclin Clb2 (Schulman et al., 1998, Loog and

Morgan, 2005, Ord et al., 2019). Cdc13 interacts with the N-terminus of the SPB-localised protein Cdc11, which contains several RXL motifs that could be candidate binding sites (Morrell et al., 2004, Wood et al., 2002, Wood et al., 2012). The interaction of Cdc13 and Cdc11 is supported by a high-throughput yeast-two-hybrid interaction study, which also identified the SPB-localised proteins Ppc89 and Sad1 as interactors of Cdc13 (Vo et al., 2016), both of which also contain R/KXL and LXF motifs (Wood et al., 2002, Wood et al., 2012). A first step to identifying if these SPB proteins interact with Cdc13 via the hydrophobic patch could therefore be to mutate the potential binding sites on Cdc11, Ppc89 and Sad1. However, for a more unbiased study, and to identify other hydrophobic patch-dependent interactions, a comparative pull-down study with $Cdc13^{HPM}$ and $Cdc13^{WT}$ would be informative. It is also worth noting that whilst Cdc13-sfGFP can be seen colocalised with an SPB component, this does not mean that Cdc13 interacts with SPB components directly. Cdc13 could be localised to another structure/protein close to the SPB, for example the centromere. Identifying the interactors of Cdc13 would therefore provide more detailed information on Cdc13 localisation.

The lack of $Cdc13^{HPM}$-sfGFP concentration increase with cell length in a *cdc25-22* G2 arrest at the restrictive temperature of 36 °C is an unexpected result. It is not clear if the difference in $Cdc13^{WT}$-sfGFP and $Cdc13^{HPM}$-sfGFP accumulation is due to a transcriptional or translational difference between the strains, or a difference in the rate of Cdc13-sfGFP protein turnover. The concentration increase of $Cdc13^{HPM}$-sfGFP in a *cdc2(as)-M17* G2 arrest by addition of 1-NmPP1 demonstrates that this lack of $Cdc13^{HPM}$-sfGFP super-scaling with cell length is not a feature of all conditions leading to a G2 arrest.

The identification that $Cdc13^{HPM}$-sfGFP does not localise to the SPB in early G2 provides an opportunity to study the importance of Cdc13 localisation to the SPB. It is possible that this SPB localisation defect is the reason why cells driven by $Cdc13^{HPM}$ do not enter mitosis. Supporting this theory, phosphoproteomic data from cells expressing either $Cdc13^{WT/HPM}$ released from a G2 arrest demonstrates that $Cdc13^{HPM}$ phosphorylates nuclear CDK substrates to similar levels to $Cdc13^{WT}$, but has significantly reduced phosphorylation of SPB and cytoplasmic targets (data from (Basu et al., 2020) and reproduced in Figure 8.1). Hydrophobic patch

dependent (HP-dependent) sites, defined as mitotic CDK sites that were not phosphorylated in the Cdc13^{HPM} condition to at least the level seen in the mitotic timepoint for Cdc13^{WT}, also had lower IC_{50} values to 1-NmPP1 on average than HP-independent sites (Figure 8.1B) (Basu et al., 2020, Swaffer et al., 2016). This means these sites require less CDK inhibitor to have steady-state phosphorylation reduced to 50 % of maximal phosphorylation, suggesting that they generally require higher levels of CDK activity in order to be fully phosphorylated. Interestingly, analysis of substrate IC_{50} values for all CDK substrates categorised by substrate localisation suggests that substrates in the SPB and cytoplasm generally require the highest CDK activity to be phosphorylated (Figure 8.1C) (Basu et al., 2020, Swaffer et al., 2016). These results indicate that Cdc2 in complex with Cdc13^{HPM} has defects in phosphorylating SPB-localised and cytoplasmic-localised substrates at mitosis, which are also the substrates that require the highest levels of CDK activity to be phosphorylated.

The lack of Cdc13^{HPM} localisation to the SPB could result in a lower CDK activity experienced at the SPB and cytoplasm; if the Cdc13-Cdc2 accumulated at the SPB cycles on and off the SPB then the SPB may act as a source of Cdc13-Cdc2 for substrates located in the cytoplasm as well. If this hypothesis is correct, sufficient overexpression of Cdc13^{HPM}-Cdc2 may overcome the defects of Cdc13^{HPM}. It is also possible that the mitotic defect of Cdc13^{HPM} is not due to the lack of SPB localisation; given that the hydrophobic patch has a role as a substrate docking region, it is possible that some critical substrates are not phosphorylated due to a lack of direct interaction with Cdc13. In order to distinguish between these two scenarios the general substrate-docking role of the hydrophobic patch will need to be uncoupled from its SPB-localisation role, which could be achieved by disrupting the specific Cdc13 docking site(s) on the SPB, or by artificially tethering Cdc13^{HPM} to the SPB. These questions are investigated later in the Results section.

The work in this chapter also reveals that there is a hydrophobic patch-independent mechanism of Cdc13-sfGFP localisation to the SPB in late G2/early mitosis, after Plo1-mCherry accumulation at the SPB. At mitotic entry the cell undergoes numerous changes, including changes in cellular signalling, SPB remodelling and insertion into the nuclear envelope, and spindle formation. There are therefore

multiple events that correlate with the timing of Cdc13^{HPM}-sfGFP localisation to the SPB.

Further investigation into the mechanism for this second, hydrophobic patch-independent localisation of Cdc13^{HPM}-sfGFP to the SPB suggested that mutants of *cut12* or *plo1* that accelerate Plo1 localisation to the SPB also accelerate Cdc13^{HPM}-sfGFP localisation to the SPB (Basu et al., 2020), reproduced in (Figure 8.2A). In this experiment, the strain backgrounds *cut12.s11, cut12T75DT78D* and *plo1.S402E* were used, all of which result in an acceleration of Plo1 localisation to the SPB without an acceleration in mitosis or an alteration of cell size at division in complex media (Mulvihill et al., 1999, MacIver et al., 2003, Grallert et al., 2013a, Petersen and Hagan, 2005). Investigation of Cdc13^{HPM}-sfGFP localisation in these strains found that Cdc13^{HPM}-sfGFP forms a nuclear focus at shorter cell lengths in these strains, suggesting that SPB localisation is accelerated. This work also showed that in a temperature-sensitive *plo1-24c* mutant (Bahler et al., 1998) at restrictive temperature, Cdc13^{HPM}-sfGFP foci did not form upon release from a G2 arrest (reproduced in Figure 8.2B)(Basu et al., 2020). This suggests that Plo1 activity is needed for Cdc13^{HPM}-sfGFP localisation to the SPB, either because of a direct requirement for Plo1 activity, or because *plo1-24C* mutants arrest before Cdc13^{HPM}-sfGFP SPB localisation.

Taken together, these findings suggest that the hydrophobic patch-independent localisation of Cdc13^{HPM}-sfGFP may be downstream and dependent on Plo1 activity at the SPB. Importantly, these experiments indicate that Cdc13^{HPM}-sfGFP SPB localisation is due to an event that is accelerated in mutant backgrounds in which Plo1 localisation to the SPB is accelerated, without an acceleration of mitosis. The advancement of Polo kinase recruitment to the SPB in the *cut12.s11* mutant is mirrored by an early SPB staining by the antibody MPM2, which detects phosphorylated epitope(s) at the SPB dependent on Polo activity, indicating that Polo is activated early at the SPB in this background (MacIver et al., 2003). Investigating a potential involvement of Polo kinase activity would therefore be an important focus for future experiments investigating the SPB localisation of Cdc13^{HPM}-sfGFP (discussed further in Chapter 7).

The work in this Chapter identifies that the hydrophobic patch plays an important role in Cdc13-sfGFP SPB localisation. In the following Chapters, I investigate whether this is similar in human Cyclin B1, and whether the lack of G2 SPB localisation of $Cdc13^{HPM}$ might be responsible for the G2 arrest of $Cdc13^{HPM}$ cells.

Chapter 4. Localisation of Cyclin B1 to the centrosome

Human Cyclin B1 shows some differences in its localisation pattern to *S. pombe* Cdc13 but some aspects of its localisation are similar. Cyclin B1 shuttles between the nucleus and cytoplasm in interphase, with a higher rate of nuclear export than import leading to a predominantly cytoplasmic localisation (Pines and Hunter, 1991, Hagting et al., 1998, Toyoshima et al., 1998). In prophase, Cyclin B1 undergoes rapid net nuclear accumulation that has been suggested to be due to phosphorylation of its cytoplasmic retention sequence (CRS) leading to decreased nuclear export and increased nuclear import, though this theory is contested (Pines and Hunter, 1991, Pines and Hunter, 1994, Hagting et al., 1999, Gavet and Pines, 2010a, Santos et al., 2012). *S. pombe* Cdc13 also accumulates in the nucleus, but does so throughout G2 (Decottignies et al., 2001).

Similarly to Cdc13, human Cyclin B1 localises to the centrosome in late G2 and mitosis, and the spindle in mitosis (Pines and Hunter, 1991, Hagting et al., 1998). Cyclin B1 has also been reported to localise to microtubules, mitotic chromosomes, and unattached kinetochores (Pines and Hunter, 1991, Jackman et al., 1995, Hagting et al., 1998, Bentley et al., 2007, Santos et al., 2012). The discovery that the first population of active Cyclin B1-Cdk1, which was detected by immunofluorescence to locate phosphorylated Cyclin B1, is found at the centrosome, suggests that the mammalian centrosome could play an important role at mitotic entry (Jackman et al., 2003). However, the importance of the centrosome in cell cycle control is controversial, as fully intact centrosomes are not essential for any aspect of cell division in *Drosophila* (Basto et al., 2006), whilst they are dispensable for spindle formation but required for the G1-S transition in vertebrate cells (Khodjakov et al., 2000, Khodjakov and Rieder, 2001). In *Xenopus*, the nucleus, not the centrosome, is suggested to be the initiation site for the mitotic trigger wave (Nolet et al., 2020, Afanzar et al., 2020).

The work in the previous Chapter demonstrates that the hydrophobic patch of *S. pombe* Cdc13 is necessary for its SPB accumulation in G2 before Plo1 SPB

localisation, but not in mitosis. The hydrophobic patch sequence of Cdc13 is highly conserved with human Cyclin B1, leading to the possibility that the hydrophobic patch also acts as the centrosomal localisation sequence for human Cyclin B1. A previous study of truncated regions of Cyclin B1 has identified a 45 amino-acid region of Cyclin B1 that is necessary for centrosomal localisation, which contains the hydrophobic patch (Bentley et al., 2007). The hydrophobic patch is therefore a strong candidate for the centrosomal localisation sequence of Cyclin B1, but this possibility has not been tested by specifically disrupting the hydrophobic patch in the full-length Cyclin B1. It is also unknown if a hydrophobic patch-independent method of Cdc13 SPB localisation is also operative for human Cyclin B1. In this Chapter, I investigate the localisation of Cyclin $B1^{HPM}$-mCherry to the centrosome in a U2OS cell line.

4.1 Expressing Cyclin B1^{HPM} in human cells

Due to the high level of sequence conservation in the hydrophobic patch between Cyclin B1 and Cdc13 (Figure 4.1), the same mutations first described to disrupt the Cyclin A hydrophobic patch (Schulman et al., 1998), and used in our work with Cdc13 (Basu et al., 2020), were made in human Cyclin B1 constructs fused to a fluorophore.

A



B

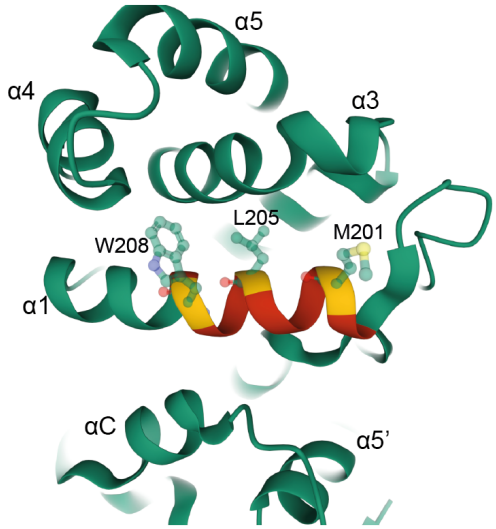


Figure 4.1 | Cdc13 and Cyclin B1 hydrophobic patch sequence conservation

A: Sequences of the hydrophobic patch region in *S. pombe* Cdc13 and human Cyclin B1, with the residues mutated in the HPM mutant marked with red asterisks (*).
B: Location of key residues in the hydrophobic patch of human Cyclin B1. The residues in the sequence NMRAILIDWL from the α1 helix shown in (A) are shown in red. R/KXL containing peptides dock into the binding groove created between α1, α3 and α4 helices. The key residues mutated in the HPM mutant are shown in yellow with their side chains shown in ball and stick format. PDB ID 2B9R, structure from (Petri et al., 2007), diagram made using Mol* (Sehnal et al., 2021) and RSCB PDB.

The Cyclin B1 constructs were initially introduced into two different cell lines: a HeLa Kyoto cell line was transiently transfected with Cyclin $B1^{WT}$-YFP or Cyclin $B1^{HPM}$-YFP as well as Centrin 1-mCherry (to mark the centrosome); and in parallel a U2OS cell line that stably expressed γ-tubulin-eGFP (to mark the centrosome) (Dai et al., 2009) was transiently transfected with just Cyclin $B1^{WT}$-mCherry or Cyclin $B1^{HPM}$-mCherry. The first approach resulted in a higher level of cell death after transfection and also resulted in fewer cells expressing both the centrosome marker and Cyclin B1-YFP, possibly due to it involving a co-transfection of both Cyclin B1-YFP and Centrin 1-mCherry constructs. Therefore, for all future experiments, the U2OS cell line stably expressing γ-tubulin-eGFP was used, with Cyclin $B1^{WT}$-mCherry or Cyclin $B1^{HPM}$-mCherry introduced by transient transfection.

To check that both Cyclin B1-mCherry constructs were expressed at full length, whole cell lysates were prepared from U2OS cells after transfection and endogenous Cyclin B1 and transfected Cyclin B1-mCherry were detected by immunoblotting (Figure 4.2). To confirm that the transfected Cyclin $B1^{WT}$-mCherry and Cyclin $B1^{HPM}$-mCherry could interact with the endogenous Cdk1, the transfected constructs were pulled down using RFP-trap and probed for bound Cdk1 (Figure 4.3). Both transfected constructs were able to pull-down endogenous Cdk1, though this was more clearly shown on the high exposure blot for Cyclin $B1^{HPM}$-mCherry due to a lower level of Cyclin $B1^{HPM}$-mCherry in the input lysate and to a lower efficiency capture of Cyclin $B1^{HPM}$-mCherry by RFP-trap in this experiment (see IP lane). The experiment was not able to distinguish any differences in affinity between Cyclin $B1^{WT}$-mCherry and Cyclin $B1^{HPM}$-mCherry with Cdk1, in part due to the varying efficiency in Cyclin $B1^{WT}$-mCherry and Cyclin $B1^{HPM}$-mCherry pull-down, and also as variation in transfection efficiency could result in different ratios of transfected Cyclin B1-mCherry and Cdk1. However, it does demonstrate that both transfected constructs can bind endogenous Cdk1. Having confirmed this, I next investigated the localisation of the constructs.

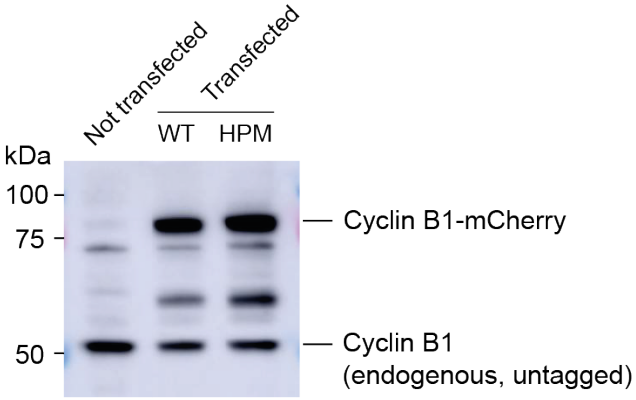


Figure 4.2 | Western blot of transfected Cyclin B1-mCherry constructs

Western blots of whole-cell lysates from U2OS cells stably expressing γ-tubulin-eGFP that were transiently transfected with either Cyclin $B1^{WT}$-mCherry, Cyclin $B1^{HPM}$-mCherry, or left untransfected. Membranes were probed with an anti-Cyclin B1 antibody.

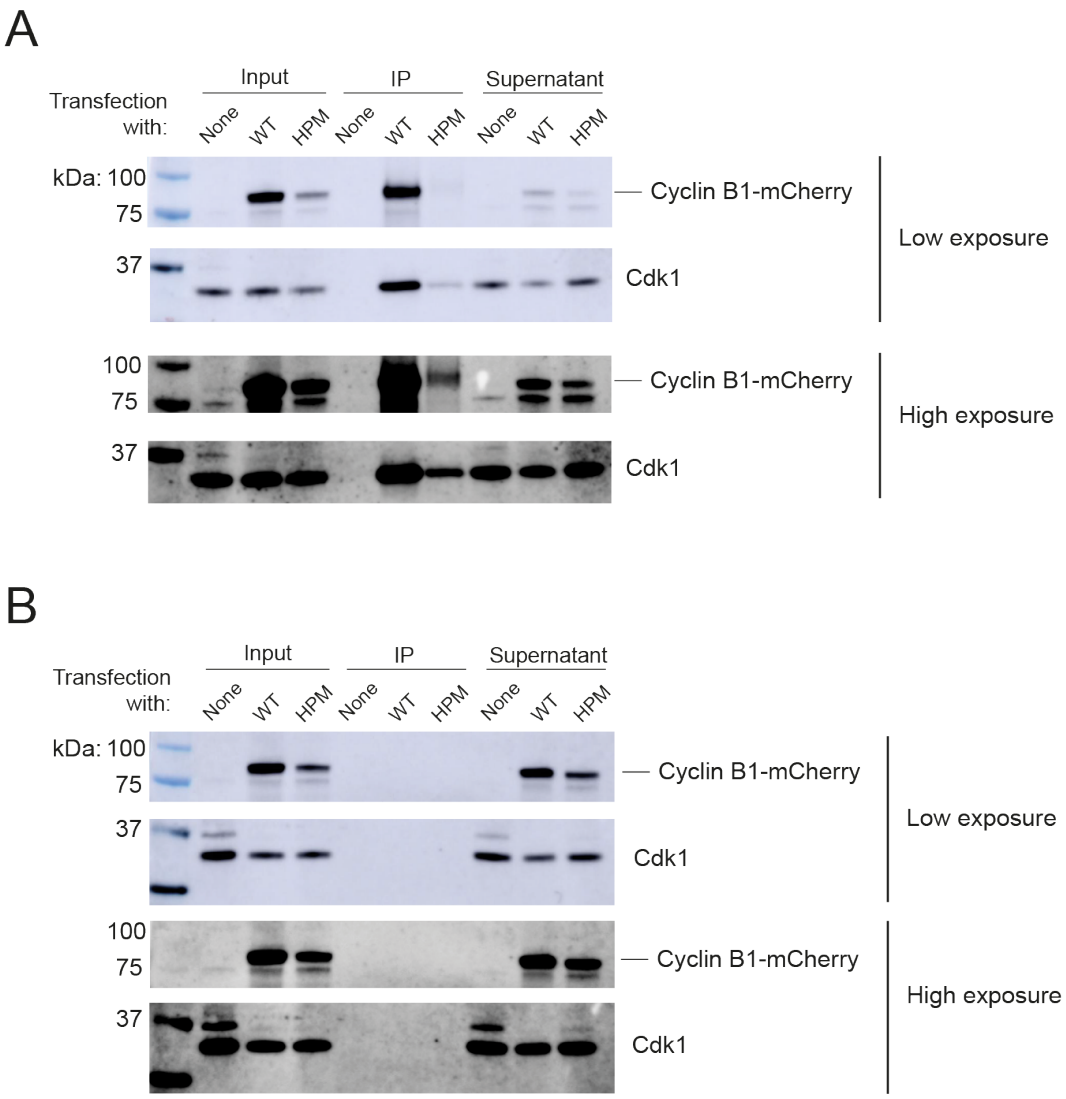


Figure 4.3 | Transfected Cyclin B1-mCherry constructs can interact with Cdk1

A: Co-immunoprecipitation using RFP-trap to capture transfected Cyclin B1-mCherry constructs. Membranes were probed with anti-Cyclin B1 antibody to detect captured Cyclin B1-mCherry, and anti-Cdk1 antibody to detect bound Cdk1. Two exposures of the same membrane are shown (low and high exposure). In the low exposure image, none of the signal saturates the displayed pixel range. The high exposure image is set to better display low intensity bands, meaning that the higher-intensity signal saturates the detected and displayed pixel range. One of two biological replicates is shown.
B: Control coimmunoprecipitation of extracts from (A) with binding control agarose beads that do not contain the RFP-nano-trap, to check for non-specific binding. As for (A), two exposures of the same membrane are shown (low and high exposure).

4.2 Localisation of Cyclin B1^{HPM}-mCherry

U2OS γ-tubulin-eGFP cells were transfected with Cyclin B1^{WT}-mCherry or Cyclin B1^{HPM}-mCherry and imaged after 24 hours. Images were taken of an asynchronous population at one point in time, and these images were analysed for a centrosomal focus of Cyclin B1-mCherry. The majority of cells displayed the expected interphase cytoplasmic localisation of Cyclin B1-mCherry (Pines and Hunter, 1991, Hagting et al., 1998), and a significant proportion of the population had a focus of Cyclin B1^{WT}-mCherry at the centrosome. However, no examples of centrosomal Cyclin B1^{HPM}-mCherry signal were observed (Figure 4.4). As transient transfection can result in a wide range of expression levels of the transfected construct, only cells below a certain signal intensity (~9000 AU) were included as high expression levels may have resulted in protein mislocalisation or sequestration. Even after excluding these very high-expressing cells, there were some cells that displayed Cyclin B1-mCherry localisation that differed from the multiple previous reports of Cyclin B1 localisation, for example displaying non-homogenous localisation in the cytoplasm (Figure 4.4C). The analysis of Cyclin B1^{WT}-mCherry and Cyclin B1^{HPM}-mCherry centrosomal localisation was performed both including and excluding these cells to establish whether the analysis of the experiment was affected. Whilst the percentage of cells with centrosomal Cyclin B1^{WT}-mCherry was reduced from ~35% to ~20% of the population when all cells were included, there were no examples of Cyclin B1^{HPM}-mCherry centrosomal localisation in any cells (Figure 4.4B). These results suggest that an intact hydrophobic patch is necessary for Cyclin B1 localisation to the centrosome in all cell cycle stages.

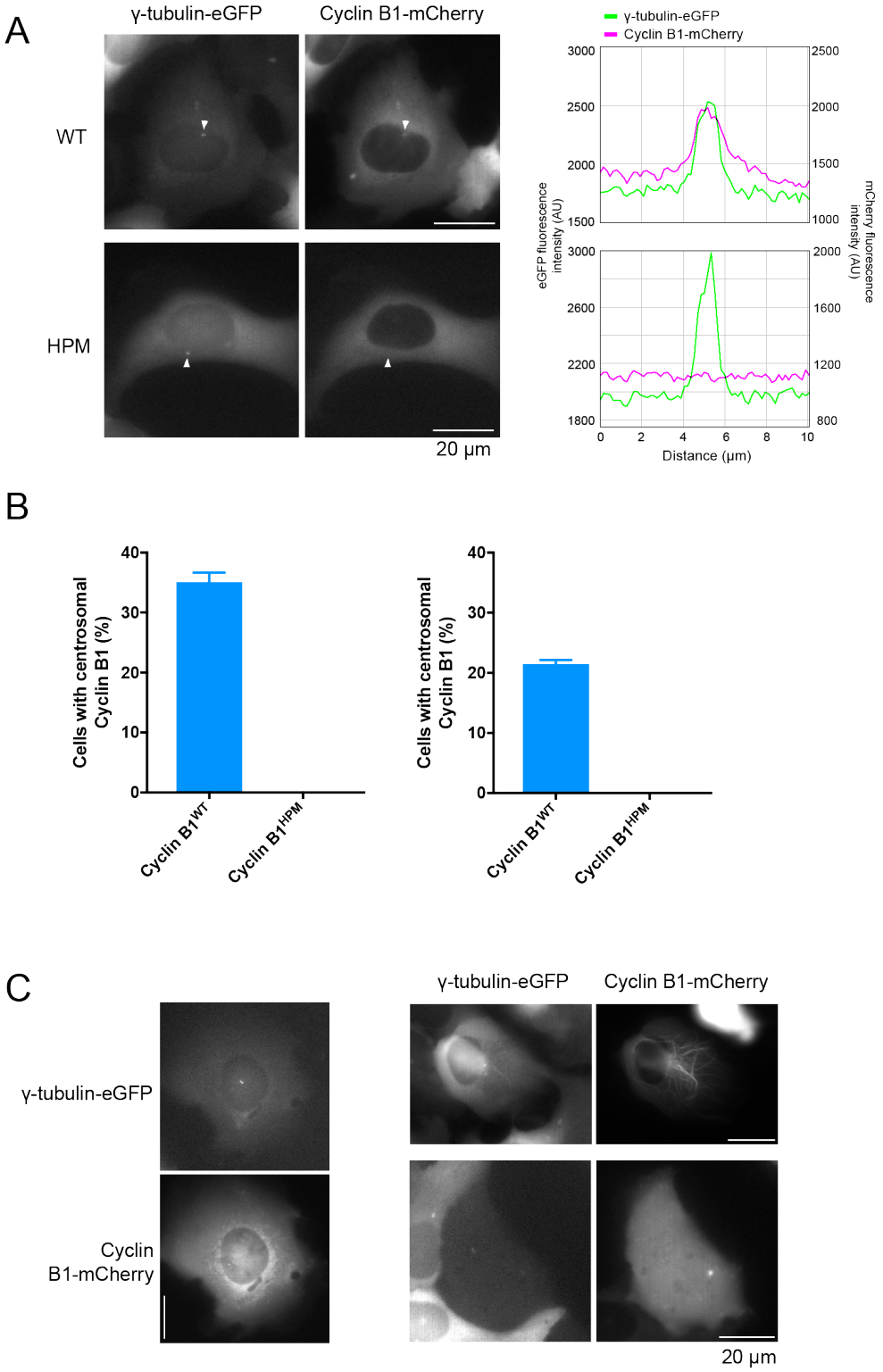


Figure 4.4 | Cyclin B1^{HPM}-mCherry is not enriched at the centrosome

A: Representative U2OS cells stably expressing γ-tubulin-eGFP (to mark the centrosome) that were transiently transfected with Cyclin B1^{WT}-mCherry or Cyclin B1^{HPM}-mCherry. Images show just the in-focus z-slice (judged by γ-tubulin-eGFP signal); graphs show vertically-averaged pixel intensity along a line scan 3 pixels in height drawn through the centrosome.

Figure 4.4 ***caption continued from previous page***
B: Cells from (A) (an asynchronous population) were analysed at one point in time for the presence of a focus of Cyclin B1-mCherry signal at the centrosome. Cells with Cyclin B1-mCherry signal intensity of higher than roughly 9000 AU were excluded as high levels of overexpression could lead to mislocalisation. Mean and SD of three biological replicates are shown. **Left-hand graph**: analysis performed while excluding cells that are judged to have mislocalised or sequestered Cyclin B1. Cyclin $B1^{WT}$-mCherry n > 50 per replicate, total n = 154. Cyclin $B1^{HPM}$-mCherry n > 50 per replicate, total n = 156. **Right-hand graph**: analysis performed including cells that are judged to have mislocalised or sequestered Cyclin B1. Cyclin $B1^{WT}$-mCherry n > 80 per replicate, total n = 294. Cyclin $B1^{HPM}$-mCherry n > 70 per replicate, total n = 287.
C: Example cells judged to have mislocalised or sequestered Cyclin B1-mCherry (included in B, right hand graph). Examples were found in populations transfected with both WT and HPM Cyclin B1-mCherry constructs. Images show just the in-focus z-slice (judged by γ-tubulin-eGFP signal); all scale bars show 20 μm.

I next followed cells in an asynchronous population by timelapse microscopy, to be able to follow cells through mitosis. Wild-type Cyclin B1 is known to localise to the centrosome in mitosis (Hagting et al., 1998), so this allows me to confirm that the Cyclin $B1^{WT}$-mCherry construct is localising as expected and compare Cyclin $B1^{HPM}$-mCherry localisation in the same cell cycle stage. It also allows the confirmation that a focus of Cyclin B1-mCherry signal at the centrosome is seen consistently through several time points, in contrast to the previous experiment, which only looks at one point in time and is therefore more sensitive to random fluctuations in signal intensity. Furthermore, given the previous findings that $Cdc13^{HPM}$-sfGFP still localises to the SPB in mitosis, yet no cells in an asynchronous population had Cyclin $B1^{HPM}$-mCherry at the centrosome, the time-lapse imaging allows me to ask specifically if cells in mitosis have centrosomal Cyclin $B1^{HPM}$-mCherry. Cells were judged to be in mitosis when Cyclin B1-mCherry (cytoplasmic in interphase) was imported into the nucleus, and the cell rounded.

Cells had a clear focus of Cyclin $B1^{WT}$-mCherry at the centrosome throughout mitosis until cyclin degradation (Figure 4.5). However, Cyclin $B1^{HPM}$-mCherry was not enriched at the centrosome even in mitotic cells (Figure 4.6). Together, the results in this Chapter suggest that the hydrophobic patch is necessary for Cyclin B1 localisation to the centrosome in all cell cycle stages, and that there is not a hydrophobic patch-independent mechanism of Cyclin B1 centrosomal localisation.

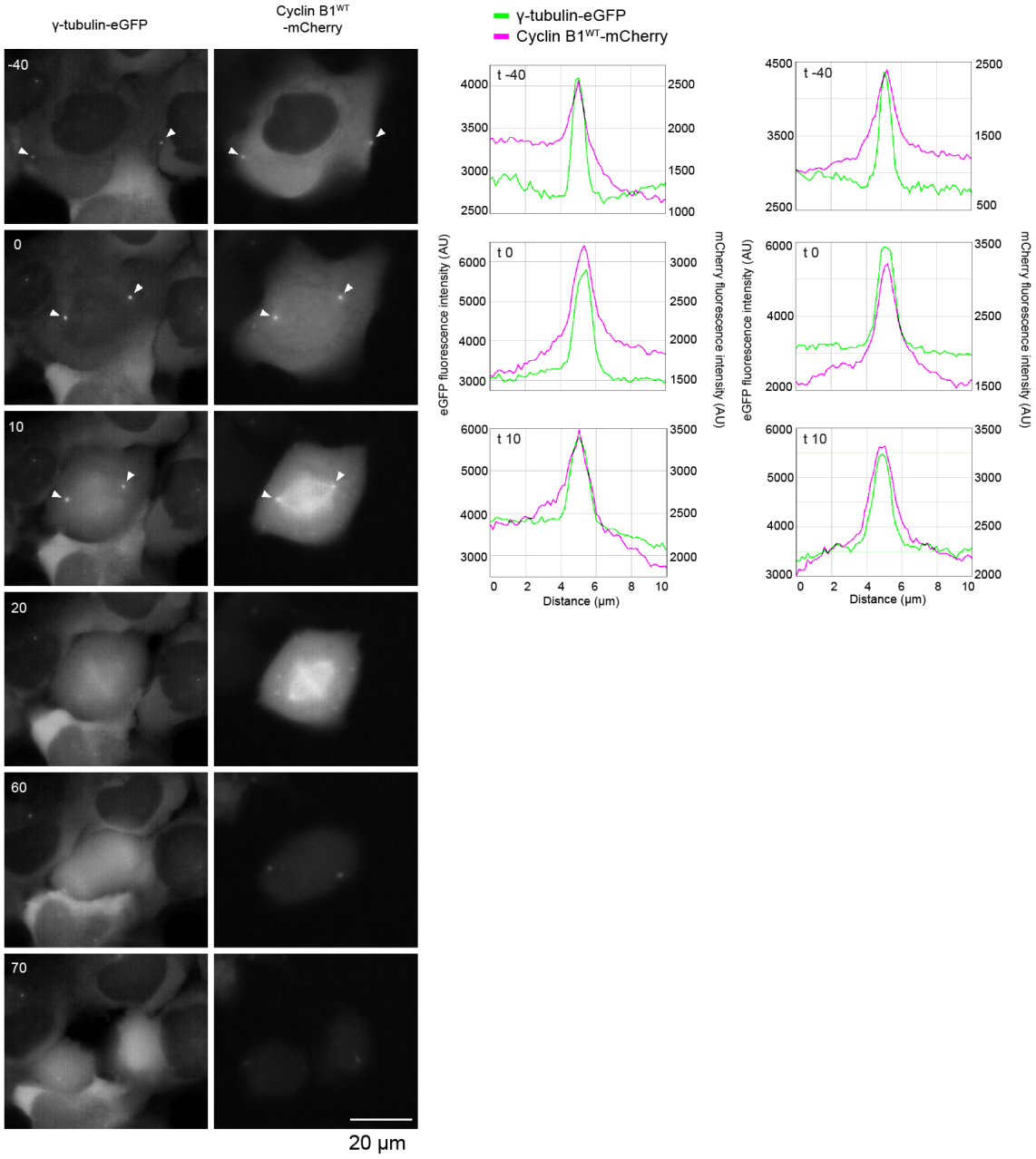


Figure 4.5 | Cyclin B1^{WT}-mCherry localisation in mitosis

U2OS cells stably expressing γ-tubulin-eGFP (to mark the centrosome) were transfected with Cyclin B1^{WT}-mCherry and followed with timelapse imaging. Images show a maximum projection of a representative cell as it goes through mitosis; in the last few frames the centrosome moved out of focus as the cell rounded. Timestamps refer to time from the first frame in which nuclear Cyclin B1-mCherry signal was seen (taken as the start of mitosis). Arrows mark the location of in-focus γ-tubulin-eGFP. Graphs show vertically-averaged pixel intensity along a line scan 3 pixels in height drawn through the centrosome, measured on the in-focus z-slice as judged by γ-tubulin-eGFP signal. Graphs correspond to the timepoint shown in the neighbouring image, and timestamps are also shown in the top left-hand corner of the graphs.

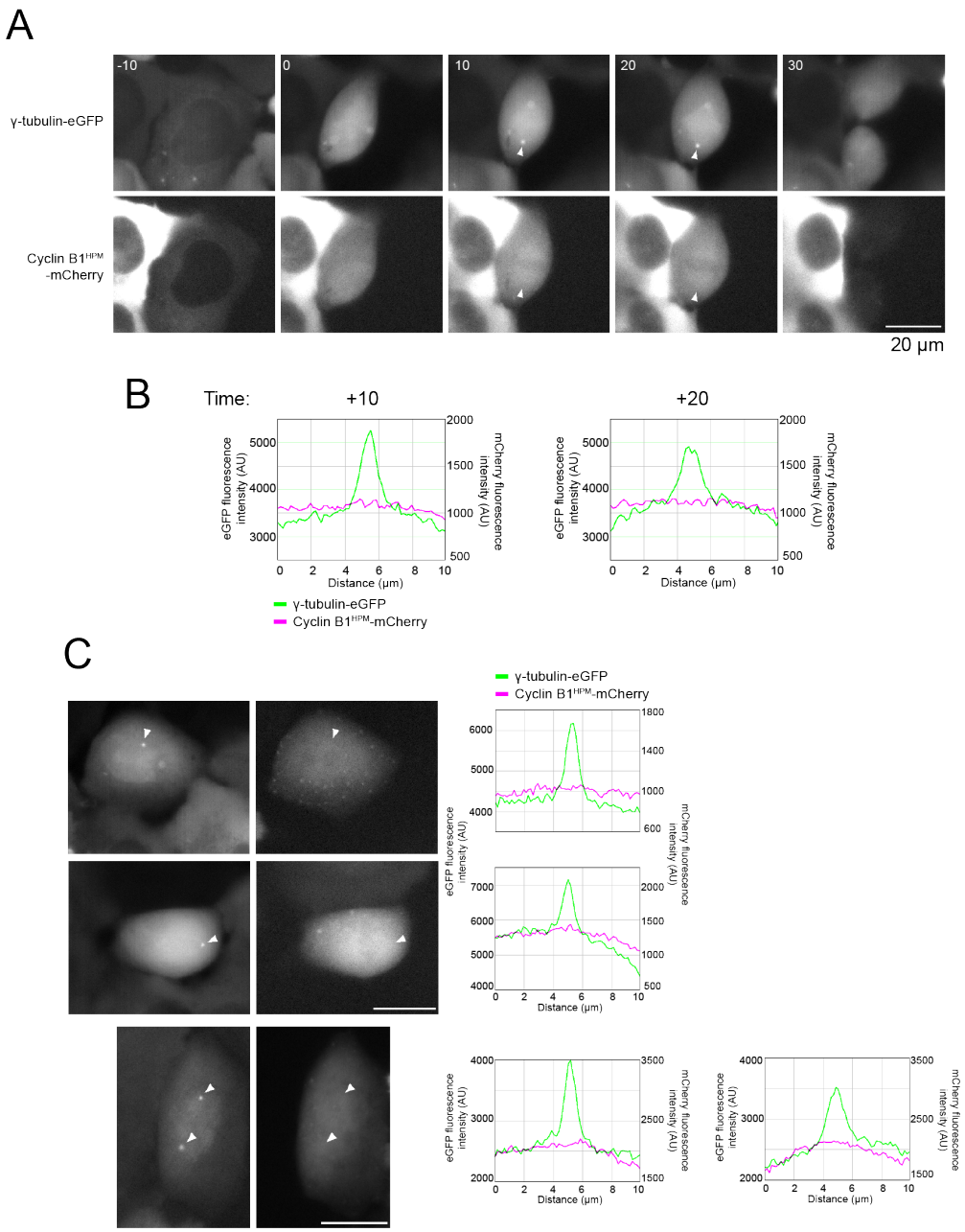


Figure 4.6 | Cyclin B1^{HPM}-mCherry localisation in mitosis

U2OS cells stably expressing γ-tubulin-eGFP (to mark the centrosome) were transfected with Cyclin B1^{HPM}-mCherry, and followed with timelapse imaging.
A: Images show the in-focus z slice (judged by γ-tubulin-eGFP signal) of a representative cell as it goes through mitosis; in the last few frames the centrosome moved out of focus as the cell rounded. Timestamps refer to time (min) from the first frame in which nuclear Cyclin B1^{HPM}-mCherry signal was seen (taken as the start of mitosis). Arrows mark the location of in-focus γ-tubulin-eGFP.
B: Graphs show vertically-averaged pixel intensity along a line scan 3 pixels in height drawn through the centrosome, for the +10 minute (left hand graph) and +20 minute (right hand graph) timepoints from (A).
C: One time point in mitosis from three more example cells, with line scans as in (B).

4.3 Discussion

The results from this Chapter suggest that the role of the hydrophobic patch in SPB and centrosomal localisation is similar between the major mitotic B-type cyclins in *S. pombe* (Cdc13) and human cells (Cyclin B1). The SPB and centrosome carry out the same function but are structurally different, and the similarity in cyclin localisation to the centrosome and SPB in these evolutionarily distant organisms is suggestive that the role of Cyclin B1/Cdc13 at the centrosome and SPB is important. The suggestion that both Cdc13 and Cyclin B1 rely on the hydrophobic patch to localise to the SPB and centrosome may indicate that they interact with homologous targets, although it is also possible that they dock to non-homologous proteins. The interaction is likely to involve R/KXL motifs. Mammalian Cyclin A also uses its hydrophobic patch to localise to the centrosome (Pascreau et al., 2010), and whilst Cyclin E does not, expressing a mammalian Cyclin E CLS (centrosomal localisation sequence) peptide interfered with the localisation of both Cyclin A and E to the centrosome, suggesting that they may dock to the same target(s) (Matsumoto and Maller, 2004). It is therefore also possible that the same or homologous protein(s) at the centrosome and SPB are interacting with Cyclins E, A, B1 and Cdc13.

The three SPB-localised proteins so far that have been suggested to interact with Cdc13 are Cdc11, Ppc89 and Sad1 (Morrell et al., 2004, Vo et al., 2016), all of which have orthologues in human cells (Centriolin, CEP57/CEP57L1 and SUN1-5 respectively) (Wood et al., 2012). Potential interactors of Cyclin E1, A2 and B1 have been identified through a series of pull-downs at specific cell cycle stages followed by quantitative proteomics (Pagliuca et al., 2011). PCM1 and Plk1 were the only proteins displaying centrosomal localisation identified in both the Cyclin A and Cyclin B1 pull-downs, and Plk1 was the only one identified in all three Cyclin pull-downs. CLASP1 (Peg1 in *S. pombe*) (Wood et al., 2012) was the only other centrosomal component pulled down by Cyclin B1, but several more components were identified as potential interactors of Cyclin A (Pagliuca et al., 2011). These putative centrosomal cyclin interactors could be a starting point for identifying

potential hydrophobic patch-interacting protein(s) at the centrosome, as would the orthologs of the suggested interactors of Cdc13.

The results presented in this Chapter also suggest that the hydrophobic patch-independent mechanism of Cdc13^{HPM}-sfGFP SPB localisation that occurs in mitosis is not conserved in Cyclin B1. Potential roles for this hydrophobic patch independent accumulation of Cdc13 and why it might not be conserved in human Cyclin B1 are discussed further in the Discussion (Chapter 7). Identifying the interactor(s) at the SPB that facilitate this mitotic localisation of Cdc13 or the region of Cdc13 required, and subsequently interfering with mitotic Cdc13 SPB accumulation, could shed more light on what role this plays in *S. pombe* and why it does not occur in human cells.

The work in this Chapter suggests that the hydrophobic patch not only plays an important role in *S. pombe* Cdc13 localisation to the SPB, but also in human Cyclin B1 localisation to the centrosome. In the following Chapter I investigate the role of the hydrophobic patch in *S. pombe* Cdc13, asking whether restoring SPB localisation of Cdc13^{HPM}-Cdc2 affects the phenotype of cells expressing Cdc13^{HPM}.

Chapter 5. Raising Cdc13^{HPM} activity at the SPB

The work in the previous Chapters has demonstrated that Cdc13^{HPM} has a severe defect in localisation to the SPB in G2. It has also been observed that cells driven by Cdc13^{HPM} perform S phase but not mitosis, and that they have reduced phosphorylation of a number of mitotic substrates, particularly those at the SPB and cytoplasm (Basu et al., 2020). These results lead to the working hypothesis that the SPB localisation defect of Cdc13^{HPM} results in a lower CDK activity at the SPB and in the cytoplasm, leading to reduced phosphorylation in these compartments and a lack of mitotic entry (Basu et al., 2020).

It is also possible that the localisation defect of Cdc13^{HPM} is not the reason, or not the only reason, that it does not drive mitosis in these experiments. It is documented that the hydrophobic patch of cyclins acts as a substrate docking region (Schulman et al., 1998, Loog and Morgan, 2005) and it is possible that one or multiple critical substrate(s) are not sufficiently phosphorylated by Cdc2 if the Cdc13 hydrophobic patch is not intact, regardless of the SPB localisation of the complex.

The results gathered so far with Cdc13^{HPM} do not distinguish between the above hypotheses, meaning that it is unknown if the necessary function of the hydrophobic patch is due to its SPB localisation role, or a more general substrate-docking role, or both. If restoring SPB localisation of Cdc13^{HPM} rescues the mitotic defect of cells driven by Cdc13^{HPM}, it would suggest that cyclin-substrate docking interactions via the hydrophobic patch are not essential for mitosis, but that cyclin SPB localisation is. This is therefore a critical experiment to gain insight into the relative importance of SPB localisation and substrate docking via the Cdc13 hydrophobic patch. The work in this Chapter addresses this question.

5.1 Localisation of Cdc13^{HPM} in the absence of wild-type Cdc13

The work outlined earlier demonstrates that in the presence of a wild-type copy of Cdc13, Cdc13^{HPM} has defective SPB localisation in early/mid G2, but accumulates at the SPB after Plo1 does, in late G2/early mitosis (Mulvihill et al., 1999, Grallert et al., 2013b). Given that cells driven solely by Cdc13^{HPM} do not enter mitosis (Basu et al., 2020), I hypothesise that these cells never reach the stage of the cell cycle in which Cdc13^{HPM} accumulates at the SPB. To test this, I investigated the localisation of Cdc13^{HPM} when wild-type Cdc13 is not present. I utilised the same system used to test whether Cdc13^{HPM} could drive mitosis (Basu et al., 2020). I used a strain background in which wild-type *cdc13* was placed under the thiamine-repressible *nmt41* promoter, and the endogenous copy of *cdc13* was deleted. The cyclins *cig1* and *cig2* were also deleted in this background. In order to study Cdc13^{HPM} localisation to the SPB, I used *sid4-mRFP* to mark the SPB, and added an exogenous copy of *cdc13^{WT}-sfGFP* or *cdc13^{HPM}-sfGFP* under the Cdc13 promoter to cells. This resulted in the following strains: *nmt41:cdc13 cig1Δ cig2Δ sid4-mRFP leu::cdc13^{WT}-sfGFP* or *nmt41:cdc13 cig1Δ cig2Δ sid4-mRFP leu::cdc13^{HPM}-sfGFP*.

Cells were arrested in G1 by nitrogen starvation, and thiamine was added to the media 1 hour before release in order to repress transcription of the wild-type *cdc13*. Cells were analysed for progression through the cell cycle and Cdc13^{WT}-sfGFP or Cdc13^{HPM}-sfGFP localisation as they were released from G1 with just the expression of the exogenous Cdc13^{WT}-sfGFP or Cdc13^{HPM}-sfGFP. Monitoring DNA content by flow cytometry showed that both populations with Cdc13^{WT}-sfGFP and Cdc13^{HPM}-sfGFP went through DNA replication with similar timings as expected from previous observations (Figure 5.1A) (Basu et al., 2020). Also in agreement with previous work, cells driven by Cdc13^{WT}-sfGFP began to binucleate, whilst cells driven by Cdc13^{HPM}-sfGFP did not (Figure 5.1B). Analysing the localisation of Cdc13-sfGFP in these populations showed that whilst both Cdc13^{WT}-sfGFP and Cdc13^{HPM}-sfGFP accumulated in cells after release from the G1 arrest, only Cdc13^{WT}-sfGFP accumulated at the SPB (Figure 5.2). From this I conclude that cells driven by Cdc13^{HPM} arrest in G2 before Cdc13^{HPM}-sfGFP accumulates at the SPB.

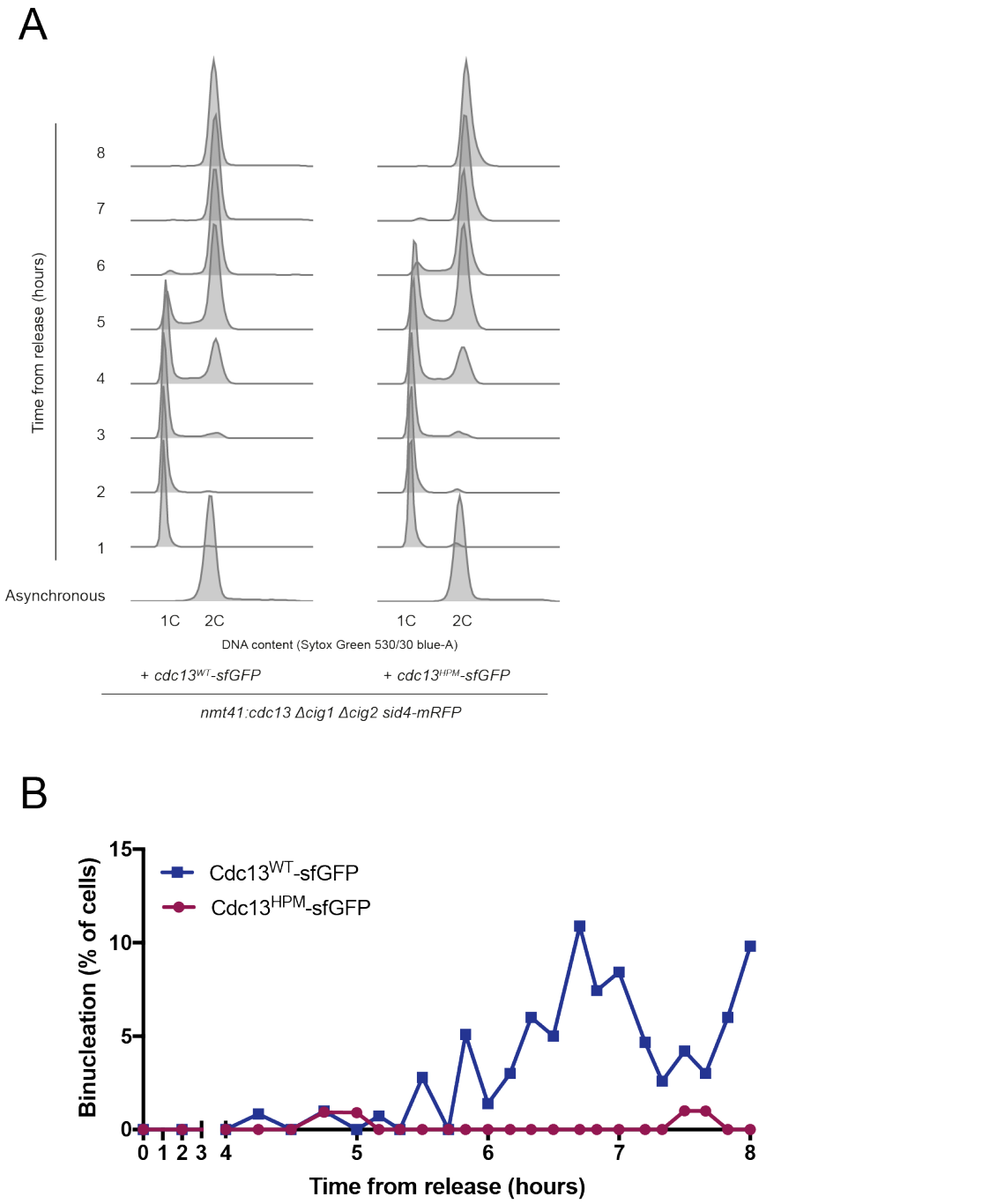


Figure 5.1 | Release from G1 arrest of cells expressing Cdc13$^{WT/HPM}$-sfGFP

A: DNA content of cells after release from a G1 arrest, measured by flow cytometry. Cells were grown in EMM + adenine at 32 °C and arrested in G1 by removing nitrogen from the media and holding at 25 °C. Arrested cells were released after 18 hours by washing into media containing nitrogen. Thiamine was added to the media 1 hour before release in order to repress transcription of wild-type *cdc13*.
B: Heat-fixed cells from the experiment in (A) were scored for binucleation (defined as cells with two separate nuclei and no septation). N > 70 cells per time point.

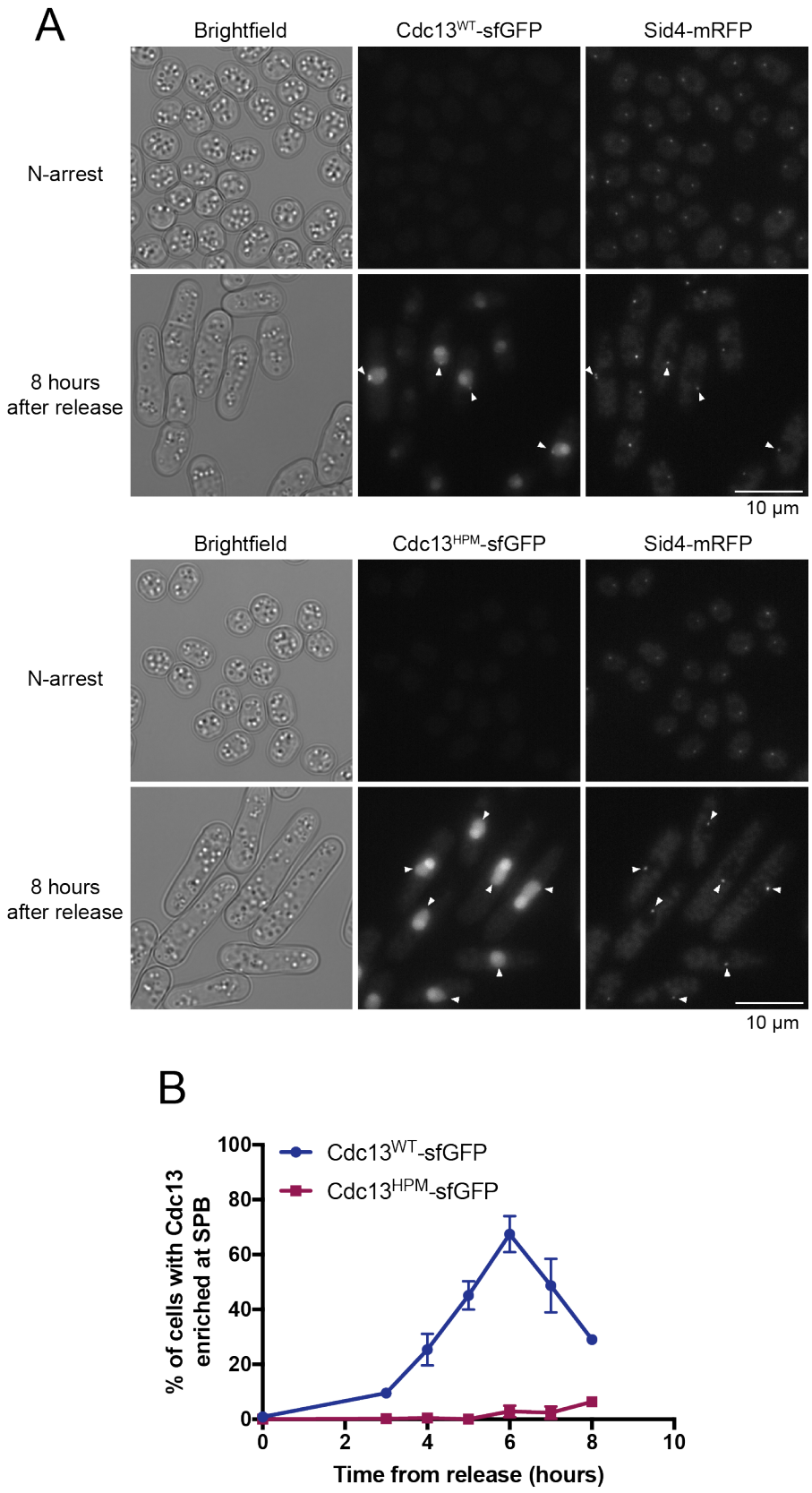


Figure 5.2 | Localisation of Cdc13^{HPM}-sfGFP when wild-type Cdc13 is not present

Figure 5.2 ***caption continued from previous page***
A: Images showing Cdc13-sfGFP accumulation and localisation in cells arrested in G1 by nitrogen starvation (N-arrest) and 8 hours after release. Fluorescence images are maximum projection images, and the same pixel range has been applied to all images of the same channel. Arrows mark the location of SPBs.
B: Cells from (A) were scored by eye for a focus of Cdc13-sfGFP at the SPB. Mean and SD of two biological replicates are shown. N ≥ 110 cells per strain per timepoint.

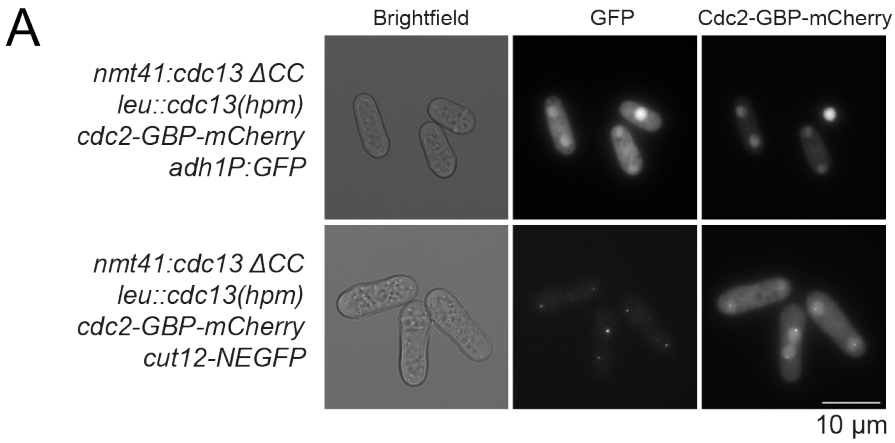
5.2 Developing a system to relocalise Cdc13^{HPM}/Cdc2 to the SPB

To separate the SPB localisation role of the hydrophobic patch from its general substrate-docking role, I sought to artificially tether Cdc13^{HPM}/Cdc2 to the SPB, to restore SPB localisation. Whilst this artificial localisation may not exactly recapitulate the dynamics and localisation of Cdc13-Cdc2 accumulation at the SPB, it may provide enough activity at the SPB to mimic the lost SPB localisation of Cdc13^{HPM}. To tether Cdc2 to the SPB, I opted to use the GFP/GBP binding system (Rothbauer et al., 2008), using Cdc2 tagged with GBP-mCherry, and Cut12-NEGFP (Bridge et al., 1998). I chose this system as it has previously been used successfully to tether active Cdc2 to the SPB resulting in an acceleration of mitotic commitment, and the strongest phenotype was seen when Cdc2 was tethered to Cut12 (Grallert et al., 2013b). I relocalised Cdc2 rather than Cdc13, as Cdc2 better tolerates being tagged (Kamenz et al., 2015).

An initial attempt was made by mating strains in order to obtain a strain with *cdc2-GBP-mCherry cut12-NEGFP* (at endogenous loci) and an exogenous copy of *cdc13^{HPM}* (under the Cdc13 promoter, in the *leu1* locus) in the background used previously (*nmt41:cdc13 cig1Δ cig2Δ*, in which the endogenous *cdc13* is deleted). Strains with no GFP, or with GFP expressed (under the *adh1* promoter) but not fused to any protein, were used as controls. Fluorescence microscopy showed that Cdc2-GBP-mCherry was co-localised with Cut12-NEGFP in *nmt41:cdc13 cig1Δ cig2Δ leu::cdc13^{HPM} cdc2-GBP-mCherry cut12-NEGFP* cells, as well as being localised in the nucleus and cytoplasm (Figure 5.3A). However, it was difficult to tell by eye if the cells were short diploid cells or long haploid cells (Figure 5.3B), so patches of cells from plates were analysed for DNA content by flow cytometry to ascertain if the strains were haploid or diploid. This showed clearly that the strain with *cut12-NEGFP* was a stable diploid (Figure 5.4). Whilst the strain had one copy of endogenous *cdc13* deleted, there was also an intact allele of *cdc13* present at its endogenous locus (not under the *nmt41* promoter) in the cells meaning the strains were no longer used in experiments. Other isolates screened from the cross were

either visibly diploid or unstable, losing expression of either Cut12-NEGFP or Cdc2-GBP-mCherry, suggesting that the cells do not tolerate the genotype.

Reasoning that forcing constitutive Cdc2 activity to the SPB throughout the cell cycle could be detrimental to cells, I next attempted to improve the cell tolerance to having a copy of Cdc2 tethered to the SPB by tethering a copy of the Cdc13-L-Cdc2(as) fusion protein, that is sensitive to inhibition by the ATP analogue 1-NmPP1 (Bishop et al., 2000, Coudreuse and Nurse, 2010). This resulted in a strain with the genotype *nmt41:cdc13 cig1Δ cig2Δ leu::cdc13^{HPM}-L-cdc2(as)-GBP-mCherry cut12-NEGFP*, and the endogenous *cdc2* remained intact in these cells. Growth on media containing 1-NmPP1 should inhibit the kinase activity of the fusion protein until the 1-NmPP1 is removed. However, even when grown on EMM4S agar plates + 1 μM 1-NmPP1, where *nmt41:cdc13* is not repressed and the kinase activity of the fusion protein is restricted, the population was unstable, with the majority of cells losing expression of either Cut12-NEGFP or Cdc13^{HPM}-L-Cdc2(as)-GBP-mCherry (Figure 5.5). It is possible that the small percentage of cells that retained both Cut12-NEGFP and Cdc13^{HPM}-L-Cdc2(as)-GBP-mCherry have mutations that permit the retention of both constructs. Growing cells on higher concentrations of 1-NmPP1 did not solve the issue. It is possible that there was still enough residual kinase activity even when 1-NmPP1 was present to make the fusion protein intolerable to cells over multiple generations. I therefore next put the tethered construct under an inducible promoter, so I could restrict expression during growth before the experiment.



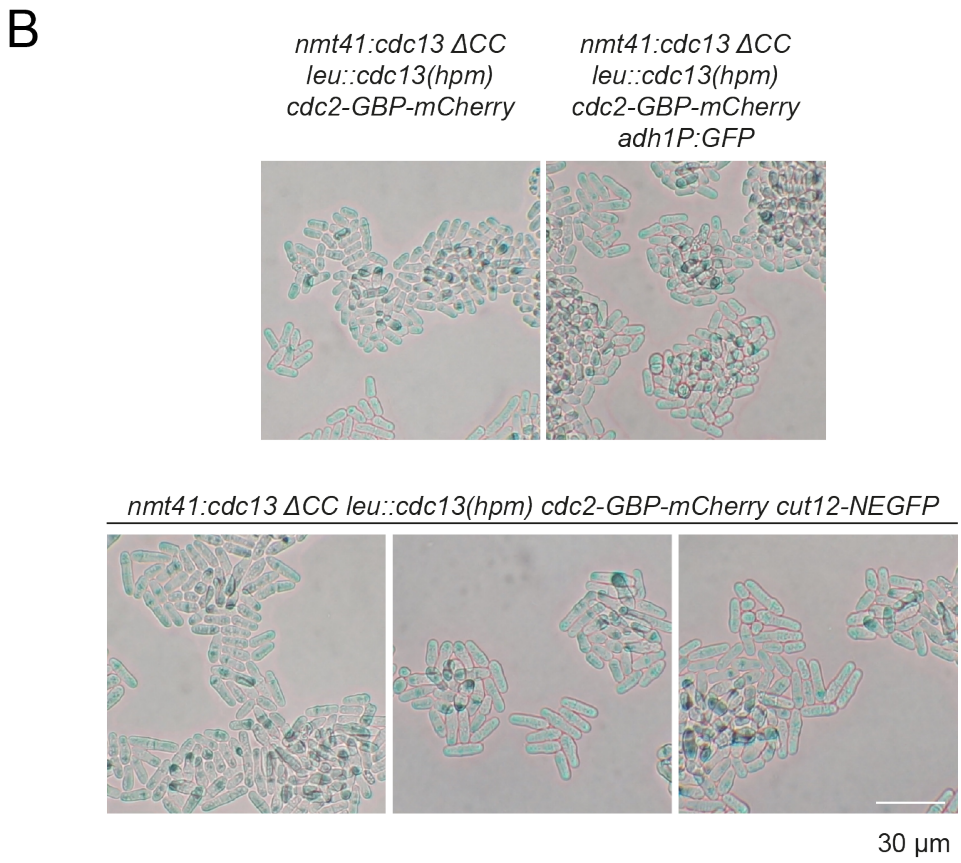


Figure 5.3 | Cdc2-GBP-mCherry colocalises with Cut12-NEGFP

A: Fluorescence microscopy to show the localisation of Cdc2-GBP-mCherry in strains containing GFP or Cut12-NEGFP. Fluorescence images show a maximum projection. Samples were grown on agar plates and transferred from plates directly to slides (suspended in EMM4S media) and imaged immediately. *ΔCC* stands for *cig1Δ cig2Δ*. Cells have expression of the endogenous *cdc13* on due to the absence of thiamine in the media
B: Cells were imaged on plates 17 hours after patching on EMM4S and placing at 25 °C. Cells in the bottom three images are from different colonies of the same original isolate. *ΔCC* stands for *cig1Δ cig2Δ*.

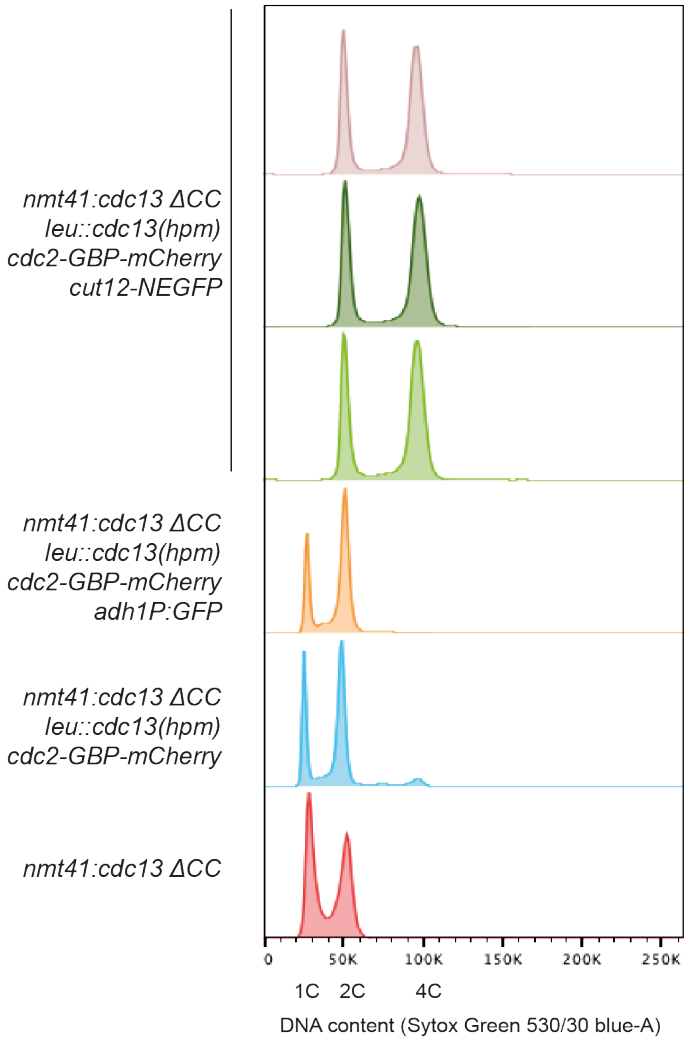


Figure 5.4 | Strains with Cdc2 tethered at the SPB are diploids

DNA content of the indicated strains, determined by flow cytometry. All samples were taken from patches on plates and suspended in 70% ethanol and processed as described in the methods before staining with Sytox Green to stain DNA. The top 3 plots represent 3 different colonies from the same original isolate.

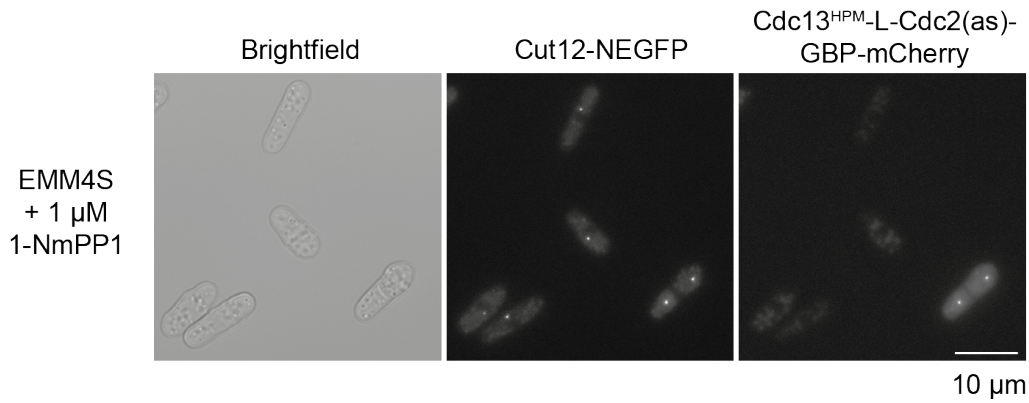


Figure 5.5 | The Cdc13-Cdc2 fusion protein tethered to the SPB is not tolerated well even in the presence of inhibitor

Cells expressing Cdc13^{HPM}-L-Cdc2(as)-GBP-mCherry under the Cdc13 promoter and Cut12-NEGFP in the strain background *nmt41:cdc13 cig1Δ cig2Δ* were grown at 25 °C on EMM4S + 1 µM 1-NmPP1 agar plates before transferring onto microscope slides for imaging. Fluorescence images are maximum projection images. The cells were scored for presence of both Cut12-NEGFP and Cdc13-L-Cdc2(as)-GBP-mCherry, with 4 % of cells retaining both constructs; n = 74 cells.

I made use of a system previously used in our lab to induce cyclin-CDK fusion proteins and test their potential to drive mitosis (Basu et al., 2021). Cells contained a temperature-sensitive allele of *cdc2*, *cdc2-M26*, which inactivates Cdc2 at the restrictive temperature of 36 °C. The cells also contained a copy of Cdc13^{HPM}-L-Cdc2(as)-GBP-mCherry under a tetracycline-inducible promoter based on the *eno101* promoter (enotetP), and a copy of the tetracycline repressor (TetR-tup11Δ70) to prevent expression in the absence of anhydrotetracycline hydrochloride (from here on referred to as tetracycline/tet) (Patterson et al., 2019, Zilio et al., 2012). The cells expressed either *cut12-NEGFP* or *cut12*$^{+}$ to have the fusion protein tethered at the SPB or untethered. Therefore the genotype of the 'tethered' strain was *cdc2-m26 tetR-tup11Δ70 enotetP-Cdc13^{HPM}-L-Cdc2(as)-GBP-mCherry cut12-NEGFP*, while the genotype of the 'untethered' strain was *cdc2-m26 tetR-tup11Δ70 enotetP-Cdc13^{HPM}-L-Cdc2(as)-GBP-mCherry*.

A preliminary experiment was carried out to test that addition of tetracycline induced fusion protein expression. Cells were shifted to 36 °C for 30 min, and

tetracycline and 1 μM 1-NmPP1 were added to induce expression of the fusion protein but restrict the kinase activity. After 1 hour, tetracycline and 1-NmPP1 were both washed out to release inhibition of the accumulated fusion protein. Both the 'tethered' and 'untethered' strains had visible Cdc13^{HPM}-L-Cdc2(as)-GBP-mCherry, indicating that the fusion protein had been induced (Figure 5.6A). Surprisingly, spindles could be seen in both conditions, suggesting that the induced Cdc13^{HPM}-L-Cdc2(as)-GBP-mCherry was able to drive spindle formation whether tethered to the SPB or untethered. To test if the untethered Cdc13^{HPM}-L-Cdc2(as)-GBP-mCherry could drive mitosis, the experiment was repeated and cells were heat fixed and stained with DAPI and calcofluor to score for binucleation and septation. A wave of binucleation could be seen after inhibitor removal, followed by a wave of septation, indicating that the cells were able to go through mitosis (Figure 5.6B).

This system is therefore unusable to ask whether tethering Cdc13^{HPM}/Cdc2 to the SPB rescues the mitotic defect of Cdc13^{HPM}. This ability of the untethered Cdc13^{HPM}-L-Cdc2(as)-GBP-mCherry to drive mitosis was unexpected given the previous findings that cells driven by Cdc13^{HPM} arrest in G2 (Figure 5.1) (Basu et al., 2020). However, there were a number of conditions that were different between the two experiments. The strain background and method of inactivating endogenous Cdc13-Cdc2 activity were different, with the original experiments using the *nmt41:cdc13 cig1Δ cig2Δ* system in the presence of thiamine and the latest experiment using *cdc2-m26* and shifting to 36 °C. The latest experiment was also using the Cdc13^{HPM}-L-Cdc2 fusion protein, and expression under a different promoter. I therefore next investigated the phenotype of the Cdc13^{HPM}-L-Cdc2 fusion protein in different strain backgrounds, in order to ask whether the fusion protein can rescue Cdc13^{HPM} in the tested conditions, and to find conditions in which the SPB-tethering rescue can be performed.

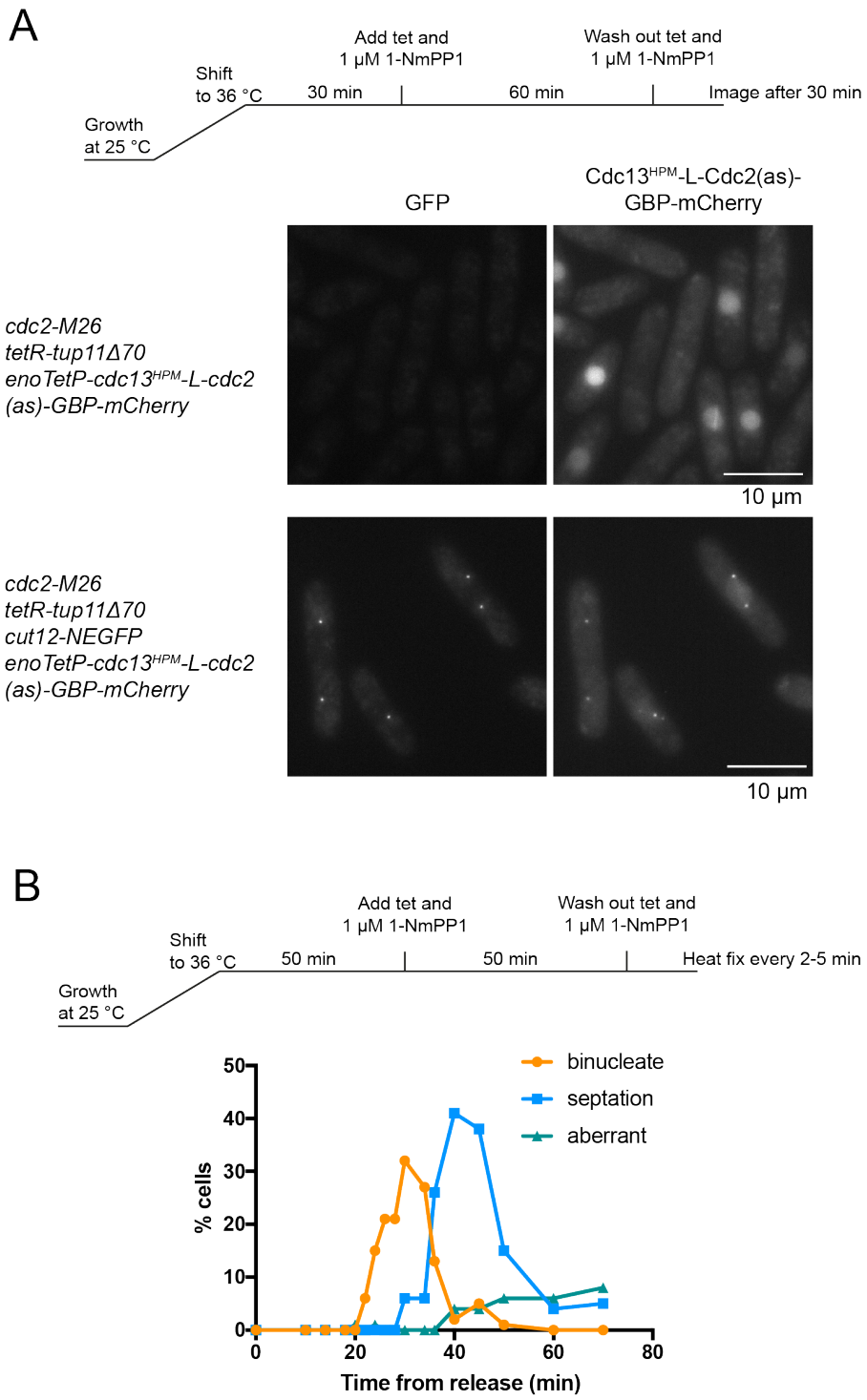


Figure 5.6 | Inducing Cdc13^{HPM}-L-Cdc2(as)-GBP-mCherry can drive mitosis in the absence of GFP

A: Cells were shifted to 36 °C to inactivate Cdc2-M26, and tetracycline and 1 µM 1-NmPP1 were added to induce the expression of the Cdc13^{HPM}-L-Cdc2(as)-GBP-mCherry fusion protein but restrict the kinase activity. After 60 minutes of induction, tetracycline and 1-NmPP1 were washed out and images were taken 30 minutes later. A schematic of the experimental outline is shown (top), with maximum

Figure 5.6 ***caption continued from previous page***
projection images from the strains with and without *cut12-NEGFP* (bottom). The same pixel range has been applied to all images from the same channel.
B: Cells without *cut12-NEGFP* were tested for their ability to perform mitosis. The top schematic shows the experimental outline, which is similar to the approach described in (A) but with a shorter induction time. Cells were heat fixed and stained with DAPI and calcofluor to measure binucleation and septation (bottom). N ≥ 100 cells per time point. Aberrant refers to aberrant mitoses and includes any mitoses that do not result in 2 nuclei separated with a single septum in the middle of the cell, for example cut phenotypes.

5.3 Can the mitotic defect of Cdc13^{HPM} be rescued by fusing Cdc13 and Cdc2 or raising Cdc2 activity?

I considered that the untethered Cdc13^{HPM}-L-Cdc2(as)-GBP-mCherry might be able to drive mitosis in the experiment in Figure 5.6 due to one of, or a combination of, the following conditions: the use of a *cdc2-M26* allele to reduce endogenous CDK activity leaves endogenous cyclins intact, and it is conceivable that they could interact with the induced fusion protein; the shift to 36 °C; the use of a Cdc13-L-Cdc2 fusion protein; or high expression from the enoTetP promoter. I therefore tested whether some of these conditions were able to rescue the mitotic defect of Cdc13^{HPM}. It is worth noting that whilst the interaction of Cdc13^{HPM} with Cdc2 has not been directly measured, it has been shown that Cdc13^{HPM} is able to drive S phase in the absence of *cig1* and *cig2*, with no differences detected in the G1/S transition rate when compared with Cdc13^{WT} (Figure 5.1) (Basu et al., 2020). Cdc13^{HPM} is also able to direct phosphorylation of early CDK substrates as well as Cdc13^{WT} does in a G2 arrest, and is able to direct phosphorylation of a number of mitotic substrates efficiently (Basu et al., 2020), indicating that it does not have a severe binding defect with Cdc2. However, it is possible that fusing Cdc13^{HPM} and Cdc2 may increase the efficiency of their binding and therefore increase the activity of Cdc2 in these strains.

I first sought to test whether the induction of Cdc13^{HPM}-L-Cdc2(as)-GBP-mCherry resulted in an overexpression in comparison to endogenous Cdc2. To do this, I repeated the shift to 36 °C and addition of tetracycline and 1-NmPP1 as outlined in Figure 5.6B, but instead of assaying for mitotic progression took samples for protein extraction at various time points after tetracycline addition. I performed this experiment using the untethered strain (*cdc2-m26 tetR-tup11Δ70 enotetP-Cdc13^{HPM}-L-Cdc2(as)-GBP-mCherry*), taking samples at 0, 15, 30, 40, 50 and 60 minutes after tetracycline addition. I also took a sample from 60 minutes after induction in the tethered strain (*cdc2-m26 tetR-tup11Δ70 enotetP-Cdc13^{HPM}-L-Cdc2(as)-GBP-mCherry cut12-NEGFP*). Serial dilutions of this sample were included on the blot to test whether the antibody concentration used was in the linear range and reflected differences in protein concentration. Western blotting of

these samples suggests that there is not a strong overexpression of Cdc13^{HPM}-L-Cdc2(as)-GBP-mCherry compared to endogenous Cdc2, however the signal of the Cdc13^{HPM}-L-Cdc2(as)-GBP-mCherry protein was smeared in the lanes above the expected band (Figure 5.7). This prevents an accurate measure of protein concentration, and therefore this cannot rule out a mild/moderate overexpression of Cdc13^{HPM}-L-Cdc2(as)-GBP-mCherry compared to Cdc2.

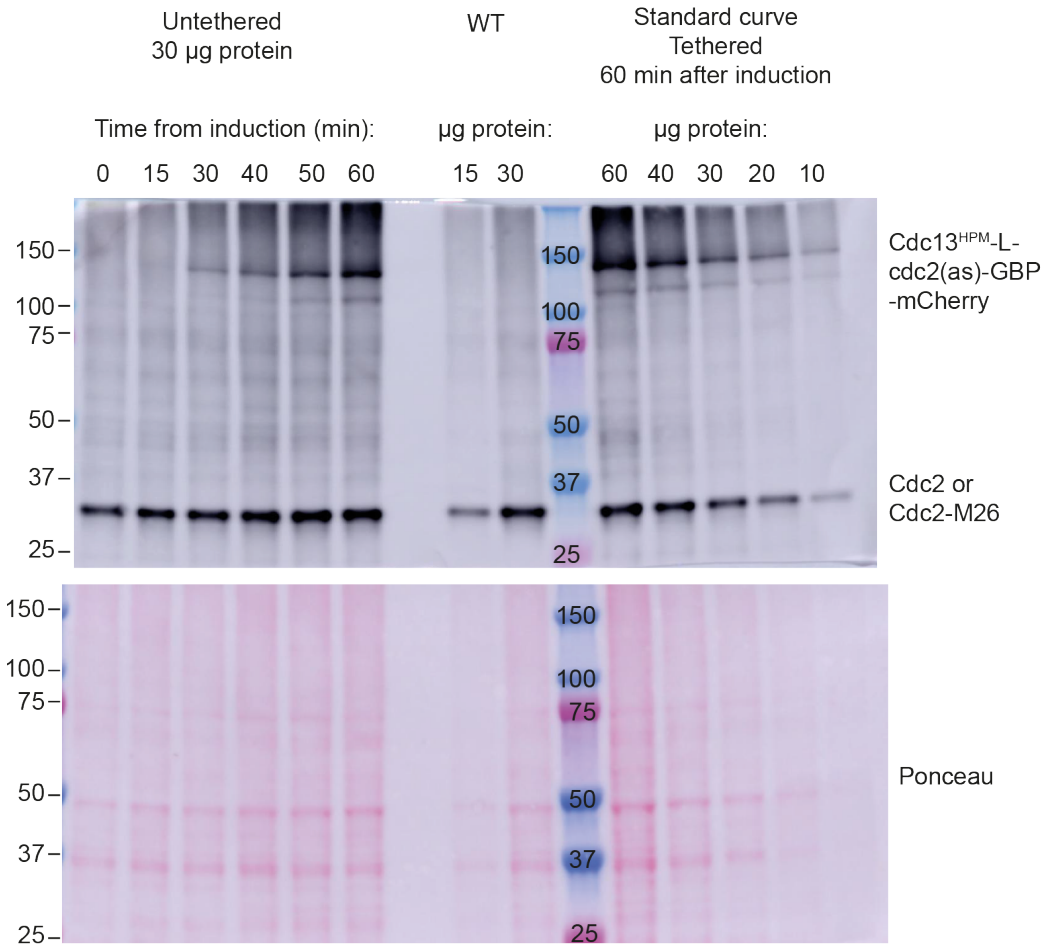


Figure 5.7 | Induction of Cdc13^{HPM}-L-Cdc2(as)-GBP-mCherry

Left hand lanes: *cdc2-M26 tetR:tup11Δ70 enoTetP-cdc13^{HPM}-L-cdc2(as)-GBP-mCherry* cells (where the induced fusion protein is not tethered to the SPB) were shifted to 36 °C. After 50 min, tetracycline and 1 µM 1-NmPP1 were added and samples taken for protein extraction at the indicated time points. 30 µg of each sample is loaded. **Middle lanes:** two dilutions (15 µg and 30 µg) of an extract from an asynchronous population of wild-type cells, to indicate endogenous levels of Cdc2. **Right hand lanes:** serial dilutions of one sample, taken from a strain with the induced fusion protein tethered at the SPB (*cdc2-M26 tetR:tup11Δ70 enoTetP-cdc13^{HPM}-L-cdc2(as)-GBP-mCherry cut12-NEGFP*). The sample was taken 60 min

Figure 5.7 ***caption continued from previous page***
after tetracycline and 1-NmPP1 addition. The top blot shows the membrane blotted with an anti-Cdc2 antibody (used at 1:40000 dilution). The bottom blot shows the same membrane stained with Ponceau-S to stain total protein.

I next tested whether the Cdc13^{HPM}-L-Cdc2(as) fusion protein could drive mitosis when expressed under the Cdc13 promoter in different strain backgrounds. To do this, Cdc13^{HPM}-L-Cdc2(as) and Cdc13^{HPM}-L-Cdc2(as)-GBP-mCherry fusion constructs under the Cdc13 promoter were introduced into the *cdc2-M26* or *nmt41:cdc13 cig1Δ cig2Δ* backgrounds, and a background with *cdc2-M26 nmt41:cdc13 cig1Δ cig2Δ*.

Cdc2-M26 cells were plated at 36 °C on YE4S, and 5 hours later cells were elongated with no septation. Cdc2-M26 with either Cdc13^{HPM}-L-Cdc2(as) or Cdc13^{HPM}-L-Cdc2(as)-GBP-mCherry on the other hand were not as elongated and septa were observed (Figure 5.8A). The cells appeared somewhat elongated, suggesting that entry into mitosis was delayed. Septa were also observed in the strain with *cdc2-M26 nmt41:cdc13 cig1Δ cig2Δ cdc13^{HPM}-L-Cdc2(as)-GBP-mCherry* on YE4S at 36 °C, in which the cyclins *cdc13, cig1* and *cig2* are repressed or deleted, suggesting that the low levels of mitotic events were not dependent solely on the expression of wild-type *cdc13, cig1* and *cig2* in these cells (Figure 5.8A-C). Quantification of septation in these images suggests that the level of septation in the Cdc2-M26 Cdc13^{HPM}-L-Cdc2(as)-GBP-mCherry cells was particularly high, and multiseptated cells could be seen, which could suggest a high level of aberrant mitoses (Figure 5.8B). To test this, the experiment was repeated and cells from the plates were stained with DAPI and calcofluor to score for binucleation and septation. This shows that a large proportion of mitoses were aberrant (Figure 5.8C). Aberrant mitoses were defined as any mitoses that did not result in two separate nuclei either side of a septum placed in the middle of the cell, and included cut cells (where the septum bisects the nucleus or nuclei), multiseptated cells (which could have multiple septa between two nuclei), and cells with two nuclei on one side of a septum.

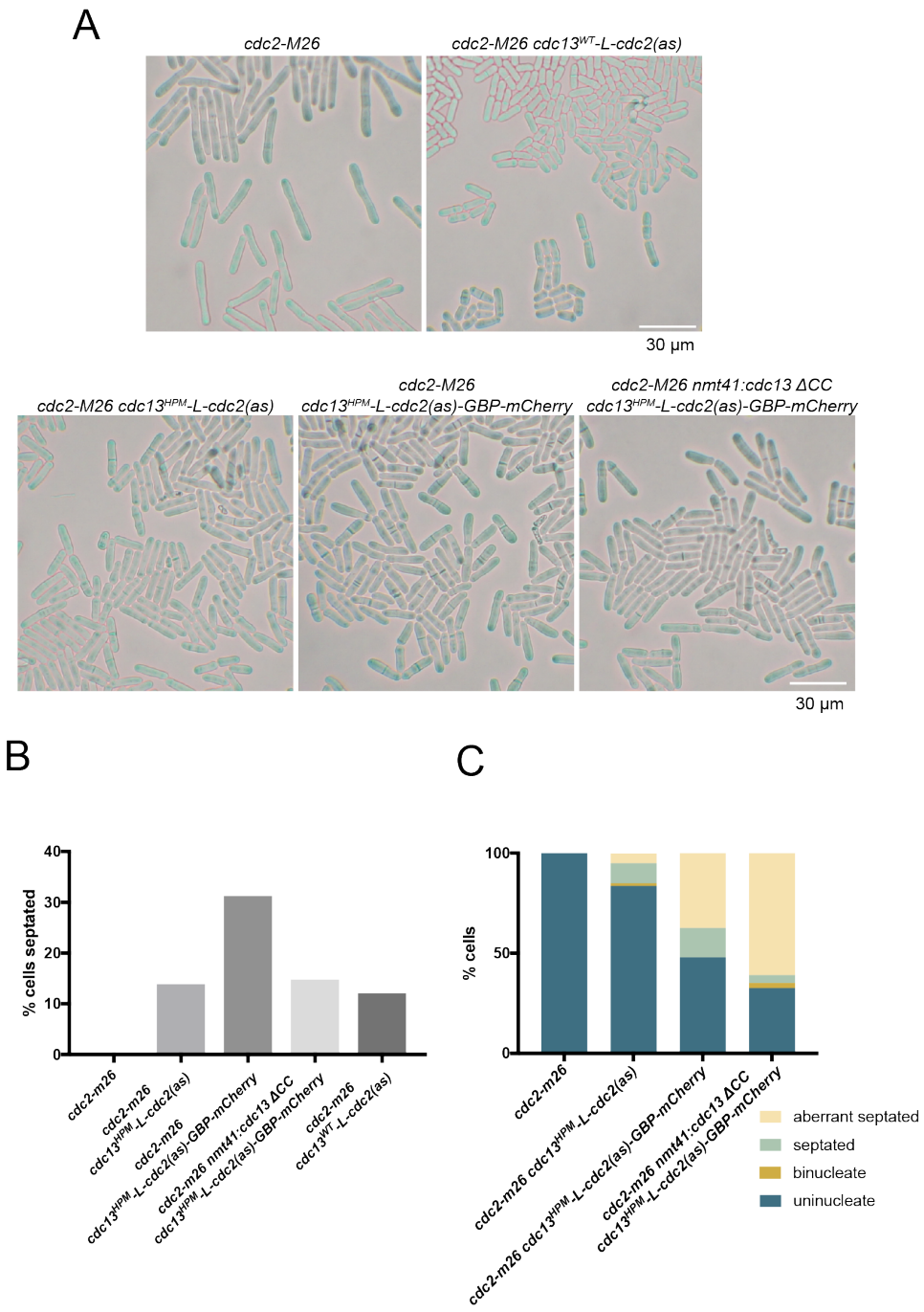


Figure 5.8 | Phenotype of cells driven by Cdc13^{HPM}-L-Cdc2 in a Cdc2-M26 background

A: Cells expressing Cdc2-M26 and an exogenous copy of the indicated Cdc13-L-Cdc2(as) fusion protein were grown on EMM4S agar plates at 25 °C. Cells were patched to YE4S agar plates at 36 °C before being imaged on plates after 5 hours.
B: Quantitation of the percentage of septated cells from (A), scored by detecting septa by eye. N ≥ 150 cells for all conditions.
C: The experiment in (A) was repeated, but cells were transferred to slides and stained with DAPI and Calcofluor 7.5 hours after shifting to 36 °C. Cells were scored for binucleation and septation. N ≥ 74 cells for all conditions.

Similar experiments were carried out in the *nmt41:cdc13 cig1Δ cig2Δ* background. After patching cells onto YE4S agar plates at 32 °C, which contain thiamine and therefore repress the wild-type *cdc13*, control cells without the Cdc13-L-Cdc2 fusion protein were elongated with no septation (Figure 5.9A). Cells with $Cdc13^{HPM}$-L-Cdc2(as) and $Cdc13^{HPM}$-L-Cdc2(as)-GBP-mCherry appeared slightly less elongated and septa could be observed, though in a lower percentage of cells than the strain with $Cdc13^{WT}$-L-Cdc2(as) (Figure 5.9A, Figure 5.10A). When the same strains were patched at 36 °C, higher levels of septation could be seen (Figure 5.9B, Figure 5.10A). A later time point was also checked in case the difference in septation level was due to the cells at 36 °C cycling more quickly, but the pattern remained the same with a higher level of septation being seen at 36 °C (Figure 5.10A). Staining the cells with DAPI and calcofluor indicated that most of the septation events at 36 °C were aberrant (Figure 5.10B).

These data suggest that there may be a low level of certain mitotic events when $Cdc13^{HPM}$ is fused to Cdc2, and expressed under the Cdc13 promoter, but it is not a full rescue of mitosis. The septation events seen in the Cdc2-M26 background do not appear to be solely due to the presence of Cdc13, Cig1 and Cig2, as these septation events still occur when these cyclins are not present. Whilst fusing $Cdc13^{HPM}$ and Cdc2 and carrying out the experiments at 36 °C may contribute to $Cdc13^{HPM}$ being able to drive a low level of some mitotic events, even when combined they do not confer a full rescue of mitosis. It is worth noting that these experiments were all carried out with Cdc13-L-Cdc2 fusion proteins expressed from the Cdc13 promoter. The mitosis driven by the tetracycline-induced $Cdc13^{HPM}$-L-Cdc2(as)-GBP-mCherry may have also been aided by a mild overexpression of the fusion protein; if the defect of $Cdc13^{HPM}$ is a lack of activity in certain subcellular compartments, a rescue should be able to be achieved by sufficiently increasing the whole-cell CDK activity. However, whilst a mild overexpression of $Cdc13^{HPM}$-L-Cdc2(as)-GBP-mCherry cannot be ruled out from the Western blot in Figure 5.7, the data is suggestive that there is not a very strong overexpression of $Cdc13^{HPM}$-L-Cdc2(as)-GBP-mCherry compared to endogenous Cdc2.

I also tested whether using a constitutively active allele of Cdc2 that cannot be phosphorylated on threonine 14 or tyrosine 15 ($Cdc2^{AF}$) (Gould and Nurse, 1989, Den Haese et al., 1995, Coudreuse and Nurse, 2010) affected the phenotype of cells driven by $Cdc13^{HPM}$-L-Cdc2(as). I tested this in the *nmt41:cdc13 cig1Δ cig2Δ* background, as this system appeared to have the lowest levels of $Cdc13^{HPM}$-L-Cdc2(as) mitotic events in the previous experiments. When cells with $Cdc13^{HPM}$-L-$Cdc2(as)^{AF}$ were plated on YE4S, they appeared shorter when compared to $Cdc13^{HPM}$-L-Cdc2(as) (Figure 5.11A). The same trend could be seen for fusion proteins that also had sfGFP (Figure 5.11B). It is possible that this partial rescue of mitotic events could be caused by generally increased CDK activity, although it is also possible that there is an alternative explanation, for example that the $Cdc2^{AF}$ allele is able to localise to the SPB through the hydrophobic patch-independent mitotic localisation pathway discussed earlier.

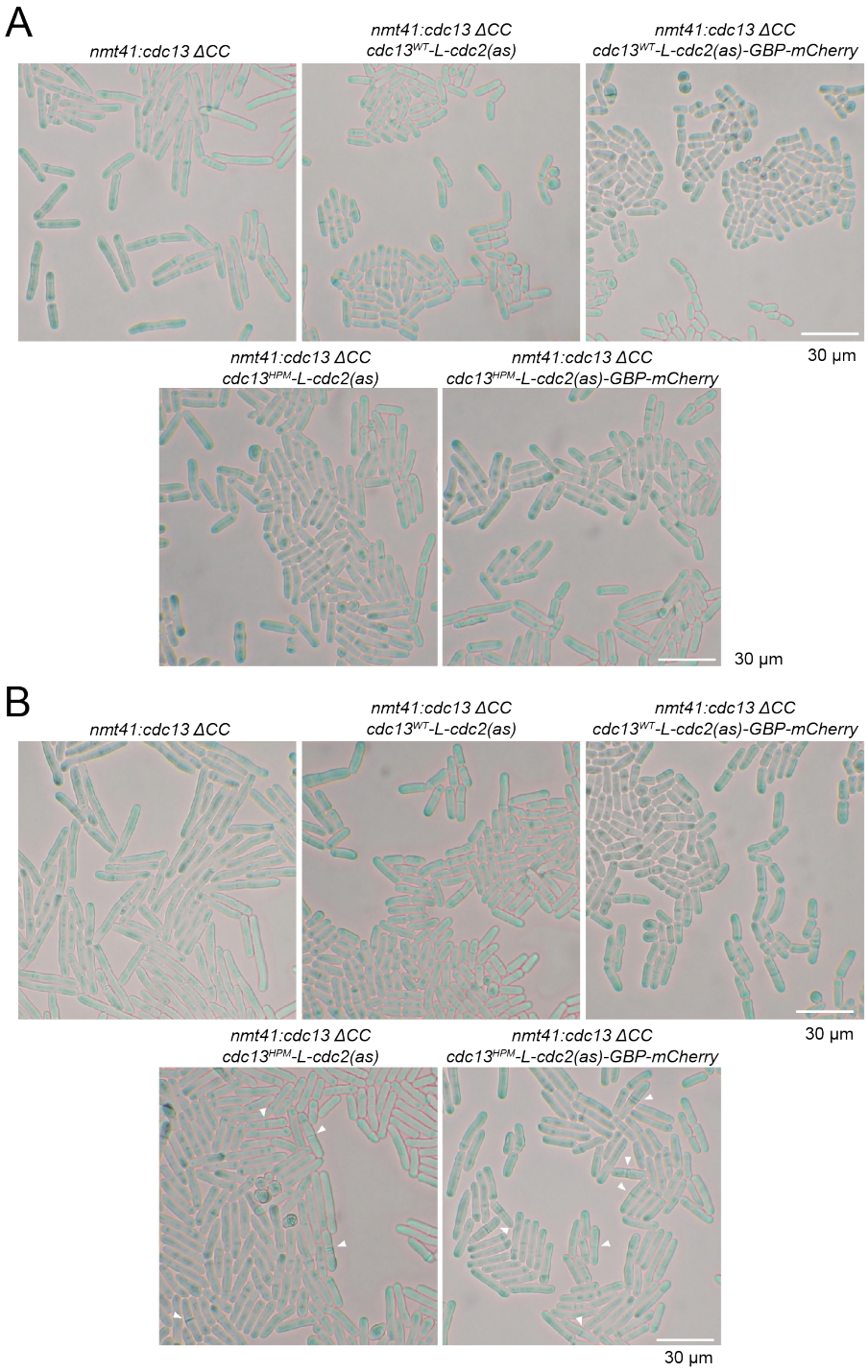


Figure 5.9 | Phenotype of cells driven by Cdc13^{HPM}-L-Cdc2 in an *nmt41:cdc13 ΔCC* background

A: Cells expressing *nmt41:cdc13 ΔCC* and an exogenous copy of the indicated Cdc13-L-Cdc2(as) fusion protein were grown on EMM4S agar plates at 32 °C. Cells were patched to YE4S agar plates at 32 °C before being imaged on plates after 5 hours 20 min.
B: As in (A), but cells were placed at 36 °C and imaged after 6 hours. Arrows indicate septa in the HPM strains.

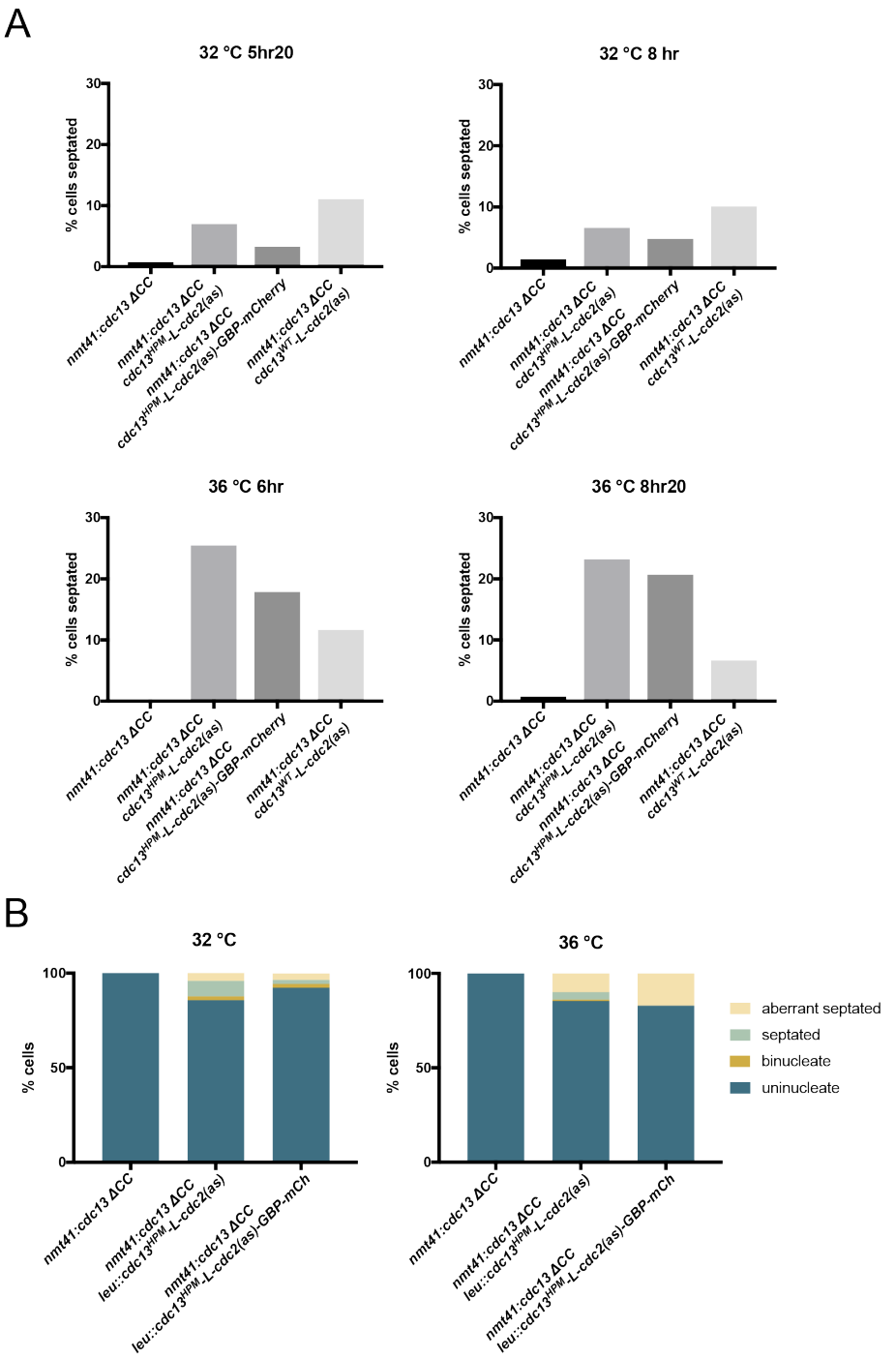


Figure 5.10 | Quantitation of septation events in cells driven by Cdc13^{HPM}-L-Cdc2 in an *nmt41:cdc13 ΔCC* background

A: Quantitation of the percentage of septated cells from (Figure 5.9) and a later time point for both temperatures, scored by detecting septa by eye. N ≥ 130 cells per condition.
B: Cells were patched onto YE4S agar plates at the indicated temperature, and transferred to slides and stained with DAPI and Calcofluor 6 hours after shifting to 32 °C or 6.5 hours after shifting to 36 °C. Cells were scored for binucleation and septation. N ≥ 115 cells per condition

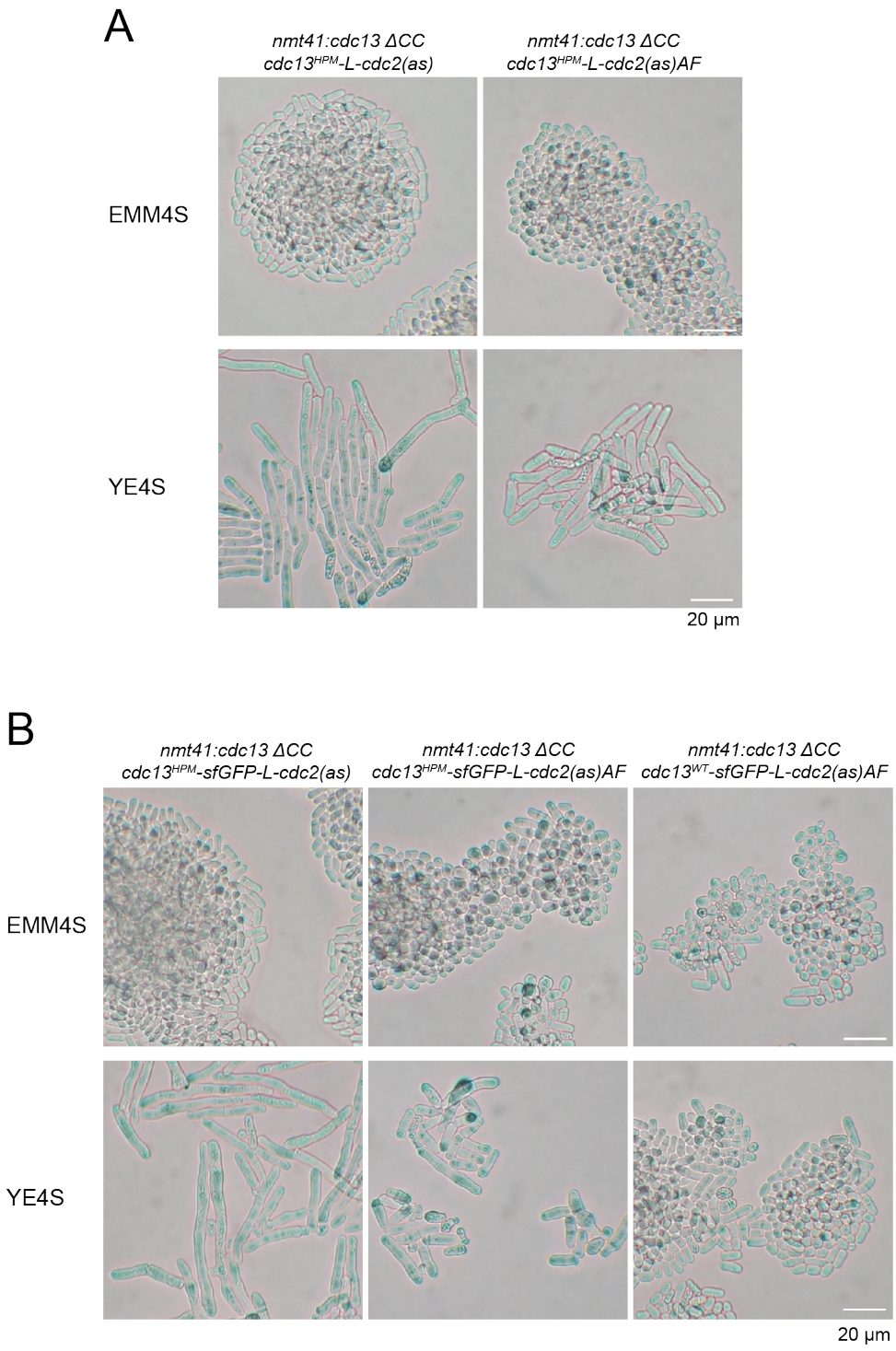


Figure 5.11 | Phenotype of cells driven by Cdc13^{HPM}-L-Cdc2(as)^{AF}

A: Images of cells expressing either Cdc13^{HPM}-L-Cdc2(as) or Cdc13^{HPM}-L-Cdc2(as)^{AF} on media without thiamine (EMM4S) and with thiamine (YE4S), which represses the expression of *nmt41::cdc13*. Cells were grown on EMM4S agar plates at 25 °C and patched onto either EMM4S or YE4S agar plates also at 25 °C. Cells on YE4S were imaged at 16 hours after patching; cells on EMM4S were imaged after 24 hours.
B: As (A), with Cdc13^{HPM}-sfGFP-L-Cdc2(as) or Cdc13^{HPM}-sfGFP-L-Cdc2(as)^{AF}

5.4 Relocalising Cdc13^{HPM}-Cdc2 to the SPB

The work outlined in the previous sections indicates that artificial alteration of CDK signalling at the SPB is not tolerated well by cells, perhaps due to the specific localisation and regulation of CDK needed at the SPB. It also suggests that some or all of: the use of the Cdc13-L-Cdc2 fusion protein, a temperature shift to 36 °C, the *cdc2-M26* background, or a potential mild overexpression of the Cdc13-L-Cdc2 construct may have been obstacles that contributed to the mitosis driven by the untethered Cdc13^{HPM}-L-Cdc2(as)-GBP-mCherry. I therefore sought to develop a system in which to test whether restoring SPB localisation of Cdc13^{HPM}-Cdc2 restored its ability to perform mitosis, in conditions which avoided the obstacles that may have been issues in the above attempts. I aimed to use a system that minimised exogenous Cdc2 signalling at the SPB during cell growth before the experiment and that resulted in exogenous Cdc2 expression levels similar to endogenous Cdc2 levels.

To remove the endogenous wild-type cyclins, I utilised the *nmt41:cdc13 ΔCC* system as before, and introduced an exogenous copy of Cdc13^{HPM} under the Cdc13 promoter into the *leu1* locus. To tether Cdc2 at the SPB, I introduced an exogenous copy of the analogue-sensitive allele Cdc2(as)-M17 (Aoi et al., 2014) fused to GBP-mCherry under a previously described tetracyline-inducible promoter (Zilio et al., 2012). The endogenous *cdc2* was left intact and unaltered. This allowed me to minimise exogenous CDK signalling at the SPB during cell growth before the experiment, by only inducing Cdc2(as)-M17-GBP-mCherry expression during the experiment and growing cells in 10 μM 1-NmPP1 to inactivate any Cdc2(as)-M17-GBP-mCherry produced by leaky expression. This tetracycline inducible promoter (referred to as TetP) results in an expression level similar to that of the *nmt81* promoter when induced, which has an expression level similar to that of endogenous *cdc2* (Zilio et al., 2012, Grallert et al., 2013b), suggesting that the expression level of the TetP-Cdc2(as)-M17-GBP-mCherry construct will be similar to that of endogenous Cdc2. Protein induction from TetP is reported to plateau between 4-6 hours after tetracycline addition (Zilio et al., 2012). The tetracycline repressor *tetR-tup11Δ70* was introduced to the strain to repress expression of

Cdc2(as)-M17-GBP-mCherry in the absence of tetracycline (Zilio et al., 2012). The strain also expressed either *cut12-NEGFP* (to tether Cdc2(as)-M17-GBP-mCherry at the SPB), or unaltered *cut12*$^{+}$ (to have Cdc2(as)-M17-GBP-mCherry untethered) (Bridge et al., 1998, Grallert et al., 2013b). The resulting strains were: *nmt41:cdc13 ΔCC leu::cdc13*^{HPM} *tetR-tup11Δ70 lys*$^{+}$*::tetP-cdc2(as)-M17-GBP-mCherry* (for the non-tethered strain); or *nmt41:cdc13 ΔCC leu::cdc13*^{HPM} *tetR-tup11Δ70 lys*$^{+}$*::tetP-cdc2(as)-M17-GBP-mCherry cut12-NEGFP* (for the SPB-tethered strain).

The experimental design was as follows (shown in Figure 5.12). The cells were grown at 32 °C in EMM + adenine + leucine + 10 μM 1-NmPP1, meaning that during growth both *nmt41:cdc13* and *leu::cdc13*^{HPM} were expressed, whilst *tetP-cdc2(as)-M17-GBP-mCherry* was repressed and any protein produced by leaky expression was inhibited. The cells were nitrogen-starved (N-starved/N-arrested) at 25 °C in order to arrest cells in G1 and degrade Cdc13 as performed previously (Figure 5.1) (Basu et al., 2020). Thiamine, tetracycline and 1-NmPP1 were added to the cells 1 hour before release from the N-arrest in order to repress transcription of *nmt41:cdc13*, and induce and inhibit *tetP-cdc2(as)-M17-GBP-mCherry*. Cells were then released from the N-arrest in the presence of thiamine, tetracycline and 1-NmPP1. At this stage *nmt41:cdc13* was repressed, and Cdc2(as)-M17-GBP-mCherry was expressed but inhibited, meaning that the only functional copies of Cdc13 and Cdc2 were the exogenous Cdc13^{HPM} and the endogenous Cdc2. Cdc13^{HPM}-Cdc2 complexes can drive S-phase but not mitosis, meaning that after release from an N-arrest cells perform S-phase and then accumulate in G2 (shown in Figure 5.1 and (Basu et al., 2020)). Fluorescence microscopy was performed 6 hours after release from the N-arrest (which is 7 hours after tetracycline addition) to visualise Cdc2(as)-M17-GBP-mCherry induction. Seven hours after release from the N-arrest cells were expected to be in G2, so 1-NmPP1 was washed out to remove the inhibition of the exogenous Cdc2(as)-M17-GBP-mCherry. Cells were heat fixed at intervals after 1-NmPP1 wash-out to score for mitotic entry and progression.

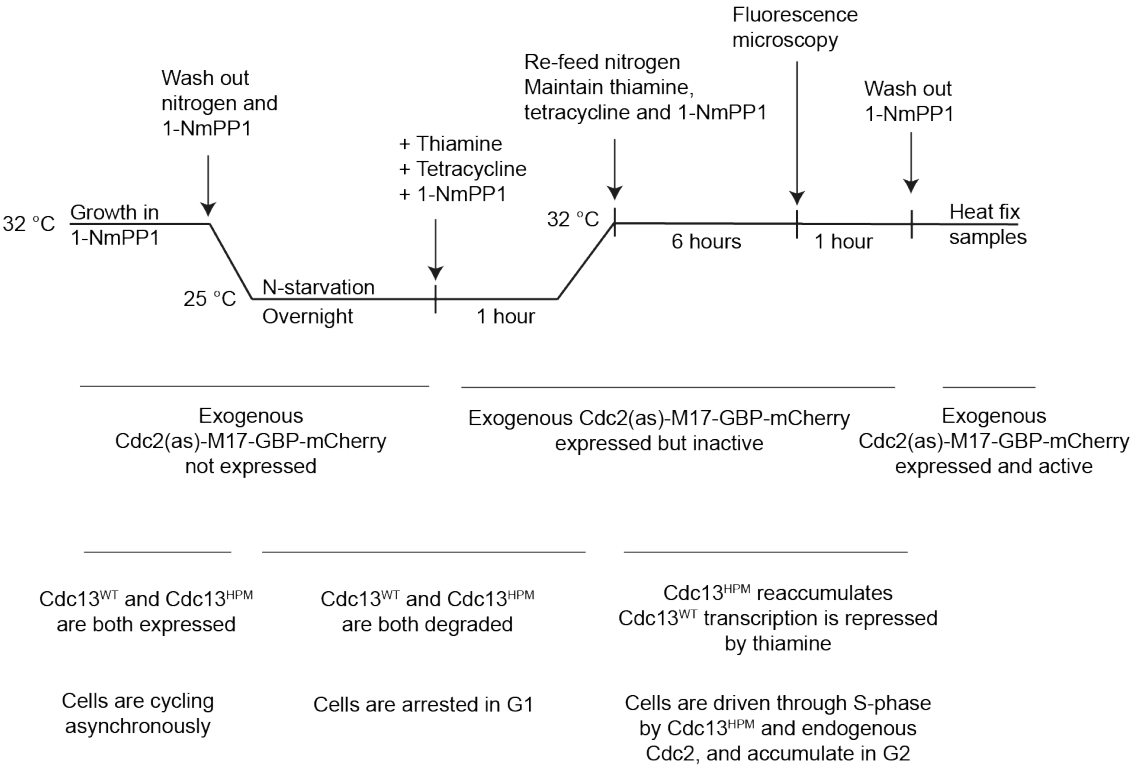


Figure 5.12 | Experimental design for Cdc13^{HPM}-Cdc2 SPB tethering experiment

Schematic of experimental design, linked to data from Figure 5.13, Figure 5.14 and Figure 5.15.

Samples for flow cytometry and heat fixation were taken during the N-arrest and every hour after until the 1-NmPP1 wash-out. Monitoring DNA content by flow cytometry shows that the N-arrest resulted in the large majority of cells having 1C DNA content (demonstrating a G1 arrest) (Figure 5.13A). Between 3-5 hours after release cells in both the non-tethered and SPB-tethered populations underwent S-phase. The heat-fixed samples were stained with DAPI and calcofluor to score for binucleation and septation (as markers of mitotic progression). These showed that there were negligible levels of mitotic progression after release from the N-arrest and before the 1-NmPP1 washout, indicating that the cells were accumulating in G2 as expected (Figure 5.13B).

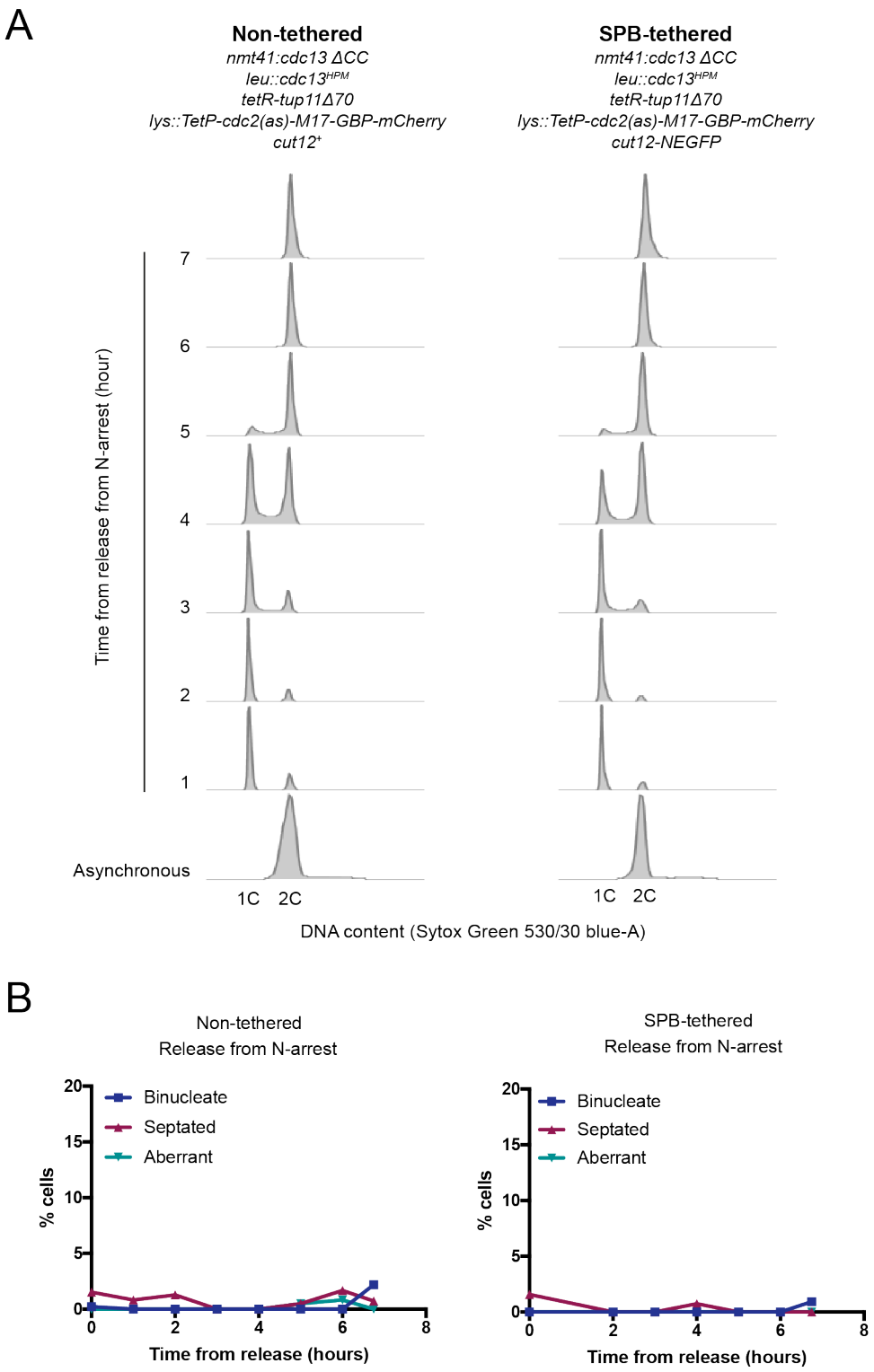


Figure 5.13 | G2 accumulation after release from N-arrest

A: DNA content of cells after release from a nitrogen starvation induced G1 arrest, measured by flow cytometry. Arrested cells were released after 17-18 hours by washing into media containing nitrogen.
B: Cells were heat-fixed at the indicated time-points and scored for binucleation and septation. n > 100 cells per time point.

Six hours after release from the N-arrest cells were imaged by fluorescence microscopy to visualise Cdc2(as)-M17-GBP-mCherry induction and localisation. As tetracycline was added 1 hour before release, this time point was 7 hours after tetracycline addition and therefore after the point at which Cdc2(as)-M17-GBP-mCherry expression is expected to plateau (Zilio et al., 2012). Whilst images taken during the N-arrest (immediately after tetracycline addition) showed no detectable Cdc2(as)-M17-GBP-mCherry, 6 hours after release from the N-arrest Cdc2(as)-M17-GBP-mCherry could be detected in both strains (Figure 5.14A). In the non-tethered strain, Cdc2(as)-M17-GBP-mCherry accumulated in the nucleus, which was expected as Cdc2(as)-M17-GBP-mCherry is expected to form a complex with $Cdc13^{HPM}$. Also as expected, no foci resembling SPB accumulation could be detected in the non-tethered strain. In contrast, in the SPB-tethered strain foci of Cdc2(as)-M17-GBP-mCherry signal were detected that colocalise with Cut12-NEGFP, indicating that the tethering to the SPB was successful. Cdc2(as)-M17-GBP-mCherry signal could also be seen in the nucleus in some cells in the SPB-tethered strain. In both the non-tethered and SPB-tethered strains, Cdc2(as)-M17-GBP-mCherry expression level appeared variable between cells. To ascertain whether the protein induction was similar between both strains, the whole-cell fluorescence intensity of Cdc2(as)-M17-GBP-mCherry was measured. The spread of mean cellular Cdc2(as)-M17-GBP-mCherry intensities was similar in both strains, indicating that there is not a major difference in average protein induction across the population in the non-tethered and SPB-tethered strains (Figure 5.14B).

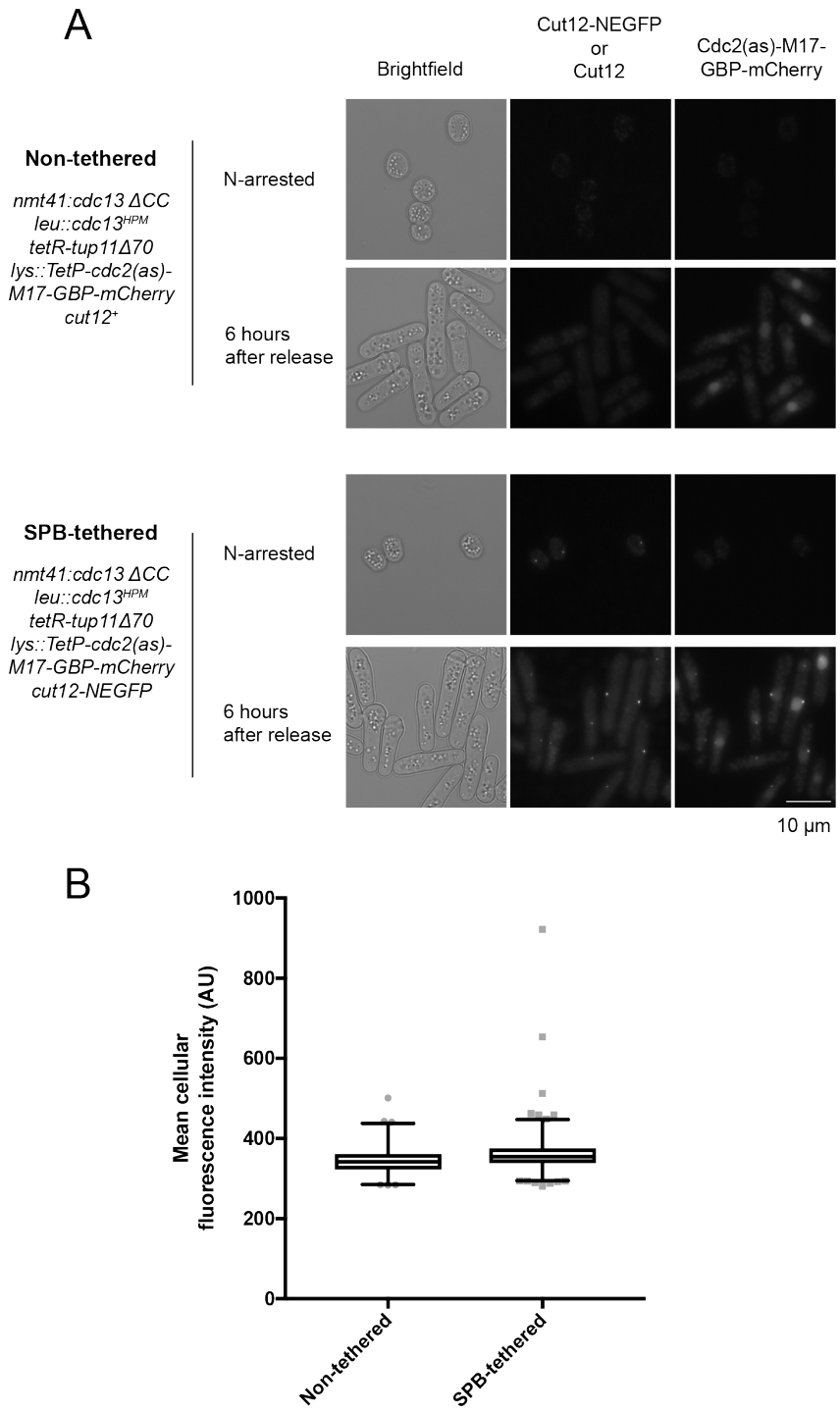


Figure 5.14 | Cdc2(as)-M17-GBP-mCherry induction

A: Representative images of the indicated strains during the N-arrest (immediately after tetracycline addition) and 6 hours after release from the N-arrest (7 hours after tetracycline addition). Fluorescence images are maximum projections, with the same pixel range applied to all images of the same fluorescent channel.
B: Images of cells 6 hours after release were segmented based on the brightfield image to mask the whole cell. The mean fluorescence intensity within each mask was plotted. Boxes show median and IQR; whiskers show 1st-99th percentile. Non-tethered n = 356 cells; SPB-tethered n = 762 cells.

Seven hours after release from the N-arrest, when cells had accumulated in G2, 1-NmPP1 was washed out to release the inhibition on Cdc2(as)-M17-GBP-mCherry. Samples were taken for heat fixation following the 1-NmPP1 wash-out to score for mitotic progression. In the SPB-tethered strain there was a wave of binucleation followed by a wave of septation, indicating that cells entered mitosis (Figure 5.15). There was also an accumulation of cells exhibiting an aberrant mitosis (including multiseptated cells and cut cells where the septum bisects the nucleus or nuclei). In the non-tethered strain, there was also a small wave of binucleation and septation, however it was notably reduced compared to the wave seen in the SPB-tethered strain. The binucleation wave peaked at around 7 % in the non-tethered strain, compared to roughly 25 % in the SPB-tethered strain. Septation rose to around 15 % in the non-tethered strain, compared to 40 % in the SPB-tethered strain. There was no accumulation of cells with aberrant mitoses in the non-tethered strain. These data show that tethering Cdc2(as)-M17-GBP-mCherry to Cut12-NEGFP promoted a significantly increased wave of mitotic entry compared to the non-tethered strain.

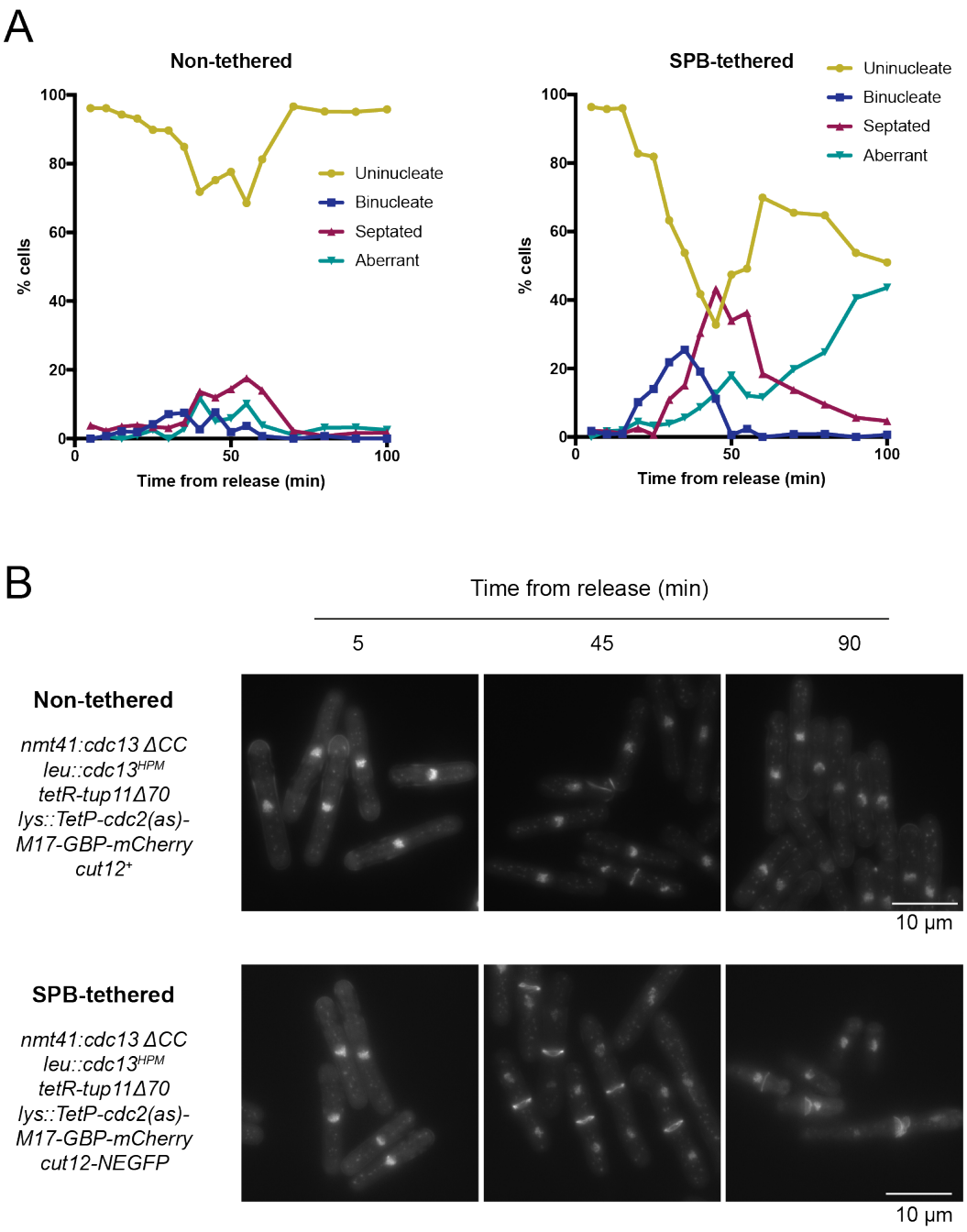


Figure 5.15 | Restoring SPB localisation of Cdc13^{HPM}-Cdc2 promotes a wave of mitotic entry

A: Cells were heat fixed at the indicated time points after 1-NmPP1 wash-out and stained for DAPI and calcofluor to score for binucleation and septation. 'Aberrant' includes multiseptate and cut cells. n ≥ 90 cells per time point.
B: Example maximum-projection images from the indicated time points. Pixel range is the same for all images of the same strain, but not between strains; pixel range is chosen to best represent DNA and septum staining.

5.5 Discussion

The work in this Chapter has focussed on testing the hypothesis that the reason that $Cdc13^{HPM}$ does not drive mitosis in the experiments in (Basu et al., 2020) is due to a lack of activity at the SPB. I first show that cells driven by $Cdc13^{HPM}$ alone, with no expression of $Cdc13^{WT}$, arrest before SPB separation with no detectable $Cdc13^{HPM}$ accumulation at the SPB.

I then show that, in cells expressing just $Cdc13^{HPM}$, tethering an exogenous copy of Cdc2 to the SPB promotes a significantly increased wave of mitosis compared to cells where the exogenous Cdc2 is not tethered to the SPB. This strongly suggests that the restoring the SPB localisation of $Cdc13^{HPM}$-Cdc2 is sufficient to drive mitotic entry. This is indicative that CDK activity at the SPB is essential for mitotic entry, and that the sole essential role of the hydrophobic patch for mitotic entry is to mediate this SPB localisation.

The waves of binucleation and septation were followed by an accumulation of cells exhibiting aberrant mitoses in the SPB-tethered strain, including multiseptate cells, cut cells, and cells with one nucleus on one side of a septum. This accumulation of cells with aberrant mitoses was not seen with the non-tethered strain. This observation suggests that whilst tethering the exogenous copy of Cdc2 to the SPB drives mitotic entry, this is followed by frequent defects in progression through mitosis and mitotic exit. One reason for this could be that specific hydrophobic patch-substrate docking, in addition to SPB localisation, is required for cells to progress through and exit mitosis. Another reason could be that tethering Cdc2 to the SPB component Cut12 does not reconstitute physiological CDK signalling at the SPB, and that this affects mitotic progression and exit. The septation initiation network (SIN) in fission yeast is coordinated by signalling at the SPB, involving the CDK-counteracting phosphatase Clp1, and requires mitotic cyclin-CDK inactivation (Bardin and Amon, 2001, Krapp et al., 2004, Chan et al., 2017). Altered CDK signalling at the SPB may affect these processes. The accumulation of cells with multiple septa could also be influenced to some degree by the experimental set-up. In this experiment, cells were held in G2 until 7 hours after release from the N-

arrest, by which point many cells are longer than they would be in an unperturbed cell cycle. Septum placement is influenced by the DYRK kinase Pom1, which is localised to cell tips, creating a Pom1 gradient that is high at the cell tips and decreases towards the centre of the cell (Bahler and Pringle, 1998, Padte et al., 2006). Pom1 contributes to inhibition of septum placement at the cell tips (Padte et al., 2006). As cells grow, Pom1 concentration in the centre of the cell decreases, contributing to septum placement in the middle of the cell once the cell has attained a critical size. Thus cells that are elongated have a low Pom1 concentration across a larger proportion of the cell (Padte et al., 2006), which might result in the placement of multiple septa in the cell. Increased cell length at the time of division is therefore one possible explanation for some of the multiseptate cells seen. Multiple septa are also seen in roughly 30% of cells upon release from a *cdc25-22* G2 arrest, in which cells are also long, with this increased cell length at division a possible explanation for the multiple septa (Singh et al., 2021). Subsequent division of these multiseptate cells can result in formation of cells with one nucleus on one side of a septum, which are also observed in later time-points.

There was a small wave of mitosis in the non-tethered strain upon the release of inhibition of exogenous Cdc2. This suggests that releasing the inhibition of the Cdc13^{HPM}-Cdc2(as)-M17 complexes caused a spike in activity that, in a small proportion of cells, was sufficient to drive mitotic entry. One explanation of this could be that these cells had sufficient Cdc13^{HPM}-Cdc2 activity in the vicinity of the SPB, despite not being specifically enriched there, to overcome the low activity experienced there. As Cdc13 concentration increases with cell length, it is likely that Cdc13^{HPM} is expressed at higher levels at the later time-points in this experiment than in an unperturbed cell cycle. To measure this, protein extracts for Western blotting could be taken in future investigations. These extracts would also allow comparisons of the expression level of the exogenous Cdc2(as)-M17-GBP-mCherry and the endogenous Cdc2, and detect whether Cdc2(as)-M17-GBP-mCherry expression level has reached a plateau as expected by the time of 1-NmPP1 wash-out.

This Chapter outlines several attempts to develop a system to test whether tethering Cdc13^{HPM}-Cdc2 to the SPB rescues the mitotic defect of Cdc13^{HPM}. The

failure of the initial attempts suggests that cells do not tolerate altered CDK signalling at the SPB well, consistent with the theory that CDK signalling at the SPB needs to be finely balanced. These initial attempts were followed by an attempt involving the induction of SPB-tethered/non-tethered Cdc13^{HPM}-L-Cdc2(as)-GBP-mCherry, using a tetracycline-inducible promoter based on the relatively strong *eno101* promoter (enoTetP). However, the induced Cdc13^{HPM}-L-Cdc2(as)-GBP-mCherry was able to drive mitosis even in the absence of SPB-localised GFP, indicating that in certain conditions Cdc13^{HPM} can drive mitosis, and rendering the system unusable to test whether tethering Cdc2 to the SPB rescues the mitotic defect of Cdc13^{HPM}. Western blotting suggests that the induced Cdc13^{HPM}-L-Cdc2(as)-GBP-mCherry was not strongly overexpressed compared to endogenous Cdc2, however smearing of the samples in the lane prevents a reliable measurement of protein concentration and therefore cannot rule out some degree of overexpression. Experiments testing whether fusing Cdc13^{HPM} to Cdc2 could provide a rescue of the mitotic defect of Cdc13^{HPM} suggest that whilst it may drive a low level of mitotic events, particularly at 36 °C, it does not provide a full rescue of mitosis when expressed under the Cdc13 promoter. This indicates that whether cells driven by Cdc13^{HPM} perform mitosis is dependent on the conditions of the experiment. It is possible that the tetracycline-induced Cdc13^{HPM}-L-Cdc2(as)-GBP-mCherry may have been able to drive mitosis due to a combination of using the Cdc13-L-Cdc2 fusion protein, a potential moderate overexpression, and possibly other factors including the presence of other wild-type cyclins in the background of the strain and performing the experiment at 36 °C. Some or all of these factors may combine to increase the Cdc2 activity in cells sufficiently to phosphorylate substrates that are otherwise poorly phosphorylated in cells driven by Cdc13^{HPM}. The slight increase in mitotic events offered by the constitutively dephosphorylated Cdc2^{AF} allele may also be due to increased activity of Cdc2 in these strains, though it is also possible that it may be by another mechanism, for example if Cdc2^{AF} were able to localise to the SPB independently of the Cdc13 hydrophobic patch.

In the course of studying CDK substrate phosphorylation in cells driven by Cdc13^{HPM}, it was noted that CDK substrate sensitivity to CDK inhibitor is correlated with substrate subcellular localisation (Basu et al., 2020, Swaffer et al., 2016). With the future aim of addressing whether CDK substrate phosphorylation is affected by

its subcellular location, in the following Chapter I describe initial work on developing a system for use in measuring CDK substrate phosphorylation in different subcellular locations.

Chapter 6. Measuring CDK substrate phosphorylation in different cellular compartments

The work presented in the previous Chapters suggests that Cdc13-Cdc2 localisation to the SPB may be necessary for cells to enter mitosis. This adds to a significant body of work that suggests that the SPB and centrosome play a critical role in cell cycle regulation, including at mitotic entry (covered in the Introduction). The findings that cells driven by $Cdc13^{HPM}$ have phosphorylation of nuclear substrates to the same level as cells driven by $Cdc13^{WT}$, but cytoplasmic and SPB substrate phosphorylation is compromised, suggests that Cdc13 localisation is critical to ensuring correct substrate phosphorylation across all subcellular compartments. Furthermore, the suggestion that substrates at the SPB tend to require the highest levels of CDK activity in order to be phosphorylated indicates a link between substrate sensitivity and localisation (Basu et al., 2020, Swaffer et al., 2016).

Analysis of global CDK phosphorylation has provided evidence of the key importance of the temporal regulation of CDK activity in the *S. pombe* cell cycle (Swaffer et al., 2016), but this does not provide information of how CDK activity is regulated spatially. Therefore, while this demonstrated that global CDK activity increases as cells progress through the cell cycle, with a significant jump in CDK activity in mitosis, it is not clear if this is true in all subcellular compartments. In *S. pombe* it is unknown if different subcellular compartments experience different CDK activity levels, or if CDK activation at G2/M occurs in all compartments simultaneously.

A FRET sensor developed to assay human Cyclin B1-Cdk1 activity has demonstrated the increasing activation of Cyclin B1-Cdk1 at mitosis, triggering different mitotic events at different activity levels, whilst also providing broad spatial information to suggest that the rapid nuclear import of Cyclin B1 helps synchronise Cdk1 activation in the cytoplasm and nucleus (Gavet and Pines, 2010a, Gavet and Pines, 2010b). Whilst this provides crucial temporal information of the activation of Cyclin B1-Cdk1, it does not have the spatial resolution to distinguish between

smaller subpopulations of Cyclin B1-Cdk1, such as the centrosomal population. However, studies in human cells illustrate that CDK activity and activation is not homogenous throughout the cell. The nuclear fraction of HeLa cells has a higher level of Cdk1 activity in H1 kinase assays than the cytoplasmic fraction throughout the cell cycle (Santos et al., 2012), and using phosphospecific antibodies against an autophosphorylation site on Cyclin B1 has identified that the first active population of Cyclin B1-Cdk1 is at the centrosome (Jackman et al., 2003). Whilst there has not been a direct measurement of Cdc2 activity in different subcellular locations in *S. pombe*, there is genetic evidence to suggest that Cdc2 is activated at the SPB before other regions in the cell (Grallert et al., 2013b), suggesting that there may also be spatial regulation of CDK activity in *S. pombe*. It would therefore be of interest to measure CDK substrate phosphorylation in different subcellular locations in *S. pombe*, and to test if the same substrate is phosphorylated at different times or different rates in different subcellular locations. Kinase activity in different subcellular locations has been measured before for mTORC2 in cultured mammalian cells, using a phosphospecific antibody against a mTORC2 substrate that is relocalised to different subcellular compartments (Ebner et al., 2017).

In this Chapter, I test novel antibodies generated against phosphosites on 5 CDK substrates for their use in Western blotting and immunofluorescence. I find that an antibody against Spo15, a late CDK substrate, can be used in immunofluorescence to detect CDK-dependent phosphorylation specifically of Spo15 late in the cell cycle, at the SPB and throughout the cell. I also find that antibodies against Spo15 and Bqt4 can be used to measure CDK substrate phosphorylation by Western blotting. These resources may be able to function as a novel CDK activity assay in *S. pombe* that would provide spatial information of CDK substrate phosphorylation.

6.1 Novel phosphospecific antibodies against CDK substrates

I first identified 5 candidate proteins from a previously defined list of CDK substrates to raise phosphospecific antibodies against (Table 6.1) (Swaffer et al., 2016). The substrates were selected on the basis that they were not essential (Kim et al., 2010), which allows for straightforward validation of the antibody using a strain genetically deleted for the protein of interest, and they represented a range of phosphorylation timings during the cell cycle (Figure 6.1) (Swaffer et al., 2016). The selected substrates had a range of published subcellular localisation and did not have another experimentally confirmed phosphosite in the immediate vicinity the phosphosite of interest (Wood et al., 2012).

Phosphosite	Protein function	Localisation	References
Bit61 S132 (mid)	Involved in TORC2 signalling pathway	Cell periphery, cytosol	(Hayashi et al., 2007, Tatebe et al., 2010)
Bqt4 T272 (late)	Telomere tethering to the nuclear periphery	Nuclear membrane	(Chikashige et al., 2009)
Crf1 T316 (mid)	Transcription corepressor for ribosomal proteins	Cytosol	(Martin et al., 2004, Matsuyama et al., 2006)
Dnt1 T225 (early)	Regulation of septation initiation signalling, G2/M transition	Nucleolus	(Jin et al., 2007, Yu et al., 2013)
Spo15 S121 (-)	Initiation of spore membrane formation	Spindle pole body	(Ikemoto et al., 2000)

Table 6.1 | Selected CDK substrates

Function and localisation of selected CDK substrates. Early/mid/late refers to the timing of phosphorylation, defined in (Swaffer et al., 2016), '(-)' signifies that the site did not fall into any of these clusters.

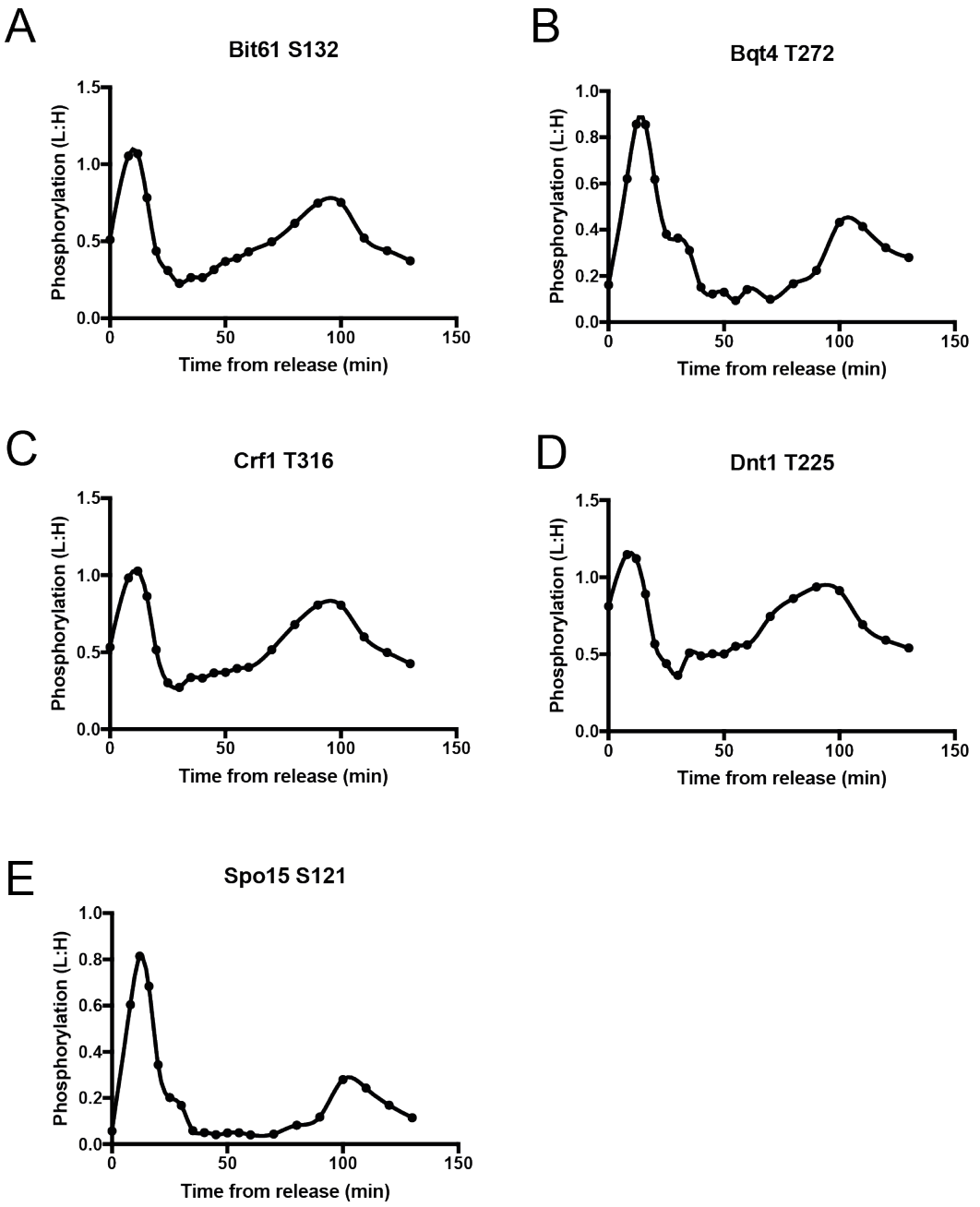


Figure 6.1 | Phosphorylation of selected CDK substrates after release from a G2 block

Graphs made using phosphorylation data from (Swaffer et al., 2016). Cells with the analogue-sensitive allele *cdc2(as)* and the simplified cell cycle network *cdc13-L-cdc2 ΔCCP* were arrested in G2 and released into mitosis. Samples from an unlabelled culture (L) were taken following release and analysed for phosphorylation relative to a mitotic heavy labelled reference sample (H). Graphs show data after imputation and smoothing for the following phosphosites: (A) Bit61 S132; (B) Bqt4 T272; (C) Crf1 T316; (D) Dnt1 T225; (E) Spo15 S121. Connecting line is a smoothed line (spline).

The antibodies were generated in rabbits against a peptide encompassing the phosphosite of interest and purified by an external company, Covalab. To purify the antibodies, the serum produced was first incubated against a non-phosphorylated peptide, and the antibodies that bound formed the 'control' antibody. The remaining serum was then incubated with the phosphorylated peptide to form the 'phosphospecific' antibody. Therefore, the phosphospecific antibodies should bind exclusively the phosphorylated target protein, whilst the control antibody should include any antibodies that bind the unphosphorylated protein, even if they have a higher affinity for the phosphorylated protein. I then tested the purified antibodies provided by Covalab by Western blotting (Figure 6.2).

Three of the antibody pairs, Bit61, Bqt4, and Spo15, recognised proteins that migrated at approximately the expected position in the gel and were not present in an extract from cells with the target gene deleted (Figure 6.2). It was concluded from this that these antibodies recognised the intended target protein. The phosphospecific Bit61-pS132 and Bqt4-pT272 antibodies also failed to recognise the protein in a Cdc2 kinase-dead extract, demonstrating that they were specific to the phosphorylated form of the protein (Figure 6.2A-B). It is also possible that the Bit61 and Bqt4 control antibodies may be more reactive to the phosphorylated form of the protein, but they both still recognise the unphosphorylated protein in the kinase-dead extract. The antibodies against Bit61 and Bqt4 also recognised multiple other proteins of varying sizes to produce background bands of a similar or stronger intensity than the target band.

The Spo15 control antibody recognises a protein of the expected length that is not present in the *spo15Δ* extract, indicating it is recognising Spo15, and it is possible that it recognises Spo15 in a partially phosphorylation-dependent way (Figure 6.2E). The phosphospecific Spo15-pS121 antibody only recognises a protein of the expected length in a mitotic extract, where CDK activity is highest. Given that Spo15 S121 is phosphorylated late in the cell cycle, at mitosis, and the band of interest is at the same size as Spo15, it is likely that this antibody is specifically recognising phosphorylated Spo15. The lack of Spo15-pS121 reactivity in an asynchronous wild-type extract is likely due to the vast majority of Spo15 being dephosphorylated in this extract, as only a small proportion of cells would be in

mitosis. This means that the kinase-dead and *spo15Δ* extracts are not informative for the Spo15-pS121 antibody, as they are also extracts from an asynchronous population. Both the phosphospecific and control Spo15 antibodies produce background bands that are very faint in comparison to the Spo15 band.

The phosphospecific and control Crf1 antibodies both recognised multiple bands that disappeared in both the kinase-dead and *crf1Δ* extract (Figure 6.2C). Whilst the lower band corresponds more closely with the size of Crf1, this complicates the use of these antibodies. Neither of the Dnt1 antibodies recognised a band of the expected size that disappeared in the *dnt1Δ* extract, meaning that these antibodies were not used any further (Figure 6.2D).

In summary, I tested antibodies against the 5 selected CDK substrates and conclude that the phosphospecific antibodies against Bqt4, Bit61 and Spo15 recognise a phosphorylated form of the target protein, and the control antibodies recognise the unphosphorylated target protein. I next tested whether the antibodies could be used to measure substrate phosphorylation in Western blotting and immunofluorescence.

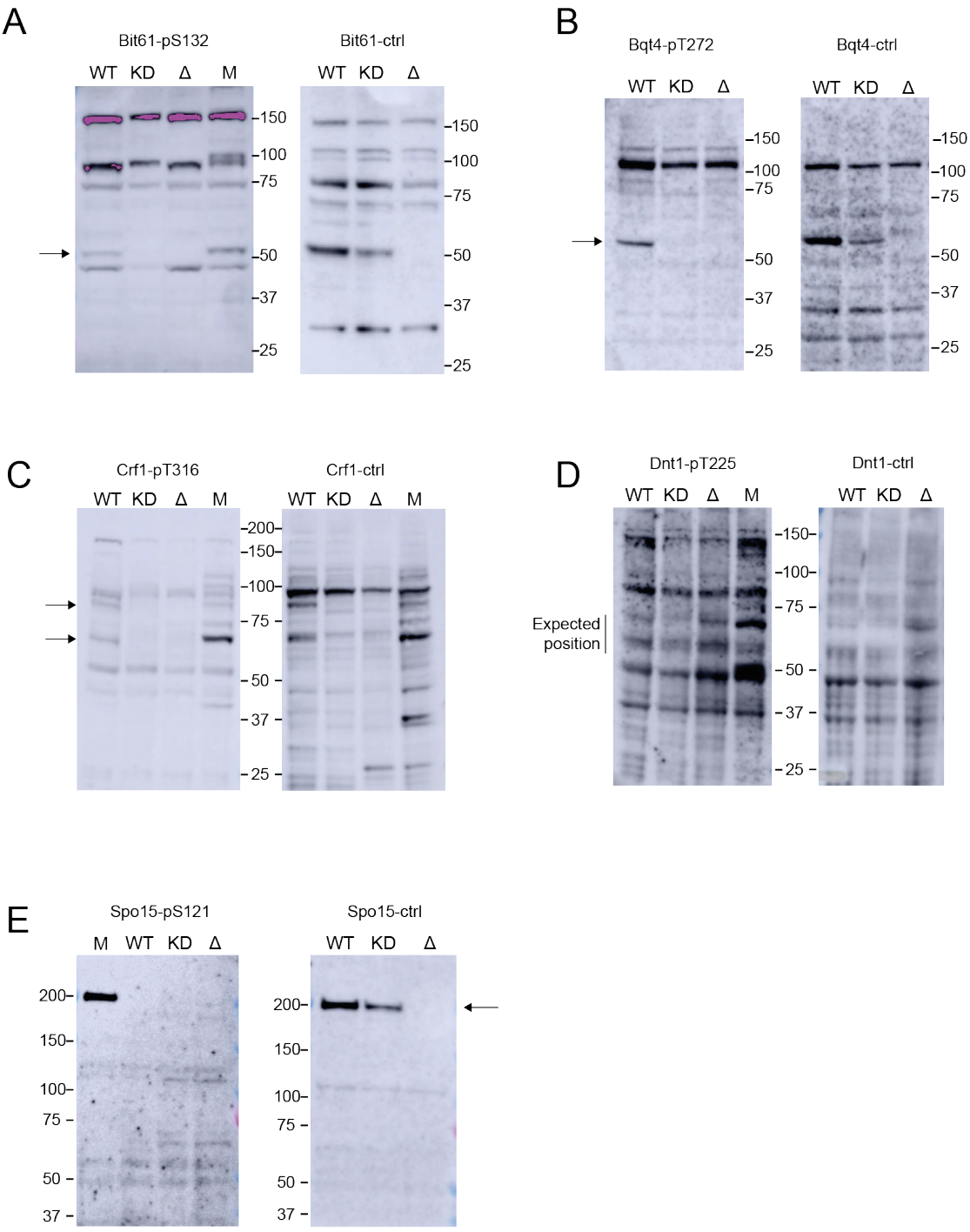


Figure 6.2 | Validating antibodies against selected CDK substrates

Western blots with phosphospecific (left) and control (right) purified antibodies against selected CDK substrates. Extracts are as follows: WT is an extract from an asynchronous wild-type population; KD (kinase-dead) is an extract from a population of *cdc2(as)* cells taken 30 minutes after 10 μM NmPP1 addition to inhibit CDK activity; Δ is an extract from a population in which the gene encoding the target protein is deleted; M (mitotic) is an extract from *cdc2(as)* cells that were arrested in G2 by addition of 1 μM NmPP1 for 1 generation and subsequently

Figure 6.2 ***caption continued from previous page***
released by washing out the inhibitor (the extract was taken 8-10 minutes after release).
A: Antibodies against Bit61 S132, protein size 47 kDa. Phosphospecific antibody dilution 1:500; control antibody dilution 1:1000. Arrow indicates the band presumed to be Bit61. Pink bands are saturated at the shown exposure.
B: Antibodies against Bqt4 T272, protein size 48 kDa. Phosphospecific antibody dilution 1:500; control antibody dilution 1:1000. Arrow indicates the band presumed to be Bqt4.
C: Antibodies against Crf1 T316, protein size 71 kDa. Phosphospecific antibody dilution 1:500; control antibody dilution 1:1000. Arrows indicate two bands that both disappear in the *crf1Δ* extract.
D: Antibodies against Dnt1 T225. Phosphospecific antibody dilution 1:500; control antibody dilution 1:1000. Protein size 66 kDa. There are no obvious bands that may represent Dnt1.
E: Antibodies against Spo15 S121, protein size 223 kDa. Phosphospecific antibody dilution 1:500; control antibody dilution 1:3000. Arrow indicates the band presumed to be Spo15.

6.2 Measuring CDK substrate phosphorylation on Western blots

To test the Bqt4, Bit61 and Spo15 antibodies in quantifying CDK substrate phosphorylation I utilised samples already collected and used for phosphoproteomics as part of a separate study in our lab (Basu et al., 2021). This had the advantage of being able to directly compare the results of the Western blot quantification with the phosphoproteomics for Spo15 S121 phosphorylation. Bqt4 T272 and Bit61 S132 were not identified in the phosphoproteomic data set so the same comparison could not be made for these sites.

CDK substrate phosphorylation was measured at mitotic entry in response to increasing level of Cdc13-L-Cdc2^{WT} or Cdc13-L-Cdc2^{AF}, where the AF allele of Cdc2 cannot be phosphorylated on T14 and Y15 (Gould and Nurse, 1989, Den Haese et al., 1995, Coudreuse and Nurse, 2010). The Cdc13 degron box was deleted from these fusion proteins to prevent fusion protein degradation. Cells contained a temperature-sensitive allele of Cdc2, *cdc2-M26*, that results in CDK inactivation at the restrictive temperature of 36 °C, and an exogenous copy of Cdc13-L-Cdc2^{WT} or Cdc13-L-Cdc2^{AF} under a previously described tetracycline-inducible promoter (Patterson et al., 2019). These cells also contained a copy of the tetracycline repressor (Zilio et al., 2012), so expression was repressed until tetracycline addition. Cells were shifted to 36 °C for 2 hours to inactivate Cdc2-M26, causing an accumulation of cells in G2. Tetracycline was then added to cells, and samples collected for protein extraction at various time points to compare substrate phosphorylation by Cdc13-L-Cdc2^{WT} or Cdc13-L-Cdc2^{AF}. Sample collection was performed by Souradeep Basu and phosphoproteomic sample preparation and analysis was performed by Andrew Jones and Souradeep Basu.

Cdc13-L-Cdc2^{WT} or Cdc13-L-Cdc2^{AF} protein induction was measured using an antibody against Cdc2. A standard curve of a serially diluted protein extract was on the same gel to confirm that the antibody dilution used gave the expected linear relationship and therefore could be used for quantitation of the other samples; sample quantitation was only performed if the standard curve gave a linear

relationship to a signal that exceeded that of the brightest band on the measured samples. Quantifying the Cdc2 antibody staining showed a linear induction of both Cdc13-L-Cdc2^{WT} and Cdc13-L-Cdc2^{AF} after 15 minutes, giving very similar results to the protein induction measured by proteomic analysis of the samples (Figure 6.3).

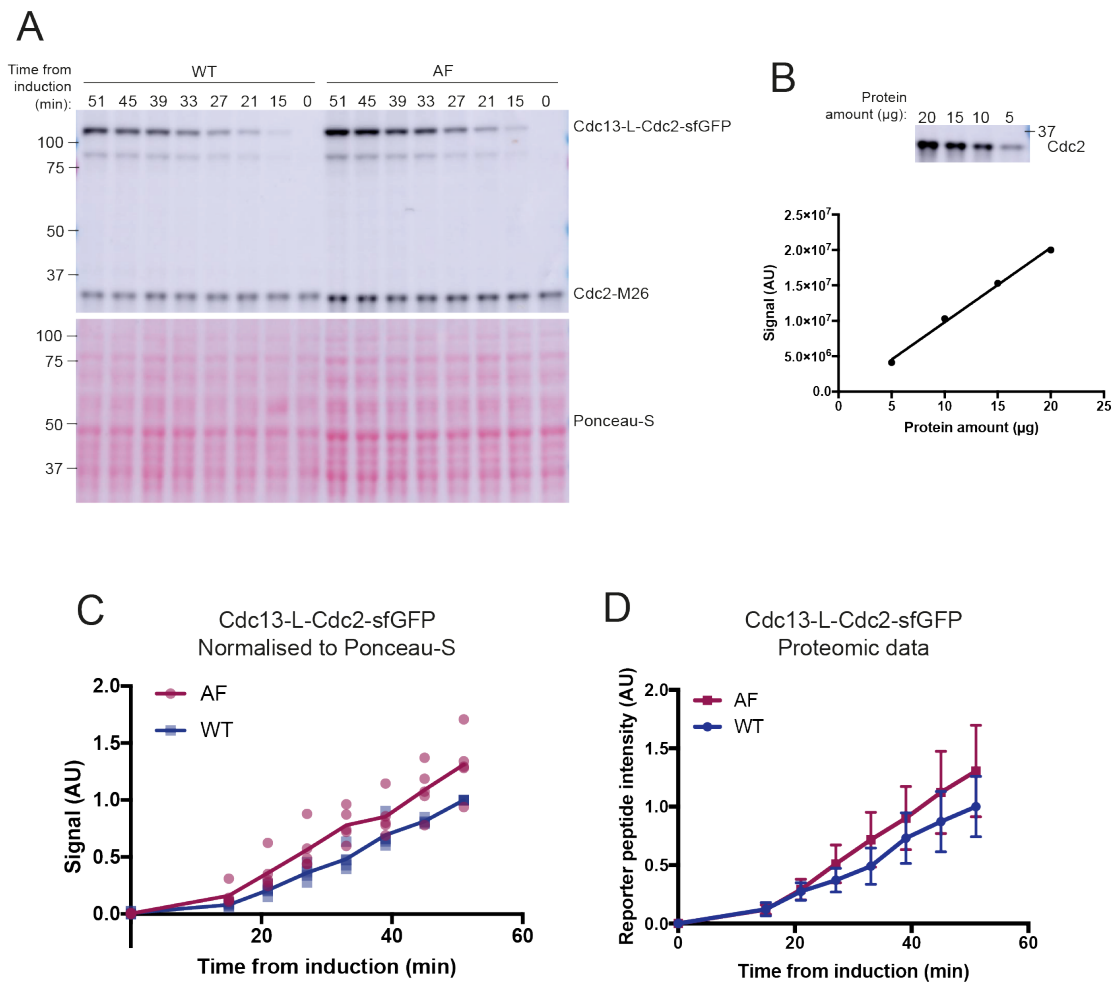


Figure 6.3 | Cdc13-L-Cdc2$^{WT/AF}$ protein level through the time course

A: Western blot showing Cdc13-L-Cdc2^{WT} and Cdc13-L-Cdc2^{AF} induction and endogenous Cdc2-M26, detected using Y63.2 anti-Cdc2 antibody at 1:40,000 dilution, with Ponceau staining shown as a loading control
B: Dilution curve of a mitotic protein extract to act as a standard curve to check that Cdc2 staining reflects the expected linear response. This dilution curve was on the same gel (and subsequently membrane) as the samples from (A).
C: Quantification of Cdc13-L-Cdc2^{WT} and Cdc13-L-Cdc2^{AF} signal from (A) and 4 more technical replicates, normalised to Ponceau staining. Data is normalised to set the WT sample at 51 min to 1. Circles/squares show individual technical replicates and the connecting line shows the mean for each time point.

Figure 6.3 ***caption continued from previous page***
D: Proteomic data showing the protein level of Cdc13-L-Cdc2^{WT} and Cdc13-L-Cdc2^{AF}. The mean and SEM of all peptides assigned to Cdc13, Cdc2 or sfGFP is shown, n = 13 peptides. Data is normalised to set the protein level at 0 min to zero, and the WT sample at 51 min to 1. Data provided and analysed by Souradeep Basu and Andrew Jones (Basu et al., 2021).

Substrate phosphorylation was then measured using the Bqt4-pT272, Bit61-pS132 and Spo15-pS121 antibodies. Quantification of Bit61-pS132 phosphorylation gave inconsistent results on two technical replicates of the same samples, leading me to stop using this antibody for quantitation on Western blots. However, quantitation using Bqt4-pT272 and Spo15-pS121 gave results that were consistent across technical replicates. Bqt4 T272 phosphorylation increased more rapidly and to a higher level with Cdc13-L-Cdc2^{AF} induction than Cdc13-L-Cdc2^{WT} (Figure 6.4). Plotting phosphorylation against fusion protein level as measured by Western blotting in Figure 6.3 to account for the higher level of AF fusion protein removed the difference in initial rate of phosphorylation increase. However, whilst phosphorylation continued to increase as Cdc13-L-Cdc2^{AF} protein level increased, phosphorylation plateaued once Cdc13-L-Cdc2^{WT} protein level reached ~70% of its maximum.

Spo15 S121 phosphorylation as measured by the Spo15-pS121 antibody increased significantly more in response to Cdc13-L-Cdc2^{AF} than Cdc13-L-Cdc2^{WT} (Figure 6.5). Similarly to Bqt4, Spo15 phosphorylation continued to increase with Cdc13-L-Cdc2^{AF}, while it plateaued once Cdc13-L-Cdc2^{WT} protein reached roughly 70% of the maximum. This would suggest that Spo15 S121 is phosphorylated significantly more by Cdc13-L-Cdc2^{AF} than Cdc13-L-Cdc2^{WT} at the higher levels of expression seen in this experiment. However, whilst the phosphorylation data from the phosphoproteomic analysis did show a slightly higher phosphorylation by Cdc13-L-Cdc2^{AF} than Cdc13-L-Cdc2^{WT} it was a much smaller difference than suggested by the Western blots. The phosphoproteomics data also shows Spo15 S121 phosphorylation plateauing at higher levels of Cdc13-L-Cdc2^{AF} whilst the Western blot data suggests that phosphorylation by Cdc13-L-Cdc2^{AF} kept

increasing (Figure 6.5C-D). Thus the phosphoproteomics analysis and Western blot quantitation do not give completely consistent results in this situation.

It is not clear which method of measuring phosphorylation provided the most accurate reflection of Spo15-S121 phosphorylation dynamics. One possibility is that the antibody is detecting multiple phosphorylation sites on Spo15; this could be tested using an S121A mutant of Spo15. Another possibility is that the phosphoproteomics analysis does not detect high levels of Spo15 S121 phosphorylation; there are several potential phosphorylation sites nearby Spo15 S121 that could result in a high m/z ratio of the peptide when it is highly phosphorylated, which may result in the highly phosphorylated peptide binding the beads used to phospho-enrich the sample so strongly that it is not eluted off (Wood et al., 2002, Wood et al., 2012).

In summary, two of the phosphospecific antibodies, Bqt4-pS272 and Spo15-pS121 gave consistent measurements of substrate phosphorylation across technical repeats of the same experimental samples, suggesting that they could be used for measuring substrate phosphorylation by Western blotting.

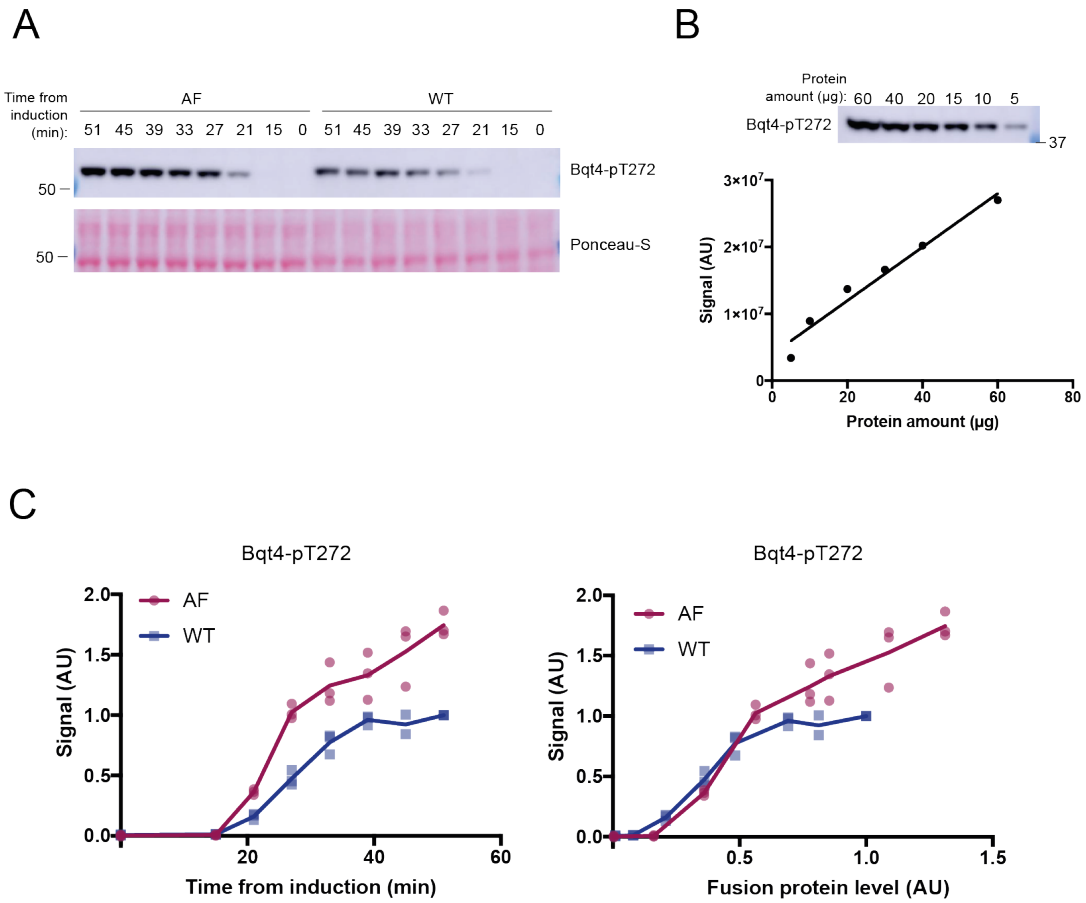


Figure 6.4 | Bqt4 phosphorylation by Cdc13-L-Cdc2$^{WT/AF}$

A: Western blot showing Bqt4-T272 phosphorylation in response to Cdc13-L-Cdc2^{WT} and Cdc13-L-Cdc2^{AF} induction, with Ponceau staining shown as a loading control. Bqt4-pT272 antibody was used at 1:2000 dilution.
B: Dilution curve of a mitotic (high kinase activity) protein extract to act as a standard curve to check that Bqt4-pT272 staining reflects the expected linear response. This dilution curve was on the same gel (and subsequently membrane) as the samples from (A).
C: Quantification of the blot from (A) and two more technical replicates, compared to both time from induction (left) and Cdc13-L-Cdc2^{WT} or Cdc13-L-Cdc2^{AF} fusion protein level (right). All replicates and their mean are shown, normalised to the WT sample at 51 min. Fusion protein level was measured from the Western blot quantification from Figure 6.3

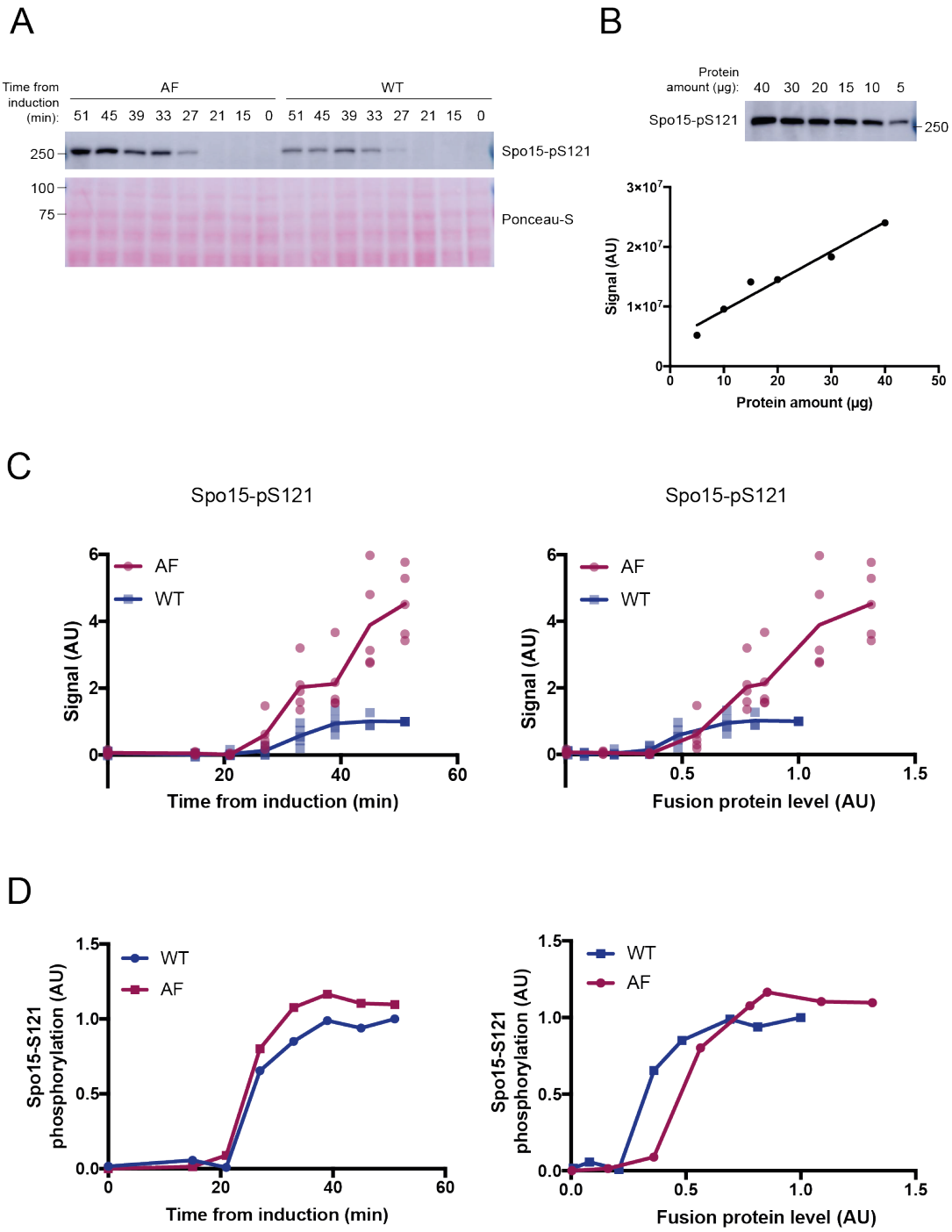


Figure 6.5 | Spo15 phosphorylation by Cdc13-L-Cdc2$^{WT/AF}$

A: Western blot showing Spo15-S121 phosphorylation in response to Cdc13-L-Cdc2^{WT} or Cdc13-L-Cdc2^{AF} induction, with Ponceau staining shown as a loading control. Spo15-pS121 antibody was used at 1:500 dilution.
B: Dilution curve of a mitotic (high kinase activity) protein extract to act as a standard curve to check that Spo15-pT121 staining reflects the expected linear response. This dilution curve was on the same gel (and subsequently membrane) as the samples from (A).

Figure 6.5 ***caption continued from previous page***
C: Quantification of the blot from (A) and 4 more technical replicates, compared to both time from induction (left) and Cdc13-L-Cdc2^{WT} or Cdc13-L-Cdc2^{AF} fusion protein level (right). All replicates and the mean are shown. Data is normalised to the WT sample at 51 min. Fusion protein level was measured from the Western blot quantification from Figure 6.3
D: Spo15-S121 phosphorylation detected by phosphoproteomics, compared to time from induction (left) and Cdc13-L-Cdc2^{WT} or Cdc13-L-Cdc2^{AF} fusion protein level (right). Data is normalised to the WT sample at 51 min. Fusion protein level was measured from the Western blot quantification from Figure 6.3. Data provided and analysed by Souradeep Basu and Andrew Jones (Basu et al., 2021).

6.3 Testing Spo15 antibodies for use in immunofluorescence

Detecting CDK substrate phosphorylation by immunofluorescence has the advantage of being able to provide spatial information of CDK activity, so I next set out to test the antibodies for use in immunofluorescence. I started with the Spo15 antibodies, as background staining can interfere with signal detection and they provided the highest signal to background ratio in Western blotting (Figure 6.2E).

Staining cells with the phosphospecific Spo15-pS121 antibody resulted in seemingly non-specific staining with no evidence of staining at the SPB and no apparent difference in staining in *spo15*$^{+}$ and *spo15Δ* cells (Figure 6.6). However, staining cells with the Spo15-ctrl antibody resulted in some cells with foci of signal adjacent to the nucleus that were likely to be SPBs (Figure 6.7). The Spo15-ctrl antibody did not stain foci in all cells in the population, and in many cells with stained foci it stained 2 foci, assumed to be separated SPBs. I therefore considered that the Spo15-ctrl antibody might be staining phosphorylated Spo15 more than non-phosphorylated Spo15, and therefore staining Spo15 more strongly later in the cell cycle.

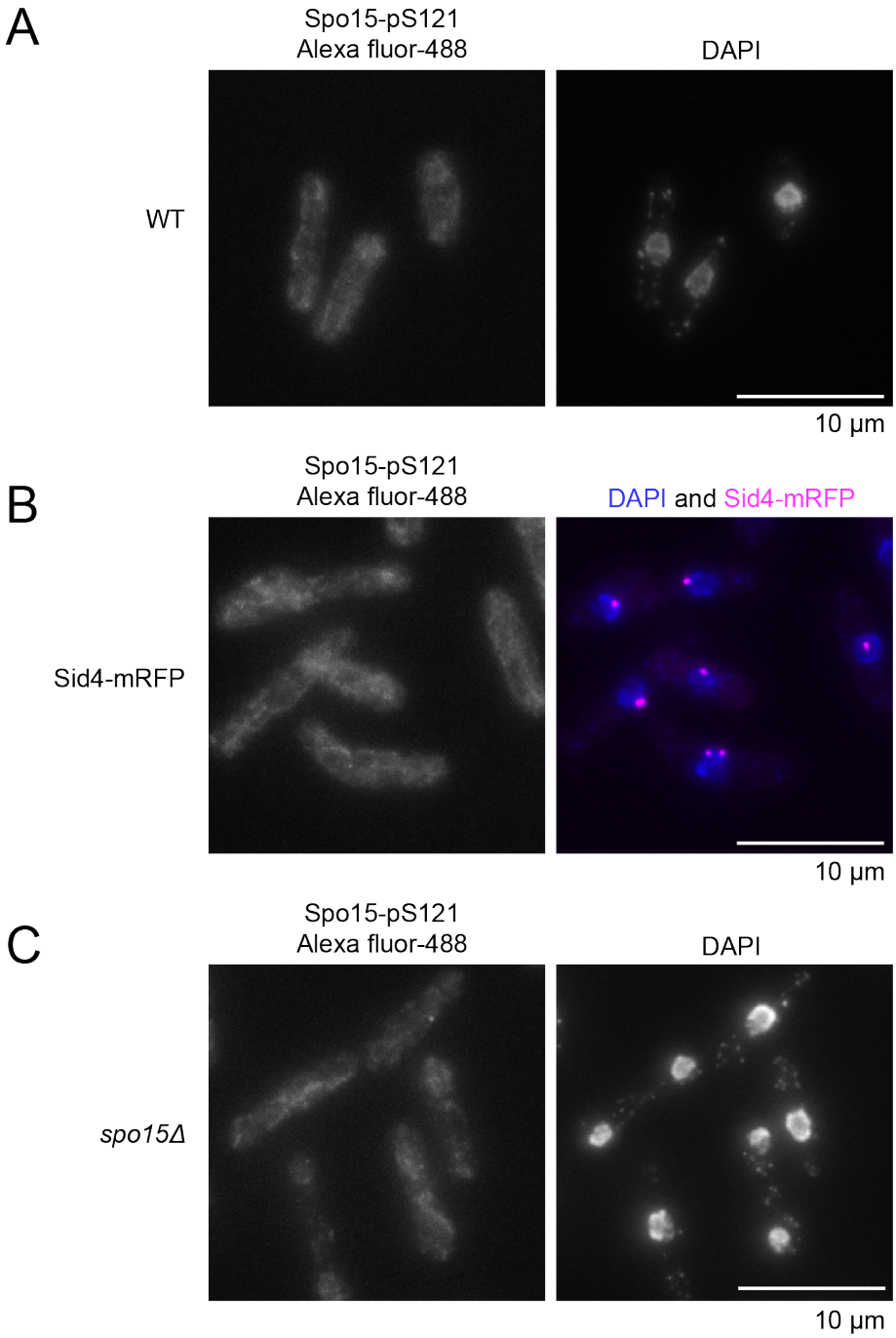


Figure 6.6 | Immunofluorescence with Spo15 phosphospecific pS121 antibody

Asynchronous cultures were formaldehyde-fixed, permeabilised and incubated with Spo15-pS121 antibody followed by an anti-rabbit secondary coupled to Alexa-fluor 488. Images show maximum projections of antibody staining (left) and DAPI staining (right). The same pixel range has been applied to all images of the same channel.
A: Wild-type cells
B: Sid4-mRFP cells. Right image shows a merged image of Sid4-mRFP and DAPI.
C: *spo15Δ* cells

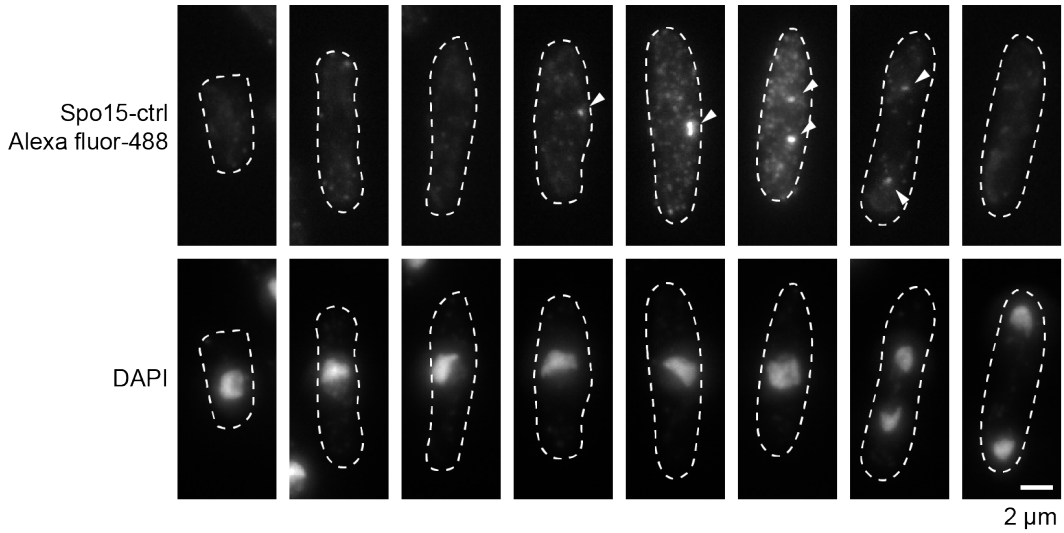


Figure 6.7 | Immunofluorescence with the Spo15-ctrl antibody

Wild-type cells were formaldehyde fixed and permeabilised according to the same protocol as Figure 6.6. Maximum projection images of cells assumed to represent progressive stages of the cell cycle, based on cell length, possible SPB dynamics and nuclear dynamics. DAPI staining (bottom) and Spo15-ctrl staining (top) are shown. All images from the same channel are set to the same pixel range. Some pixels in the Spo15-ctrl channel are saturated in the displayed pixel range in order to better display the whole-cell staining. Arrows mark foci adjacent to the nucleus that are possible SPBs.

To test whether the Spo15-ctrl antibody was detecting phosphorylated Spo15 at the SPB, I used the SPB marker Sid4-mRFP and the analogue-sensitive allele of *cdc2*, *cdc2(as)-M17*, and treated cells with 10 µM 1-NmPP1 for 20 minutes to inhibit CDK activity to allow substrate dephosphorylation. I compared Spo15-ctrl staining in this kinase-dead condition with DMSO-treated *cdc2(as)-M17* cells, or 1-NmPP1-treated *cdc2*$^{+}$ cells. In the *sid4-mRFP* 1-NmPP1-treated cells and the *cdc2(as)-M17 sid4-mRFP* DMSO-treated cells bright foci could be seen in some cells that colocalised with the SPB, often in cells that had separated SPBs (Figure 6.8A). The cells that had Spo15-ctrl staining at the SPB also often had punctate signal throughout the cell. In the *cdc2(as)-M17 sid4-mRFP* 1-NmPP1-treated cells the SPB and punctate cellular signal was lost even in cells that had separated SPBs indicating that they were mitotic (Figure 6.8A). Quantifying all cells with separated SPBs 5 µm apart or less (to focus on early mitotic cells) showed that whilst roughly 80% of them had Spo15-ctrl enriched at the SPB in the Cdc2-active conditions, Spo15-ctrl SPB staining was abolished when Cdc2 was inhibited (Figure 6.8B).

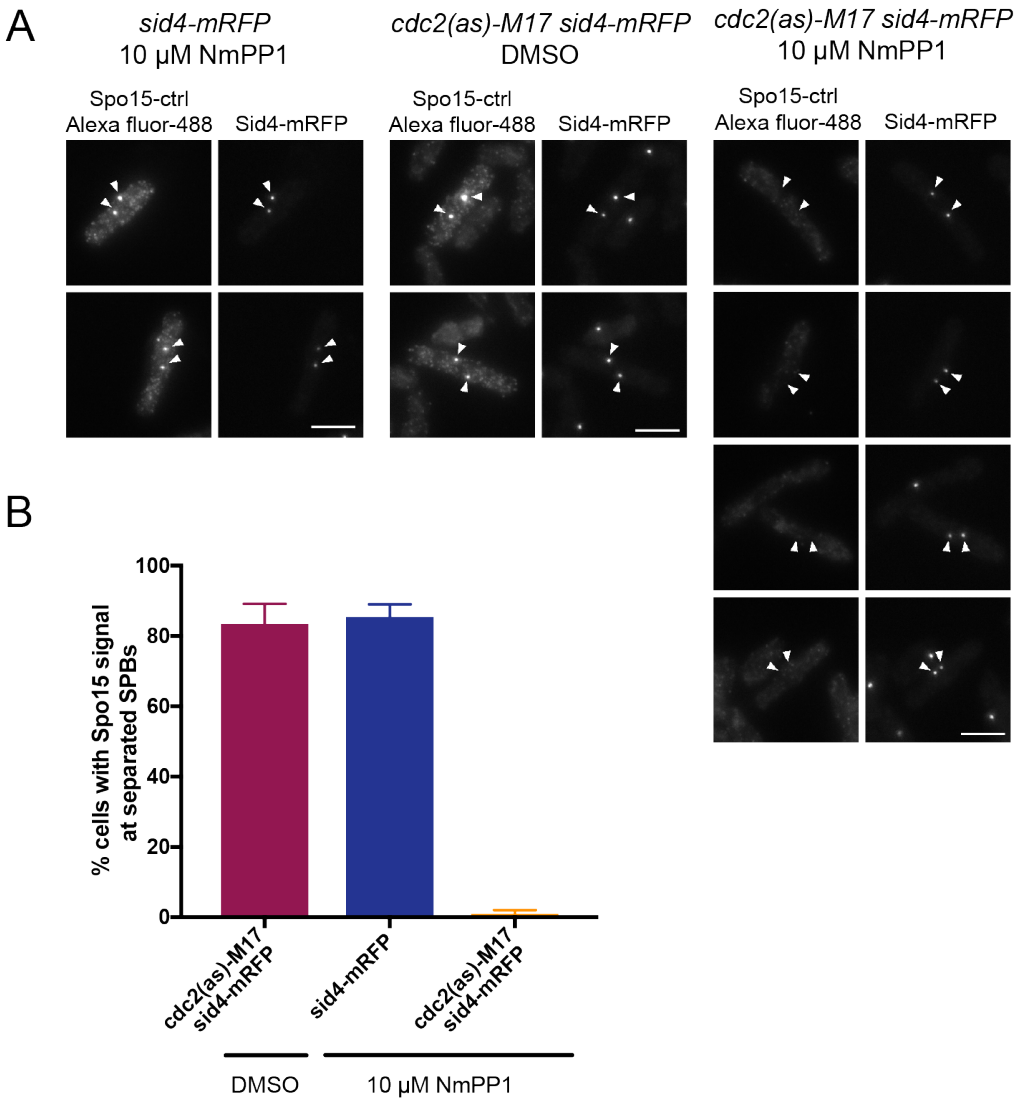


Figure 6.8 | Testing what Spo15-ctrl staining is dependent on CDK activity

A: Asynchronous populations of *cdc2(as)-M17 sid4-mRFP* cells were treated with DMSO or 10 μM 1-NmPP1, and *sid4-mRFP* cells were treated with 10 μM 1-NmPP1, for 20 minutes before formaldehyde fixation. Maximum projection images are shown of example cells that have separated SPBs less than 5 μm apart (judged by Sid4-mRFP signal). Scale bars show 5 μm.
B: Cells with separated SPBs ≤5 μm apart were scored for Spo15-ctrl staining at the SPB. Scoring was done by eye, and for ambiguous cells a line was drawn through the SPB and the signal intensity plotted in ImageJ. Cells were counted as having Spo15 enriched at the SPB if the signal from one SPB was at least two times the background signal in the cell. Graph shows mean and SD of 3 replicates. n ≥ 29 per strain for each replicate. Across all 3 replicates total n = 266 for *cdc2(as) sid4-mRFP* DMSO treatment; n = 253 for *sid4-mRFP* 1-NmPP1 treatment; n = 136 for *cdc2(as) sid4-mRFP* 1-NmPP1 treatment.

Measuring the pixel intensity at the SPB shows that at longer cell lengths, Spo15-ctrl intensity increases dramatically in some cells when Cdc2 remains active (Figure 6.9A). SPBs with high Spo15-ctrl staining are more likely to belong to a cell that has 2 SPBs (mitotic and binucleate cells). Inhibiting Cdc2 activity removes this high-intensity SPB staining of Spo15-ctrl. The same pattern, though less extreme, can be seen with whole-cell intensity; when Cdc2 is active, there is a population of cells with high cellular intensity of Spo15-ctrl, and this population is enriched for cells with 2 SPBs and long cells (Figure 6.9B). This high-intensity staining is also dependent on Cdc2 activity. To test if this high whole-cell intensity of Spo15-ctrl was due to high SPB signal affecting the whole-cell mean, or higher staining outside of the SPB, the mean intensity of the cell minus the SPB (Cell-SPB) was measured (Figure 6.9C). The high-intensity population could still be seen, suggesting that Spo15-ctrl staining increases at the SPB but also elsewhere in the cell at mitosis. The ratio of the SPB staining to the Cell-SPB staining still showed a dramatic increase in some cells at longer lengths, indicating that Spo15-ctrl staining at the SPB increased in concentration more than in the rest of the cell, which is unsurprising given that the concentration of Spo15 is higher at the SPB (Figure 6.9D) (Ikemoto et al., 2000). These data strongly suggest that Spo15-ctrl is detecting a phosphorylated substrate(s) both at the SPB and also elsewhere in the cell in a manner that is dependent on CDK activity. This is consistent with the timing of phosphorylation of Spo15 S121 identified in phosphoproteomics (Figure 6.1), which indicates a very low level of phosphorylation in a G2 arrest, followed by a rapid increase in mitosis.

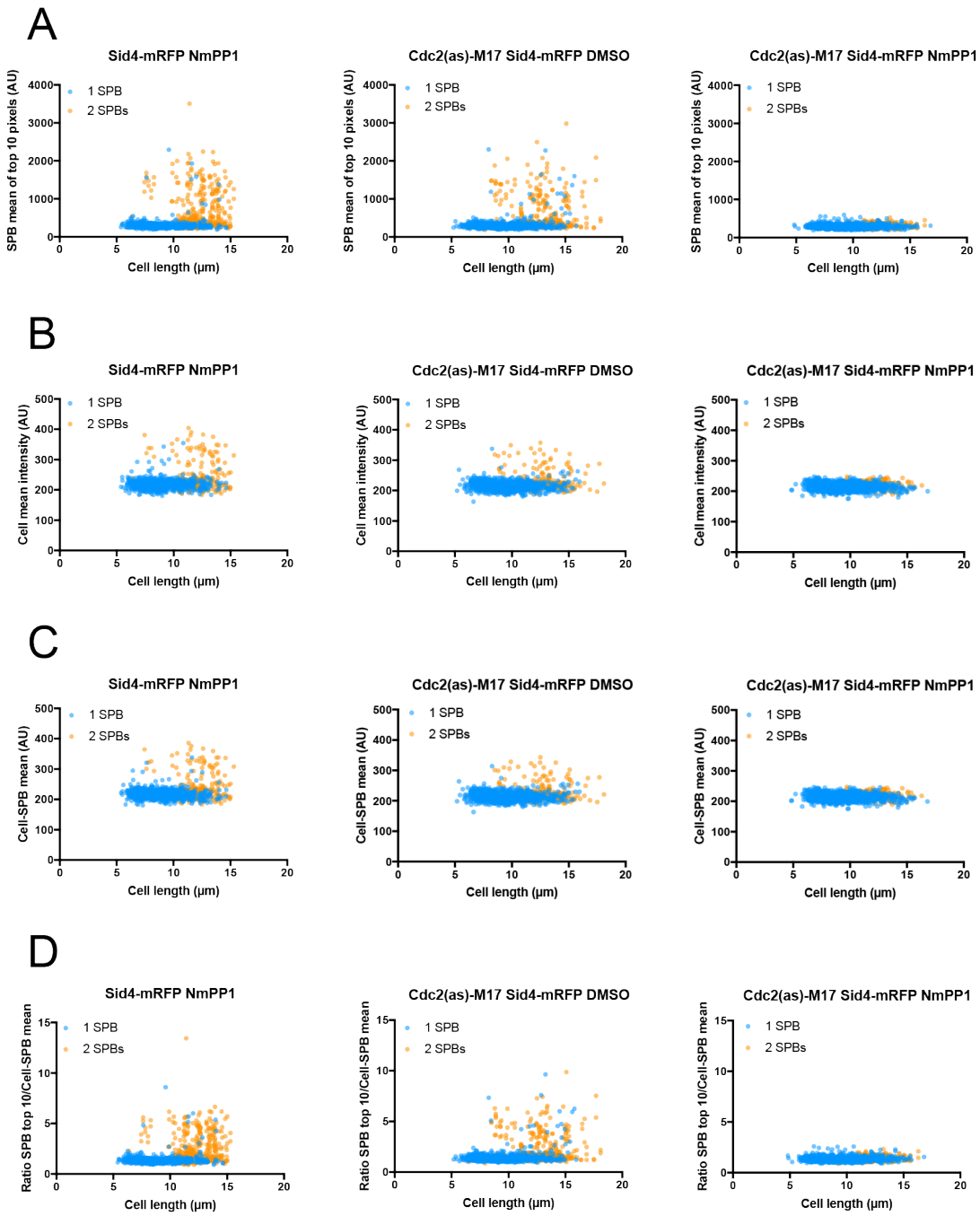


Figure 6.9 | Intensity measurements of Spo15-ctrl staining in Cdc2-inhibited cells

Cells were segmented using brightfield images to generate a whole cell mask, and Sid4-mRFP signal to generate an SPB mask. Cell length was determined from the whole cell mask, and the number of SPBs in a given cell was determined by how many SPB masks intersected with the cell mask.
A: Mean of the highest ten Spo15-ctrl pixels from the SPB mask plotted against cell length. n = 1160 SPBs for Sid4-mRFP 1-NmPP1-treated; n = 1276 SPBs for Cdc2(as)-M17 Sid4-mRFP DMSO-treated; n = 1156 SPBs for Cdc2(as)-M17 Sid4-mRFP 1-NmPP1-treated.

Figure 6.9 ***caption continued from previous page***
B: Mean Spo15-ctrl pixel intensity from the whole cell mask plotted against cell length. n = 910 cells for Sid4-mRFP 1-NmPP1-treated; n = 1041 cells for Cdc2(as)-M17 Sid4-mRFP DMSO-treated; n = 1009 cells for Cdc2(as)-M17 Sid4-mRFP 1-NmPP1-treated.
C: Mean Spo15-ctrl pixel intensity from the whole cell mask excluding the SPB mask, plotted against cell length. n = 910 cells for Sid4-mRFP 1-NmPP1-treated; n = 1041 cells for Cdc2(as)-M17 Sid4-mRFP DMSO-treated; n = 1009 cells for Cdc2(as)-M17 Sid4-mRFP 1-NmPP1-treated.
D: The ratio of the mean of the top 10 pixels in the SPB mask from (A) divided by the mean of the cell excluding SPB mask from (C). n = 1160 SPBs for Sid4-mRFP 1-NmPP1-treated; n = 1276 SPBs for Cdc2(as)-M17 Sid4-mRFP DMSO-treated; n = 1156 SPBs for Cdc2(as)-M17 Sid4-mRFP 1-NmPP1-treated.

I next tested whether the Spo15-ctrl staining was specific to Spo15 by comparing the staining in wild-type and *spo15Δ* cells. Whilst roughly 6% of cells in an asynchronous population of wild-type cells had high Spo15-ctrl signal at the SPB, not a single example was found in the *spo15Δ* strain (Figure 6.10A-B). Intensity measurements of the whole-cell signal intensity also showed that the population of high-intensity cells at longer cell lengths disappeared in the *spo15Δ* strain (Figure 6.10C). This suggests that both the SPB and non-SPB high-intensity staining of the Spo15-ctrl antibody is specific to Spo15. Taken together, the experiments in this section suggest that the Spo15-ctrl antibody is detecting phosphorylated Spo15, both at the SPB and as punctate signal throughout the cell. Immunofluorescence with the Spo15-ctrl antibody could therefore provide an opportunity to detect phosphorylation of the same substrate in different subcellular compartments.

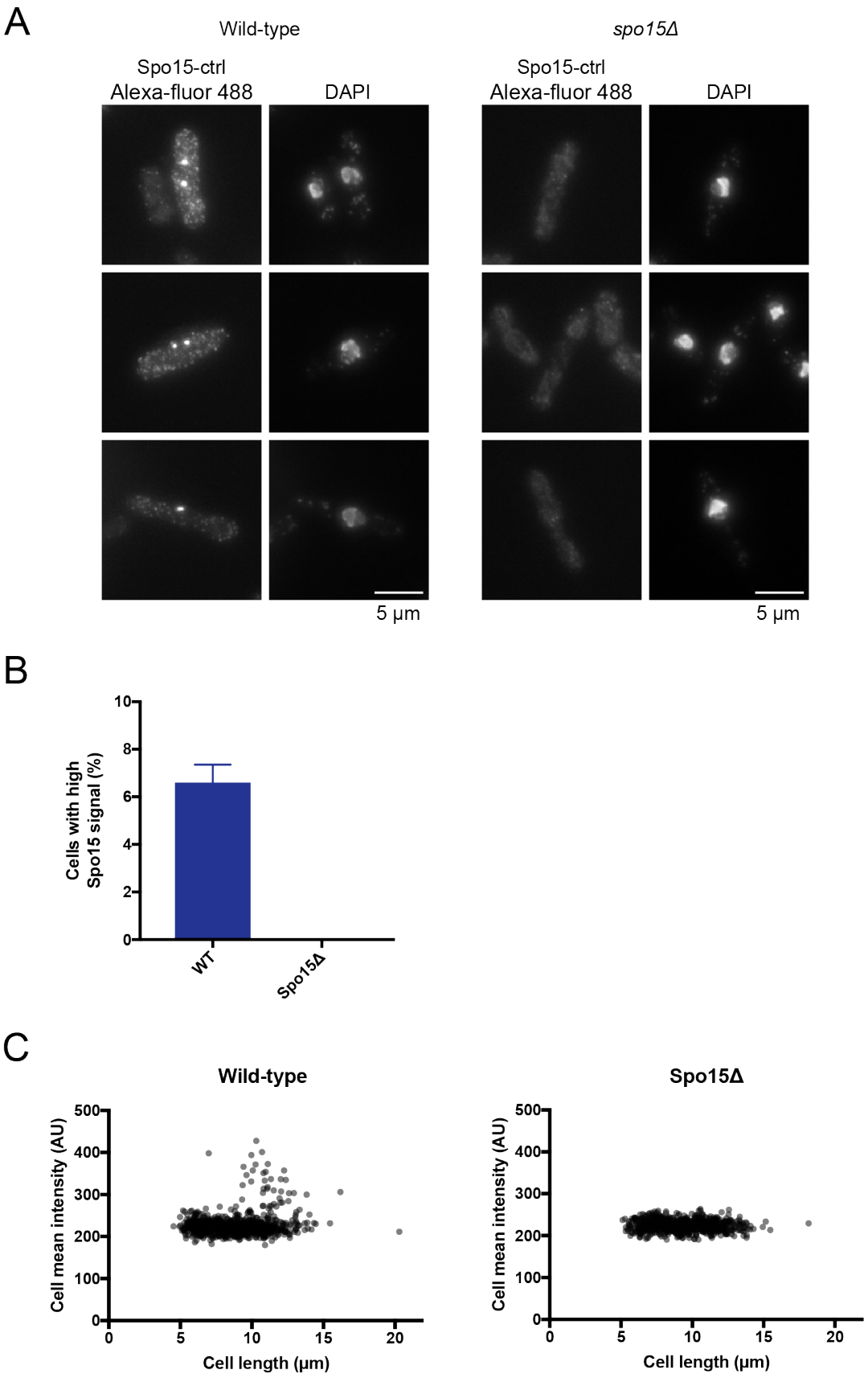


Figure 6.10 | Testing what Spo15-ctrl signal is specific to Spo15

Figure 6.10 ***caption continued from previous page***
A: Example cells demonstrating Spo15-ctrl antibody staining in a wild-type (left) and *spo15Δ* (right) strain. Cells were selected as being representative of longer uninucleate cells. The same pixel range has been applied to all images of the same channel, with some pixels in the wild-type Spo15-ctrl images saturating the shown range.
B: Percentage of wild-type and *spo15Δ* cells from an asynchronous population with one or two foci of high Spo15-ctrl antibody signal near the nucleus, which is assumed to be staining of the SPB. Cells were judged by eye and if ambiguous, a signal intensity profile was plotted through the focus of signal, and the cell classed as 'high intensity' if the focus was at least twice as high as the background signal. Graph shows mean and SD of 3 replicates. n > 275 cells for each strain and each replicate. Across all 3 replicates, total n = 967 cells for WT, and n = 933 cells for *spo15Δ*.
C: Wild-type and *spo15Δ* cells from one replicate of (B) were segmented based on their brightfield images, and the resulting masks used to measure the mean signal intensity and cell length. n = 843 wild-type cells and n = 771 *spo15Δ* cells.

6.4 Discussion

The work in this Chapter describes the development of reagents that may be used to measure CDK substrate phosphorylation in different subcellular locations. Of the 5 sets of antibodies generated, the antibodies against Bqt4 and Spo15 look most promising.

The work in this Chapter strongly suggests that the Spo15-ctrl antibody detects phosphorylated Spo15 (in a CDK-activity dependent manner) in immunofluorescence. The observation that the antibody is detecting phosphorylated Spo15 both concentrated at the SPB but also throughout the cell in punctate foci provides an opportunity to measure Spo15 phosphorylation in different subcellular compartments. It would be of interest to arrest cells in G2 and release them synchronously into mitosis, to see if Spo15-ctrl intensity measurements can be made at several time points at the SPB and throughout the cell to measure the rate of substrate phosphorylation. This could be used to ask if the rate and timing of phosphorylation of Spo15 is different at the SPB compared to the rest of the cell.

To compare substrate phosphorylation in different subcellular compartments, the substrate of interest, or a peptide encompassing the phosphosite, could also be targeted to different subcellular compartments, and the rate of phosphorylation measured in these different scenarios. If the substrate relocalisation was efficient and resulted in a large proportion of the substrate being targeted to the location of interest, substrate phosphorylation could also be measured in a population by Western blotting. This would have the advantage of being able to measure Bqt4 phosphorylation, as although the Bqt4 antibodies have not been tested in immunofluorescence, the work in this Chapter suggests that the Bqt4 phosphospecific antibody can give repeatable measurements of substrate phosphorylation by Western blotting. It is worth noting however that protein retargeting can perturb the cell as shown in the previous Chapter. If this poses an issue, retargeting a peptide encompassing the phosphosite, rather than the full protein, may reduce the impact on cell physiology.

Thus, the systems developed in this Chapter could potentially be used to ask if altering the localisation of Bqt4 and Spo15 affects their sensitivity to CDK activity. The work in the previous results Chapters, in combination with insights from (Basu et al., 2020), suggest that cyclin-CDK localisation to the SPB plays an important role in CDK substrate phosphorylation and cell cycle progression. The work in this Chapter outlines the initial steps towards developing a system that could provide an insight into the role that substrate localisation plays in the phosphorylation of the CDK substrates Bqt4 and Spo15. These experiments would be particularly interesting in light of the observation that substrate sensitivity to Cdc2 inhibition is correlated with substrate localisation (Swaffer et al., 2016, Basu et al., 2020).

Chapter 7. Discussion

The aim of this project was to further our understanding of cyclin-CDK localisation and its influence on the cell cycle. The work presented here first demonstrates that the hydrophobic patch of Cdc13 is necessary for its enrichment at the SPB in early G2. This identified a key mechanism regulating Cdc13 localisation and a potential explanation for the failure of cells driven by $Cdc13^{HPM}$ to perform mitosis. The work in this thesis also indicates that restoring the SPB localisation of $Cdc13^{HPM}$-Cdc2 allows mitotic entry. This suggests that Cdc2 activity at the SPB is essential for mitotic entry, and highlights the importance of considering compartmentalised CDK activity in the quantitative model. It also suggests that the sole essential role of the Cdc13 hydrophobic patch for mitotic entry is to mediate SPB localisation. Although it promotes mitotic entry, tethering $Cdc13^{HPM}$-Cdc2 to the SPB results in frequent defects in mitotic progression and exit. It therefore remains possible that Cdc13 hydrophobic patch-substrate docking interactions, or a more precise SPB localisation not mimicked by tethering to Cut12, is essential for full mitotic progression and exit.

The data presented here also indicate that the hydrophobic patch of human Cyclin B1 is required for its localisation to the centrosome, suggesting the role of the hydrophobic patch in spatial enrichment in fission yeast Cdc13 and human Cyclin B1 may be conserved. This work has also shown that there is a hydrophobic patch-independent mechanism of Cdc13 localisation to the SPB, that occurs after Polo kinase localises to the SPB in late G2/early mitosis.

Finally, phosphospecific antibodies against CDK substrates are described that may be able to provide a method to measure CDK substrate phosphorylation in different subcellular locations. Antibodies against the CDK substrates Bqt4 and Spo15 have been optimised for use in Western blotting, and an antibody against Spo15 has also been optimised for use in immunofluorescence. Future work will build on this to test whether these systems can be used to ask if the timing of phosphorylation of these substrates is affected by subcellular location.

In this Discussion I first outline my favoured model to explain the observations of the phenotype of cells driven by Cdc13^{HPM}. I will then discuss the key points in this model in more detail and how they relate to what is already known about the role and importance of the hydrophobic patch and cyclin SPB/centrosomal localisation in other systems. I will also discuss the other key findings of my work and areas of interest for future work.

7.1 A localisation model to explain the effect of Cdc13^{HPM}

Based on the data presented in this thesis, data from the related work in (Basu et al., 2020), and published work in the field, the following model is favoured (referred to as the localisation model from here on). Wild-type Cdc13 docks with a subset of CDK substrates via R/KXL motifs. It also docks with an/multiple SPB component(s) that may also be CDK substrates, again likely via R/KXL motif(s). This docking of Cdc13 with SPB components concentrates Cdc13 at the SPB, providing Cdc13-Cdc2 activity to neighbouring Cdc2 substrates at the SPB even if these substrates themselves do not directly dock to Cdc13 via the hydrophobic patch. In this way, the interactor(s) at the SPB with docking motifs act as a platform by which Cdc13-Cdc2 can reach neighbouring substrates. This accumulation of Cdc13-Cdc2 at the SPB also provides a source of Cdc2 activity for cytoplasmic CDK substrates, which I propose is due to Cdc13-Cdc2 cycling on and off the SPB. Disruption of the Cdc13 hydrophobic patch disrupts not only the direct docking of Cdc13 to Cdc2 substrates, but also the accumulation of Cdc13 at the SPB. This results in lower Cdc13-Cdc2 activity experienced at the SPB and cytoplasm, resulting in reduced phosphorylation of substrates at the SPB and cytoplasm even if they do not contain R/KXL motifs. I propose that a lack of Cdc2 activity at the SPB in cells driven by Cdc13^{HPM} results in the observed failure of these cells to enter mitosis. Two essential processes that seem likely to be affected by a lack of Cdc2 activity at the SPB are SPB insertion into the nuclear envelope, and activation of the feedback loops involving Plo1 and Cdc25 that drive mitotic commitment. I therefore suggest that Cdc2 Y15 is unlikely to be dephosphorylated in cells driven by Cdc13^{HPM}.

Given that the data presented here also suggests that the hydrophobic patch is involved in Cyclin B1 localisation to the centrosome in human cells, I propose that this work supports the theory that Cyclin B1-Cdk1 localisation to the centrosome is important for cell cycle progression in human cells. In the next sections I will discuss the suggestions from this localisation model, and how they relate to the published literature in *S. pombe* and other systems. I will first discuss the role of the hydrophobic patch in substrate docking and localisation, followed by the potential importance of these roles in cell cycle progression.

7.2 The role of the cyclin hydrophobic patch in substrate docking and localisation

It has previously been suggested that the hydrophobic patch of G1/S cyclins in *S. cerevisiae* mediates the preferential targeting of these cyclins to substrates phosphorylated early in the cell cycle (Loog and Morgan, 2005). Given that the entire *S. pombe* cell cycle can be driven by one cyclin-CDK complex, Cdc13-Cdc2 (Fisher and Nurse, 1996, Coudreuse and Nurse, 2010), the Cdc13 hydrophobic patch provided a possible mechanism by which this single cyclin-CDK complex might order substrate phosphorylation, by preferentially targeting CDK activity to early substrates. However, it was demonstrated that *S. pombe* cells driven by $Cdc13^{HPM}$ perform S-phase, but not mitosis (Basu et al., 2020) (also shown in Figure 5.1). This suggested that the primary role of the hydrophobic patch of Cdc13 is not to mediate early CDK substrate phosphorylation as might have been expected, but that it is still required for cell cycle progression.

The work in this thesis demonstrates that the Cdc13 hydrophobic patch is necessary for its G2 localisation to the SPB, with cells driven by $Cdc13^{HPM}$-sfGFP arresting in G2 with no $Cdc13^{HPM}$-sfGFP enrichment at the SPB. Therefore, one of the key suggestions of this work is that a major role of the Cdc13 hydrophobic patch is to mediate SPB localisation. This suggestion is supported by the observation that restoring $Cdc13^{HPM}$-Cdc2 SPB localisation promotes mitotic entry.

Whilst the proposed localisation model suggests that disrupting the hydrophobic patch of Cdc13 prevents direct docking to SPB components or SPB-localised proteins, it is important to note that this is not the only explanation of these results. For example, these data could also be explained by mutations in the hydrophobic patch disrupting nuclear export of Cdc13, resulting in nuclear retention of Cdc13 and thus indirectly reducing Cdc13 SPB localisation. However this explanation cannot be true for the localisation of human $Cyclin\ B1^{HPM}$, which displays the expected cytoplasmic localisation in interphase, and nuclear import at mitosis, but does not visibly enrich at the centrosome. It is also possible that Cdc13 is localising to a distinct structure near the SPB, such as the centromere. However, the role of

the SPB as a signalling hub at mitotic entry, and the confirmed interaction of Cdc13 with several SPB components (as discussed in section 3.4), are both consistent with the suggested hypothesis that Cdc13 interacts with SPB components via its hydrophobic patch. The restoration of mitotic entry seen upon tethering of $Cdc13^{HPM}$-Cdc2 to Cut12, an SPB component, also suggests that Cdc13 localises to the SPB.

It is likely that the Cdc13 hydrophobic patch is used to dock to substrates directly as well as its SPB localisation role. However, the suggestion that the major essential role of the Cdc13 hydrophobic patch is in mediating localisation contrasts with the suggestion that the role of the hydrophobic patch in G1/S cyclins in *S. cerevisiae* is to mediate early substrate phosphorylation (Loog and Morgan, 2005). This raises the questions of whether there are different primary roles for the hydrophobic patch between G1/S and mitotic cyclins, or between different organisms.

7.2.1 Are there different roles for the hydrophobic patch in G1/S vs mitotic cyclins?

Whilst the role of the hydrophobic patch in substrate docking has been clearly demonstrated *in vitro* for G1/S cyclins, it is suggested that the mitotic cyclins in *S. cerevisiae* are less reliant on the hydrophobic patch for targeted substrate phosphorylation, though some Clb2-specific substrates dependent on the hydrophobic patch have been identified (Schulman et al., 1998, Koivomagi et al., 2011, Loog and Morgan, 2005, Ord et al., 2019). The hydrophobic patch has been implicated in localisation of the *S. cerevisiae* mitotic cyclin Clb2 to the bud neck (Bailly et al., 2003), and the work in this thesis suggests that the hydrophobic patch also mediates human Cyclin B1 localisation to the centrosome, as has previously been hypothesised (Bentley et al., 2007), indicating that the hydrophobic patch region is involved in localisation of other mitotic cyclins. The work in this thesis is consistent with the theory that the hydrophobic patch of B-type cyclins may be well conserved due to a conserved role in localisation (Bentley et al., 2007).

Reconciling these observations, it may be that the hydrophobic patch has different primary roles in different cyclins, with G1/S cyclins predominantly using it for targeting early substrate phosphorylation, and mitotic cyclins using it primarily for localisation. However, it may not be this clear cut, as the G1/S mammalian Cyclin A hydrophobic patch is involved in centrosomal localisation as well as substrate docking, and the centrosomal localisation role of the hydrophobic patch is important for its activity in S-phase (Schulman et al., 1998, Pascreau et al., 2010). More detailed studies are needed to separate the localisation and more general substrate docking role of the hydrophobic patch in different cyclins in order to test the importance of each role. Investigation of the localisation and S-phase promoting ability of the hydrophobic patch mutant of the fission yeast B-type G1/S cyclin Cig2, which acts earlier in the cycle than Cdc13, but has a relatively well conserved hydrophobic patch and localises to the SPB (Decottignies et al., 2001), could also inform this discussion.

7.2.2 Are there different roles for the hydrophobic patch between different organisms?

It is also possible that the reason that the localisation model suggested here contrasts with the model resulting from the work in *S. cerevisiae* is because the balance of importance of the different roles of the hydrophobic patch varies between species. Whilst ordered cell cycle progression in *S. cerevisiae* can be driven by a single cyclin-CDK, G1/S cyclin specificity is required for cell polarisation and bud emergence and therefore cell viability (Pirincci Ercan et al., 2021). This contrasts with *S. pombe* cells, which are viable with just Cdc13-Cdc2 (Fisher and Nurse, 1996, Coudreuse and Nurse, 2010). The different requirements for multiple cyclins between *S. pombe* and *S. cerevisiae* may be reflected in differing importance of the general substrate docking and localisation roles of the hydrophobic patch between these organisms.

It may also be affected by the difference in timing of cell cycle events in these organisms. S-phase and spindle formation are temporally separated in *S. pombe*,

with spindle formation being restricted to mitosis as it is in the majority of eukaryotic cells including mammalian cells. These two processes are not as temporally distinct in *S. cerevisiae*, in which a bipolar spindle is formed during S phase (Winey and O'Toole, 2001). It is possible that substrate-specific docking interactions may play a more important role in *S. cerevisiae* cyclins in part due to the unusual overlap in timing of these events. If it is true that the importance of cyclin mediated localisation and direct substrate docking varies between organisms, more studies will be required in more complex eukaryotic systems such as human cells to ascertain what role the hydrophobic patch plays in these organisms. However, the observation in this thesis that the hydrophobic patch of human Cyclin B1 mediates its localisation to the centrosome suggests that what is found in *S. pombe* may be relevant for human cells.

7.2.3 The involvement of the cyclin hydrophobic patch in SPB and centrosomal localisation

The work in this thesis suggests that the role of the hydrophobic patch in SPB and centrosomal localisation specifically is similar in fission yeast Cdc13 and human Cyclin B1. This adds to the previous finding that the hydrophobic patch of human Cyclin A directs it to the centrosome (Pascreau et al., 2010) and the more recent suggestion that the hydrophobic patch of the G2 *S. cerevisiae* cyclin Clb3 can influence its localisation to the SPB (Faustova et al., 2021). However, it is clearly not a universal feature of the cyclin hydrophobic patch, as mammalian Cyclin E and budding yeast Clb2 both do not require their hydrophobic patch to localise to the centrosome and SPB respectively (Matsumoto and Maller, 2004, Bailly et al., 2003). It is worth noting however that the Clb2 hydrophobic patch (NRDILVNW) has some sequence differences with the Cdc13, Cyclin B1 and Cyclin A hydrophobic patches, including an asparagine (N) in place of the highly conserved methionine (M). Furthermore, when compared to Cyclin A and Cyclin B1, the region surrounding the Cyclin E hydrophobic patch has structural and electrostatic differences that may affect the hydrophobic patch binding groove (Pascreau et al., 2010). It is possible that these differences in the hydrophobic patch regions of Cyclin E and Clb2 may not favour binding with the interacting protein(s) at the

centrosome and SPB. It is also possible that the hydrophobic patch region of Clb2 is involved in its localisation to the SPB, but that there is also a hydrophobic patch-independent mechanism of Clb2 SPB localisation similar to the mechanism that operates in *S. pombe* after Plo1 localisation to the SPB (discussed later in section 7.4). Interestingly, mammalian Cyclin E relies on a different hydrophobic region for centrosomal localisation, raising the question of whether the same is true for budding yeast Clb2 (Matsumoto and Maller, 2004). It is also unknown whether the *S. cerevisiae* G1/S phase cyclin Clb5 uses its hydrophobic patch to mediate localisation, though it does localise to the nucleus and SPB (Huisman et al., 2007).

The work to date on the cyclin hydrophobic patch therefore suggests that cyclins in multiple systems rely on the hydrophobic patch for substrate docking and/or localisation, with a particular but not exclusive emphasis on localisation to the SPB or centrosome. The relative importance of the general substrate docking and the localisation roles of the hydrophobic patch may vary between cyclins, with the possibility that in G1/S cyclins, the main role of the hydrophobic patch is to mediate substrate docking, while in mitotic cyclins, the primary role is to influence localisation. However, more study is required to ascertain whether this general categorisation is true.

7.3 Importance of the hydrophobic patch and SPB localisation

7.3.1 Is Cdc13 SPB localisation essential for cell cycle progression?

One of the main suggestions of the localisation model is that the reason cells driven by $Cdc13^{HPM}$ do not enter mitosis is due to a lack of Cdc2 activity at the SPB and cytoplasm, caused by the defective localisation of $Cdc13^{HPM}$ to the SPB. The model therefore suggests that Cdc13 localisation to the SPB is essential for mitosis. As discussed in the Introduction (section 1.6.4), the importance of the centrosome in more complex eukaryotes is contested. However, the observation that the first active population of Cyclin B1-Cdk1 in human cells is at the centrosome suggests a role for centrosomal Cyclin B1-Cdk1 in mitotic entry, indicating that mitotic cyclin-CDK signalling at the SPB and centrosome may be important in both fission yeast and human cells (Jackman et al., 2003).

The wave of mitotic entry seen upon restoration of $Cdc13^{HPM}$-Cdc2 SPB localisation suggests that the mitotic entry defect of $Cdc13^{HPM}$ is due to a lack of SPB localisation, and therefore supports the hypothesis that CDK activity at the SPB is essential for mitotic entry. The importance of CDK signalling at the SPB is further supported by the previous observation that Cdc2Y15F tethered to the SPB specifically can promote mitotic commitment, whereas when tethered to other locations Cdc2Y15F does not promote mitotic entry (Grallert et al., 2013b). However, the observation in this thesis that tetracycline-induced $Cdc13^{HPM}$-L-Cdc2(as)-GBP-mCherry was able to drive mitosis even when untethered to the SPB was an unexpected result and contrasts with the initial finding that cells driven by $Cdc13^{HPM}$ (expressed under the Cdc13 promoter) do not perform mitosis. It is possible that a combination of a potential mild overexpression, increased efficiency of Cdc13-Cdc2 binding when using the fusion protein, the presence of other cyclins in the strain, and/or performing the experiment at 36 °C result in increased Cdc2 activity in these strains. This proposal would be consistent with the suggested localisation model, as an increase in CDK activity throughout the cell would result in an increase in activity in the cytoplasm and around the SPB, even if Cdc2 is not specifically enriched at the SPB. Therefore, one model to reconcile these experimental results is that a threshold level of CDK activity is needed at the SPB

for mitotic entry, which is provided by Cdc13-Cdc2 enrichment at the SPB dependent on the hydrophobic patch. When this enrichment is abolished, an increase in whole-cell CDK activity may be sufficient to meet the activity threshold at the SPB. Thus, according to this model, SPB localisation of Cdc13 is essential for mitotic entry in a normal cell cycle, and only becomes dispensable in conditions of increased cyclin-CDK activity.

Another prediction of the localisation model is that SPB-localised Cdc13-Cdc2 provides activity in the cytoplasm as well as the SPB. To investigate this, future work will ask whether restoring the SPB localisation of $Cdc13^{HPM}$-Cdc2 restores CDK substrate phosphorylation at the cytoplasm as well as the SPB. This will be done by using the Spo15 antibody immunofluorescence protocol developed in Chapter 6. Spo15-S121 is a hydrophobic patch-dependent substrate, only being phosphorylated by $Cdc13^{HPM}$-Cdc2 to roughly 40 % of wild-type phosphorylation levels (Basu et al., 2020). As Spo15 phosphorylation can be detected both at the SPB and throughout the cell by immunofluorescence, this technique can be used to test whether Spo15 phosphorylation at the SPB and cytoplasm is restored in the SPB-tethering experiment described in Section 5.4.

To further understand the role and importance of the hydrophobic patch it is also worth considering the arrest point of $Cdc13^{HPM}$. Whilst work in this thesis demonstrates that $Cdc13^{HPM}$ arrests before the hydrophobic patch-independent localisation of $Cdc13^{HPM}$ to the SPB, and before SPB separation can be detected, phosphoproteomics carried out in (Basu et al., 2020) suggests that nuclear-localised mitotic substrates are phosphorylated to similar levels by $Cdc13^{HPM}$- and $Cdc13^{WT}$-bound Cdc2. This raises the question of how $Cdc13^{HPM}$-Cdc2 reaches the activity levels necessary to phosphorylate these substrates. The Cdc2 Y15 phosphorylation state in cells driven by $Cdc13^{HPM}$ has not yet been assessed. If Cdc2 Y15 is not dephosphorylated, it would suggest that nuclear mitotic substrates do not need Cdc2 Y15 dephosphorylation and feedback loop activation in order to be phosphorylated, raising the question of how their phosphorylation is temporally restricted to mitosis. If Cdc2 Y15 is dephosphorylated, it would indicate that $Cdc13^{HPM}$ can carry out some events considered to be mitotic and would suggest that SPB localisation is not necessary for Cdc2 Y15 dephosphorylation. The

reduction in cell length when cells are driven by the Cdc13^{HPM}-L-Cdc2(as)^{AF} fusion rather than the Cdc13^{HPM}-L-Cdc2(as) fusion may suggest that it is more likely that Cdc2 Y15 is not dephosphorylated when cells are driven by Cdc13^{HPM} (Figure 5.3.4).

7.3.2 What might be the essential roles of Cdc13-Cdc2 at the SPB?

The suggestion that CDK activity at the SPB is essential for mitotic entry raises the question of what essential function(s) Cdc13-Cdc2 is carrying out at the SPB. It is possible that Cdc2 activity at the SPB is needed to phosphorylate substrates localised at the SPB, or locally activate other mitotic regulators that may be necessary for major mitotic events at the SPB such as SPB insertion, SPB activation and/or mitotic spindle assembly. It is also possible that SPB localisation is necessary to concentrate enough Cdc2 to overcome the inhibitory action of Wee1 and phosphatases, and/or recruit activators such as Plo1, to initiate feedback loop amplification resulting in global activation of Cdc2 via Y15 dephosphorylation.

It has been suggested that the SPB may be the site at which the mitotic entry switch is initiated (Grallert et al., 2013b, Hagan and Grallert, 2013), consistent with the observation that the first detectable active population of Cyclin B1-Cdk1 in human cells is at the centrosome (Jackman et al., 2003). Therefore, Cdc2 localisation to the SPB may be essential in order to trigger Cdc2 Y15 dephosphorylation and mitotic commitment. If this were the only essential function of the hydrophobic patch, the mitotic defect of Cdc13^{HPM} should be rescued in a Cdc2^{AF} background (where Cdc2 cannot be phosphorylated on T14 or Y15). The reduction in cell length in cells driven by Cdc13^{HPM}-L-Cdc2(as)^{AF} when compared to those driven by Cdc13^{HPM}-L-Cdc2(as) suggests that some defects of Cdc13^{HPM} may be reduced in the context of Cdc2 Y15 dephosphorylation, though it does not provide a full rescue in these preliminary experiments. However, this would be an interesting area for further study.

In addition to this, Cdc2 activity at the SPB may be needed for SPB insertion. Global Cdc2 inactivation prevents Plo1 association with SPBs (Grallert et al., 2013b), so it is possible that Cdc2 activity at the SPB specifically is needed for Plo1 SPB recruitment. The mutant of the SPB component Cut12, *cut12.1*, exhibits enhanced Dis2 (PP1 catalytic subunit) binding to Cut12 and a failure to activate and properly insert one SPB into the nuclear envelope (Bridge et al., 1998, Tallada et al., 2009, Grallert et al., 2013a). Dis2 binding to the SPB influences Plo1 recruitment to the SPB, indicating that the defect in *cut12.1* may be a result of reduced Plo1 activation and Cdc2 activity at the SPB (Tallada et al., 2009, Grallert et al., 2013a). Thus, the SPB insertion defect of *cut12.1* mutants is proposed to be due to an inability to reach the threshold Cdc2 activity at the SPB needed for SPB insertion (Tallada et al., 2009). Supporting this, overproducing Cdc25 can rescue the monopolar spindle defect of *cut12.1* (Tallada et al., 2007). These data strongly suggest that Cdc2 activity at the SPB is important for SPB insertion.

Therefore, SPB insertion and activation of the feedback loops that drive mitotic commitment are both possible essential functions of Cdc13-Cdc2 activity at the SPB.

7.3.3 Importance of substrate specific docking via the hydrophobic patch

Whilst restoring Cdc13^{HPM}-Cdc2 SPB localisation promoted a wave of mitotic entry, it also promoted an accumulation of cells with aberrant divisions. These aberrant divisions included the cut phenotype (where a septum bisects the nucleus/nuclei), multiseptate cells, and cells with one nucleus one side of a septum. One possibility for these aberrant divisions is that general substrate specific docking mediated by the Cdc13 hydrophobic patch (in addition to SPB docking) is necessary for normal mitotic progression and mitotic exit. It is also possible that the experimental system used with artificial tethering of Cdc2 to the SPB component Cut12 resulted in altered CDK signalling at the SPB in comparison to wild-type unperturbed cells, which could affect signalling important for the SIN. Furthermore, it is possible that the long cell lengths at the time of 1-NmPP1 wash-out generated by the

experimental procedure contribute to some of the aberrant divisions seen (discussed in section 5.5). It is therefore not clear what causes the observed defects in mitotic division in this experiment, and it remains a possibility that hydrophobic patch mediated substrate docking is necessary for full mitotic progression.

The other major outputs of this thesis were the observation that Cdc13^{HPM}-sfGFP localises to the SPB after Plo1 SPB localisation, and the development of a system that may be used to measure Cdc2 substrate phosphorylation in different subcellular locations. These are discussed in the next sections.

7.4 Hydrophobic patch-independent localisation of Cdc13

One of the findings from this work is that Cdc13^{HPM}-sfGFP accumulates at the SPB independently of the hydrophobic patch, after Polo kinase localisation to the SPB, if there is a wild-type copy of Cdc13 in cells. An acceleration of Cdc13^{HPM}-sfGFP SPB localisation is observed in mutants of *cut12* (including *cut12.s11*) or *plo1* that accelerate Plo1 localisation to the SPB, and there is a lack of Cdc13^{HPM}-sfGFP SPB localisation in a *plo1-24C* mutant at restrictive temperature (Basu et al., 2020). This suggests that Cdc13^{HPM}-sfGFP localisation is downstream and possibly dependent on Plo1 activity at the SPB. The antibody MPM2, which recognises phosphorylated epitope(s) at the SPB dependent on Plo1 activity, stains the SPB early in the *cut12.s11* mutants, suggesting that the Plo1 recruited to the SPB is active (MacIver et al., 2003).

Given that an acceleration of Plo1 activity at the SPB also accelerates Cdc13^{HPM}-sfGFP SPB localisation, considering Plo1 activities at the SPB would be a logical starting point when considering the mechanism of Cdc13^{HPM}-sfGFP SPB localisation. Polo kinase plays a key role in multiple signalling pathways at the SPB in late G2/early mitosis. As discussed in the Introduction, one major role of Plo1 at the SPB is in mitotic commitment, being involved in the feedback loops that act on Cdc2 Y15 dephosphorylation. Another key role of Polo kinase is in SPB maturation. Plo1 is required for the increased incorporation of some SPB components prior to mitosis, and for the redistribution of some SPB components that is seen before SPB insertion, suggesting that Plo1 recruitment to the SPB precedes SPB remodelling (Walde and King, 2014, Bestul et al., 2021). Furthermore, perturbing Plo1 recruitment to the SPB has been linked to defects in SPB insertion. Temperature-sensitive mutants in two SPB components, *cut12.1* and *pcp1-18*, are defective in Plo1 recruitment to the SPB, and in SPB insertion (Fong et al., 2010, MacIver et al., 2003, Tallada et al., 2009). Therefore, Plo1 signalling at the SPB in G2/M is important for SPB remodelling, SPB insertion, and mitotic commitment.

7.4.1 How might Polo kinase activity at the SPB influence Cdc13 SPB recruitment?

Given the wide range of roles Plo1 has been reported to have at the SPB at G2/M, it is not immediately clear exactly how Polo activity might influence $Cdc13^{HPM}$ localisation to the SPB in mitosis. One possibility is that $Cdc13^{HPM}$ localisation is driven by Plo1-dependent SPB remodelling at mitotic entry; perhaps this remodelling recruits a binding partner of $Cdc13^{HPM}$-Cdc2 that was not previously enriched at the SPB. For example, Cut11 and Brr6 both transiently associate with the SPB at mitosis demonstrating that some proteins are recruited to the SPB specifically at mitosis (West et al., 1998, Tamm et al., 2011, Walde and King, 2014). It is also possible that SPB remodelling could drive a structural change that exposes a new epitope on an existing SPB component that can then be bound by $Cdc13^{HPM}$-Cdc2.

It could also be that Plo1 phosphorylation of a substrate at the SPB promotes $Cdc13^{HPM}$ localisation. CDK is known to associate with the accessory factor Suc1 (Cks1 and Cks2 in human cells), which contains a phospho-binding pocket that mediates Suc1 binding with phosphorylated residues (Arvai et al., 1995). It is possible that $Cdc13^{HPM}$-Cdc2-Suc1 is able to bind a phosphorylated epitope at the SPB. However the consensus binding motif identified for budding yeast Cks1 is Φ-X-pT-P, where Φ denotes a hydrophobic amino acid (McGrath et al., 2013). The strong requirement for a proline at the +1 position for Cks1 binding contrasts with the observation that Plk1 does not phosphorylate (S/T)P sites well (Santamaria et al., 2011), reducing the likelihood that Suc1 is binding to a Plo1 phosphosite at the SPB. There has also been a phosphate binding pocket recently identified in a region of Cyclin B1 that is conserved with Cdc13, which could conceivably bind to a phosphosite on the SPB (Yu et al., 2021).

Plo1 is also involved in SPB insertion, and it is possible that SPB insertion could be affecting Cdc13 accumulation at the SPB. Before SPB insertion, the SPB is cytoplasmic, with the nuclear face of the SPB adjacent to the nuclear envelope. After insertion, the nuclear face of the SPB is exposed to the nucleus, which could result in the exposure of previously inaccessible Cdc13-Cdc2-Suc1 binding sites,

and therefore hydrophobic patch-independent accumulation of Cdc13 to the SPB. It has also been proposed that there is an alteration in the nuclear membrane adjacent to the SPB after Plo1 SPB recruitment and prior to SPB insertion, which is suggested to make the nuclear face of the SPB accessible to Wee1 (Masuda et al., 2011). Such a mechanism could also potentially explain Cdc13^{HPM} SPB recruitment.

As Plo1 is thought to be involved in the activation of Cdc2, it could also be considered that locally activated Cdc2 is able to accumulate at the SPB independently of the hydrophobic patch. For example, this may be able to occur if activated Cdc2 drives phosphorylation of an SPB component or a structural change in the SPB that allows the Cdc13^{HPM}-Cdc2-Suc1 complex to bind. The Y15 phosphorylation state of Cdc2 at the SPB after Plo1 early recruitment to the SPB in *cut12.s11* cells has not been directly measured. However, the observation that the Plo1 that is recruited to the SPB is active has led to the proposal that there is local activation of the feedback loops that result in Cdc2 Y15 dephosphorylation at the SPB (Grallert et al., 2013b). It is therefore possible that Cdc13^{HPM}-sfGFP may be able to accumulate at the SPB due to Cdc2 Y15 dephosphorylation; this could be tested by investigating the G2 localisation of Cdc13^{HPM} in cells with Cdc2^{AF}. In human cells, activation of Cyclin B1-Cdk1 is coincident with its nuclear import. It is contested whether this import is due to phosphorylation of Cyclin B1 or changes in nuclear import machinery, but regardless of the mechanism involved it is clear that activating Cyclin B1-Cdk1 is linked to its redistribution (Hagting et al., 1999, Gavet and Pines, 2010a, Santos et al., 2012). Thus it is worth considering that the activation of Cdc13-Cdc2 triggers its accumulation at the SPB.

7.4.2 What is the role of the hydrophobic patch independent mechanism of Cdc13 SPB accumulation in late G2/mitosis?

It is not clear why there is a hydrophobic patch-independent mechanism of Cdc13 SPB accumulation in late G2/mitosis, but the results from this thesis suggest that it is not conserved in human Cyclin B1. This difference in Cdc13 and Cyclin B1 localisation regulation could reflect the difference in architecture of the SPB and

centrosome. Whilst these components are functionally equivalent they differ in structure, with the centrosome consisting of a pair of centrioles surrounded by a pericentriolar matrix (PCM), whilst the SPB is a laminar structure that does not contain centrioles (Bornens, 2002, Bestul et al., 2017).

This difference in Cdc13 and Cyclin B1 regulation could also be due to differences in events during mitosis. Human cells perform an open mitosis, with the nuclear envelope breaking down early in mitosis, whereas the nuclear envelope remains predominantly intact in the *S. pombe* closed mitosis. Perhaps these different approaches to mitosis result in different requirements for Cdc13/Cyclin B1 localisation.

It could also be due to differences in the regulation of mitotic entry; whilst this regulation is broadly similar, certain aspects of Cdc13 and Cyclin B1 regulation differ. For example, Cyclin B1 is predominantly cytoplasmic in interphase, and its abrupt nuclear import at the start of mitosis is part of a spatial positive feedback loop that has been proposed to contribute to a switch-like entry into mitosis (Santos et al., 2012). In contrast, Cdc13 accumulates in the nucleus throughout G2 (Decottignies et al., 2001). Given that the activation of Cdc13-Cdc2 has been suggested to initiate at the SPB (Grallert et al., 2013b), perhaps the mitosis-specific hydrophobic patch-independent accumulation of Cdc13 at the SPB could play a similar role to nuclear accumulation of Cyclin B1 in human cells, by acting as a mechanism to ensure that there is rapid activation of bulk Cdc13-Cdc2 at mitotic entry.

Another possible role for the mitotic hydrophobic patch-independent accumulation of Cdc13 at the SPB could be to concentrate Cdc13-Cdc2 in proximity to SPB substrates which generally require high levels of CDK activity in order to be phosphorylated (Basu et al., 2020, Swaffer et al., 2016). It is not known if centrosomal substrates in human cells require relatively high levels of Cyclin B1-Cdk1 activity in order to be phosphorylated; if not, this could explain why human Cyclin B1 does not have a mitotic, hydrophobic patch-independent mechanism of accumulation at the centrosome.

Identifying the mechanism for the hydrophobic patch-independent localisation of Cdc13, and perturbing this localisation, would be an interesting area for further study to understand what role this localisation might play in *S. pombe*. This would also provide insight on whether this localisation fulfils a role that is also involved in cell cycle regulation in more complex eukaryotes, such as spatial positive feedback, albeit by a different mechanism.

It should also be considered whether the hydrophobic-patch independent localisation to the SPB is possibly conserved in cyclins in other yeasts such as *S. cerevisiae*. *S. pombe* and *S. cerevisiae* share certain biological processes that they do not share with human cells, such as a closed mitosis and therefore SPB insertion. It therefore might be expected that if the hydrophobic patch-independent localisation of Cdc13 to the SPB involves a structure or process that is conserved between the two yeasts, that this mechanism of cyclin localisation may also be conserved. As discussed above, *S. cerevisiae* Clb2 does not require its hydrophobic patch for localisation to the SPB (Bailly et al., 2003). There is therefore a hydrophobic patch-independent mechanism for Clb2 localisation to the SPB, and it is possible that it is by the same mechanism as Cdc13^{HPM}-sfGFP localisation. Whilst the Clb2^{HPM} SPB localisation was not reported to be restricted to mitosis, the difference in timings in SPB insertion and spindle formation between the organisms, occurring at G2/M in *S. pombe* and S-phase in *S. cerevisiae*, could explain the difference in the timing of cyclin SPB localisation by this mechanism.

7.5 The role of localisation in substrate sensitivity to CDK activity

One of the key remaining questions in cell cycle control is how CDK can temporally order substrate phosphorylation to ensure that the key physiological processes involved in the cell division cycle occur in the correct sequence. *S. pombe* provides an ideal system in which to study this, and the finding that cell cycle events and CDK substrate phosphorylation can both be ordered by the increasing global activity of a single cyclin-CDK complex, that has a large dynamic range of activity, refines this question to how a wide range of substrate sensitivities to CDK activity can be generated (Fisher and Nurse, 1996, Coudreuse and Nurse, 2010, Swaffer et al., 2016). There are a number of factors that may influence substrate sensitivity to CDK activity, including cyclin docking regions (such as the cyclin hydrophobic patch), accessory factors that bind CDK (e.g. Suc1), phosphatase substrate specificity and sensitivity, and substrate localisation. The activity model developed to explain these observations, whereby increasing CDK activity drives ordered substrate phosphorylation and cell cycle progression, considers CDK activity in the whole cell. There is still an open question as to how the spatial regulation of CDK activity fits into this model. It is worth noting that when ‘CDK activity’ is referred to in this situation, it is the net balance of CDK activity and phosphatase activity, as the measure of CDK activity used is substrate phosphorylation.

It has been observed that substrate sensitivity to a CDK inhibitor is correlated with localisation, raising the possibility that substrate sensitivity to global CDK activity may be influenced by its cellular localisation (Basu et al., 2020, Swaffer et al., 2016). The localisation of many cell cycle regulators is clearly not homogenous throughout the cell, and therefore this raises the possibility that different subcellular locations experience different levels of CDK activity. Substrate phosphorylation in any given location will be affected by both CDK and phosphatase activities, and intrinsic CDK activity itself could be influenced by other cell cycle regulators. Supporting the theory that CDK activity may not be homogenous throughout the cell, in human cells, Cdk1 activity is higher in the nucleus than in the cytoplasm (Santos et al., 2012).

It is interesting that the substrates with the lowest IC_{50} values (i.e. those that required lower amounts of the Shokat CDK inhibitor in order to be dephosphorylated to 50 % of their mitotic levels) were those localised to the SPB, despite the SPB having a high local concentration of Cdc13-Cdc2 (Basu et al., 2020, Swaffer et al., 2016). In general, SPB substrates had the lowest IC_{50} values, followed by cytoplasmic substrates, followed by nuclear substrates. It is worth considering that if inhibitor concentration is homogenous throughout the cell, different subcellular populations of Cdc2 would experience different local ratios of Cdc2 to inhibitor. However, if this were to explain the observed difference in sensitivity of these substrates to CDK inhibitor, it would be expected that cytoplasmic substrates would require the least inhibitor to reduce phosphorylation, with SPB substrates requiring high levels of inhibitor (and therefore having high IC_{50} values), as Cdc2 is more highly concentrated at the SPB than the cytoplasm. Given that the observed sensitivity to CDK inhibitor of SPB substrates is the opposite of what would be expected, with SPB substrates sensitive to low levels of inhibitor, the difference in distribution of Cdc2 and its inhibitor cannot explain all of the observed differences in CDK substrate sensitivities. This supports the view that there might be different CDK activity levels in different subcellular locations. It cannot simply be down to local concentration of Cdc2, as this would also result in high levels of inhibitor being required for SPB substrate dephosphorylation. However, it could be down to the local balance of Cdc2, its activators such as Cdc25 and Plo1, and regulators that counteract CDK activity such as Wee1 and phosphatases. As these regulators change localisation through the cell cycle, the balance of CDK activity level across different subcellular locations may alter. For example, Dis2 (PP1) localisation to the SPB may result in low CDK activity at the SPB in early G2, but Dis2 eviction and subsequent Plo1 recruitment to the SPB late in G2 may result in a local net CDK activity increase at the SPB that is higher than the whole-cell net CDK activity increase in G2.

If it is true that CDK activity varies across subcellular locations, it might be observed that the same substrate is phosphorylated at different times, or at different rates, when in different subcellular locations. The work in this thesis has described the development of an experimental system that will be tested for use in

measuring CDK substrate phosphorylation in different subcellular locations. The Spo15 immunofluorescence protocol described here will be used in future work to test if SPB-localised and non-SPB-localised Spo15 phosphorylation dynamics can be measured and compared. As Spo15 can be detected at the SPB and throughout the cell, this can be done without relocalising Spo15, and allows us to compare the different subpopulations of Spo15 in the cell. It has not yet been assessed if the immunofluorescence with the Spo15 antibody will give robust enough measurements to be able to compare phosphorylation across multiple samples, but if it does, this system could be a valuable tool to provide spatial information of substrate phosphorylation. For example, it could be used to measure Spo15 phosphorylation in cultures released from a G2 arrest, to track phosphorylation of different subcellular populations over time. Furthermore, both the Spo15 and Bqt4 antibodies can be tested for use in Western blotting with the substrates re-localised to different cellular compartments. If successful, these experiments would allow us to test whether the phosphorylation dynamics of these substrates is affected by their localisation.

7.6 Concluding remarks

The cell cycle is one of the most fundamental processes in eukaryotic biology. It has long been appreciated that the temporal control of CDK signalling is highly regulated and critical for cell cycle progression but, more recently, increasing evidence has shown that the spatial regulation of CDK signalling is also crucial in cell cycle control. The work in this thesis contributes to this existing body of work in supporting the view that cyclin-CDK localisation to the SPB plays a critical role in mitotic entry.

The main open questions following on from this work are whether restoring $Cdc13^{HPM}$-Cdc2 localisation restores SPB and cytoplasmic substrate phosphorylation, and whether cyclin-substrate specific docking is essential for mitotic progression and exit. It is also important to determine whether the importance of cyclin hydrophobic patch-mediated localisation to the SPB and centrosome proposed here is conserved in other eukaryotes. Further work will be required to understand the dynamics of CDK activity in different subcellular locations, including whether CDK activity is higher in certain subcellular locations, and whether localisation affects substrate sensitivity to CDK activity.

Chapter 8. Appendix

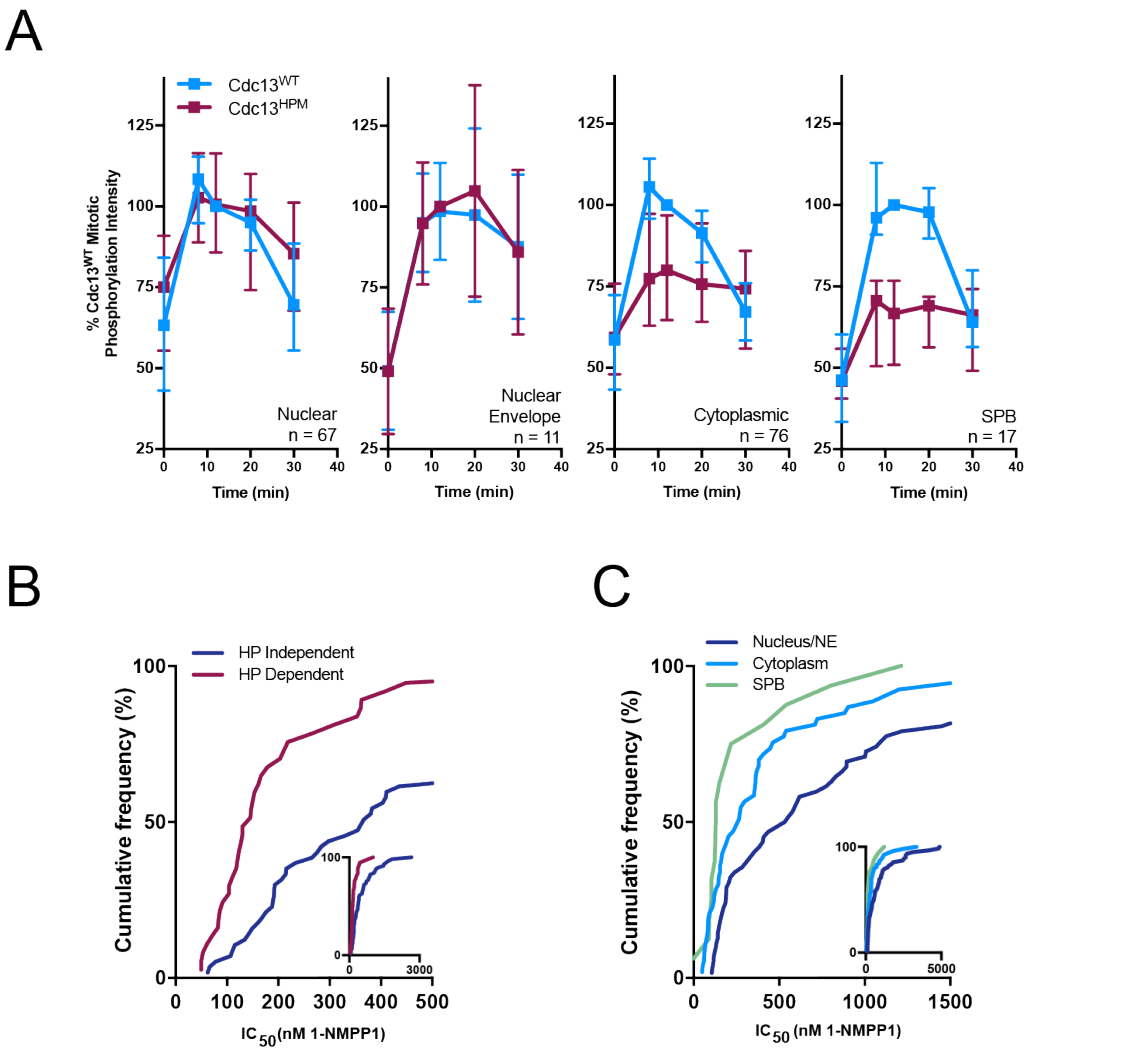


Figure 8.1 | Identification of phosphosites dependent on the Cdc13 hydrophobic patch

Experiments and analysis carried out by Souradeep Basu and Andrew Jones; figure reproduced with permission from the authors (Basu et al., 2020).
Cells expressing wild-type *cdc13* under the thiamine-repressible *nmt41* promoter, and *cdc2(as)-M17 cig1Δ cig2Δ* and an exogenous copy of either $cdc13^{WT}$ or $cdc13^{HPM}$ were arrested in G2 by addition of 1 μM 1-NmPP1. Thiamine was added to the culture (and kept in the media in all subsequent steps) to repress transcription of wild-type *cdc13* and cells were released into mitosis resulting in the degradation of the Cdc13 protein. After progression through S phase cells were once again arrested in G2, and upon 1-NmPP1 wash-out were released into mitosis with expression of only the exogenous copy of Cdc13. Samples for phosphoproteomics were taken at 0, 8, 12, 20 and 30 minutes after release from

G2 arrest. For $Cdc13^{WT}$, t = 12 is taken as the peak mitotic time point in this experiment.
A: Phosphorylation of CDK mitotic phosphosites in different subcellular locations. Phosphosite phosphorylation was normalised to t = 12 for $Cdc13^{WT}$, and the median plotted with error bars representing interquartile range.
B: Cumulative frequency of average phosphosite IC_{50} to NmPP1 inhibition for hydrophobic patch (HP) dependent and independent sites. Sites were classed as HP-dependent if in the $Cdc13^{HPM}$ condition they were not phosphorylated to at least the level in the $Cdc13^{WT}$ t = 12 time point. Site IC_{50} data is from (Swaffer et al., 2016). Inset shows entire range of data. One data point is beyond axis limits but is included in statistical analysis. Mann-Whitney rank comparison $p < 0.0001$.
C: Cumulative frequency of average phosphosite IC_{50} to NmPP1 inhibition for all CDK substrates localised to the nucleus/nuclear envelope, cytoplasm and SPB. Inset shows full range of data. 3 data points are beyond axis limits but included in statistical analysis. Nucleus/NE vs cytoplasm difference $p < 0.01$. Difference between nucleus/NE and SPB < 0.001 (Mann-Whitney rank comparison).

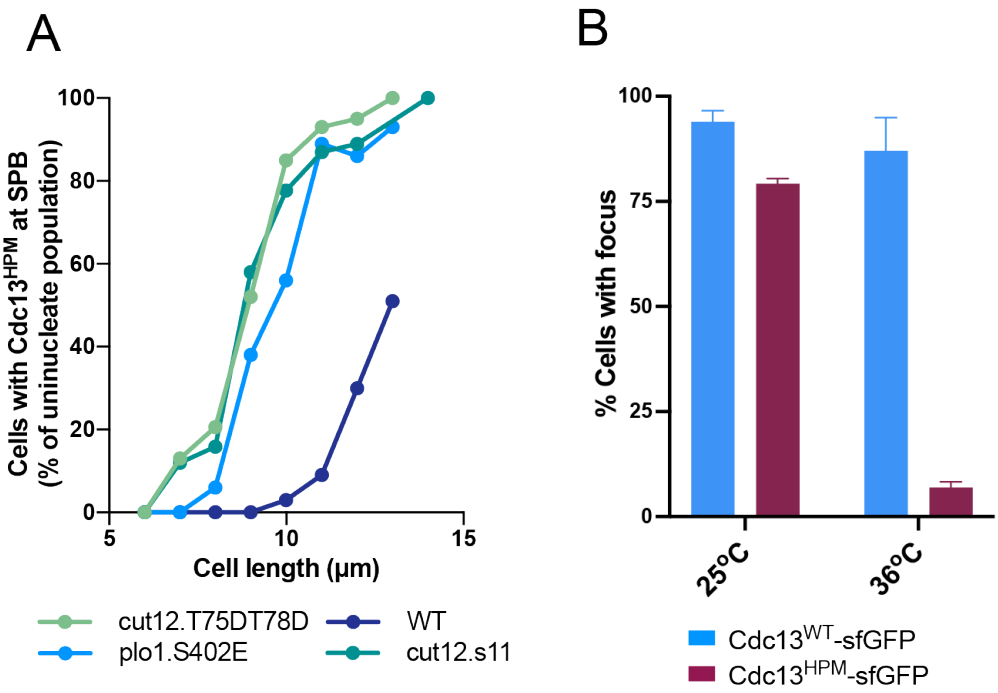


Figure 8.2 | Cdc13^{HPM}-sfGFP SPB localisation is downstream of Plo1 SPB localisation

Experiments performed by Souradeep Basu, figure reproduced with permission from the author (Basu et al., 2020).
A: Uninucleate cells were scored for Cdc13^{HPM}-sfGFP foci compared to cell length in an otherwise wild-type strain background, or strains in which Plo1 localisation to the SPB is accelerated (*cut12.s11, cut12.T75DT78D, plo1.S402E*). Data from 3 replicates was pooled and sorted into 1 µm bins. N > 100 cells per strain per replicate.
B: Cells with *cdc2(as)-M17 plo1-24C* and an exogenous copy of Cdc13$^{WT/HPM}$-sfGFP were arrested in G2 by addition of 1 µM 1-NmPP1 for 3.5 hours, and either kept at 25 °C for the whole block, or shifted to the restrictive temperature of 36 °C 90 minutes before 1-NmPP1 was washed out. 1-NmPP1 was removed to release cells into mitosis, and cells were imaged after 6 minutes. Graph shows the percentage of cells with Cdc13-sfGFP foci. Mean and SD of 3 replicates are shown, with n > 75 cells per replicate per strain.

Reference List

ABRIEU, A., BRASSAC, T., GALAS, S., FISHER, D., LABBE, J. C. & DOREE, M. 1998. The Polo-like kinase Plx1 is a component of the MPF amplification loop at the G2/M-phase transition of the cell cycle in Xenopus eggs. *J Cell Sci,* 111 (Pt 12)**,** 1751-7.

AFANZAR, O., BUSS, G. K., STEARNS, T. & FERRELL, J. E., JR. 2020. The nucleus serves as the pacemaker for the cell cycle. *Elife,* 9.

ALFA, C. E., BOOHER, R., BEACH, D. & HYAMS, J. S. 1989. Fission yeast cyclin: subcellular localisation and cell cycle regulation. *J Cell Sci Suppl,* 12**,** 9-19.

ALFA, C. E., DUCOMMUN, B., BEACH, D. & HYAMS, J. S. 1990. Distinct nuclear and spindle pole body population of cyclin-cdc2 in fission yeast. *Nature,* 347**,** 680-2.

ALLARD, C. A. H., OPALKO, H. E., LIU, K. W., MEDOH, U. & MOSELEY, J. B. 2018. Cell size-dependent regulation of Wee1 localization by Cdr2 cortical nodes. *J Cell Biol,* 217**,** 1589-1599.

AOI, Y., KAWASHIMA, S. A., SIMANIS, V., YAMAMOTO, M. & SATO, M. 2014. Optimization of the analogue-sensitive Cdc2/Cdk1 mutant by in vivo selection eliminates physiological limitations to its use in cell cycle analysis. *Open Biol,* 4.

APRELIKOVA, O., XIONG, Y. & LIU, E. T. 1995. Both p16 and p21 families of cyclin-dependent kinase (CDK) inhibitors block the phosphorylation of cyclin-dependent kinases by the CDK-activating kinase. *J Biol Chem,* 270**,** 18195-7.

ARQUINT, C., GABRYJONCZYK, A. M. & NIGG, E. A. 2014. Centrosomes as signalling centres. *Philos Trans R Soc Lond B Biol Sci,* 369.

ARVAI, A. S., BOURNE, Y., HICKEY, M. J. & TAINER, J. A. 1995. Crystal structure of the human cell cycle protein CksHs1: single domain fold with similarity to kinase N-lobe domain. *J Mol Biol,* 249**,** 835-42.

ASFAHA, J. B., ORD, M., CARLSON, C. R., FAUSTOVA, I., LOOG, M. & MORGAN, D. O. 2022. Multisite phosphorylation by Cdk1 initiates delayed negative feedback to control mitotic transcription. *Curr Biol,* 32**,** 256-263 e4.

BAHLER, J. & PRINGLE, J. R. 1998. Pom1p, a fission yeast protein kinase that provides positional information for both polarized growth and cytokinesis. *Genes Dev,* 12**,** 1356-70.

BAHLER, J., STEEVER, A. B., WHEATLEY, S., WANG, Y., PRINGLE, J. R., GOULD, K. L. & MCCOLLUM, D. 1998. Role of polo kinase and Mid1p in determining the site of cell division in fission yeast. *J Cell Biol,* 143**,** 1603-16.

BAILLY, E., CABANTOUS, S., SONDAZ, D., BERNADAC, A. & SIMON, M. N. 2003. Differential cellular localization among mitotic cyclins from Saccharomyces cerevisiae: a new role for the axial budding protein Bud3 in targeting Clb2 to the mother-bud neck. *J Cell Sci,* 116**,** 4119-30.

BAILLY, E., DOREE, M., NURSE, P. & BORNENS, M. 1989. p34cdc2 is located in both nucleus and cytoplasm; part is centrosomally associated at G2/M and enters vesicles at anaphase. *EMBO J,* 8**,** 3985-95.

BALDIN, V. & DUCOMMUN, B. 1995. Subcellular localisation of human wee1 kinase is regulated during the cell cycle. *J Cell Sci,* 108 (Pt 6)**,** 2425-32.

BALDIN, V., LUKAS, J., MARCOTE, M. J., PAGANO, M. & DRAETTA, G. 1993. Cyclin D1 is a nuclear protein required for cell cycle progression in G1. *Genes Dev,* 7**,** 812-21.

BARBERIS, M., DE GIOIA, L., RUZZENE, M., SARNO, S., COCCETTI, P., FANTUCCI, P., VANONI, M. & ALBERGHINA, L. 2005. The yeast cyclin-dependent kinase inhibitor Sic1 and mammalian p27Kip1 are functional homologues with a structurally conserved inhibitory domain. *Biochem J,* 387**,** 639-47.

BARDIN, A. J. & AMON, A. 2001. Men and sin: what's the difference? *Nat Rev Mol Cell Biol,* 2**,** 815-26.

BARR, A. R., HELDT, F. S., ZHANG, T., BAKAL, C. & NOVAK, B. 2016. A Dynamical Framework for the All-or-None G1/S Transition. *Cell Syst,* 2**,** 27-37.

BARTHOLOMEW, C. R., WOO, S. H., CHUNG, Y. S., JONES, C. & HARDY, C. F. 2001. Cdc5 interacts with the Wee1 kinase in budding yeast. *Mol Cell Biol,* 21**,** 4949-59.

BASTO, R., LAU, J., VINOGRADOVA, T., GARDIOL, A., WOODS, C. G., KHODJAKOV, A. & RAFF, J. W. 2006. Flies without centrioles. *Cell,* 125**,** 1375-86.

BASU, S., JONES, A. W. & NURSE, P. 2021. Core Control Principles of the Eukaryotic Cell Cycle. *Nature Portfolio*.

BASU, S., ROBERTS, E. L., JONES, A. W., SWAFFER, M. P., SNIJDERS, A. P. & NURSE, P. 2020. The Hydrophobic Patch Directs Cyclin B to Centrosomes to Promote Global CDK Phosphorylation at Mitosis. *Curr Biol,* 30**,** 883-892 e4.

BENTLEY, A. M., NORMAND, G., HOYT, J. & KING, R. W. 2007. Distinct sequence elements of cyclin B1 promote localization to chromatin, centrosomes, and kinetochores during mitosis. *Mol Biol Cell,* 18**,** 4847-58.

BERG, S., KUTRA, D., KROEGER, T., STRAEHLE, C. N., KAUSLER, B. X., HAUBOLD, C., SCHIEGG, M., ALES, J., BEIER, T., RUDY, M., EREN, K., CERVANTES, J. I., XU, B., BEUTTENMUELLER, F., WOLNY, A., ZHANG, C., KOETHE, U., HAMPRECHT, F. A. & KRESHUK, A. 2019. ilastik: interactive machine learning for (bio)image analysis. *Nat Methods,* 16**,** 1226-1232.

BESSON, A., DOWDY, S. F. & ROBERTS, J. M. 2008. CDK inhibitors: cell cycle regulators and beyond. *Dev Cell,* 14**,** 159-69.

BESTUL, A. J., YU, Z., UNRUH, J. R. & JASPERSEN, S. L. 2017. Molecular model of fission yeast centrosome assembly determined by superresolution imaging. *J Cell Biol,* 216**,** 2409-2424.

BESTUL, A. J., YU, Z., UNRUH, J. R. & JASPERSEN, S. L. 2021. Redistribution of centrosomal proteins by centromeres and Polo kinase controls partial nuclear envelope breakdown in fission yeast. *Mol Biol Cell,* 32**,** 1487-1500.

BHADURI, S., VALK, E., WINTERS, M. J., GRUESSNER, B., LOOG, M. & PRYCIAK, P. M. 2015. A docking interface in the cyclin Cln2 promotes multi-site phosphorylation of substrates and timely cell-cycle entry. *Curr Biol,* 25**,** 316-325.

BISHOP, A. C., UBERSAX, J. A., PETSCH, D. T., MATHEOS, D. P., GRAY, N. S., BLETHROW, J., SHIMIZU, E., TSIEN, J. Z., SCHULTZ, P. G., ROSE, M. D., WOOD, J. L., MORGAN, D. O. & SHOKAT, K. M. 2000. A chemical switch for inhibitor-sensitive alleles of any protein kinase. *Nature,* 407**,** 395-401.

BOOHER, R. & BEACH, D. 1988. Involvement of cdc13+ in mitotic control in Schizosaccharomyces pombe: possible interaction of the gene product with microtubules. *EMBO J,* 7**,** 2321-7.

BOOHER, R. N., ALFA, C. E., HYAMS, J. S. & BEACH, D. H. 1989. The fission yeast cdc2/cdc13/suc1 protein kinase: regulation of catalytic activity and nuclear localization. *Cell,* 58**,** 485-97.

BOOHER, R. N., HOLMAN, P. S. & FATTAEY, A. 1997. Human Myt1 is a cell cycle-regulated kinase that inhibits Cdc2 but not Cdk2 activity. *J Biol Chem,* 272**,** 22300-6.

BORNENS, M. 2002. Centrosome composition and microtubule anchoring mechanisms. *Curr Opin Cell Biol,* 14**,** 25-34.

BOURNE, Y., WATSON, M. H., HICKEY, M. J., HOLMES, W., ROCQUE, W., REED, S. I. & TAINER, J. A. 1996. Crystal structure and mutational analysis of the human CDK2 kinase complex with cell cycle-regulatory protein CksHs1. *Cell,* 84**,** 863-74.

BRIDGE, A. J., MORPHEW, M., BARTLETT, R. & HAGAN, I. M. 1998. The fission yeast SPB component Cut12 links bipolar spindle formation to mitotic control. *Genes Dev,* 12**,** 927-42.

BRIZUELA, L., DRAETTA, G. & BEACH, D. 1987. p13suc1 acts in the fission yeast cell division cycle as a component of the p34cdc2 protein kinase. *EMBO J,* 6**,** 3507-14.

BUCK, V., RUSSELL, P. & MILLAR, J. B. 1995. Identification of a cdk-activating kinase in fission yeast. *EMBO J,* 14**,** 6173-83.

CASTILHO, P. V., WILLIAMS, B. C., MOCHIDA, S., ZHAO, Y. & GOLDBERG, M. L. 2009. The M phase kinase Greatwall (Gwl) promotes inactivation of PP2A/B55delta, a phosphatase directed against CDK phosphosites. *Mol Biol Cell,* 20**,** 4777-89.

CHAN, K. Y., ALONSO-NUNEZ, M., GRALLERT, A., TANAKA, K., CONNOLLY, Y., SMITH, D. L. & HAGAN, I. M. 2017. Dialogue between centrosomal entrance and exit scaffold pathways regulates mitotic commitment. *J Cell Biol,* 216**,** 2795-2812.

CHANG, F. & HERSKOWITZ, I. 1990. Identification of a gene necessary for cell cycle arrest by a negative growth factor of yeast: FAR1 is an inhibitor of a G1 cyclin, CLN2. *Cell,* 63**,** 999-1011.

CHANG, Y. L., TSENG, S. F., HUANG, Y. C., SHEN, Z. J., HSU, P. H., HSIEH, M. H., YANG, C. W., TOGNETTI, S., CANAL, B., SUBIRANA, L., WANG, C. W., CHEN, H. T., LIN, C. Y., POSAS, F. & TENG, S. C. 2017. Yeast Cip1 is activated by environmental stress to inhibit Cdk1-G1 cyclins via Mcm1 and Msn2/4. *Nat Commun,* 8**,** 56.

CHEN, Y. H., WANG, G. Y., HAO, H. C., CHAO, C. J., WANG, Y. & JIN, Q. W. 2017. Facile manipulation of protein localization in fission yeast through binding of GFP-binding protein to GFP. *J Cell Sci,* 130**,** 1003-1015.

CHIKASHIGE, Y., YAMANE, M., OKAMASA, K., TSUTSUMI, C., KOJIDANI, T., SATO, M., HARAGUCHI, T. & HIRAOKA, Y. 2009. Membrane proteins Bqt3 and -4 anchor telomeres to the nuclear envelope to ensure chromosomal bouquet formation. *J Cell Biol,* 187**,** 413-27.

CISMOWSKI, M. J., LAFF, G. M., SOLOMON, M. J. & REED, S. I. 1995. KIN28 encodes a C-terminal domain kinase that controls mRNA transcription in Saccharomyces cerevisiae but lacks cyclin-dependent kinase-activating kinase (CAK) activity. *Mol Cell Biol,* 15**,** 2983-92.

CORREA-BORDES, J., GULLI, M. P. & NURSE, P. 1997. p25rum1 promotes proteolysis of the mitotic B-cyclin p56cdc13 during G1 of the fission yeast cell cycle. *EMBO J,* 16**,** 4657-64.

CORREA-BORDES, J. & NURSE, P. 1995. p25rum1 orders S phase and mitosis by acting as an inhibitor of the p34cdc2 mitotic kinase. *Cell,* 83**,** 1001-9.

COUDREUSE, D. & NURSE, P. 2010. Driving the cell cycle with a minimal CDK control network. *Nature,* 468**,** 1074-9.

CROSS, F. R. & JACOBSON, M. D. 2000. Conservation and function of a potential substrate-binding domain in the yeast Clb5 B-type cyclin. *Mol Cell Biol,* 20**,** 4782-90.

D'URSO, G., MARRACCINO, R. L., MARSHAK, D. R. & ROBERTS, J. M. 1990. Cell cycle control of DNA replication by a homologue from human cells of the p34cdc2 protein kinase. *Science,* 250**,** 786-91.

DAI, J., KATENEVA, A. V. & HIGGINS, J. M. 2009. Studies of haspin-depleted cells reveal that spindle-pole integrity in mitosis requires chromosome cohesion. *J Cell Sci,* 122**,** 4168-76.

DALAL, S. N., SCHWEITZER, C. M., GAN, J. & DECAPRIO, J. A. 1999. Cytoplasmic localization of human cdc25C during interphase requires an intact 14-3-3 binding site. *Mol Cell Biol,* 19**,** 4465-79.

DECOTTIGNIES, A., ZARZOV, P. & NURSE, P. 2001. In vivo localisation of fission yeast cyclin-dependent kinase cdc2p and cyclin B cdc13p during mitosis and meiosis. *J Cell Sci,* 114**,** 2627-40.

DEN HAESE, G. J., WALWORTH, N., CARR, A. M. & GOULD, K. L. 1995. The Wee1 protein kinase regulates T14 phosphorylation of fission yeast Cdc2. *Mol Biol Cell,* 6**,** 371-85.

DEVAULT, A., MARTINEZ, A. M., FESQUET, D., LABBE, J. C., MORIN, N., TASSAN, J. P., NIGG, E. A., CAVADORE, J. C. & DOREE, M. 1995. MAT1 ('menage a trois') a new RING finger protein subunit stabilizing cyclin H-cdk7 complexes in starfish and Xenopus CAK. *EMBO J,* 14**,** 5027-36.

DING, R., WEST, R. R., MORPHEW, D. M., OAKLEY, B. R. & MCINTOSH, J. R. 1997. The spindle pole body of Schizosaccharomyces pombe enters and leaves the nuclear envelope as the cell cycle proceeds. *Mol Biol Cell,* 8**,** 1461-79.

DOHADWALA, M., DA CRUZ E SILVA, E. F., HALL, F. L., WILLIAMS, R. T., CARBONARO-HALL, D. A., NAIRN, A. C., GREENGARD, P. & BERNDT, N. 1994. Phosphorylation and inactivation of protein phosphatase 1 by cyclin-dependent kinases. *Proc Natl Acad Sci U S A,* 91**,** 6408-12.

DOXSEY, S., ZIMMERMAN, W. & MIKULE, K. 2005. Centrosome control of the cell cycle. *Trends Cell Biol,* 15**,** 303-11.

DRAVIAM, V. M., ORRECHIA, S., LOWE, M., PARDI, R. & PINES, J. 2001. The localization of human cyclins B1 and B2 determines CDK1 substrate specificity and neither enzyme requires MEK to disassemble the Golgi apparatus. *J Cell Biol,* 152**,** 945-58.

DUNPHY, W. G., BRIZUELA, L., BEACH, D. & NEWPORT, J. 1988. The Xenopus cdc2 protein is a component of MPF, a cytoplasmic regulator of mitosis. *Cell,* 54**,** 423-31.

DUTERTRE, S., CAZALES, M., QUARANTA, M., FROMENT, C., TRABUT, V., DOZIER, C., MIREY, G., BOUCHE, J. P., THEIS-FEBVRE, N., SCHMITT, E., MONSARRAT, B., PRIGENT, C. & DUCOMMUN, B. 2004. Phosphorylation of CDC25B by Aurora-A at the centrosome contributes to the G2-M transition. *J Cell Sci,* 117**,** 2523-31.

EBNER, M., SINKOVICS, B., SZCZYGIEL, M., RIBEIRO, D. W. & YUDUSHKIN, I. 2017. Localization of mTORC2 activity inside cells. *J Cell Biol,* 216**,** 343-353.

EDELSTEIN, A. D., TSUCHIDA, M. A., AMODAJ, N., PINKARD, H., VALE, R. D. & STUURMAN, N. 2014. Advanced methods of microscope control using muManager software. *J Biol Methods,* 1.

ENSERINK, J. M. & KOLODNER, R. D. 2010. An overview of Cdk1-controlled targets and processes. *Cell Div,* 5**,** 11.

EVANS, T., ROSENTHAL, E. T., YOUNGBLOM, J., DISTEL, D. & HUNT, T. 1983. Cyclin: a protein specified by maternal mRNA in sea urchin eggs that is destroyed at each cleavage division. *Cell,* 33**,** 389-96.

FAUSTOVA, I., BULATOVIC, L., MATIYEVSKAYA, F., VALK, E., ORD, M. & LOOG, M. 2021. A new linear cyclin docking motif that mediates exclusively S-phase CDK-specific signaling. *EMBO J,* 40**,** e105839.

FEATHERSTONE, C. & RUSSELL, P. 1991. Fission yeast p107wee1 mitotic inhibitor is a tyrosine/serine kinase. *Nature,* 349**,** 808-11.

FERGUSON, R. L. & MALLER, J. L. 2010. Centrosomal localization of cyclin E-Cdk2 is required for initiation of DNA synthesis. *Curr Biol,* 20**,** 856-60.

FERRELL, J. E., JR. 1998. How regulated protein translocation can produce switch-like responses. *Trends Biochem Sci,* 23**,** 461-5.

FISHER, D. L. & NURSE, P. 1996. A single fission yeast mitotic cyclin B p34cdc2 kinase promotes both S-phase and mitosis in the absence of G1 cyclins. *EMBO J,* 15**,** 850-60.

FISHER, R. P., JIN, P., CHAMBERLIN, H. M. & MORGAN, D. O. 1995. Alternative mechanisms of CAK assembly require an assembly factor or an activating kinase. *Cell,* 83**,** 47-57.

FISHER, R. P. & MORGAN, D. O. 1994. A novel cyclin associates with MO15/CDK7 to form the CDK-activating kinase. *Cell,* 78**,** 713-24.

FONG, C. S., SATO, M. & TODA, T. 2010. Fission yeast Pcp1 links polo kinase-mediated mitotic entry to gamma-tubulin-dependent spindle formation. *EMBO J,* 29**,** 120-30.

FU, J., HAGAN, I. M. & GLOVER, D. M. 2015. The centrosome and its duplication cycle. *Cold Spring Harb Perspect Biol,* 7**,** a015800.

FUKUURA, M., NAGAO, K., OBUSE, C., TAKAHASHI, T. S., NAKAGAWA, T. & MASUKATA, H. 2011. CDK promotes interactions of Sld3 and Drc1 with Cut5 for initiation of DNA replication in fission yeast. *Mol Biol Cell,* 22**,** 2620-33.

FURNARI, B., BLASINA, A., BODDY, M. N., MCGOWAN, C. H. & RUSSELL, P. 1999. Cdc25 inhibited in vivo and in vitro by checkpoint kinases Cds1 and Chk1. *Mol Biol Cell,* 10**,** 833-45.

GABRIELLI, B. G., CLARK, J. M., MCCORMACK, A. K. & ELLEM, K. A. 1997. Ultraviolet light-induced G2 phase cell cycle checkpoint blocks cdc25-dependent progression into mitosis. *Oncogene,* 15**,** 749-58.

GAUTIER, J., NORBURY, C., LOHKA, M., NURSE, P. & MALLER, J. 1988. Purified maturation-promoting factor contains the product of a Xenopus homolog of the fission yeast cell cycle control gene cdc2+. *Cell,* 54**,** 433-9.

GAUTIER, J., SOLOMON, M. J., BOOHER, R. N., BAZAN, J. F. & KIRSCHNER, M. W. 1991. cdc25 is a specific tyrosine phosphatase that directly activates p34cdc2. *Cell,* 67**,** 197-211.

GAVET, O. & PINES, J. 2010a. Activation of cyclin B1-Cdk1 synchronizes events in the nucleus and the cytoplasm at mitosis. *J Cell Biol,* 189**,** 247-59.

GAVET, O. & PINES, J. 2010b. Progressive activation of CyclinB1-Cdk1 coordinates entry to mitosis. *Dev Cell,* 18**,** 533-43.

GHARBI-AYACHI, A., LABBE, J. C., BURGESS, A., VIGNERON, S., STRUB, J. M., BRIOUDES, E., VAN-DORSSELAER, A., CASTRO, A. & LORCA, T. 2010. The substrate of Greatwall kinase, Arpp19, controls mitosis by inhibiting protein phosphatase 2A. *Science,* 330**,** 1673-7.

GOLSTEYN, R. M., MUNDT, K. E., FRY, A. M. & NIGG, E. A. 1995. Cell cycle regulation of the activity and subcellular localization of Plk1, a human protein kinase implicated in mitotic spindle function. *J Cell Biol,* 129**,** 1617-28.

GONG, D., POMERENING, J. R., MYERS, J. W., GUSTAVSSON, C., JONES, J. T., HAHN, A. T., MEYER, T. & FERRELL, J. E., JR. 2007. Cyclin A2 regulates nuclear-envelope breakdown and the nuclear accumulation of cyclin B1. *Curr Biol,* 17**,** 85-91.

GOULD, K. L., MORENO, S., OWEN, D. J., SAZER, S. & NURSE, P. 1991. Phosphorylation at Thr167 is required for Schizosaccharomyces pombe p34cdc2 function. *EMBO J,* 10**,** 3297-309.

GOULD, K. L. & NURSE, P. 1989. Tyrosine phosphorylation of the fission yeast cdc2+ protein kinase regulates entry into mitosis. *Nature,* 342**,** 39-45.

GRALLERT, A., BOKE, E., HAGTING, A., HODGSON, B., CONNOLLY, Y., GRIFFITHS, J. R., SMITH, D. L., PINES, J. & HAGAN, I. M. 2015. A PP1-PP2A phosphatase relay controls mitotic progression. *Nature,* 517**,** 94-98.

GRALLERT, A., CHAN, K. Y., ALONSO-NUNEZ, M. L., MADRID, M., BISWAS, A., ALVAREZ-TABARES, I., CONNOLLY, Y., TANAKA, K., ROBERTSON, A.,

ORTIZ, J. M., SMITH, D. L. & HAGAN, I. M. 2013a. Removal of centrosomal PP1 by NIMA kinase unlocks the MPF feedback loop to promote mitotic commitment in S. pombe. *Curr Biol,* 23**,** 213-22.
GRALLERT, A., KRAPP, A., BAGLEY, S., SIMANIS, V. & HAGAN, I. M. 2004. Recruitment of NIMA kinase shows that maturation of the S. pombe spindle-pole body occurs over consecutive cell cycles and reveals a role for NIMA in modulating SIN activity. *Genes Dev,* 18**,** 1007-21.
GRALLERT, A., PATEL, A., TALLADA, V. A., CHAN, K. Y., BAGLEY, S., KRAPP, A., SIMANIS, V. & HAGAN, I. M. 2013b. Centrosomal MPF triggers the mitotic and morphogenetic switches of fission yeast. *Nat Cell Biol,* 15**,** 88-95.
HAGAN, I. & YANAGIDA, M. 1995. The product of the spindle formation gene sad1+ associates with the fission yeast spindle pole body and is essential for viability. *J Cell Biol,* 129**,** 1033-47.
HAGAN, I. M. 2016. Immunofluorescence Microscopy of Schizosaccharomyces pombe Using Chemical Fixation. *Cold Spring Harb Protoc,* 2016.
HAGAN, I. M. & GRALLERT, A. 2013. Spatial control of mitotic commitment in fission yeast. *Biochem Soc Trans,* 41**,** 1766-71.
HAGTING, A., JACKMAN, M., SIMPSON, K. & PINES, J. 1999. Translocation of cyclin B1 to the nucleus at prophase requires a phosphorylation-dependent nuclear import signal. *Curr Biol,* 9**,** 680-9.
HAGTING, A., KARLSSON, C., CLUTE, P., JACKMAN, M. & PINES, J. 1998. MPF localization is controlled by nuclear export. *EMBO J,* 17**,** 4127-38.
HALOVA, L. & PETERSEN, J. 2011. Aurora promotes cell division during recovery from TOR-mediated cell cycle arrest by driving spindle pole body recruitment of Polo. *J Cell Sci,* 124**,** 3441-9.
HARTWELL, L. H., CULOTTI, J. & REID, B. 1970. Genetic control of the cell-division cycle in yeast. I. Detection of mutants. *Proc Natl Acad Sci U S A,* 66**,** 352-9.
HARTWELL, L. H., MORTIMER, R. K., CULOTTI, J. & CULOTTI, M. 1973. Genetic Control of the Cell Division Cycle in Yeast: V. Genetic Analysis of cdc Mutants. *Genetics,* 74**,** 267-86.
HAYASHI, T., HATANAKA, M., NAGAO, K., NAKASEKO, Y., KANOH, J., KOKUBU, A., EBE, M. & YANAGIDA, M. 2007. Rapamycin sensitivity of the Schizosaccharomyces pombe tor2 mutant and organization of two highly phosphorylated TOR complexes by specific and common subunits. *Genes Cells,* 12**,** 1357-70.
HAYLES, J., AVES, S. & NURSE, P. 1986a. suc1 is an essential gene involved in both the cell cycle and growth in fission yeast. *EMBO J,* 5**,** 3373-9.
HAYLES, J., BEACH, D., DURKACZ, B. & NURSE, P. 1986b. The fission yeast cell cycle control gene cdc2: isolation of a sequence suc1 that suppresses cdc2 mutant function. *Mol Gen Genet,* 202**,** 291-3.
HAYLES, J., WOOD, V., JEFFERY, L., HOE, K. L., KIM, D. U., PARK, H. O., SALAS-PINO, S., HEICHINGER, C. & NURSE, P. 2013. A genome-wide resource of cell cycle and cell shape genes of fission yeast. *Open Biol,* 3**,** 130053.
HEALD, R., MCLOUGHLIN, M. & MCKEON, F. 1993. Human wee1 maintains mitotic timing by protecting the nucleus from cytoplasmically activated Cdc2 kinase. *Cell,* 74**,** 463-74.
HEGARAT, N., CRNCEC, A., SUAREZ PEREDO RODRIGUEZ, M. F., ECHEGARAY ITURRA, F., GU, Y., BUSBY, O., LANG, P. F., BARR, A. R., BAKAL, C., KANEMAKI, M. T., LAMOND, A. I., NOVAK, B., LY, T. & HOCHEGGER, H. 2020. Cyclin A triggers Mitosis either via the Greatwall kinase pathway or Cyclin B. *EMBO J,* 39**,** e104419.

HEINRICH, S., WINDECKER, H., HUSTEDT, N. & HAUF, S. 2012. Mph1 kinetochore localization is crucial and upstream in the hierarchy of spindle assembly checkpoint protein recruitment to kinetochores. *J Cell Sci,* 125**,** 4720-7.

HERMAND, D., PIHLAK, A., WESTERLING, T., DAMAGNEZ, V., VANDENHAUTE, J., COTTAREL, G. & MAKELA, T. P. 1998. Fission yeast Csk1 is a CAK-activating kinase (CAKAK). *EMBO J,* 17**,** 7230-8.

HERMAND, D., WESTERLING, T., PIHLAK, A., THURET, J. Y., VALLENIUS, T., TIAINEN, M., VANDENHAUTE, J., COTTAREL, G., MANN, C. & MAKELA, T. P. 2001. Specificity of Cdk activation in vivo by the two Caks Mcs6 and Csk1 in fission yeast. *EMBO J,* 20**,** 82-90.

HINCHCLIFFE, E. H., MILLER, F. J., CHAM, M., KHODJAKOV, A. & SLUDER, G. 2001. Requirement of a centrosomal activity for cell cycle progression through G1 into S phase. *Science,* 291**,** 1547-50.

HOFFMANN, I., CLARKE, P. R., MARCOTE, M. J., KARSENTI, E. & DRAETTA, G. 1993. Phosphorylation and activation of human cdc25-C by cdc2--cyclin B and its involvement in the self-amplification of MPF at mitosis. *EMBO J,* 12**,** 53-63.

HOFFMANN, I., DRAETTA, G. & KARSENTI, E. 1994. Activation of the phosphatase activity of human cdc25A by a cdk2-cyclin E dependent phosphorylation at the G1/S transition. *EMBO J,* 13**,** 4302-10.

HUDSON, J. D., FEILOTTER, H. & YOUNG, P. G. 1990. stf1: non-wee mutations epistatic to cdc25 in the fission yeast Schizosaccharomyces pombe. *Genetics,* 126**,** 309-15.

HUISMAN, S. M., SMEETS, M. F. & SEGAL, M. 2007. Phosphorylation of Spc110p by Cdc28p-Clb5p kinase contributes to correct spindle morphogenesis in S. cerevisiae. *J Cell Sci,* 120**,** 435-46.

IKEMOTO, S., NAKAMURA, T., KUBO, M. & SHIMODA, C. 2000. S. pombe sporulation-specific coiled-coil protein Spo15p is localized to the spindle pole body and essential for its modification. *J Cell Sci,* 113 (Pt 3)**,** 545-54.

INOUE, D. & SAGATA, N. 2005. The Polo-like kinase Plx1 interacts with and inhibits Myt1 after fertilization of Xenopus eggs. *EMBO J,* 24**,** 1057-67.

JACKMAN, M., FIRTH, M. & PINES, J. 1995. Human cyclins B1 and B2 are localized to strikingly different structures: B1 to microtubules, B2 primarily to the Golgi apparatus. *EMBO J,* 14**,** 1646-54.

JACKMAN, M., KUBOTA, Y., DEN ELZEN, N., HAGTING, A. & PINES, J. 2002. Cyclin A- and cyclin E-Cdk complexes shuttle between the nucleus and the cytoplasm. *Mol Biol Cell,* 13**,** 1030-45.

JACKMAN, M., LINDON, C., NIGG, E. A. & PINES, J. 2003. Active cyclin B1-Cdk1 first appears on centrosomes in prophase. *Nat Cell Biol,* 5**,** 143-8.

JEFFREY, P. D., RUSSO, A. A., POLYAK, K., GIBBS, E., HURWITZ, J., MASSAGUE, J. & PAVLETICH, N. P. 1995. Mechanism of CDK activation revealed by the structure of a cyclinA-CDK2 complex. *Nature,* 376**,** 313-20.

JIN, Q. W., RAY, S., CHOI, S. H. & MCCOLLUM, D. 2007. The nucleolar Net1/Cfi1-related protein Dnt1 antagonizes the septation initiation network in fission yeast. *Mol Biol Cell,* 18**,** 2924-34.

KALDIS, P. 1999. The cdk-activating kinase (CAK): from yeast to mammals. *Cell Mol Life Sci,* 55**,** 284-96.

KALDIS, P., SUTTON, A. & SOLOMON, M. J. 1996. The Cdk-activating kinase (CAK) from budding yeast. *Cell,* 86**,** 553-64.

KALLSTROM, H., LINDQVIST, A., POSPISIL, V., LUNDGREN, A. & ROSENTHAL, C. K. 2005. Cdc25A localisation and shuttling: characterisation of sequences mediating nuclear export and import. *Exp Cell Res,* 303**,** 89-100.

KAMENZ, J., MIHALJEV, T., KUBIS, A., LEGEWIE, S. & HAUF, S. 2015. Robust Ordering of Anaphase Events by Adaptive Thresholds and Competing Degradation Pathways. *Mol Cell,* 60**,** 446-59.

KARAISKOU, A., JESSUS, C., BRASSAC, T. & OZON, R. 1999. Phosphatase 2A and polo kinase, two antagonistic regulators of cdc25 activation and MPF auto-amplification. *J Cell Sci,* 112 (Pt 21)**,** 3747-56.

KHODJAKOV, A., COLE, R. W., OAKLEY, B. R. & RIEDER, C. L. 2000. Centrosome-independent mitotic spindle formation in vertebrates. *Curr Biol,* 10**,** 59-67.

KHODJAKOV, A. & RIEDER, C. L. 2001. Centrosomes enhance the fidelity of cytokinesis in vertebrates and are required for cell cycle progression. *J Cell Biol,* 153**,** 237-42.

KIM, D. U., HAYLES, J., KIM, D., WOOD, V., PARK, H. O., WON, M., YOO, H. S., DUHIG, T., NAM, M., PALMER, G., HAN, S., JEFFERY, L., BAEK, S. T., LEE, H., SHIM, Y. S., LEE, M., KIM, L., HEO, K. S., NOH, E. J., LEE, A. R., JANG, Y. J., CHUNG, K. S., CHOI, S. J., PARK, J. Y., PARK, Y., KIM, H. M., PARK, S. K., PARK, H. J., KANG, E. J., KIM, H. B., KANG, H. S., PARK, H. M., KIM, K., SONG, K., SONG, K. B., NURSE, P. & HOE, K. L. 2010. Analysis of a genome-wide set of gene deletions in the fission yeast Schizosaccharomyces pombe. *Nat Biotechnol,* 28**,** 617-623.

KIM, S. Y. & FERRELL, J. E., JR. 2007. Substrate competition as a source of ultrasensitivity in the inactivation of Wee1. *Cell,* 128**,** 1133-45.

KING, R. W., PETERS, J. M., TUGENDREICH, S., ROLFE, M., HIETER, P. & KIRSCHNER, M. W. 1995. A 20S complex containing CDC27 and CDC16 catalyzes the mitosis-specific conjugation of ubiquitin to cyclin B. *Cell,* 81**,** 279-88.

KINOSHITA, N., YAMANO, H., NIWA, H., YOSHIDA, T. & YANAGIDA, M. 1993. Negative regulation of mitosis by the fission yeast protein phosphatase ppa2. *Genes Dev,* 7**,** 1059-71.

KOIVOMAGI, M. & LOOG, M. 2011. Cdk1: a kinase with changing substrate specificity. *Cell Cycle,* 10**,** 3625-6.

KOIVOMAGI, M., ORD, M., IOFIK, A., VALK, E., VENTA, R., FAUSTOVA, I., KIVI, R., BALOG, E. R., RUBIN, S. M. & LOOG, M. 2013. Multisite phosphorylation networks as signal processors for Cdk1. *Nat Struct Mol Biol,* 20**,** 1415-24.

KOIVOMAGI, M., VALK, E., VENTA, R., IOFIK, A., LEPIKU, M., MORGAN, D. O. & LOOG, M. 2011. Dynamics of Cdk1 substrate specificity during the cell cycle. *Mol Cell,* 42**,** 610-23.

KRAMER, A., MAILAND, N., LUKAS, C., SYLJUASEN, R. G., WILKINSON, C. J., NIGG, E. A., BARTEK, J. & LUKAS, J. 2004. Centrosome-associated Chk1 prevents premature activation of cyclin-B-Cdk1 kinase. *Nat Cell Biol,* 6**,** 884-91.

KRAPP, A., GULLI, M. P. & SIMANIS, V. 2004. SIN and the art of splitting the fission yeast cell. *Curr Biol,* 14**,** R722-30.

KREK, W. & NIGG, E. A. 1991a. Differential phosphorylation of vertebrate p34cdc2 kinase at the G1/S and G2/M transitions of the cell cycle: identification of major phosphorylation sites. *EMBO J,* 10**,** 305-16.

KREK, W. & NIGG, E. A. 1991b. Mutations of p34cdc2 phosphorylation sites induce premature mitotic events in HeLa cells: evidence for a double block to p34cdc2 kinase activation in vertebrates. *EMBO J,* 10**,** 3331-41.

KUMAGAI, A. & DUNPHY, W. G. 1996. Purification and molecular cloning of Plx1, a Cdc25-regulatory kinase from Xenopus egg extracts. *Science,* 273**,** 1377-80.

KUMAGAI, A. & DUNPHY, W. G. 1999. Binding of 14-3-3 proteins and nuclear export control the intracellular localization of the mitotic inducer Cdc25. *Genes Dev,* 13**,** 1067-72.

KUMAGAI, A., YAKOWEC, P. S. & DUNPHY, W. G. 1998. 14-3-3 proteins act as negative regulators of the mitotic inducer Cdc25 in Xenopus egg extracts. *Mol Biol Cell,* 9**,** 345-54.

KUME, K., CANTWELL, H., BURRELL, A. & NURSE, P. 2019. Nuclear membrane protein Lem2 regulates nuclear size through membrane flow. *Nat Commun,* 10**,** 1871.

LABAER, J., GARRETT, M. D., STEVENSON, L. F., SLINGERLAND, J. M., SANDHU, C., CHOU, H. S., FATTAEY, A. & HARLOW, E. 1997. New functional activities for the p21 family of CDK inhibitors. *Genes Dev,* 11**,** 847-62.

LABBE, J. C., CAPONY, J. P., CAPUT, D., CAVADORE, J. C., DERANCOURT, J., KAGHAD, M., LELIAS, J. M., PICARD, A. & DOREE, M. 1989a. MPF from starfish oocytes at first meiotic metaphase is a heterodimer containing one molecule of cdc2 and one molecule of cyclin B. *EMBO J,* 8**,** 3053-8.

LABBE, J. C., PICARD, A., PEAUCELLIER, G., CAVADORE, J. C., NURSE, P. & DOREE, M. 1989b. Purification of MPF from starfish: identification as the H1 histone kinase p34cdc2 and a possible mechanism for its periodic activation. *Cell,* 57**,** 253-63.

LEE, M. G. & NURSE, P. 1987. Complementation used to clone a human homologue of the fission yeast cell cycle control gene cdc2. *Nature,* 327**,** 31-5.

LI, J., MEYER, A. N. & DONOGHUE, D. J. 1995. Requirement for phosphorylation of cyclin B1 for Xenopus oocyte maturation. *Mol Biol Cell,* 6**,** 1111-24.

LI, J., MEYER, A. N. & DONOGHUE, D. J. 1997. Nuclear localization of cyclin B1 mediates its biological activity and is regulated by phosphorylation. *Proc Natl Acad Sci U S A,* 94**,** 502-7.

LINDQVIST, A., KALLSTROM, H. & KARLSSON ROSENTHAL, C. 2004. Characterisation of Cdc25B localisation and nuclear export during the cell cycle and in response to stress. *J Cell Sci,* 117**,** 4979-90.

LINDQVIST, A., KALLSTROM, H., LUNDGREN, A., BARSOUM, E. & ROSENTHAL, C. K. 2005. Cdc25B cooperates with Cdc25A to induce mitosis but has a unique role in activating cyclin B1-Cdk1 at the centrosome. *J Cell Biol,* 171**,** 35-45.

LOCK, A., RUTHERFORD, K., HARRIS, M. A., HAYLES, J., OLIVER, S. G., BAHLER, J. & WOOD, V. 2019. PomBase 2018: user-driven reimplementation of the fission yeast database provides rapid and intuitive access to diverse, interconnected information. *Nucleic Acids Res,* 47**,** D821-D827.

LOOG, M. & MORGAN, D. O. 2005. Cyclin specificity in the phosphorylation of cyclin-dependent kinase substrates. *Nature,* 434**,** 104-8.

LOPEZ-GIRONA, A., FURNARI, B., MONDESERT, O. & RUSSELL, P. 1999. Nuclear localization of Cdc25 is regulated by DNA damage and a 14-3-3 protein. *Nature,* 397**,** 172-5.

LORCA, T., LABBE, J. C., DEVAULT, A., FESQUET, D., CAPONY, J. P., CAVADORE, J. C., LE BOUFFANT, F. & DOREE, M. 1992. Dephosphorylation of cdc2 on threonine 161 is required for cdc2 kinase inactivation and normal anaphase. *EMBO J,* 11**,** 2381-90.

LU, L. X., DOMINGO-SANANES, M. R., HUZARSKA, M., NOVAK, B. & GOULD, K. L. 2012. Multisite phosphoregulation of Cdc25 activity refines the mitotic entrance and exit switches. *Proc Natl Acad Sci U S A,* 109**,** 9899-904.

LUNDGREN, K., WALWORTH, N., BOOHER, R., DEMBSKI, M., KIRSCHNER, M. & BEACH, D. 1991. mik1 and wee1 cooperate in the inhibitory tyrosine phosphorylation of cdc2. *Cell,* 64**,** 1111-22.

MACIVER, F. H., TANAKA, K., ROBERTSON, A. M. & HAGAN, I. M. 2003. Physical and functional interactions between polo kinase and the spindle pole component Cut12 regulate mitotic commitment in S. pombe. *Genes Dev,* 17**,** 1507-23.

MAGIDSON, V., CHANG, F. & KHODJAKOV, A. 2006. Regulation of cytokinesis by spindle-pole bodies. *Nat Cell Biol,* 8**,** 891-3.
MARTIN, D. E., SOULARD, A. & HALL, M. N. 2004. TOR regulates ribosomal protein gene expression via PKA and the Forkhead transcription factor FHL1. *Cell,* 119**,** 969-79.
MARTIN-CASTELLANOS, C., BLANCO, M. A., DE PRADA, J. M. & MORENO, S. 2000. The puc1 cyclin regulates the G1 phase of the fission yeast cell cycle in response to cell size. *Mol Biol Cell,* 11**,** 543-54.
MARTIN-CASTELLANOS, C., LABIB, K. & MORENO, S. 1996. B-type cyclins regulate G1 progression in fission yeast in opposition to the p25rum1 cdk inhibitor. *EMBO J,* 15**,** 839-49.
MASUDA, H., FONG, C. S., OHTSUKI, C., HARAGUCHI, T. & HIRAOKA, Y. 2011. Spatiotemporal regulations of Wee1 at the G2/M transition. *Mol Biol Cell,* 22**,** 555-69.
MASUI, Y. & MARKERT, C. L. 1971. Cytoplasmic control of nuclear behavior during meiotic maturation of frog oocytes. *J Exp Zool,* 177**,** 129-45.
MATSUMOTO, Y. & MALLER, J. L. 2004. A centrosomal localization signal in cyclin E required for Cdk2-independent S phase entry. *Science,* 306**,** 885-8.
MATSUOKA, S., HUANG, M. & ELLEDGE, S. J. 1998. Linkage of ATM to cell cycle regulation by the Chk2 protein kinase. *Science,* 282**,** 1893-7.
MATSUYAMA, A., ARAI, R., YASHIRODA, Y., SHIRAI, A., KAMATA, A., SEKIDO, S., KOBAYASHI, Y., HASHIMOTO, A., HAMAMOTO, M., HIRAOKA, Y., HORINOUCHI, S. & YOSHIDA, M. 2006. ORFeome cloning and global analysis of protein localization in the fission yeast Schizosaccharomyces pombe. *Nat Biotechnol,* 24**,** 841-7.
MCCULLY, E. K. & ROBINOW, C. F. 1971. Mitosis in the fission yeast Schizosaccharomyces pombe: a comparative study with light and electron microscopy. *J Cell Sci,* 9**,** 475-507.
MCGOWAN, C. H. & RUSSELL, P. 1993. Human Wee1 kinase inhibits cell division by phosphorylating p34cdc2 exclusively on Tyr15. *EMBO J,* 12**,** 75-85.
MCGOWAN, C. H. & RUSSELL, P. 1995. Cell cycle regulation of human WEE1. *EMBO J,* 14**,** 2166-75.
MCGRATH, D. A., BALOG, E. R., KOIVOMAGI, M., LUCENA, R., MAI, M. V., HIRSCHI, A., KELLOGG, D. R., LOOG, M. & RUBIN, S. M. 2013. Cks confers specificity to phosphorylation-dependent CDK signaling pathways. *Nat Struct Mol Biol,* 20**,** 1407-14.
MENDENHALL, M. D. 1993. An inhibitor of p34CDC28 protein kinase activity from Saccharomyces cerevisiae. *Science,* 259**,** 216-9.
MILLAR, J. B., LENAERS, G. & RUSSELL, P. 1992. Pyp3 PTPase acts as a mitotic inducer in fission yeast. *EMBO J,* 11**,** 4933-41.
MILLAR, J. B., MCGOWAN, C. H., LENAERS, G., JONES, R. & RUSSELL, P. 1991. p80cdc25 mitotic inducer is the tyrosine phosphatase that activates p34cdc2 kinase in fission yeast. *EMBO J,* 10**,** 4301-9.
MITCHISON, J. M. 1970. Chapter 7 Physiological and Cytological Methods for Schizosaccharomyces pombe. *In:* PRESCOTT, D. M. (ed.) *Methods in Cell Biology.* Academic Press.
MOCCIARO, A. & SCHIEBEL, E. 2010. Cdc14: a highly conserved family of phosphatases with non-conserved functions? *J Cell Sci,* 123**,** 2867-76.
MOCHIDA, S. & HUNT, T. 2012. Protein phosphatases and their regulation in the control of mitosis. *EMBO Rep,* 13**,** 197-203.
MOCHIDA, S., MASLEN, S. L., SKEHEL, M. & HUNT, T. 2010. Greatwall phosphorylates an inhibitor of protein phosphatase 2A that is essential for mitosis. *Science,* 330**,** 1670-3.

MOORE, J. D., KIRK, J. A. & HUNT, T. 2003. Unmasking the S-phase-promoting potential of cyclin B1. *Science,* 300**,** 987-90.
MORENO, S., HAYLES, J. & NURSE, P. 1989. Regulation of p34cdc2 protein kinase during mitosis. *Cell,* 58**,** 361-72.
MORENO, S., KLAR, A. & NURSE, P. 1991. Molecular genetic analysis of fission yeast Schizosaccharomyces pombe. *Methods Enzymol,* 194**,** 795-823.
MORENO, S. & NURSE, P. 1994. Regulation of progression through the G1 phase of the cell cycle by the rum1+ gene. *Nature,* 367**,** 236-42.
MORIS, N., SHRIVASTAVA, J., JEFFERY, L., LI, J. J., HAYLES, J. & NURSE, P. 2016. A genome-wide screen to identify genes controlling the rate of entry into mitosis in fission yeast. *Cell Cycle,* 15**,** 3121-3130.
MORRELL, J. L., TOMLIN, G. C., RAJAGOPALAN, S., VENKATRAM, S., FEOKTISTOVA, A. S., TASTO, J. J., MEHTA, S., JENNINGS, J. L., LINK, A., BALASUBRAMANIAN, M. K. & GOULD, K. L. 2004. Sid4p-Cdc11p assembles the septation initiation network and its regulators at the S. pombe SPB. *Curr Biol,* 14**,** 579-84.
MOSELEY, J. B., MAYEUX, A., PAOLETTI, A. & NURSE, P. 2009. A spatial gradient coordinates cell size and mitotic entry in fission yeast. *Nature,* 459**,** 857-60.
MUELLER, P. R., COLEMAN, T. R. & DUNPHY, W. G. 1995a. Cell cycle regulation of a Xenopus Wee1-like kinase. *Mol Biol Cell,* 6**,** 119-34.
MUELLER, P. R., COLEMAN, T. R., KUMAGAI, A. & DUNPHY, W. G. 1995b. Myt1: a membrane-associated inhibitory kinase that phosphorylates Cdc2 on both threonine-14 and tyrosine-15. *Science,* 270**,** 86-90.
MULVIHILL, D. P., PETERSEN, J., OHKURA, H., GLOVER, D. M. & HAGAN, I. M. 1999. Plo1 kinase recruitment to the spindle pole body and its role in cell division in Schizosaccharomyces pombe. *Mol Biol Cell,* 10**,** 2771-85.
NAVARRO, F. J. & NURSE, P. 2012. A systematic screen reveals new elements acting at the G2/M cell cycle control. *Genome Biol,* 13**,** R36.
NOGUCHI, E., SHANAHAN, P., NOGUCHI, C. & RUSSELL, P. 2002. CDK phosphorylation of Drc1 regulates DNA replication in fission yeast. *Curr Biol,* 12**,** 599-605.
NOLET, F. E., VANDERVELDE, A., VANDERBEKE, A., PINEROS, L., CHANG, J. B. & GELENS, L. 2020. Nuclei determine the spatial origin of mitotic waves. *Elife,* 9.
NURSE, P. 1975. Genetic control of cell size at cell division in yeast. *Nature,* 256**,** 547-551.
NURSE, P. & BISSETT, Y. 1981. Gene required in G1 for commitment to cell cycle and in G2 for control of mitosis in fission yeast. *Nature,* 292**,** 558-60.
NURSE, P., THURIAUX, P. & NASMYTH, K. 1976. Genetic control of the cell division cycle in the fission yeast Schizosaccharomyces pombe. *Mol Gen Genet,* 146**,** 167-78.
O'CONNELL, M. J., RALEIGH, J. M., VERKADE, H. M. & NURSE, P. 1997. Chk1 is a wee1 kinase in the G2 DNA damage checkpoint inhibiting cdc2 by Y15 phosphorylation. *EMBO J,* 16**,** 545-54.
OHTSUBO, M., THEODORAS, A. M., SCHUMACHER, J., ROBERTS, J. M. & PAGANO, M. 1995. Human cyclin E, a nuclear protein essential for the G1-to-S phase transition. *Mol Cell Biol,* 15**,** 2612-24.
ORD, M., PUSS, K. K., KIVI, R., MOLL, K., OJALA, T., BOROVKO, I., FAUSTOVA, I., VENTA, R., VALK, E., KOIVOMAGI, M. & LOOG, M. 2020. Proline-Rich Motifs Control G2-CDK Target Phosphorylation and Priming an Anchoring Protein for Polo Kinase Localization. *Cell Rep,* 31**,** 107757.
ORD, M., VENTA, R., MOLL, K., VALK, E. & LOOG, M. 2019. Cyclin-Specific Docking Mechanisms Reveal the Complexity of M-CDK Function in the Cell Cycle. *Mol Cell,* 75**,** 76-89 e3.

PADTE, N. N., MARTIN, S. G., HOWARD, M. & CHANG, F. 2006. The cell-end factor pom1p inhibits mid1p in specification of the cell division plane in fission yeast. *Curr Biol,* 16**,** 2480-7.

PAGLIUCA, F. W., COLLINS, M. O., LICHAWSKA, A., ZEGERMAN, P., CHOUDHARY, J. S. & PINES, J. 2011. Quantitative proteomics reveals the basis for the biochemical specificity of the cell-cycle machinery. *Mol Cell,* 43**,** 406-17.

PASCREAU, G., ECKERDT, F., CHURCHILL, M. E. & MALLER, J. L. 2010. Discovery of a distinct domain in cyclin A sufficient for centrosomal localization independently of Cdk binding. *Proc Natl Acad Sci U S A,* 107**,** 2932-7.

PATTERSON, J. O., BASU, S., REES, P. & NURSE, P. 2021. CDK control pathways integrate cell size and ploidy information to control cell division. *Elife,* 10.

PATTERSON, J. O., REES, P. & NURSE, P. 2019. Noisy Cell-Size-Correlated Expression of Cyclin B Drives Probabilistic Cell-Size Homeostasis in Fission Yeast. *Curr Biol,* 29**,** 1379-1386 e4.

PENG, C. Y., GRAVES, P. R., THOMA, R. S., WU, Z., SHAW, A. S. & PIWNICA-WORMS, H. 1997. Mitotic and G2 checkpoint control: regulation of 14-3-3 protein binding by phosphorylation of Cdc25C on serine-216. *Science,* 277**,** 1501-5.

PETERSEN, J. & HAGAN, I. M. 2005. Polo kinase links the stress pathway to cell cycle control and tip growth in fission yeast. *Nature,* 435**,** 507-12.

PETERSEN, J. & NURSE, P. 2007. TOR signalling regulates mitotic commitment through the stress MAP kinase pathway and the Polo and Cdc2 kinases. *Nat Cell Biol,* 9**,** 1263-72.

PETRI, E. T., ERRICO, A., ESCOBEDO, L., HUNT, T. & BASAVAPPA, R. 2007. The crystal structure of human cyclin B. *Cell Cycle,* 6**,** 1342-9.

PINES, J. & HUNTER, T. 1991. Human cyclins A and B1 are differentially located in the cell and undergo cell cycle-dependent nuclear transport. *J Cell Biol,* 115**,** 1-17.

PINES, J. & HUNTER, T. 1994. The differential localization of human cyclins A and B is due to a cytoplasmic retention signal in cyclin B. *EMBO J,* 13**,** 3772-81.

PIRINCCI ERCAN, D., CHRETIEN, F., CHAKRAVARTY, P., FLYNN, H. R., SNIJDERS, A. P. & UHLMANN, F. 2021. Budding yeast relies on G1 cyclin specificity to couple cell cycle progression with morphogenetic development. *Sci Adv,* 7.

POMERENING, J. R., SONTAG, E. D. & FERRELL, J. E., JR. 2003. Building a cell cycle oscillator: hysteresis and bistability in the activation of Cdc2. *Nat Cell Biol,* 5**,** 346-51.

POON, R. Y., YAMASHITA, K., ADAMCZEWSKI, J. P., HUNT, T. & SHUTTLEWORTH, J. 1993. The cdc2-related protein p40MO15 is the catalytic subunit of a protein kinase that can activate p33cdk2 and p34cdc2. *EMBO J,* 12**,** 3123-32.

RICHARDSON, H. E., WITTENBERG, C., CROSS, F. & REED, S. I. 1989. An essential G1 function for cyclin-like proteins in yeast. *Cell,* 59**,** 1127-33.

ROTHBAUER, U., ZOLGHADR, K., MUYLDERMANS, S., SCHEPERS, A., CARDOSO, M. C. & LEONHARDT, H. 2008. A versatile nanotrap for biochemical and functional studies with fluorescent fusion proteins. *Mol Cell Proteomics,* 7**,** 282-9.

RUSSELL, P. & NURSE, P. 1986. cdc25+ functions as an inducer in the mitotic control of fission yeast. *Cell,* 45**,** 145-53.

RUSSO, A. A., JEFFREY, P. D., PATTEN, A. K., MASSAGUE, J. & PAVLETICH, N. P. 1996a. Crystal structure of the p27Kip1 cyclin-dependent-kinase inhibitor bound to the cyclin A-Cdk2 complex. *Nature,* 382**,** 325-31.

RUSSO, A. A., JEFFREY, P. D. & PAVLETICH, N. P. 1996b. Structural basis of cyclin-dependent kinase activation by phosphorylation. *Nat Struct Biol,* 3**,** 696-700.

RUTHNICK, D. & SCHIEBEL, E. 2018. Duplication and Nuclear Envelope Insertion of the Yeast Microtubule Organizing Centre, the Spindle Pole Body. *Cells,* 7.

SANTAMARIA, A., WANG, B., ELOWE, S., MALIK, R., ZHANG, F., BAUER, M., SCHMIDT, A., SILLJE, H. H., KORNER, R. & NIGG, E. A. 2011. The Plk1-dependent phosphoproteome of the early mitotic spindle. *Mol Cell Proteomics,* 10**,** M110 004457.

SANTAMARIA, D., BARRIERE, C., CERQUEIRA, A., HUNT, S., TARDY, C., NEWTON, K., CACERES, J. F., DUBUS, P., MALUMBRES, M. & BARBACID, M. 2007. Cdk1 is sufficient to drive the mammalian cell cycle. *Nature,* 448**,** 811-5.

SANTOS, S. D., WOLLMAN, R., MEYER, T. & FERRELL, J. E., JR. 2012. Spatial positive feedback at the onset of mitosis. *Cell,* 149**,** 1500-13.

SATYANARAYANA, A. & KALDIS, P. 2009. Mammalian cell-cycle regulation: several Cdks, numerous cyclins and diverse compensatory mechanisms. *Oncogene,* 28**,** 2925-39.

SCHINDELIN, J., ARGANDA-CARRERAS, I., FRISE, E., KAYNIG, V., LONGAIR, M., PIETZSCH, T., PREIBISCH, S., RUEDEN, C., SAALFELD, S., SCHMID, B., TINEVEZ, J. Y., WHITE, D. J., HARTENSTEIN, V., ELICEIRI, K., TOMANCAK, P. & CARDONA, A. 2012. Fiji: an open-source platform for biological-image analysis. *Nat Methods,* 9**,** 676-82.

SCHMUCKER, S. & SUMARA, I. 2014. Molecular dynamics of PLK1 during mitosis. *Mol Cell Oncol,* 1**,** e954507.

SCHULMAN, B. A., LINDSTROM, D. L. & HARLOW, E. 1998. Substrate recruitment to cyclin-dependent kinase 2 by a multipurpose docking site on cyclin A. *Proc Natl Acad Sci U S A,* 95**,** 10453-8.

SEHNAL, D., BITTRICH, S., DESHPANDE, M., SVOBODOVA, R., BERKA, K., BAZGIER, V., VELANKAR, S., BURLEY, S. K., KOCA, J. & ROSE, A. S. 2021. Mol* Viewer: modern web app for 3D visualization and analysis of large biomolecular structures. *Nucleic Acids Res,* 49**,** W431-W437.

SHERR, C. J. & ROBERTS, J. M. 1999. CDK inhibitors: positive and negative regulators of G1-phase progression. *Genes Dev,* 13**,** 1501-12.

SIMANIS, V. & NURSE, P. 1986. The cell cycle control gene cdc2+ of fission yeast encodes a protein kinase potentially regulated by phosphorylation. *Cell,* 45**,** 261-8.

SINGH, P., HALOVA, L. & HAGAN, I. M. 2021. Highly Synchronous Mitotic Progression in Schizosaccharomyces pombe Upon Relief of Transient Cdc2-asM17 Inhibition. *Methods Mol Biol,* 2329**,** 123-142.

SONGYANG, Z., BLECHNER, S., HOAGLAND, N., HOEKSTRA, M. F., PIWNICA-WORMS, H. & CANTLEY, L. C. 1994. Use of an oriented peptide library to determine the optimal substrates of protein kinases. *Curr Biol,* 4**,** 973-82.

STERN, B. & NURSE, P. 1996. A quantitative model for the cdc2 control of S phase and mitosis in fission yeast. *Trends Genet,* 12**,** 345-50.

SUDAKIN, V., GANOTH, D., DAHAN, A., HELLER, H., HERSHKO, J., LUCA, F. C., RUDERMAN, J. V. & HERSHKO, A. 1995. The cyclosome, a large complex containing cyclin-selective ubiquitin ligase activity, targets cyclins for destruction at the end of mitosis. *Mol Biol Cell,* 6**,** 185-97.

SUTANI, T., YUASA, T., TOMONAGA, T., DOHMAE, N., TAKIO, K. & YANAGIDA, M. 1999. Fission yeast condensin complex: essential roles of non-SMC subunits for condensation and Cdc2 phosphorylation of Cut3/SMC4. *Genes Dev,* 13**,** 2271-83.

SWAFFER, M. P., JONES, A. W., FLYNN, H. R., SNIJDERS, A. P. & NURSE, P. 2016. CDK Substrate Phosphorylation and Ordering the Cell Cycle. *Cell,* 167**,** 1750-1761 e16.

TAKIZAWA, C. G. & MORGAN, D. O. 2000. Control of mitosis by changes in the subcellular location of cyclin-B1-Cdk1 and Cdc25C. *Curr Opin Cell Biol,* 12**,** 658-65.

TALLADA, V. A., BRIDGE, A. J., EMERY, P. A. & HAGAN, I. M. 2007. Suppression of the Schizosaccharomyces pombe cut12.1 cell-cycle defect by mutations in cdc25 and genes involved in transcriptional and translational control. *Genetics,* 176**,** 73-83.

TALLADA, V. A., TANAKA, K., YANAGIDA, M. & HAGAN, I. M. 2009. The S. pombe mitotic regulator Cut12 promotes spindle pole body activation and integration into the nuclear envelope. *J Cell Biol,* 185**,** 875-88.

TAMM, T., GRALLERT, A., GROSSMAN, E. P., ALVAREZ-TABARES, I., STEVENS, F. E. & HAGAN, I. M. 2011. Brr6 drives the Schizosaccharomyces pombe spindle pole body nuclear envelope insertion/extrusion cycle. *J Cell Biol,* 195**,** 467-84.

TANAKA, K., PETERSEN, J., MACIVER, F., MULVIHILL, D. P., GLOVER, D. M. & HAGAN, I. M. 2001. The role of Plo1 kinase in mitotic commitment and septation in Schizosaccharomyces pombe. *EMBO J,* 20**,** 1259-70.

TANG, Z., COLEMAN, T. R. & DUNPHY, W. G. 1993. Two distinct mechanisms for negative regulation of the Wee1 protein kinase. *EMBO J,* 12**,** 3427-36.

TASSAN, J. P., JAQUENOUD, M., FRY, A. M., FRUTIGER, S., HUGHES, G. J. & NIGG, E. A. 1995. In vitro assembly of a functional human CDK7-cyclin H complex requires MAT1, a novel 36 kDa RING finger protein. *EMBO J,* 14**,** 5608-17.

TASSAN, J. P., SCHULTZ, S. J., BARTEK, J. & NIGG, E. A. 1994. Cell cycle analysis of the activity, subcellular localization, and subunit composition of human CAK (CDK-activating kinase). *J Cell Biol,* 127**,** 467-78.

TATEBE, H., MORIGASAKI, S., MURAYAMA, S., ZENG, C. T. & SHIOZAKI, K. 2010. Rab-family GTPase regulates TOR complex 2 signaling in fission yeast. *Curr Biol,* 20**,** 1975-82.

THOMAS, Y., CIRILLO, L., PANBIANCO, C., MARTINO, L., TAVERNIER, N., SCHWAGER, F., VAN HOVE, L., JOLY, N., SANTAMARIA, A., PINTARD, L. & GOTTA, M. 2016. Cdk1 Phosphorylates SPAT-1/Bora to Promote Plk1 Activation in C. elegans and Human Cells. *Cell Rep,* 15**,** 510-518.

TIBELIUS, A., MARHOLD, J., ZENTGRAF, H., HEILIG, C. E., NEITZEL, H., DUCOMMUN, B., RAUCH, A., HO, A. D., BARTEK, J. & KRAMER, A. 2009. Microcephalin and pericentrin regulate mitotic entry via centrosome-associated Chk1. *J Cell Biol,* 185**,** 1149-57.

TOYOSHIMA, F., MORIGUCHI, T., WADA, A., FUKUDA, M. & NISHIDA, E. 1998. Nuclear export of cyclin B1 and its possible role in the DNA damage-induced G2 checkpoint. *EMBO J,* 17**,** 2728-35.

TRAUTMANN, S., WOLFE, B. A., JORGENSEN, P., TYERS, M., GOULD, K. L. & MCCOLLUM, D. 2001. Fission yeast Clp1p phosphatase regulates G2/M transition and coordination of cytokinesis with cell cycle progression. *Curr Biol,* 11**,** 931-40.

TRUNNELL, N. B., POON, A. C., KIM, S. Y. & FERRELL, J. E., JR. 2011. Ultrasensitivity in the Regulation of Cdc25C by Cdk1. *Mol Cell,* 41**,** 263-74.

UZAWA, S., LI, F., JIN, Y., MCDONALD, K. L., BRAUNFELD, M. B., AGARD, D. A. & CANDE, W. Z. 2004. Spindle pole body duplication in fission yeast occurs at the G1/S boundary but maturation is blocked until exit from S by an event downstream of cdc10+. *Mol Biol Cell,* 15**,** 5219-30.

VERMA, R., ANNAN, R. S., HUDDLESTON, M. J., CARR, S. A., REYNARD, G. & DESHAIES, R. J. 1997. Phosphorylation of Sic1p by G1 Cdk required for its degradation and entry into S phase. *Science,* 278**,** 455-60.

VISINTIN, R., CRAIG, K., HWANG, E. S., PRINZ, S., TYERS, M. & AMON, A. 1998. The phosphatase Cdc14 triggers mitotic exit by reversal of Cdk-dependent phosphorylation. *Mol Cell,* 2**,** 709-18.

VO, T. V., DAS, J., MEYER, M. J., CORDERO, N. A., AKTURK, N., WEI, X., FAIR, B. J., DEGATANO, A. G., FRAGOZA, R., LIU, L. G., MATSUYAMA, A., TRICKEY, M., HORIBATA, S., GRIMSON, A., YAMANO, H., YOSHIDA, M., ROTH, F. P., PLEISS, J. A., XIA, Y. & YU, H. 2016. A Proteome-wide Fission Yeast Interactome Reveals Network Evolution Principles from Yeasts to Human. *Cell,* 164**,** 310-323.

VOROBJEV, I. A. & CHENTSOV YU, S. 1982. Centrioles in the cell cycle. I. Epithelial cells. *J Cell Biol,* 93**,** 938-49.

WALDE, S. & KING, M. C. 2014. The KASH protein Kms2 coordinates mitotic remodeling of the spindle pole body. *J Cell Sci,* 127**,** 3625-40.

WATANABE, N., ARAI, H., NISHIHARA, Y., TANIGUCHI, M., WATANABE, N., HUNTER, T. & OSADA, H. 2004. M-phase kinases induce phospho-dependent ubiquitination of somatic Wee1 by SCFbeta-TrCP. *Proc Natl Acad Sci U S A,* 101**,** 4419-24.

WELBURN, J. P., TUCKER, J. A., JOHNSON, T., LINDERT, L., MORGAN, M., WILLIS, A., NOBLE, M. E. & ENDICOTT, J. A. 2007. How tyrosine 15 phosphorylation inhibits the activity of cyclin-dependent kinase 2-cyclin A. *J Biol Chem,* 282**,** 3173-81.

WEST, R. R., VAISBERG, E. V., DING, R., NURSE, P. & MCINTOSH, J. R. 1998. cut11(+): A gene required for cell cycle-dependent spindle pole body anchoring in the nuclear envelope and bipolar spindle formation in Schizosaccharomyces pombe. *Mol Biol Cell,* 9**,** 2839-55.

WINEY, M. & O'TOOLE, E. T. 2001. The spindle cycle in budding yeast. *Nat Cell Biol,* 3**,** E23-7.

WOOD, V., GWILLIAM, R., RAJANDREAM, M. A., LYNE, M., LYNE, R., STEWART, A., SGOUROS, J., PEAT, N., HAYLES, J., BAKER, S., BASHAM, D., BOWMAN, S., BROOKS, K., BROWN, D., BROWN, S., CHILLINGWORTH, T., CHURCHER, C., COLLINS, M., CONNOR, R., CRONIN, A., DAVIS, P., FELTWELL, T., FRASER, A., GENTLES, S., GOBLE, A., HAMLIN, N., HARRIS, D., HIDALGO, J., HODGSON, G., HOLROYD, S., HORNSBY, T., HOWARTH, S., HUCKLE, E. J., HUNT, S., JAGELS, K., JAMES, K., JONES, L., JONES, M., LEATHER, S., MCDONALD, S., MCLEAN, J., MOONEY, P., MOULE, S., MUNGALL, K., MURPHY, L., NIBLETT, D., ODELL, C., OLIVER, K., O'NEIL, S., PEARSON, D., QUAIL, M. A., RABBINOWITSCH, E., RUTHERFORD, K., RUTTER, S., SAUNDERS, D., SEEGER, K., SHARP, S., SKELTON, J., SIMMONDS, M., SQUARES, R., SQUARES, S., STEVENS, K., TAYLOR, K., TAYLOR, R. G., TIVEY, A., WALSH, S., WARREN, T., WHITEHEAD, S., WOODWARD, J., VOLCKAERT, G., AERT, R., ROBBEN, J., GRYMONPREZ, B., WELTJENS, I., VANSTREELS, E., RIEGER, M., SCHAFER, M., MULLER-AUER, S., GABEL, C., FUCHS, M., DUSTERHOFT, A., FRITZC, C., HOLZER, E., MOESTL, D., HILBERT, H., BORZYM, K., LANGER, I., BECK, A., LEHRACH, H., REINHARDT, R., POHL, T. M., EGER, P., ZIMMERMANN, W., WEDLER, H., WAMBUTT, R., PURNELLE, B., GOFFEAU, A., CADIEU, E., DREANO, S., GLOUX, S., et al. 2002. The genome sequence of Schizosaccharomyces pombe. *Nature,* 415**,** 871-80.

WOOD, V., HARRIS, M. A., MCDOWALL, M. D., RUTHERFORD, K., VAUGHAN, B. W., STAINES, D. M., ASLETT, M., LOCK, A., BAHLER, J., KERSEY, P. J. & OLIVER, S. G. 2012. PomBase: a comprehensive online resource for fission yeast. *Nucleic Acids Res,* 40**,** D695-9.

WU, J. Q., GUO, J. Y., TANG, W., YANG, C. S., FREEL, C. D., CHEN, C., NAIRN, A. C. & KORNBLUTH, S. 2009. PP1-mediated dephosphorylation of phosphoproteins at mitotic exit is controlled by inhibitor-1 and PP1 phosphorylation. *Nat Cell Biol,* 11**,** 644-51.

YANG, J., BARDES, E. S., MOORE, J. D., BRENNAN, J., POWERS, M. A. & KORNBLUTH, S. 1998. Control of cyclin B1 localization through regulated binding of the nuclear export factor CRM1. *Genes Dev,* 12**,** 2131-43.

YANG, J., SONG, H., WALSH, S., BARDES, E. S. & KORNBLUTH, S. 2001. Combinatorial control of cyclin B1 nuclear trafficking through phosphorylation at multiple sites. *J Biol Chem,* 276**,** 3604-9.

YU, J., RAIA, P., GHENT, C. M., RAISCH, T., SADIAN, Y., CAVADINI, S., SABALE, P. M., BARFORD, D., RAUNSER, S., MORGAN, D. O. & BOLAND, A. 2021. Structural basis of human separase regulation by securin and CDK1-cyclin B1. *Nature,* 596**,** 138-142.

YU, Z. Y., ZHANG, M. T., WANG, G. Y., XU, D., KEIFENHEIM, D., FRANCO, A., CANSADO, J., MASUDA, H., RHIND, N., WANG, Y. & JIN, Q. W. 2013. Fission yeast nucleolar protein Dnt1 regulates G2/M transition and cytokinesis by downregulating Wee1 kinase. *J Cell Sci,* 126**,** 4995-5004.

ZILIO, N., WEHRKAMP-RICHTER, S. & BODDY, M. N. 2012. A new versatile system for rapid control of gene expression in the fission yeast Schizosaccharomyces pombe. *Yeast,* 29**,** 425-34.